FEBRUARY 1991

ENVIRONMENTAL PROGRESS

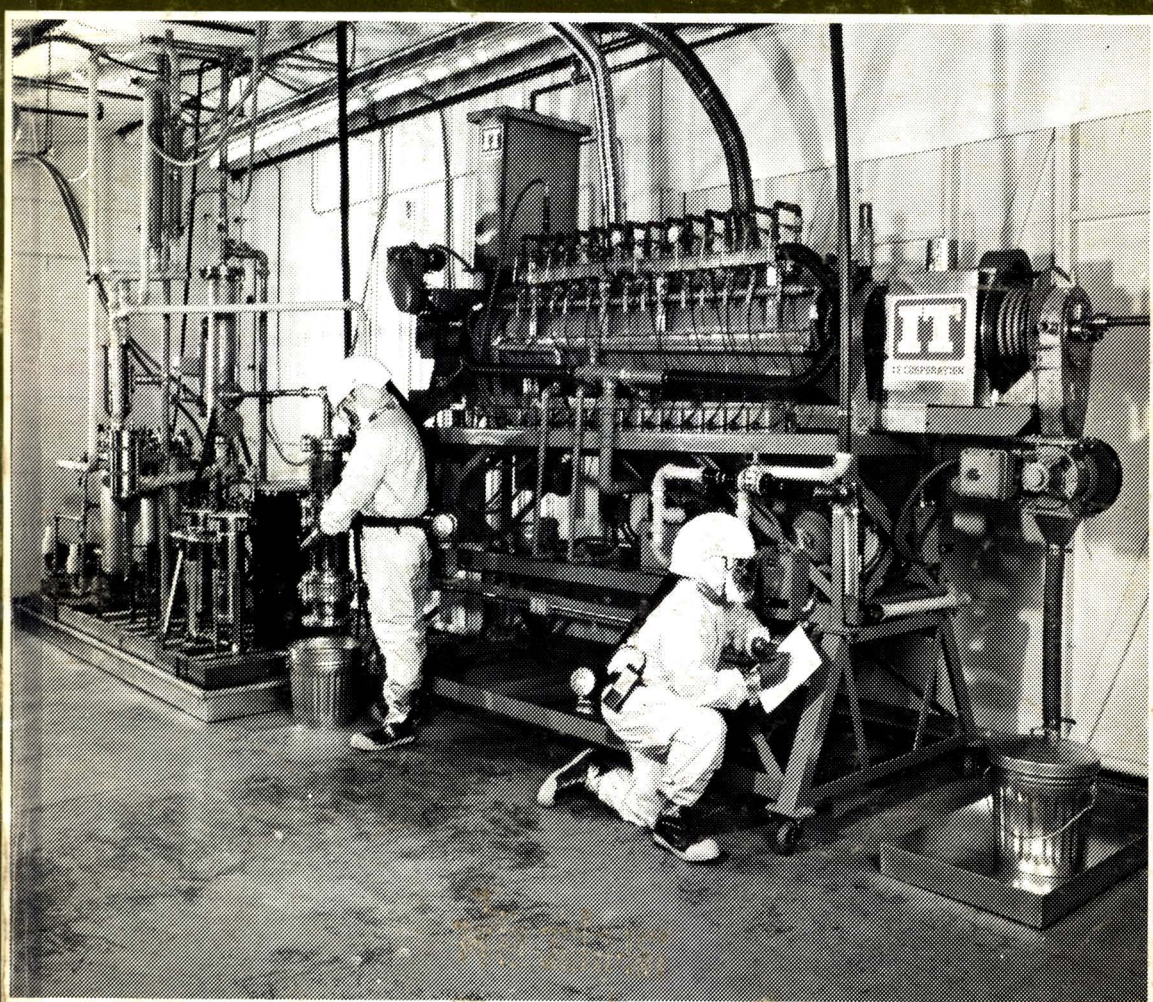

Thermal separation pilot plant (see article on page 40).
Photo courtesy of IT Corporation, St. Paul, Minnesota.

Turn your lifetime of experience into the experience of a lifetime.

We're looking for executives who know their way around the trenches as well as the front offices. Because if you're recently retired, there's a whole world out there desperately waiting to be taught what you spent a lifetime learning.

Through the International Executive Service Corps—the not-for-profit organization that sends U.S. managers to help businesses in developing nations—you can volunteer for short-term assignments in foreign countries where you're truly needed. Although you will not be paid, you and your spouse will receive all expenses, plus the personal satisfaction of teaching others while you discover more about yourself.

Think of it. Your experience can make a difference in a land much different from your own. Instead of ending your career, you could be starting the experience of a lifetime.

Send for more information today.

IESC Volunteer Gordon Swaney, a retired U.S. manager, on project site in Indonesia.

IESC

International Executive Service Corps

Ad Council
A Public Service of This Publication

YES, I'd like to share my lifetime of experience with others. I recently retired from my position as a hands-on manager with a U.S. company. I also understand that volunteers and their spouses receive expenses, but no salary. Please send me more information now.

Name_____

Address_____

City_____ State_____ Zip_____

Write to: IESC, 8 Stamford Forum, P.O. Box 10005, Stamford, CT 06904-2005.
Or, for faster response, call this number: (203) 967-6000.

ENVIRONMENTAL PROGRESS

Environmental Progress is a publication of the American Institute of Chemical Engineers. It will deal with multi-faceted aspects of the pollution problem. It will provide thorough coverage of abatement, control, and containment of effluents and emissions within compliance standards. Papers will cover all aspects including water, air, liquid and solid wastes. Progress and technological advances vital to the environmental engineer will be reported.

Publisher
Gary M. Rekstad

Published four times a year (February, May, August, and November) by the American Institute of Chemical Engineers, 345 East 47th St., New York, N.Y. 10017. (ISSN 0278-4491). Manuscripts should be submitted to the Manuscript Center, American Institute of Chemical Engineers, 345 East 47th St., New York, N.Y. 10017. Statements and opinions in *Environmental Progress* are those of the contributors, and the American Institute of Chemical Engineers assumes no responsibility for them. Subscription price per year: $100.00. AIChE Environmental Division Members: $25 included in dues. Outside the U.S. please add $7.50 per subscription for postage and handling. Single copies $30. Outside the U.S. please add $2 for postage and handling. Payment must be made in U.S. dollars. Second-class postage paid at New York, N.Y. and additional mailing offices.

Volume 10

CONTENTS

Number 1

Departments

Environmental Progress fee code: 0278-4491/91 $2.00. Postmaster: Please send change of addresses to *Environmental Progress*, AIChE, 345 East 47 Street, New York, N.Y. 10017.

Proactive Environmental Management

Coby A. Scher

Pilko & Associates, Inc., 2707 North Loop West, Suite 960, Houston, TX 77008

Proactive environmental management, as a concept, has been widely discussed but also widely misunderstood by many executives. It is best defined as follows: Doing what is prudent from a business standpoint to reduce environmental liabilities -- regardless of whether these actions are required by regulatory agencies.

The concept of proactive environmental management is simple and straightforward, but in practice most U.S. companies are operating in a Stage 1 reactive mode: struggling to be in compliance with *existing* regulations. Some companies have made the transition to Stage 2, where they are not only in compliance with existing regulations, but are also planning how to deal with proposed regulations. Surprisingly, only a handful of firms are operating in the Stage 3 or proactive mode where they are going beyond compliance to also *manage* their environmental risks.

More companies would be operating in a proactive mode if their chief executives understood the nature and magnitude of the environmental risks faced by their companies. Basically, most industrial firms should be concerned about four types of environmental risks:

Soils and Groundwater Contamination. This problem occurs at a high percentage of industrial sites, a surprising number of commercial sites, and even some supposedly "virgin" sites.

Asbestos Contamination. Asbestos is often found in buildings built prior to 1977.

Catastrophic Releases of Toxic Materials. These releases can have the most immediate and serious impact upon local residents and the environment.

Regulatory Changes. Regulatory agencies can change the ground rules for a company or an entire industry.

A company should employ the following steps to manage its environmental risks:

Step One: Identify potential environmental problems -- preferably before they occur -- related to soils and groundwater contamination, asbestos contamination, catastrophic releases of toxic materials, and regulatory changes.

Step Two: Prioritize these risks based upon the probability of their occurrence and potential severity if they do occur. This potential severity can be measured by financial exposure, human health risks, public relations impact, etc.

Step Three: Develop specific alternatives that can be used to reduce the probability of occurrence and/or the potential severity of these risks.

Step Four: Take action where appropriate. The key is "where appropriate" because the objective should be to *manage* environmental risks as opposed to simply *risk minimization.*

These four steps should be used for a company's ongoing operations, shutdown sites that it still owns, previously owned sites at which a company may have residual liabilities, and multiparty sites such as Superfund sites.

The following procedure should be employed to reduce environmental risks:

1) **Develop a "proactive" environmental policy and clearly communicate this policy to all staff.** The most important contribution a board of directors can make in this area is to encourage its CEO to develop a proactive environmental policy that includes managing environmental risks. A proactive policy is in sharp contrast to most environmental policies, which focus upon being in compliance with environmental regulations. This policy needs to be clearly communicated not only to environmental staff but also to line executives.

2) **Periodically conduct environmental risk assessments for all company operations.** The CEO should be encouraged to require periodic risk assessments. These are not merely environmental "compliance audits," which have become fashionable during the past five to eight years and tend to focus upon whether facilities have the proper permits, are in compliance, or if company staff are falsifying records. Instead, comprehensive risk assessments that are designed to identify potential problems, either before they occur, or at an early stage, should be conducted so that management will have the opportunity to take action.

3) **Identify, prioritize, and manage soils, groundwater, and asbestos problems.** This needs to be done for a company's present and past sites, including multiparty sites.

4) **Require appropriate environmental due diligence prior to all acquisitions and divestitures.** This would include real estate transactions as well.

The environmental risks of corporate acquisitions can be major due to contaminated real estate, prior offsite disposal, agency enforcement actions, etc. Adequate environmental due diligence is critical prior to consummating any acquisition or divestiture.

5) **Cultivate your public.** Regardless of precautions taken, environmental problems will still occur. Therefore, companies should develop positive, ongoing relationships with local residents, community leaders, and regulatory agency staff. The key is to establish a track record of being open and honest. These relationships will be invaluable for effective damage control and when problems occur.

In summary, companies cannot afford just to be in compliance with environmental laws, regulations, and permits. A growing number of well-managed companies are expanding their concept of environmental management to include environmental risks. When dealing with environmental risks, "an ounce of prevention is worth a *ton* of cure."

Coby Scher, P.E., is a Vice President and General Manager of the Environmental Strategy Division of Pilko & Associates. He is a member of AIChE, a registered professional engineer in Texas and a Diplomate of the American Academy of Environmental Engineers. He is past chairman of the Environmental Division of AIChE and now serves on Environmental Progress's *Editorial Advisory Board.*

Washington Environmental Newsletter

CLEAN AIR ACT (Recap)

The Clean Air Act amendments of 1990 that were signed into law on November 15, 1990, send a clear signal that industry will have to make some severe adjustments in changing from "business as usual" for compliance.

Projections of costs for implementation may run as high as $25 billion a year since the amendments significantly toughen CAA by mandating regulations to reduce acid rain, urban smog, air toxics and ozone-depleting chemicals over the next decade.

Urban smog—new provisions of the bill call for reductions in urban smog by areas that have not attained health-based ambient air quality standards. Controls will be imposed on emitters (including dry cleaners, printers and bakeries) of 10 tons of hydrocarbons and nitrogen oxides in areas which the law defines to be *extremely* polluted such as Los Angeles; 25 tons in areas which the law defines as *severely* polluted such as New York; and 50 tons in areas that the law defines as *seriously* polluted, such as Washington, D.C.

Motor vehicle emissions—new tailpipe standards will require automobiles to reduce nitrogen oxides by 60% and hydrocarbons by 30% from currently accepted standards. Target dates for accomplishment are between 1994 and 1998. The nine smoggiest cities in the U.S. will be required to sell reformulated gasolines in 1995, and cities with CO problems will be required to sell oxygenated fuels. Auto manufacturers will also be required to design and build vehicles for the California market that are capable of running on non-gasoline fuels.

Toxic air pollutants—to decrease emissions, the new law will require industrial sources of 189 listed air toxics to install Maximum Achievable Control Technologies (MACT) by the year 2003. However utility emmisions are exempted until EPA determines the need for regulation. Municipal incinerators will be subject to these air emission controls and other requirements for monitoring emissions, training operators and issuing operating permits. Ash disposal provisions and waste recycling requirements were deleted from the law pending reauthorization of the Resource Conservation and Recovery Act, up for consideration in '91.

Acid rain—controls include a cap on utility emissions of sulfur dioxide of 8.9 million tons a year by the year 2000, representing a 10 million ton reduction from 1980 levels. 111 of the dirtiest utility plants must account for the largest cuts during the first 5 years, and cleaner plants responsible for later emission reductions. The law also sets up a system to provide pollution credits to "dirty" utilities in exchange for cuts in sulfur dioxide below their required limits.

Ozone-depletion—provisions call for the phase out of CFC's and halons by 2000. HCPC production will be frozen by 2015 and eliminated by 2030. A mandated recycling program for CFC's in air conditioning and refrigeration equipment will begin in 1992.

New enforcement authority granted the federal government is one of the most controversial areas of the law. The range of penalties for violations of the law have been increased, including criminal penalties for negligent or knowing violations that endanger others and for knowingly filing false statements.

The AIChE Washington office has put together a more detailed "Executive Summary" of the new law that is available to interested members. Call or write to:

Dr. Martin Siegel, Staff Dir. Gov't. Relations
AIChE Washington
1707 L St. N.W.
Washington, DC 20036
Tel. (202) 223-0650 Fax. (202) 833-3014

This material was prepared by AIChE's Washington Representative, Siegel•Houston & Associates, Inc. Suite 333, 1707 L Street, N.W., Washington, D.C. 20036. Tel. (202) 223-0650

Clean Water Act Compliance Course

Government Institutes, Inc., will offer a special course designed to help companies structure their environmental compliance programs to meet all of the requirements under the Clean Water Act.

The program agenda will include: An Introduction & Overview of Clean Water Developments Affecting Industrial Managers; Criminal, Civil & Administrative Enforcement Trends Under the Clean Water Act; Development & Application of Toxics Water Quality Standards to Industrial and Municipal Dischargers; Development, Revision, & Application of Technology-Based Effluent Limitations for Industry, and Variances for Them; Pretreatment Requirements Affecting Industrial Dischargers; Special Issues Facing Publicly Owned Treatment Works (POTWs) and Their Effect on Industrial Pretreatment Obligations and Expenses; Developments in National Pollutant Discharge Elimination System (NPDES) Permit Program; Overview of Monitoring & BioMonitoring Requirements and Developments; Special Spill Prevention and the New National Oil Pollution Act; Non-Point Source & Stormwater Controls; Important Legislative Developments; and more.

The Clean Water Act Compliance Course will be taught by a team of experts who work daily in the field. Leading the course will be the Program Co-Chairmen, J. Gordon Arbuckle and Russell V. Randle from the law firm of Patton, Boggs & Blow.

For more information or to register please contact Colleen Sullivan at Government Institutes, Inc., 966 Hungerford Drive, #24; Rockville, MD 20850; (301) 251-9250; FAX (301) 251-0638.

Hazardous Waste Reduction: The Federal Government's Role

As a participant in the 1990 Washington Internships for Students of Engineering (WISE) Program, Adam McNeese, a chemical engineering student at the University of Kentucky, Lexington, Kentucky, authored a 36-page report entitled "Hazardous Waste Reduction: The Federal Government's Role." In his WISE Program, Mr. McNeese was supervised by Dr. Jana Milford, Assistant Professor at the University of Connecticut, Storrs, Connecticut, the faculty "member-in-residence." Mr. McNeese's project was sponsored by the AIChE.

This project and resulting support were clearly topical as Congress considers some type of legislation mandating waste reduction. And the AIChE, realizing the need for waste reduction, established the Center for Waste Reduction technologies in the fall of 1989.

In his paper, the author mades several recommendations to mitigate hazardous waste reduction problems:

1. Clearly define the terms "hazardous waste reduction" and "hazardous waste"
2. Establish data collection procedures for waste reduction
3. Increase funding projects to ease the burden of reducing waste
4. Provide motivation for reducing wastes through a facility planning law

The full paper is available through AIChE's Washington Office: Siegel and Houston, 1701 L Street NW, Suite 333, Washington, DC 20036.

Cleanup of Petroleum Contaminated Soils at Underground Storage Tanks, Pollution Technology Review No. 195, Warren J. Lyman, David C. Noonan, and Patrick J. Reidy, Noyes Data Corporation, Park Ridge, NJ, (1990), 216 pages [ISBN No.: 0-8155-1258-9] U.S. List Price: $48.00

With the identification of many sites having leaking underground storage tanks and contaminated with petroleum products, this book is indeed appropriate and relevant. This book focuses on various strategies for the cleanup of petroleum-contaminated soils in the saturated and unsaturated zones at underground storage tank sites. The book presents basic information about the subsurface environment and the released petroleum product required to conduct a site assessment. Factors critical to the successful implementation of each technology are presented and site conditions which are favorable for each technology are discussed. The technologies addressed include: soil venting, bioremediation, soil flushing, hydraulic methods, excavation, soil washing, enhanced volatilization, trench excavation, vacuum extraction, air stripping, and activated carbon adsorption.

The book is divided into two parts. Part I describes corrective action technologies and considerations for petroleum-contaminated soils in the unsaturated zone, while Part II covers remediation techniques in the saturated zone. Chapter I of Part I presents an introduction addressing the purpose and approach and organization for the book. Chapter 2 discusses how to conduct a site assessment, including what information should be collected, plus evaluation of contaminant phases in the unsaturated zone and contaminant mobility. Chapter 3 addresses technology selection in the unsaturated zone (soil venting, bioremediation, soil flushing, hydraulic methods, excavation, and above ground treatment methods), addressing factors such as experience, cost and time-scale for effective implementation. Chapter 4 discusses followup measures by specifying cleanup goals, selecting design criteria, and monitoring performance and progress. Part I contains a list of references for the entire section. It also provides a sample case history, including a description of the methodology. Part I concludes with a glossary of terms.

Part II also begins with an introduction containing background, purpose, limitations, scope, and approach and organization. Chapter 2 addresses how to conduct the site assessment for the saturated zone. Chapter 3 discusses the technology selection for non-aqueous phase liquids (NAPLs), including containment of NAPLs and/or dissolved contaminants, recovery of floating NAPLs, treatment of contaminants dissolved in groundwater, new technologies, and technology compatibility. Chapter 4 addresses monitoring and follow-up measurements. This is followed by a list of references. The appendix discusses how to use the various worksheets contained in the book, followed by a glossary of terms.

The book contains a lot of useful information for people interested in the remediation of petroleum-contaminated soils. It is also a valuable reference source for people interested in the field of cleanup of subsurface contamination.

Robert W. Peters, Ph.D., P.E.
Environmental Systems Engineer
Energy Systems Division
Argonne National Laboratory
9700 South Cass Avenue
Argonne, Illinois 60439

Technolgy and Environment, J. H. Ausubel and H. E. Sladovich, National Academy Press, Washington, D.C. (1989), 230 pages [ISBN No.: 0-309-04075-2] U.S. List Price: $35.00

Technology and Environment is one of a series of publications by the National Academy Press designed to draw attention to major technological and engineering issues.

Modern technology which provides the best hope for the remediation of present day environmental problems, and the avoidance of the recurrence, is also in many cases, the cause of such problems. Technology and Environment examines this complex issue, and identifies the gaps which prevent our understanding of the basic cause of environmental concerns, and stresses the dangers of professional compartmentalization of knowledge. Using several examples with supporting data, the book addresses the contribution of present technology to issues such as global warming, hazardous wastes, and contamination of water resources, and defines the need for an international societal approach to the design, development, and implementation of new technology. The book stresses the importance of global information transfer, and examines the promise of technological solutions to the complex environmental issues.

A timely publication, this book is well written. I would strongly recommend it to anyone interested in the development and implementation of technological and engineering solutions to growing environmental problems.

John B. Rajan, P.E.
Chemical Technology Division
Argonne National Laboratory
9700 South Cass Avenue
Argonne, IL 60439

Organic Contaminants in Waste Water, Sludge, and Sediment: Occurrence, Fate, and Disposal, D. Quaghebeur, I. Temmerman, and G. Angeletti, Elsevier Applied Science, New York, NY (1989), 213 pages [ISBN No.: 0-85166-445-9] U.S. List Price: $45.00

This book represents the proceedings of a workshop held in Brussels, Belgium, held on October 26-27, 1988, sponsored by the European Corporation in Scientific and Technological Research, organized by the Commission of the European Communities, the Study Center for Water Research, and the Institute for Hygiene and Epidemiology. The title of this book was the general topic of the workshop.

The book was divided into four main parts. Part I addresses sources and occurrence in wastewaters, sludge, and soil; this section contains three papers on the general topics of trace analysis of linear alkylbenzene sulfonate, broad spectrum analysis of organic contaminants in surface waters and wastewaters, and occurrence of organic pollutants in soil and plants after land application.

Part II which includes five papers covers analytical techniques including sampling and determinations. Techniques discussed include capillary gas chromatography, atomic absorption spectrophotometry, gas chromatography/mass spectrometry (GCMS), liquid-liquid extraction, microsteam distillation, and high pressure liquid chromatography (HPLC).

Part III addressing the behavior during treatment including sampling and determinations covers four papers. The first paper concerns the fate of organic pollutants in sludge-amended soil and sludge-only landfills. The second paper involves the elimination of linear alkylbenzene sulfonate (LAS) during sewage treatment, drying, and composting of sludges and soil-amending processes. The third paper concerns the behavior of organic micropollutants in aerobic treatment, while the fourth paper covers biodegradation of phenolic compounds and monoaromatic hydrocarbons by a mixed wastewater culture under denitrifying conditions.

Part IV concerns the environmental fate and effects for soil, groundwater, and plants, and contains three papers. The first paper covers the levels and fate of LAS in sludge-amended soils. The second paper describes investigations of the entry of selected organic pollutants into soils and plants by use of sewage sludge. The last paper discusses present and future trends for organic contaminants.

The authors of these papers are from over ten countries and represent industry, research institutions, and universities, thereby covering several perspectives. The book addresses the occurrence, fate, and disposal of pollutants from a multimedia perspective and discusses appropriate analytical techniques. This book is a useful reference text for those people interested in the occurrence, fate, and disposal of pollutants in wastewaters and sediments, including sludge-amended soils.

Robert W. Peters, Ph.D., P.E.
Environmental Systems Engineer
Energy Systems Division
Argonne National Laboratory
9700 South Cass Avenue
Argonne, Illinois 60439

Use of Bulletin Board System For Air Quality Modeling

Ashok Kumar and Sumeet Mohan

Department of Civil Engineering, The University of Toledo, Toledo, OH 43606

Environmental Engineering professionals are required to conduct environmental impact analysis for new and existing facilities. The procedure often involves the use of air quality models specified in guidelines issued by the United States (U.S.) Environmental Protection Agency (EPA) [*1*]. A large number of scientists outside the U.S. have relied on the U.S. EPA guideline models to do some of the modeling work in their own country. The need for air quality models will also increase as a result of the Clean Air Act Amendments of 1990. The models are available from National Technical Information Services, Springfield, VA (telephone #703-487-4650) or from consulting companies. However, the Source Receptor Analysis branch of the EPA, located at Research Triangle Park, NC has recently started a Support Center for Regulatory Air Models, abbreviated as SCRAM, with a Bulletin Board System (BBS) to inform all people engaged in the field of air pollution modeling [*2*]. In addition to SCRAM, the BBS also provides information on CHIEF (Clearinghouse for Inventories and Emission Factors), CAA (Clean Air Act), APTI (Air Pollution Training Institute) and EMTIC (Emission Measurement Technical Information Center). The latter three are yet to be implemented completely.

The SCRAM BBS allows remotely logged on users to be able to communicate air quality modeling knowledge and information. The users could be logged on to mini- or microcomputers (having communication software like PROCOMM, KERMIT, etc.). With the help of a modem (to be able to dial up the BBS) one can even download the various air quality

Table 1 List of Air Quality Programs Available from SCRAM

(A) Regulatory Models:	
BLP	ISCLT
CALINE3	ISCST
CDM2	MPTER
CRSTER	RAM
EKMA1 through EKMA3	UAM1 through UAM6
(B) Screening Models:	
COMPLEX1	SCREEN
LONGZ	SHORTZ
PTPLU	VALLEY
RTDM3.2	VISCREEN
RVD2	
(C) Other Models:	
CTDMP1 through CTDMP11	
DEGADIS 2.1, CMB7, FDM1, FDM2, FDM3, PLUVUE 2	
(D) Related Programs:	
CAMPRO	PCRAMMT2
CHAVG	PREPFILE
CONCOR	RAMMET
MPRM1 through MPRM6	STAR
PCRAMMT1	WINDROSE

Table 2 Brief Description of Air Quality Programs Available from SCRAM and NTIS

APPRAC3	A model to determine emission factors by treating the traffic links of transportation networks with low vehicle miles as area sources.
BLP	A Gaussian plume dispersion model, specifically suited for aluminium reduction plants and graphite electrode plants.
CALINE3	A line source dispersion model used to predict CO concentrations in vicinity of highways and arterial streets.
CDM2	A climatological dispersion model for determining the long term persistence of quasi-stable contaminant concentrations.
CMB	The chemical mass balance model apportions source contributions to pollutants measured at a receptor site, using measured profiles of the sources chemical and elemental compositions.
COMPLEX1	Multiple point source model (having terrain adjustment) used mostly for initial screening phase.
CRSTER	A model for estimating ground level concentrations (G.L.C.) resulting from emissions up to 9 co-located elevated stacks.
CTDMP	Complex terrain dispersion model (detailed 3-D calculations) which can be used in all stability conditions.
DEGADIS	A model to simulate the dispersion of spills.
EKMA	The Empirical Kinetic Modeling Approach which estimates maximum afternoon concentrations of photochemically formed ozone based on pollutants emitted in the morning.
FDM	A model to study fugitive emissions.
HIWAY & ROADWAY	Models which compute hourly concentrations of non reactive contaminants in the downwind direction on roads and also G.L.C. within a distance of 200 meters from a highway.
INPUFF	A Gaussian model used to compute impacts of accidental hazardous releases or spills for a few minutes and also of typical continuous plumes from stacks.
ISCLT	A steady state Gaussian plume dispersion model to compute long term contaminant concentrations due to co-located industrial sources.
ISCST	A steady state Gaussian plume model to compute short term contaminant concentrations due to co-located industrial sources.
LONGZ	A model used to calculate long term impact on emissions from multiple stack, buildings and area sources.
MPRM	A software which provides a multi-purpose processor for organization of the meteorological data in the format required by air quality models.
MPTER	A multiple point source model that has built-in terrain adjustment correction factors.
PAL	A point, area and line source algorithm steady state Gaussian model used to compute short term impacts.
PBM	A model used for computation of hourly averages of different components of photochemical smog for one day of simulation in an urban area.
PEM	A model used to calculate short term G.L.C. and deposition fluxes of two particulate or gaseous pollutants.
PLUVUE2	The model is designed to calculate visual range reduction and atmospheric discoloration caused by plumes consisting of primary particles, nitrogen oxides, and sulfur dioxide emitted by a single source.
PTPLU	A point source Gaussian model used to calculate maximum G.L.C. for 1 hour.
RAM	A steady state Gaussian model used for calculating short term pollutant concentrations.
RAMMET	A software to process hourly meteorological data for air quality models.
RTDM	A Gaussian model used to calculate G.L.C. of pollutants in flat or rough terrains co-located with single or multiple point sources.
RVD	Relieve Valve Discharge model used to estimate plume rise, plume touchdown distance, concentration at touchdown for short term denser-than-air gas releases from stacks or pipes.
SCREEN	A screening model used by the USEPA to estimate maximum concentrations incorporating the effects of building down wash and cavity analysis, releases from flares and inversion break-up.
SHORTZ	The model is designed to calculate the short-term concentration at a large number of receptors by emissions from multiple stack, buidling and area sources.
STAR	The program produces STAR files from raw National Weather Service data for use with long-term dispersion models.
UAM	The urban air shed model to study ozone episodes using carbon bond IV chemistry.
VALLEY	A steady state univariate Gaussian model used to calculate daily or annual levels of pollutant concentrations emitted from up to 50 point and area sources.
VISCREEN	A plume visual impact prediction model.

Table 3 Documentation of Air Quality Models Available from NTIS and SCRAM

Accession Number	Title	Date
PB82-103 763	APRAC-3 User's Guide	1981
PB 81-164-634	BLP User's Guide	1980
PB80-220 841	CALINE-3 User's Guide*	1979
PB84-229 467	CALMPRO User's Guide	1984
PB86-136 546	CDM-2.0 User's Guide*	1986
PB83-107 342	CHAVG User's Guide	1982
PB90-500 414	Complex/PFM User's Guide	1989
PB-271 360	CRSTER User's Guide	1977
PB86-242 468	CRSTER User's Guide Addendum	1987
PB-80-227 556	HIWAY 2 User's Guide	1980
PB87-145 843	INPUFF Abstract	1986
PB86-242 468	INPUFF User's Guide	1986
PB88-171 475	ISC User's Guide, Vol. I*	1987
PB88-171 475	ISC User's Guide, Vol. II	1987
PB84-181 775	MESOPUFF-2.0 User's Guide	1984
PB86-171 402	MPDA-1.1 User's Guide	1986
PB83-114 207	MPTDS User's Guide	1983
PB80-197 361	MPTER User's Guide	1980
PB86-217 163	MPTER User's Guide Addendum	1986
PB85-137 164	PBM User's Guide	1984
PB84-164 128	PEM User's Guide	1984
PB87-132 098	PEM-2 User's Guide	1986
PB84-158 302	PLUVUE-2 User's Guide	1984
PB81-164 667	PTMAX, PTDIS and PTMTP User's Guide	1980
PB83-211 235	PTPLU User's Guide	1982
PB87-145 363	PTPLU-2 User's Guide Addendum	1986
PB88-113 261	RAM and RAMMET User's Guide*	1987
PB87-171 906	ROADWAY-2.0 User's Guide	1987
PB83-146 100	SHORTZ & LONGZ User's Guide	1982
PB83-146 092	SHORTZ & LONGZ User's Guide	1982
PB80-227 572	TEM User's Guide	1979
PB81-164 626	TGM User's Guide	1980
PB86-181 310	TUPOS-2.0 User's Guide	1986
PB86-241 031	TUPOS-2.0 User's Guide Addendum	1986
PB86-181 328	TUPOS Past Processor User's Guide	1986
PB-274 054	VALLEY User's Guide	1977
PB83-228 890	VALLEY User's Guide Ammendum	1982

* Condensed guides are available on SCRAM BBS

NOTE: The cost of guides vary from $10.00 to $30.00 and are subject to change.

and dispersion models currently being used and recommended by the federal and several state environmental protection agencies.

The SCRAM Bulletin Board has been designed in an extremely user friendly and readily accessible manner. Excellent computer networking facilities permit the transfer of models and other relevant information across the nation. We did not check on the availability of information internationally. The information being provided by the SCRAM BBS includes the source codes and executable images of models program (if available), the required data for testing, several utility programs, user's guide, meteorological data, latest developments, and an electronic mail service through which messages can be communicated between different users accessing the same bulletin board system.

The electronic mail makes it possible for the messages to be directed to individual user or being brought to general public attention. Four main menu options offered by the SCRAM Bulletin Board System are: system utilities, file transfer, agency communications and public communications.

Various utility functions include communication with the system operator, called SYSOP, ability to identify previous users of the BBS, and changing the users terminal configuration. The system can be signed on using telephone number 919-541-5742. First time users are required to wait for several days in order to get their registration reviewed by the staff. The users communication software should have the following set up: eight data bits, no parity, one stop bit and capability of communication at 1200 or 2400 band. Recently, two 9600 bps lines have been added and can be accessed through telephone number 919-941-1447.

A list of programs available through the BBS is given in Table 1. Brief description for each model is shown in Table 2. Program documentations are available from BBS and/or NTIS and the accession number is listed in Table 3. The source code for the program can also be purchased from NTIS. The NTIS number is given in Table 4. Some models are available in IBM compatible PC executable format as shown in Table 4.

Availability of air quality models through BBS has several advantages for the field of air pollution. First of all, scientists will be able to obtain PC models and updates at virtually no cost. Secondly it will encourage the use of air quality models during design stage of a project in order to incorporate the impact on air quality. Thirdly, environmental managers will be able to test their intuitive feelings by running the models. And finally the process of model development for complex problems will speed up as a result of information exchange among scientists.

Future improvements in the BBS may include the following:
(1) availability of all air quality models in an IBM compatible personal computer format.

Table 4 Source Codes and Executables Available from NTIS for Air Quality Models

Accession Number		Model	Cost	
Soure Codes(S)	Executable files (E)		(S)	(E)
PB90-500851		APRAC-3	$ 50	
PB90-500281		BLP	$ 50	
PB90-500273	PB90-500406	CDM2	$ 50;	$ 50
PB90-500414		COMPLEXI	$ 50	
PB90-500323		CRSTER	$ 50	
PB90-500810		HIWAY-ROADWAY	$ 50	
PB90-500752		INPUFF	$ 50	
PB90-500380		ISCLT	$125	
PB90-500398	PB90-500257	ISCST	$125;	$125
PB90-500265		LONGZ-SHORTZ	$125	
PB90-500794		MESOPUFF	$ 50	
PB90-500422	PB90-500430	MPRM 1.1	$ 70;	$ 70
PB90-500836		MPTDS	$ 50	
PB90-500307	PB90-500356	MPTER	$ 75;	$ 75
PB90-500802	PB90-500844	PAL	$ 50;	$ 50
PB90-500786		PBM	$ 50	
PB90-500760		PEM	$ 75	
PB90-500778		PLUVUE	$ 50	
PB90-500331		PTPLU	$ 50	
PB90-500315		RAM	$ 50	
PB90-500372		RTDM	$ 50	
PB90-500877		TUPOS	$ 75	
PB90-500349		VALLEY	$ 50	

* Includes the cost of documentation (where available).

(2) addition of graphics to the programs to display concentration and other air quality variables,
(3) providing a full screen editing facility data entry (through appropriate terminal data management system software).
(4) availability of all air quality models through BITNET/Internet for university education, and
(5) availability of user's guides for all the programs on the BBS.

Overall, the SCRAM Bulletin Board System is a useful tool at The University of Toledo for teaching and research activities. We are confident that you will like to try the system and will use it for your professional needs.

LITERATURE CITED

1. U.S. EPA, Guidline on Air Quality Models (Revised), EPA-450/2-78-027, Research Triangle Park, NC, July 1986. (Also available from NTIS as PB86-245248).
2. U.S. EPA, Flyer on Support Center for Regulatory Air Models Bulletin Board System, June 1989.

Waste Reduction Methodology and Case Histories at Dow Chemical's Pittsburg, California Plant Site

Bryant C. Fischback
The Dow Chemical Co., Pittsburg, CA. 94565

The corporate environmental policy of The Dow Chemical Company states:

> *The Dow Chemical Company is committed to continued excellence, leadership and stewardship in protecting the environment. Environmental protection is a primary management responsibility as well as the responsibility of every Dow employee.*
>
> *In keeping with this policy, our objective as a company is to reduce waste and achieve minimal adverse impact on the air, water, and land through excellence in environmental control.*

The centerpiece of implementing this policy is *to reduce waste.*

The company's corporate policy guidelines spell out the waste reduction priorities, namely,

Minimize/Eliminate Generation of Waste
Reuse/Recycle
Treat (preferably by incineration for burnable wastes)
Dispose to Land Only as a Last Alternative

In addition, the policy guidelines state among other things that Dow owned sites are preferred for hazardous waste treatment and disposal.

In 1986 DOW's waste reduction program was formalized and given the title of the Waste Reduction Always Pays or "WRAP" program. The goals of this program are to reduce waste to all media, provide incentives, provide recognition for excellence create a waste reduction mentality, save money including avoided costs, and lessen future liability.

In order to evaluate the opportunities for waste reduction, all materials entering the environment, i.e., to air, water and land, are inventoried. Sustances of concern are then listed by priority; sources of losses are identified, quantified, and "indexed" to production usually as pounds of waste per pound of product. Environmental impacts are evaluated and a determination is made as to which streams to address first.

This *evaluation phase* is followed by an *action phase* where cost effective actions are determined, goals are set, resource requirements are determined and performance is monitored and documented. Future plans are also made during this phase of the program.

It is important to note that priorities for waste reduction are addressed by using statistical methods such as Pareto charts. In this way efforts are focused on the plants which have the greatest potential for waste reduction. Similarly, statistical analysis is used to assess waste reduction opportunities within the individual plant in order to determine where to expend resources, i.e., personnel, equipment and funds.

Hazardous Waste History at Dow's Pittsburg Plant Site

YEAR	TREATMENT ONSITE ($kg \times 10^3$)	DISPOSAL OFFSITE ($kg \times 10^3$)	TOTAL GENERATED ($kg \times 10^3$)
1984	58,086	8,097	66,183
1985	55,117	4,454	59,571
1986	31,397	5,188	36,567
1987	15,690	5,256	20,946
1988	0	4,627	4,627
1989	0	3,268	3,268

Incentives for continuous improvement in the waste reduction are are also part of the WRAP program. For example, a yearly WRAP award is given for the outstanding successful waste reduction project in each of Dow's major manufacturing division in the United States. The yearly WRAP award projects for the Western Division for 1986, 1987, and 1988 are described below. The 1988 award recipients from each manufacturing division were flown with their spouses or guests to Washington, D. C. and arrangements were made to receive the award plaque from the member of Congress from their respective Congressional district.

The goal of the WRAP program is *zero waste generation*. While this goal is probably unachievable, it remains a goal and is a necessary element of the program. As is true with safety, waste reduction requires a mind set, a waste reduction mentality. So, like safety which has a goal of zero lost time injuries, the waste reduction program has a goal of zero waste released to any medium, air, water, or land.

A capital budget has been established for WRAP program projects. This budget is strictly for "non-regulatory driven" projects and is limited to $200,000 per project. Capital funds for projects instituted to comply with existing laws or regulations are funded as a matter of course. However, such "compliance" projects receive funds from sources other than the WRAP capital budget. Moreover, the Western Division has an additional WRAP budget for non-regulatory driven projects of less than $50,000 per project. Projects funded by these WRAP budgets over the past three years have, on average, returned 135 percent on investment before taxes. Indeed, waste reduction always pays.

Call for Papers

Annual American Institute of Chemical Engineers (AIChE) Environmental Division Student Award

AIChE—Environmental Division

1st Place - $300
2nd Place - $200
3rd Place - $100

Certificates and awards will be presented at the Summer National AIChE Meeting to be held in Pittsburgh, Pennsylvania, in August of 1991. The AIChE will also provide the 1st place winner with the lowest cost airfare and two (2) days accommodation for attendance at the awards presentation. In addition, the paper is intended for publication in *Environmental Progress*.

Contest Entry Rules:

1) The work must be a first paper (i.e., report on original unpublished work).
2) The paper must report on research or investigation related to an environmental program (i.e., lab experiment, theoretical development, a numerical analysis or modeling).
3) The author must be the sole author of the paper and must be a full-time undergraduate student in a school with an accredited chemical engineering program (faculty guidance is encouraged).
4) The author must be a member of the student chapter of AIChE.
5) The work must be performed during the author's undergraduate enrollment and the paper must be submitted prior to or within six months of graduation.

Submit manuscript with cover letter by May 14, 1991 to the Second Vice Chairman of the Environmental Division as shown below:

Peter B. Lederman, Ph.D., P.E.
Roy F. Weston, Inc.
One Weston Way
West Chester, PA 19380
Direct Dial: (215) 430-7422
Fax: (215) 430-3158

The following two articles [Seibert *et al.* and Govind *et al.*] were originally scheduled to appear in our special issue featuring *Innovative Hazardous Waste Treatment* which was published in December 1990. We were obliged to delay publication due to space constraints.

Toxic Trace Pollutants From Incineration

Paul C. Siebert, Denise R. Alston,
Roy F. Weston Inc., Weston Way, West Chester, PA 19380
and
Kay H. Jones
Zephyr Environmental Consulting, 2600 Fairview Ave., Seattle, WA 98102

Toxic Trace Pollutant emission factors have been developed using a database of over 500 references, including 50 emission test reports for municipal solid waste (MSW) incineration. Procedures have been developed and computerized to calculate emission factors from the best available data for dioxin/furan toxic equivalents, carcinogenic PAHs, and other trace organics and metals. Statistical analyses have been performed on standardized test results to assess the relationship of emissions and various incineration and air pollution control equipment design and operating parameters. Although the data is much more limited for hazardous waste and medical waste incineration, the available data have been summarized.

INTRODUCTION

Emissions from combustion of municipal solid waste (MSW), hazardous waste, and medical waste and their potential health impacts have become an increasing concern, especially as more incineration facilities are planned and built. In particular, emissions of trace organics, such as dioxins (polychlorinated dibenzo-p-dioxins-PCDDs) and furans (polychlorinated dibenzofurans-PCDFs), and trace metals have received much attention because of their relatively high toxicity, despite the low quantities emitted. The mechanisms involved in the formation and possible control of PCDD and PCDF emissions can only be hypothesized at present. The formation of metallic compounds in the incinerator flame is the result of various oxidation-reduction processes [*1*]. Depending on the vaporization and condensation temperatures of the compounds as well as the temperature, oxygen and carbon monoxide profiles in the incinerator, different amounts of the various metallic compounds can be formed, vaporized, condensed, and adsorbed onto particles. In addition, limited emissions test data are available because of the high cost of analysis for complex organic compounds or for trace metals.

Weston has attempted to collect the best data available for the estimation of emission factors for resource recovery MSW incineration facilities and other incinerators. A database of over 500 citations has been compiled on various aspects of modern incineration facilities. Only a small number of these citations are primary sources of emissions testing results, i.e., facility test reports, which are the preferred data source for emission factor development. The current database involves the evaluation of available data from over 50 resource recovery facilities, as well as a smaller number of hazardous and medical waste incineration facilities in the U.S., Canada, and Europe covering a wide range of fuel types, combustion systems, throughputs, and air pollution control technologies. The database also considers emissions of acid gases and criteria pollutants; however, this paper focuses on only the pollutants of primary concern as toxics emissions: PCDD/PCDF, other trace organics and trace metal emissions and notes some of the statistical evidence that such emissions from mass burn resource recovery facilities may be affected by various facility and control equipment characteristics.

The use of Weston's then available database for resource recovery facilities and methodology for emission factor development has been reported in detail for dioxins/furans in a previous paper by the same authors [*2*]. Because this database and methodology are utilized in this study, the key assumptions and procedures are reviewed in this paper. An updated and

expanded database for dioxins/furans as well as an additional analysis for trace metals and a number of additional statistical analyses performed on this expanded resource recovery database were reported in a subsequent paper [3].

The available emissions data are constantly expanding as a result of the number of new test reports. Considering the new data as they become available tends to reduce the emissions uncertainty by increasing the overall confidence in the emissions estimates. When possible, these data are handled statistically, so that meaningful estimates of average and upper-limit tendencies can be determined. Although the data for dioxins from MSW resource recovery incinerators are increasing steadily because of the worldwide attention paid to these pollutants and sources, emissions information for some of the metals and other organics and from other types of incinerators is much more limited. Therefore, the use of data from different facility types and of different assumptions was necessary for each category of pollutants so that reasonable estimates of emissions could be made. In fact, there are not sufficient data available to assess the effect of control equipment and operating parameters on emissions of polychlorinated biphenyls (PCBs), polycyclic aromatic hydrocarbons (PAHs), aldehydes (RCHO), chlorobenzenes (CB), chlorophenols (CP) or trace metals. This scarcity of data is especially evident for hazardous and medical waste incinerators.

As noted previously, in addition to control equipment, differences in temperature, oxygen, and carbon monoxide profiles may affect emissions. Incinerator design characteristics such as heat recovery, modular design, combustion system (single or two stage), combustion air (excess or starved) and fuel type (mass burn or refuse-derived fuel-RDF) may affect these profiles and resulting emissions. It should be noted that differences in waste composition may also affect emissions. This effect would be expected to be most pronounced for metal emissions, because metals originate only in the waste and are not formed, but only transformed, during combustion. The reported emission test results are converted to emission factors to allow the utilization and comparison of all available data. Emission factors are calculated as mass of emissions per process weight rate (e.g., pounds per ton of refuse) or mass or volume per standardized gas flow rate (e.g., pounds per dry normal cubic meter at 12% CO_2 or parts per million, dry volume at 12% CO_2). Emission factors are thus contrasted with emission rates that are given as mass per unit time. Emission factors account for differences in emissions with facility capacity and differences in stack gas conditions (i.e., moisture content, temperature, and excess air) so that they can be used to estimate like by emissions from a proposed or untested facility that is basically similar in design and operation. The preferred basis for emission factors is measured data from similar facilities.

As much as possible, only emission testing results from modern facilities, with typical operation during testing and acceptable testing procedures, were considered. The standardized results from individual test runs were averaged to calculate one emission value for each pollutant measured at a facility.

Emission factors used to estimate expected emissions from any similar facility were derived by assuming a log-normal distribution which is common for emissions data. Environmental pollutant data, in general, are often approximately log-normal and, therefore, the log-normal distribution is the most commonly used probability density model for environmental contaminant data [4]. More specifically with regard to air pollution, Crawford [5] states that the particle size distribution having relatively simple mathematical form which best fits a wide variety of dusts and mists is the log-normal distribution. Crawford notes that White [6] discusses the applicability of the log-normal distribution function to real particulate collections. White also cites Kolomogorov [7] in a theoretical study which leads to the conclusion that physical processes forming particulate distributions tend to produce a log-normal distribution. Crawford concludes that, although real distributions do deviate some from the log-normal pattern, the deviation is no greater than would be expected with any theoretical curve.

As discussed in the following section, a log-normal distribution has been demonstrated for dioxin/furan emissions from resource recovery facilities. Therefore, log-normality was also assumed for emissions of other pollutants, for which fewer data points are available. Thus, the statistical analysis of the data was performed on the logarithms of the data points.

The statistical analyses used to develop one emission factor for like facilities from the various facility results were varied depending on the number of data points that were selected for inclusion. The geometric mean was used as the best estimate of long-term emissions, regardless of the number of data points. (Using the geometric mean of emissions from a population as the best estimate of long-term emissions is equivalent to assuming that the distribution describing the emissions from the various facilities in the population also describes the emissions of any one facility in the same population as they vary over time. Although the validity of this assumption may be questioned, it appears to be the best feasible approach and should be explicitly stated.) The upper and lower bound emission factors, however, were estimated by the 95% confidence intervals of the mean for seven or more points, the geometric mean plus or minus the geometric standard deviation for five or six points, and the maximum and minimum value reported for four or fewer points. (Based on the same assumption regarding the emissions at one plant over time, the upper range value is considered the appropriate estimate of short-term emissions such as may be measured during an emission test.)

DIOXINS/FURANS

Municipal Solid Waste Incinerators

Four criteria were used to select the facilities included in the database for mass burn, excess air resource recovery facilities, the most commonly selected type of MSW incinerator. The criteria are:

- All facilities that do not recover heat were eliminated. A statistical analysis has confirmed that the two sets of facility emissions are distinct data sets [3]. A simple linear regression analysis of the logarithm of total PCDD/PCDF emissions versus a dummy variable indicating whether or not the facility recovers heat showed that the two sets of facilities, with or without heat recovery excluding abnormal data, are significantly different with a certainty of over 99%.
- Facilities that experienced abnormal conditions during the period of tests were eliminated.
- Facilities that burn refuse-derived fuel (RDF) instead of mass-burning municipal waste were eliminated.
- Facilities that are mass-burn, but have a furnace capacity of less than 50 tons per day, were eliminated. These modular facilities usually are two-stage starved air systems, in contrast with the larger single-stage excess air systems. (Although the Pittsfield facility is a modular facility, it was retained because it is a large capacity excess air facility.)

The PCDD and PCDF emissions that were reported in the test reports for these facilities are in a variety of units and gas conditions. To use the varied emissions data from all of these facilities and to develop emission factors for each pollutant, the data were recalculated on a uniform and consistent basis. Thus, all of the emissions data had to be converted to common units and standard conditions. For most purposes, the PCDD and PCDF emissions were converted to nanograms per normal cubic meter (ng/Nm^3) on a dry basis and corrected to 12% CO_2 (where normal conditions are 1 atmosphere and 0°C or 32°F). To convert all of the data to these units required cor-

Table 1 Dioxin/Furan Emissions from MSW Incinerators (ng/NM³ @ 12% CO_2, dry)[a]

Technology/Facility	U.S. EPA Toxic Equivalent	Eadon Toxic Equivalent	New York Toxic Equivalent	California Toxic Equivalent	Ontario Toxic Equivalent	2,3,7,8-T_4CDD	T_4CDD	PCDD	T_4CDF	PCDF
Facilities with Acid Gas Control (including wet & dry scrubbers, dry lime injection, etc.)										
Commerce, California	0.034	0.069	0.075	0.170	0.677	0.011	0.067	0.554	0.956	1.393
Stockholm, Sweden	0.067	0.112	0.125	0.238	1.289	0.004	0.251	2.727	0.963	3.621
Marion County, Oregon	0.058	0.123	0.126	0.307	0.312	0.022	0.231	1.449	0.483	0.594
Wurzburg, West Germany	0.374	0.810	0.909	2.107	10.707	0.018	1.910	22.100	9.600	27.860
Stapefeld, West Germany	1.716	3.689	4.092	9.683	44.289	0.140	8.630	60.300	52.340	109.526
Stellinger Moor, West Germany	4.706	9.661	10.706	24.740	118.000	0.740	21.600	126.157	144.530	282.472
Borsigstrasse, West Germany	7.524	16.457	18.003	43.279	143.593	0.340	42.020	234.532	111.420	380.183
Bristol, Connecticut	0.178	0.463	0.492	1.363	4.252	0.020	0.348	4.092	5.188	10.364
Stanislaus, California	0.071	0.162	0.183	0.460	2.765	0.010	0.448	1.019	3.401	5.902
Milbury, Massaschusetts	0.354	0.723	0.800	1.916	11.087	0.061	0.960	9.729	13.126	32.022
Bridgeport, Connecticut	0.330	0.341	0.343	0.379	0.418	0.317	0.363	1.013	0.044	2.058
Geometric Mean	0.326	0.647	0.703	1.549	5.423	0.047	1.110	7.382	4.870	13.971
Lower 95% Confidence Interval	0.096	0.187	0.202	0.427	1.259	0.015	0.278	1.796	0.923	3.258
Upper 95% Confidence Interval	1.106	2.240	2.451	5.617	23.351	0.147	4.435	30.342	25.700	59.914
Facilities Without Acid Gas Control										
Tulsa County, Oklahoma	0.701	1.735	1.802	4.750	6.496	0.101	1.613	18.924	7.308	15.520
Pinellas, Florida	0.896	1.613	1.800	4.097	19.754	0.163	3.540	48.780	21.400	54.810
Pittsfield, Massachusetts	1.369	2.480	2.622	6.272	17.446	0.585	2.249	36.342	13.122	73.277
Westchester, New York	1.622	3.846	4.025	9.926	26.703	0.279	2.852	24.023	30.070	76.242
Zurich, Switzerland	2.828	5.971	6.417	15.339	46.626	0.242	6.051	171.085	33.733	134.478
Chicago, Illinois	3.617	7.639	8.265	20.469	92.833	0.588	0.588	56.829	10.609	259.415
North Andover, Massachusetts	6.574	15.956	16.660	43.624	76.760	1.073	14.770	122.399	85.284	251.406
Saugus, Massachusetts	9.227	19.971	21.502	50.453	172.256	1.860	34.236	181.678	194.950	441.505
Alexandria/Arlington, Virginia	0.761	1.942	2.092	5.554	19.758	0.054	2.787	13.532	25.825	42.971
Geometric Mean	2.057	4.498	4.803	11.863	34.408	0.326	3.845	51.057	27.662	97.425
Lower 95% Confidence Interval	0.998	2.166	2.318	5.740	15.774	0.136	1.526	24.520	12.558	43.583
Upper 95% Confidence Interval	4.239	9.340	9.951	24.517	75.055	0.780	9.689	106.314	60.932	217.786
Ratio of Facilities with Acid Gas Controls to Facilities without No Acid Gas Controls										
Geometric Mean	0.159	0.144	0.146	0.131	0.158	0.143	0.289	0.145	0.176	0.143
Lower 95% Confidence Interval	0.097	0.086	0.087	0.074	0.080	0.108	0.182	0.073	0.073	0.075
Upper 95% Confidence Interval	0.261	0.240	0.246	0.229	0.311	0.189	0.458	0.285	0.422	0.275

[a] Emissions were taken from the actual test reports and converted into ng/NM³ @ 12% CO_2, dry.

recting for temperature, moisture, and excess air (% CO_2) in the flue gas, as well as converting to metric units, where applicable.

The average of the standardized emission factors for each individual test run at a facility was calculated for each congener* tested. The U.S. Environmental Protection Agency (EPA) toxic equivalents for each facility are presented. The U.S. EPA** and other toxic equivalency weighting schemes (such as the Eadon, California, Ontario, and New York schemes that are also calculated and presented) weight the emissions of the various PCDD and PCDF congeners by their assumed toxicity relative to the most toxic (and the most researched) congener, 2, 3, 7, 8-T4CDD. For those facilities where the emissions of a particular congener or homologue were not measured, the toxic equivalents were calculated by assuming the ratios of the individual 2, 3, 7, 8-isomer to the homologue, and of the various homologues to the T4CDD homologue developed from the resource recovery database as a whole.

As noted previously, a log-normal distribution of dioxin/furan emissions was tested, and, as discussed below, has been demonstrated. Air pollution emissions data generally tend to be log-normally distributed, i.e., the logarithms of emissions data are normally distributed. The log-normality of the three data sets (all of the facilities considered together, only the facilities with acid gas controls, and only the facilities without acid gas controls) has been demonstrated using the Shapiro-Wilk statistic and a univariate analysis [3].

The validity of treating the facilities with and without acid gas controls as two distinct data sets was also assessed statistically [3]. A simple linear regression of the logarithm of the U.S. EPA TEF and a dummy variable indicating whether the facility was with or without acid gas controls indicated with 88% confidence that the two sets (with and without acid gas controls) were significantly different. A t-test procedure also demonstrated with a probability of 82% that the two data sets are different.

The results of the statistical analysis for the U.S. EPA toxic equivalent measure, as well as other measures of dioxins/furans, are presented in Table 1 for the two cases with and without acid gas controls, respectively. The geometric means and the 95% confidence intervals or geometric standard deviations are based on log-normal distribution. The 95% confidence intervals of the means are the best statistical predictors of two measures: the range within which there is 95% confidence that the true mean of the sample facilities would fall; and the range within which 95% of the results of new tests on the same or similar facilities would be expected to fall. It should be noted that because of the small sample sizes, extreme values may significantly influence results and may lie outside the 95% confidence intervals. The apparent distance outside the confidence intervals may appear especially large when the confidence intervals and extreme values are reported as untransformed numbers rather than the log transforms. Nevertheless, the confidence intervals based on a log-normal distribution are the statistically correct measure because the data are not normally, but are log-normally distributed.

Table 2 Summary of U.S. EPA Dioxin/Furan Toxic Equivalent Emissions from Hazardous Waste Incinerators

Facility	U. S. EPA TEF Emissions (ng/dscm)
SCA	0.197
Biebesheim	0.284
Ross	<0.0116
American Cyanamid	<0.0116
DuPont	<0.0116
UpJohn	0.0842
Mitchell	0.0400
Plant B	1.348
Rollins (Deer Park, Texas)	0.241
ENSCO	0.0615
Rollins (Bridgeport, New Jersey)	<0.309
Geometric mean	0.0856
Upper 95% confidence interval	0.248
Lower 95% confidence interval	0.0295

A stepwise multiple linear regression analysis was conducted to determine the likelihood that control equipment and operating parameters are related to the dioxin/furan emissions as represented by the U.S. EPA toxic equivalent [3]. In general, the models with the logarithm of dioxin/furan emissions as the dependent variable were better fits than those using the raw emissions data without the logarithm transform. This is consistent with the demonstrated log-normal distribution of the emissions data. The variable that was the predominate predictor whenever included is outlet temperature. Dioxin/furan emissions directly correspond to outlet temperatures; i.e., decreased emissions occur simultaneously with decreased temperature. The start-up year was also generally significant, with newer facilities tending to have lower emissions. In many cases, the control equipment or its performance is a significant variable, with filters (fabric and granular bed) and acid gas controls, particularly spray dryers and dry injection systems, having lower emissions. The control equipment variables were most often significant when temperature was not considered in the model. Because outlet temperature and type of particulate and acid gas controls, and, to a lesser degree, start-up year, appear to be interdependent, it could not be ascertained whether the type of control equipment, the reduced temperature, the newer system, or the combination of the three was the crucial factor related to reduced dioxin/furan emissions.

Hazardous Waste Incinerators

Much less definitive data are available for hazardous waste incinerators. Measured data for each congener were generally not available. Therefore, to calculate toxic equivalent emissions, the limited measured test data were supplemented with estimates based on the ratios of total homologue to total T4CDD and 2, 3, 7, 8 congener to total homologue for MSW resource recovery facilities. (The ratios based on MSW resource recovery facilities were used because insufficient data are available to develop such ratios for other incinerators.) The resulting

* *Homologue* - chemical compounds belonging to a chemical series whose successive members have a regular difference in composition; e.g., for the PCDD and PCDF series the homologues differ by a chlorine atom, i.e., tetrachlorinated (T4CDD), a pentachlorinated (P5CDD), hexachlorinated (H6CDD), and heptachlorinated (H7CDD) dibenzo p-dioxin are homologues (tetra, penta, hexa, and hepta denote 4, 5, 6, and 7, respectively).

Isomer - chemical compounds that contain the same number of atoms of the same elements, but differ in structural arrangement and properties; e.g., 2, 3, 7, 8-T4CDD and 1, 4, 7, 8-T4CDD are isomers of T4CDD with the four chlorine atoms at the 2, 3, 7, 8, and 1, 4, 7, 8 positions on the benzene rings in the T4CDD molecule, respectively.

Congener - a member of the same general class of compounds, e.g., 2, 3, 7, 8-T4CDD and 1, 2, 3, 4, 7, 8-H6CDD are congeners of dioxin.

** Since this article was drafted, the U. S. EPA has adopted a new toxic equivalency weighting system for dioxins/furans. The U.S. EPA has adopted the international toxicity equivalency factors developed under the auspices of the North Atlantic Treaty Organization's Committee on Challenges of Modern Society with participation by U. S. EPA. [7] The overall effect of the revision is that the current (1989) U.S. EPA TEF is generally about twice the value of the previous (1987) U.S. EPA TEF.

Table 3 Dioxin/Furan Emissions from Medical Waste Incinerators

Facility	U. S. EPA TEF Emissions (ng/dscm @ 12% CO_2)
Cedars-Sinai[a]	7.14
Stanford Univ.[b]	0.261
Geometric Mean	1.36

[a]Two stage starved air combustor, fabric filter.
[b]Two stage starved air combustor, sodium hydroxide venturi scrubber, stack gas reheater.

emission factors are presented in Table 2 in units of nanograms per dry standard cubic meter (ng/dscm), where a standard temperature of 68°F was used to convert data not already reported in standard conditions (which may represent 60, 68 or 70°F, but was not specified in all data sources reporting in ng/dscm).

Medical Waste Incinerator

A few congener-specific analyses of medical waste incinerators have been conducted in California. Data from two starved air, two stage combustors were used to develop the U.S. EPA toxic equivalent emission factors presented in Table 3.

TRACE METALS

The development of controlled emission factors (i.e., following air pollution controls) for trace metals is outlined in this section. These emission factors are presented in pounds of metal emitted per ton of waste combusted. Because metals are present in solid waste, some metals will be emitted in the flue gases of the facility. The amount emitted is a function of the quantity of metal in the waste stream, the properties of the metal, the combustion characteristics of the facility, and the characteristics and the performance of the air pollution control equipment.

A significant portion of most metals vaporizes during combustion. As the exhaust gases cool (during heat recovery, in ducting, and in air pollution control devices), many of the metals will condense. The temperatures of heating and cooling in conjuction with the availability of reaction components will determine what metallic compounds will be formed and condensed and at what temperatures. Usually, the condensed metals will adsorb onto the surface of particles in the gas stream. Because adsorption rates are dependent on surface area (rather than volume or mass) and small particles have more surface area per volume, there is a theoretical tendency for more of the metals to be adsorbed onto smaller, less easily controlled particles. In practice, however, only some metals clearly exhibit this tendency toward "fine particle enrichment." It should be noted that mercury is an exception because, in practice, mercury and its compounds exist almost completely as a vapor at common stack exit temperatures.

Municipal Solid Waste Incineration

The same four criteria were used to choose the selected facilities included in the final database for metals emissions from mass burn excess air resource recovery facilities that were used for PCDD and PCDF emissions. The available data for individual test runs from the selected facilities were converted to a common basis of pounds of metal per ton of refuse. Facility emission factors were then calculated by taking the average of the emission factors for the individual emission test runs.

The best estimates of controlled metal emissions for similar mass-burn facilities were developed by assuming a log-normal distribution that is usually representative of emissions data and has been demonstrated for dioxins/furans. Accordingly, a best estimate was calculated by taking the geometric mean of the values for the selected facilities.

Hexavalent chromium (VI) was estimated based upon the controlled chromium emission factors for similar mass-burn facilities and assuming hexavalent chromium to be approximately 3.4% of the total chromium value. This assumption is based on emission tests by the U.S. EPA at the Marion County facility [9]. Many of the hexavalent chromium values were below detection limits. The assumed value of 3.4% is conservatively high in that is is based on the test run with the highest hexavalent to total chromium ratio of any of the tests with both types of chromium measured and detectable.

In 1988, the data seemed to indicate that significant differences between emissions from facilities with and without acid gas controls were evident for arsenic, beryllium, and lead [3]. However, the additional data that have become available do not support a distinction between emissions from facilities with and without acid gas controls. Therefore, the emission factors for metals that are presented in Table 4 were calculated based on test data for nonmodular, heat recovery facilities with both acid gas controls as well as high-efficiency particulate controls and with high-efficiency particulate controls only. As noted previously, the range of expected values was assumed to be the 95% confidence intervals (log normal) for seven or more data points, the geometric mean plus or minus the geometric standard deviation for five or six data points, and the range of values for four or fewer data points.

It should be noted that a number of the facilities used to develop metal emission factors are located in other countries where the waste composition may be significantly different from that found in the U.S. This difference as reflected in emissions would be expected to be most pronounced for metals because metals emissions originate only in the waste and are not formed, but only transformed, during combustion. Nevertheless, since metals emissions data are limited, the foreign data were considered. However, it is possible that U.S. waste could have higher metals content.

An additional regression analysis was performed to determine if a relationship existed between particulate and trace metal emissions for the various metals [3]. For this analysis, only facilities with heat recovery were considered (with the possible exception of the Japanese facility); however, both modular and nonmodular facilities as well as controlled and uncontrolled emissions were considered. In addition, much of the data is not from primary test reports, so that various assumptions had to be made in order to estimate emission factors. Therefore, this analysis does not have the level of accuracy of the other analyses presented, but can be used to asses general trends. Consideration of the regression coefficient shows that metal emissions tend to decrease as particulate emissions decrease for arsenic, cadmium, chromium, lead, and selenium because the regression coefficients are greater than 50%. The trends are unclear for beryllium (for which fewer data points are available) and nickel. The near-zero regression coefficient for mercury lends credibility to the analysis since it shows that mercury emissions are essentially independent of particulate emissions, as would be expected for vaporous emissions.

Hazardous Waste Incinerators

Metal emissions are highly dependent on the waste stream. The waste streams of hazardous waste incinerators are generally site-specific, particularly those that burn only a specific

Table 4 Metal Emissions from MSW Incinerator Resource Recovery Facilities (all with electrostatic precipitators or fabric filters) (lb/ton of waste)[a]

Facility	Antimony	Arsenic	Barium	Beryllium	Cadmium	Chromium	Cobalt	Copper	Lead	Magnesium
Facilities With Acid Gas Control										
Wurzburg, West Germany	3.97E-06	3.96E-08	—	—	3.96E-05	3.54E-06	—	—	7.84E-05	—
Munich, West Germany	2.01E-05	3.56E-06	4.94E-05	3.86E-09	6.58E-05	8.04E-03	1.28E-04	4.57E-05	6.85E-04	—
Marion County, Oregon	—	—	—	2.36E-08	—	—	—	—	2.62E-04	—
Stockholm, Sweden	—	—	—	1.96E-07	9.81E-07	—	—	—	1.09E-04	—
Commerce, California	2.42E-06	1.45E-06	9.19E-04	1.45E-06	1.55E-05	1.84E-05	2.91E-06	4.21E-04	1.55E-05	2.11E-03
Bristol, Connecticut	—	2.99E-05	—	6.72E-08	—	1.49E-05	—	—	2.24E-04	—
Stanislaus, California	2.73E-05	1.25E-05	—	4.85E-09	1.97E-05	1.11E-04	—	1.14E-04	3.04E-04	—
Milbury, Massachusetts	3.57E-05	3.63E-05	—	3.82E-06	1.74E-04	6.77E-04	—	3.70E-04	2.70E-03	—
Bridgeport, Connecticut	—	1.23E-05	—	1.10E-05	—	2.42E-04	—	—	2.26E-05	—
Geometric Mean	1.13E-05	4.44E-06	2.13E-04	1.56E-07	2.27E-05	1.05E-04	1.93E-05	1.69E-04	1.67E-04	2.11E-03
Upper 95% Confidence Interval[b]	NA	3.98E-05	NA	1.93E-06	NA	1.19E-03	NA	NA	5.75E-04	NA
Plus Standard Deviation[c]	3.82E-05	4.76E-05	NA	3.16E-06	1.33E-04	1.45E-03	NA	NA	8.35E-04	NA
Maximum	3.57E-05	3.63E-05	9.19E-04	1.10E-05	1.74E-04	8.04E-03	1.28E-04	4.21E-04	2.70E-03	NA
Lower 95% Confidence Interval[b]	NA	4.96E-07	NA	1.26E-08	NA	9.28E-06	NA	NA	4.82E-05	NA
Minus Standard Deviation[c]	3.37E-06	4.15E-07	NA	7.71E-09	3.87E-06	7.62E-06	NA	NA	3.32E-05	NA
Minimum	2.42E-06	3.96E-08	4.94E-05	3.86E-09	9.81E-07	3.54E-06	2.91E-06	4.57E-05	1.55E-05	NA
Facilities Without Acid Gas Control										
Pinellas County, Florida	—	2.95E-05	—	1.42E-07	6.67E-05	3.82E-05	—	2.15E-04	1.34E-04	—
Hillsborough, Florida	—	—	—	1.00E-06	—	—	—	—	2.60E-03	—
Baltimore, Maryland	—	5.26E-05	—	—	—	2.67E-04	—	—	—	—
Tulsa County, Oklahoma	—	—	—	2.56E-08	—	—	—	—	4.16E-03	—
North Andover, Massachusetts	—	—	—	6.46E-06	—	—	—	—	6.12E-04	—
Prince Edward Island, Canada[d]	—	—	8.50E-04	—	—	—	—	—	—	3.67E-03
Geometric Mean	NA	3.94E-05	8.50E-04	3.91E-07	6.67E-05	1.01E-04	NA	2.15E-04	9.70E.04	3.67E-03
Upper 95% Confidence Interval[b]	NA	NA	NA	NA	NA	NA	NA	NA	NA	NA
Plus Standard Deviation[c]	NA	NA	NA	NA	NA	NA	NA	NA	NA	NA
Maximum	NA	5.26E-05	NA	6.46E-06	NA	2.67E-04	NA	NA	4.16E-03	NA
Lower 95% Confidence Interval[b]	NA	NA	NA	NA	NA	NA	NA	NA	NA	NA
Minus Standard Deviation[c]	NA	NA	NA	NA	NA	NA	NA	NA	NA	NA
Minimum	NA	2.95E-05	NA	2.56E-08	NA	3.82E-05	NA	NA	1.34E-04	NA
All Facilities										
Geometric Mean	1.13E-05	7.22E-06	3.38E-04	2.12E-07	2.65E-05	1.04E-04	1.93E-05	1.77E-04	2.86E-04	2.78E-03
Upper 95% Confidence Interval[b]	NA	4.14E-05	NA	1.21E-06	1.23E-04	6.22E-04	NA	NA	8.23E-04	NA
Plus Standard Deviation[c]	3.82E-05	7.00E-05	NA	3.30E-06	1.40E-04	1.06E-03	NA	4.43E-04	1.64E-03	NA
Maximum	3.57E-05	5.26E-05	9.19E-04	1.10E-05	1.74E-04	8.04E-03	1.28E-04	4.21E-04	4.16E-03	3.67E-03
Lower 95% Confidence Interval[b]	NA	1.26E-06	NA	3.71E-08	5.67E-06	1.75E-05	NA	NA	9.97E.05	NA
Minus Standard Deviation[c]	3.37E-06	7.44E-07	NA	1.36E-08	5.01E-06	1.02E-05	NA	7.09E-05	4.99E-05	NA
Minimum	2.42E-06	3.96E-08	4.94E-05	3.86E-09	9.81E-07	3.54E-06	2.91E-06	4.57E-05	1.55E-05	2.11E-03
Ratio of Facilities with Acid Gas Controls to Facilities without Acid Gas Controls										
Geometric Mean	NA	0.11	0.25	0.40	0.34	1.04	NA	0.79	0.17	0.57
Upper Range	NA	0.76	NA	0.30	NA	4.46	NA	NA	0.14	NA
Lower Range	NA	0.02	NA	0.49	NA	0.24	NA	NA	0.36	NA
Upper Range with acid gas controls to Lower Range without acid gas controls	NA	1.35	NA	75.46	NA	31.18	NA	NA	4.29	NA

[a] 1 Pound of pollutant per ton of waste feed is equal to 0.5 kilograms per Megagram.
[b] The 95% confidence interval was calculated for those metals which have more than 6 data points.
[c] The standard deviation was calculated for those metals which have more than 4 data points.
[d] Prince Edward Island is a modular facility, but results were used for barium, magnesium, and silver because of limited data available.

Table 4 (continued)

Facility	Manganese	Mercury	Molybdenum	Nickel	Selenium	Silver	Thallium	Tin	Vanadium	Zinc
Facilities With Acid Gas Control										
Wurzburg, West Germany	1.01E-05	—	—	1.60E-06	—	—	—	—	—	—
Munich, West Germany	8.95E-04	—	—	3.73E-03	—	—	1.26E-08	2.70E-04	2.01E-05	3.06E-03
Marion County, Oregon	—	2.20E-03	—	—	—	—	—	—	—	—
Stockholm, Sweden	—	—	—	—	—	—	—	—	—	2.40E-04
Commerce, California	7.75E-06	3.24E-04	9.68E-05	4.84E-05	2.13E-05	—	—	1.45E-05	4.84E-07	3.00E-04
Bristol, Connecticut	—	8.96E-04	—	4.48E-05	—	—	—	—	—	—
Stanislaus, California	9.74E-05	4.95E-03	—	2.06E-04	3.34E-06	—	—	2.25E-04	2.74E-05	1.17E-03
Milbury, Massachusetts	1.82E-04	1.17E-02	1.32E-04	1.76E-04	7.71E-06	—	—	1.99E-04	4.07E-05	7.51E-03
Bridgeport, Connecticut	—	3.01E-03	—	2.69E-04	—	—	—	—	—	—
Geometric Mean	6.59E-05	2.19E-05	1.13E-04	1.03E-04	8.19E-06	NA	1.26E-08	1.15E-04	1.02E-05	1.14E-03
Upper 95% Confidence Interval[b]	NA	NA	NA	9.10E-04	NA	NA	NA	NA	NA	NA
Plus Standard Deviation[c]	4.90E-04	7.79E-03	NA	1.09E-03	NA	NA	NA	NA	NA	5.00E-03
Maximum	8.95E-04	1.17E-02	1.32E-04	3.73E-03	2.13E-05	NA	NA	2.70E-04	4.07E-05	7.51E-03
Lower 95% Confidence Interval[b]	NA	NA	NA	1.18E-05	NA	NA	NA	NA	NA	NA
Minus Standard Deviation[c]	8.87E-06	6.18E-04	NA	9.85E-06	NA	NA	NA	NA	NA	2.60E-04
Minimum	7.75E-06	3.24E-04	9.68E-05	1.60E-06	3.34E-06	NA	NA	1.45E-05	4.84E-07	2.40E-04
Facilities Without Acid Gas Control										
Pinellas County, Florida	—	7.44E-03	2.92E-05	2.42E-05	—	—	—	—	—	—
Hillsborough, Florida	—	—	—	—	—	—	—	—	—	—
Baltimore, Maryland	—	—	—	—	—	—	—	—	—	—
Tulsa County, Oklahoma	—	3.84E-03	—	—	—	—	—	—	—	—
North Andover, Massachusetts	—	—	—	—	—	—	—	—	—	—
Prince Edward Island, Canada[d]	—	—	—	—	—	2.38E-04	—	—	—	—
Geometric Mean	NA	5.35E-03	2.92E-05	2.42E-05	NA	2.38E-04	NA	NA	NA	NA
Upper 95% Confidence Interval[b]	NA	NA	NA	NA	NA	NA	NA	NA	NA	NA
Plus Standard Deviation[c]	NA	NA	NA	NA	NA	NA	NA	NA	NA	NA
Maximum	NA	7.44E-03	NA	NA	NA	NA	NA	NA	NA	NA
Lower 95% Confidence Interval[b]	NA	NA	NA	NA	NA	NA	NA	NA	NA	NA
Minus Standard Deviation[c]	NA	NA	NA	NA	NA	NA	NA	NA	NA	NA
Minimum	NA	3.84E-03	NA	NA	NA	NA	NA	NA	NA	NA
All Facilities										
Geometric Mean	6.59E-05	2.74E-03	7.20E-05	8.62E-05	8.19E-06	2.38E-04	1.26E-08	1.15E-04	1.02E-05	1.14E-03
Upper 95% Confidence Interval[b]	NA	7.23E-03	NA	5.59E-04	NA	NA	NA	NA	NA	NA
Plus Standard Deviation[c]	4.90E-04	8.75E-03	NA	8.07E-04	NA	NA	NA	NA	NA	5.00E-03
Maximum	8.95E-04	1.17E-02	1.32E-04	3.73E-03	2.13E-05	NA	NA	2.70E-04	4.07E-05	7.51E-03
Lower 95% Confidence Interval[b]	NA	1.04E-03	NA	1.33E-05	NA	NA	NA	NA	NA	NA
Minus Standard Deviation[c]	8.87E-06	8.59E-04	NA	9.21E-06	NA	NA	NA	NA	NA	2.60E-04
Minimum	7.75E-06	3.24E-04	2.92E-05	1.60E-06	3.34E-06	NA	NA	1.45E-05	4.84E-07	2.40E-04
Ratio of Facilities with Acid Gas Controls to Facilities without Acid Gas Controls										
Geometric Mean	NA	0.41	3.87	4.27	NA	NA	NA	NA	NA	NA
Upper Range	NA	1.05	NA	NA	NA	NA	NA	NA	NA	NA
Lower Range	NA	0.16	NA	NA	NA	NA	NA	NA	NA	NA
Upper Range with acid gas controls to Lower Range without acid gas controls	NA	2.03	NA	NA	NA	NA	NA	NA	NA	NA

[a] 1 Pound of pollutant per ton of waste feed is equal to 0.5 kilograms per Megagram.
[b] The 95% confidence interval was calculated for those metals which have more than 6 data points.
[c] The standard deviation was calculated for those metals which have more than 4 data points.
[d] Prince Edward Island is a modular facility, but results were used for barium, magnesium, and silver because of limited data available.

Table 5 HWI Metals Emission Factors Based on Emission Test Results (lb/ton of waste)[a]

Metal	3 Runs 7-88	3 Runs 6-88	Plant X[b] 1 Run 3-88	3 Runs 8-87	3 Runs 8-84	Ross[c] 3 Runs 6-82	Dupont[d] 3 Runs 82	Geometric Mean	Maximum
Antimony	≤ 9.28E-05	≤ 1.55E-04	NA	NA	NA	1.43E-02	≤ 1.06E-03	6.83E-04	1.43E-02
Arsenic	≤ 2.32E-05	1.00E-04	≤ 7.84E-05	9.63E-06	8.08E-04	≤ 4.60E-04	≤ 4.34E-03	1.61E-04	≤ 4.34E-03
Barium	≤ 4.64E-04	4.51E-04	NA	NA	NA	1.36E-03	3.00E-03	9.61E-04	3.00E-03
Beryllium	≤ 1.11E-05	≤ 1.06E-05	1.02E-05	NA	7.94E-06	NA	1.06E-04	1.59E-05	1.06E-04
Cadmium	8.32E-03[d,e]	5.28E-02[d,e]	1.42E-02[e]	1.33E-05[e]	2.12E-04	1.45E-03	6.42E-04	1.49E-03	5.28E-02
Chromium (Total)	5.60E-04[e]	1.77E-03[e]	7.91E-04[e]	3.28E-04[e]	1.46E-03	3.78E-03	5.80E-04	9.73E-04	3.78E-03
Lead	4.66E-03[e]	7.60E-02[e]	1.58E-02[e]	5.95E-04[e]	1.89E-02	1.41E-01	1.29E-02	1.42E-02	1.41E-01
Magnesium	NA	NA	NA	NA	NA	NA	NA	NA	NA
Manganese	NA	NA	NA	NA	NA	NA	NA	NA	NA
Mercury	1.32E-05	2.18E-04	2.25E-05	NA	1.95E-02	8.59E-05	≤ 8.85E-04	2.14E-04	1.95E-02
Nickel	5.64E-04	7.03E-03[e]	5.79E-04[e]	5.50E-04	5.30E-04	6.41E-04	2.79E-03	1.03E-03	7.03E-03
Selenium	2.77E-05	≤ 4.41E-05	NA	NA	NA	9.27E-04	1.53E-02	3.63E-04	1.53E-02
Silver	3.25E-05	≤ 2.21E-05	NA	NA	NA	1.76E-05	3.93E-04	4.72E-05	3.93E-04
Thallium	≤ 2.32E-04	≤ 2.21E-05	NA	NA	NA	2.30E-04	7.87E-04	1.75E-04	7.87E-04
Tin	NA	NA	NA	NA	NA	NA	NA	NA	NA
Zinc	2.77E-02	2.63E-02	NA	NA	1.02E-02	NA	NA	1.95E-02	2.77E-02

[a] 1 Pound of pollutant per ton of waste feed is equal to 0.5 kilograms per Megagram.
[b] Controlled with wet scrubber system.
[c] Controlled with wet scrubber quench, packed scrubbers with caustic, and two-stage ionizing wet scrubber.
[d] Controlled with 3-stage scrubber system (quench, cyclone, absorber).
[e] Suspected contamination.
[f] Metal added to feed.

Table 6 Trace Metal Emissions from Medical Waste Incinerators (lb/ton of waste)[a]

Metal	Cedars Sinai		Stanford University		St. Agnes	Royal Jubilee	Uncontrolled	
	Fabric Filter	Uncontrolled	Caustic Venturi	Uncontrolled	Uncontrolled	Uncontrolled	Geometric Mean	Maximum
Arsenic	3.94E-08	2.08E-04	ND[b]	ND	1.19E-04	NA[c]	1.57E-04	2.08E-04
Cadmium	5.16E-06	4.43E-03	1.50E-03	2.02E-03	3.19E-03	2.44E-03	2.89E-03	4.43E-03
Chromium (total)	2.14E-06	1.98E-04	2.77E-04	3.34E-04	4.69E-04	1.49E-03	4.64E-04	1.49E-03
Chromium (hexavalent)	NA	NA	2.52E-04	1.67E-04	NA	NA	1.67E-04	1.67E-04
Iron	2.39E-05	5.53E-03	1.91E-02	3.73E-03	7.51E-03	1.82E-02	7.29E-03	1.82E-02
Lead	9.92E-05	4.35E-02	5.05E-02	4.65E-02	4.33E-02	4.17E-02	4.37E-02	4.65E-02
Manganese	5.16E-06	4.00E-04	2.93E-04	2.40E-04	2.88E-04	9.60E-04	4.04E-04	9.60E-04
Nickel	2.67E-05	1.10E-04	2.49E-04	1.55E-04	2.38E-04	4.30E-04	2.04E-04	4.30E-04

[a] 1 pound of pollutant per ton of waste feed is equal to 0.5 kilograms per megagram.
[b] Not detectable.
[c] Not analyzed.

Table 7 Polycyclic Aromatic Hydrocarbons Emission Factors on Test Data from Selected Facilities ($\mu g/NM^3$ @ 12% CO_2, dry)[a]

Facility Possible Carcinogens	Results for Individual Test Runs 1	 2	 3	Test Average
Alexandria, Minnesota[b]				
Benz(a)anthracene	0.720	—	—	0.720
Benzo(b)fluoranthene	0.513	—	—	0.513
Benzo(k)fluoranthene	0.568	—	—	0.568
Benzo(a)pyrene	0.643	—	—	0.643
Dibenz(a,h)anthracene	0.536	—	—	0.536
Indeno(1,2,3-cd)pyrene	0.739	—	—	0.739
Total Carcinogens				3.718
Total PAHs				12.032
Cattaraugus, New York[b]				
Benzo(a)pyrene	0.928	0.928	0.879	0.912
Total Carcinogens				0.912
Total PAHs				0.912
Commerce, California				
Benz(a)anthracene	0.0025	0.0015	—	0.0020
Benzo(b)fluoranthene	0.0026	0.0032	—	0.0029
Benzo(k)fluoranthene	0.0026	0.0032	—	0.0029
Benzo(a)pyrene	0.0043	≤ 0.0016	—	0.0030
Dibenz(a,h)anthracene	≤ 0.0017	≤ 0.0032	—	0.0025
Indeno(1,2,3-cd)pyrene	0.0019	≤ 0.0028	—	0.0024
Total Carcinogens				0.0156
Total PAHs				0.465
Hogdalen, Sweden[c]				
Total Carcinogens	0.040	—	—	0.040
Total PAHs	0.040	—	—	0.040
Nuremberg, Germany				
Benz(a)anthracene	≤ 0.0015	—	—	0.0015
Benzo(b)fluoranthene	≤ 0.0015	—	—	0.0015
Benzo(a)pyrene	≤ 0.0015	—	—	0.0015
Dibenz(a,h)anthracene	≤ 0.0031	—	—	0.0031
Total Carcinogens				0.0076
Total PAHs				0.0244
Oneida, New York[b]				
Benzo(a)pyrene	11.921	11.597	9.991	11.17
Total Carcinogens				11.17
Total PAHs				11.17
Pittsfield, Massachusetts[c]				
Total Carcinogens	0.204	0.095	—	0.149
Total PAHs	0.204	0.095	—	0.149

(Continued on opposite page)

facility's or company's waste. Therefore, when developing metal emission factors for a specific hazardous waste facility, the best approach is probably to estimate the metals content of the waste stream and assume the volatilization and air pollution control equipment removals given by the U.S. EPA in its Guidance on Metals and Hydrogen Chloride Controls for Hazardous Waste Incinerators. However, actual measured data such as in Table 5 may be significantly lower.

Medical Waste Incinerators

Medical waste incinerator metal emissions also would be expected to vary substantially with differences in the waste stream composition. A comparison of the uncontrolled emission factors for four facilities in Table 6 shows only a variation of a factor of two for most metals and a factor of four for the others. Thus, the waste streams of medical waste incinerators may be more consistent than might be expected. The metals removals achieved by the fabric filter at Cedar-Sinai generally exceed 99% (except for nickel at 75%).

OTHER TRACE ORGANICS

The formation of trace organics other than dioxins/furans is dependent on the waste stream composition in conjunction with the thermal stability of the subject compound or the compounds that could form it as a product of incomplete combustion (PIC). Very little measured data are available except for municipal solid waste incineration.

Municipal Solid Waste Incinerators

Only limited data are available for other trace organics. Emission test results for a number of relatively toxic organics,

Table 7 Polycyclic Aromatic Hydrocarbons Emission Factors on Test Data from Selected Facilities ($\mu g/NM^3$ @ 12% CO_2, dry)[a]

Facility Possible Carcinogens	Results for Individual Test Runs 1	 2	 3	Test Average
Prince Edward Island, Canada[b]				
Benz(a)anthracene	0.248	0.269	0.065	0.194
Benzo(j,k)fluoranthene & Benzo(a)pyrene	0.139	0.492	0.133	0.255
Dibenz(a,h)anthracene	0.022	ND[d]	0.007	0.014
Indeno(1,2,3-cd)pyrene	0.059	ND[d]	0.009	0.034
Total Carcinogens				0.497
Total PAHs				7.731
Bristol, Connecticut				
Benz(a)anthracene	≤ 0.007	≤ 0.006	≤ 0.003	0.005
Benzo(b)fluoranthene & Benzo(k)fluoranthene	≤ 0.01	≤ 0.01	≤ 0.007	0.009
Benzo(a)pyrene	≤ 0.007	≤ 0.007	≤ 0.003	0.006
Dibenz(a,h)anthracene	≤ 0.026	≤ 0.026	≤ 0.003	0.018
Indeno(1,2,3-cd)pyrene	≤ 0.015	≤ 0.014	≤ 0.007	0.012
Total Carcinogens				0.050
Total PAHs				0.579
Stanislaus, California				
Benz(a)anthracene	0.6676	0.4875	—	0.578
Benzo(b)fluoranthene & Benzo(k)fluoranthene	0.9125	0.6507	—	0.782
Benzo(a)pyrene	0.0993	0.0632	—	0.081
Dibenz(a,h)anthracene	0.0109	0.0104	—	0.011
Indeno(1,2,3-cd)pyrene	0.0795	0.0631	—	0.071
Total Carcinogens				1.522
Total PAHs				3.260
Total Carcinogens				
Geometric Mean				0.252
Upper 95% Confidence Interval				1.434
Lower 95% Confidence Interval				0.044
Total PAHS				
Geometric Mean				1.234
Upper 95% Confidence Interval				6.201
Lower 95% Confidence Interval				0.246

[a] Based on test results from massburn (excess air and modular) facilities
[b] Based on test results from modular unit (less than 50 tons/day/unit)
[c] An analytical analysis was not performed or given in the test report. Therefore, the most conservative assumption for risk assessment purposes was made, i.e., that all measured PAH is carcinogenic and, thus, using the EPA procedure, assumed to have the toxicity of benzo(a)pyrene.
[d] Value was at or below the detection limit, but the detection limits were not supplied; therefore, it was not included in the calculations of the average.

Table 8 Polychlorinated Biphenyls Emission Factors Based on Test Data from Selected Facilities ($\mu g/NM^3$ @ 12% CO_2, dry)[a]

Facility	Results for Individual Test Runs 1	 2	 3	 4	 5	 6	Test Average
Cattaraugus, New York[b]	0.603	2.017	1.347	—	—	—	1.322
Chicago (Northwest), Illinois	0.033	0.017	0.124	0.023	0.015	0.107	0.053
Commerce, California	≤ 0.113	≤ 0.657	—	-	-	—	0.385
Oneida, New York[b]	0.210	1.271	1.174	—	—	—	0.885
Pittsfield, Massachusetts	ND[c]	ND	—	—	-	—	NA
Prince Edward Island, Canada[b]	ND	ND	2.620	—	—	—	2.620
Stanislaus, California	≤0.1998	≤0.1849	≤0.2116	≤0.1697	≤0.1892	≤0.1793	0.189
All Facilities							
Geometric Mean							0.478
Plus 1 Standard Deviation (Geometric)							1.970
Minus 1 Standard Deviation (Geometric)							0.116

[a] Based on test results from massburn (excess air and modular) facilities
[b] Based on test results from modular unit (less than 50 tons/day/unit)
[c] Value was at or below the detection limit, but the detection limits were not supplied; therefore, it was not included in the calculations of the average.

carcinogenic polycyclic aromatic hydrocarbons (PAH), polychlorinated biphenyls (PCB), aldehydes, and chlorobenzenes and chlorophenols, are presented in Tables 7, 8, 9, and 10, respectively.

Table 9 Aldehydes Emission Factors Based on Test Data from Selected Facilities ($\mu g/Nm^3$ @ 12% CO_2, dry)[a]

Facility	Results for Individual Test Runs 1	2	3	Test Average
Cattaraugus, New York[b]	641.9	563.4	646.1	617.1
Oneida, New York[b]	213.1	215.7	212.1	213.6
Westchester, New York	745.6	397.3	512.6	551.8
All Facilities				
Geometric Mean				417.5
Maximum				617.1
Minimum				213.6

[a] Based on test results from massburn (excess air and modular) facilities
[b] Based on test results from modular unit (less than 50 tons/day/unit)

Hazardous Waste Incinerators

No data are known to be available for other trace organics from hazardous waste incinerators. Because the waste stream compositions can differ substantially, trace organics in the waste stream or formed as PICs are best estimated from thermal stability data.

Medical Waste Incinerators

No measured data are available. The Cedars-Sinai facility was tested for PCBs. However, no PCBs were detected.

SUMMARY

The readily available emissions data for toxic trace pollutants from incinerators have been reviewed and summarized. A direct comparison of measured emissions from the different waste stream/incinerator types is difficult because of the diversity of waste streams, combustor designs, and air pollution control

Table 10 Chlorobenzenes & Chlorophenols Emission Factors Based on Test Data from Selected Facilities ($\mu g/NM^3$ @ 12% CO_2, dry)[a]

Facility	Results for Individual Test Runs 1	2	3	Test Average
Chicago (Northwest), Illinois				
Carcinogenic Chlorobenzenes				
Hexachlorobenzene	149	58	424	210
Total Chlorobenzenes	1,814	1,367	4,614	2,598
Total Chlorophenols	4,514	3,298	7,596	5,136
Commerce, California				
Carcinogenic Chlorobenzenes				
1,4-Dichlorobenzene	30	40	—	35
Hexachlorobenzene	60	70	—	65
Total Chlorobenzenes	470	640	—	555
Carcinogenic Chlorophenols				
2,4,6-Trichlorophenol	50	70	—	60
Total Chlorophenols	1,050	1,470	—	1,260
Pinellas, Florida				
Total Chlorobenzenes	2,682	≤ 1,235	≤ 1,572	≤ 1,830
Total Chlorophenols[b]	1,267	1,760	≤13,370	≤ 5,466
Prince Edward Island, Canada[c]				
Carcinogenic Chlorobenzenes				
Hexachlorobenzene	1,660	4,438	ND[d]	2,033
Total Chlorobenzenes	6,194	6,071	1,885	4,717
Total Chlorophenols	1,774	6,452	6,006	4,744
Chlorobenzenes				
1,4-Dichlorobenzene Percent of Total				6.32%
Hexachlorobenzene Percent of Total				18.16%
Total Chlorobenzenes				
Geometric Mean				1,878
Maximum				4,717
Minimum				555
Chlorophenols				
2,4,6-Trichlorophenol Percent of Total				4.76%
Total Chlorophenols				
Geometric Mean				3,599
Maximum				5,466
Minimum				1,260

[a] Based on test results from massburn (excess air and modular) facilities
[b] Analyses were performed only for pentachlorophenols.
[c] Based on test results from modular unit (less than 50 tons/day/unit)
[d] Value was at or below the detection limit, but the detection limits were not supplied; therefore, it was not included in the calculations of the average.

Table 11 Comparison of Emission Factors for MSW, HW, and MW Incinerators

Pollutant	Geometric Mean			Upper Range		
	MSW	HW	MW	MSW	HW	MW
Dioxins/Furans (ng/m³) [U.S. EPA TEF-1987]	0.33 [a]	0.086 [b]	1.36 [c]	1.11 [a]	0.25 [b]	7.14 [c]
Metals (lb/ton of waste)[d]						
Antimony	1.13E-05	6.83E-04	NA	3.82E-05	1.43E-02	NA
Arsenic	7.22E-06	1.61E-04	1.57E-04	4.14E-05	4.34E-03	2.08E-04
Barium	3.38E-04	9.61E-04	NA	9.19E-04	3.00E-03	NA
Beryllium	2.12E-07	1.59E-05	NA	1.21E-06	1.06E-04	NA
Cadmium	2.65E-05	1.49E-03	2.89E-03	1.23E-04	5.28E-02	4.43E-03
Chromium	1.04E-04	9.73E-04	4.64E-04	6.22E-04	3.78E-03	1.49E-03
Cobalt	1.93E-05	NA	NA	1.28E-04	NA	NA
Copper	1.77E-04	NA	NA	4.43E-04	NA	NA
Lead	2.86E-04	1.42E-02	4.37E-02	8.23E-04	1.41E-01	4.65E-02
Magnesium	2.78E-03	NA	NA	3.67E-03	NA	NA
Manganese	6.59E-05	NA	4.04E-04	4.90E-04	NA	9.60E-04
Mercury	2.74E-03	2.14E-04	NA	7.23E-03	1.95E-02	NA
Molybdenum	7.20E-05	NA	NA	1.32E-04	NA	NA
Nickel	8.62E-05	1.03E-03	2.04E-04	5.59E-04	7.03E-03	4.30E-04
Selenium	8.19E-06	3.63E-04	NA	2.13E-05	1.53E-02	NA
Silver	2.38E-04	4.72E-05	NA	NA	3.93E-04	NA
Thallium	1.26E-08	1.75E-04	NA	NA	7.87E-04	NA
Tin	1.15E-04	NA	NA	2.70E-04	NA	NA
Vanadium	1.02E-05	NA	NA	4.07E-05	NA	NA
Zinc	1.14E-03	1.95E-02	NA	5.00E-03	2.77E-02	NA
Other Organics ($\mu g/Nm^3$ @ 12% CO_2, dry)						
PCB	0.47	NA	NA	1.90	NA	NA
Carcinogenic PAH	0.25	NA	NA	1.42	NA	NA
Aldehydes	417	NA	NA	617	NA	NA
Polychlorobenzenes	1.88	NA	NA	4.74	NA	NA
Polychlorophenols	3.59	NA	NA	5.47	NA	NA

[a] In ng/Nm³ @ 12% CO_2, dry based on mass burn resource recovery facilities with high efficiency particulate controls and acid gas controls (where normal temperature is 32°F).
[b] In ng/dscm (where standard temperature of 68°F was used when values were converted to standard temperature).
[c] In ng/dscm @ 12% CO_2, (where standard temperature of 68°F was used when values were converted to standard temperature).
[d] 1 Pound of pollutant per ton of waste feed is equal to 0.5 kilograms per megagram.

equipment. Emission factors for the three incinerator types are compared in Table 11. For dioxins/furans, the limited data suggest that emissions are highest for medical waste and lowest for hazardous waste. A possible explanation would be a decrease in organics emissions with higher combustion temperature and with the flue gas cooling of acid gas controls. Metals, on the other hand, are highest for hazardous waste and much lower for municipal solid waste. Possible mechanisms would be greater volatilization at higher combustion temperatures in conjunction with adsorption and collection in acid gas controls. Nevertheless, in the absence of any other data for the same incinerator type, emissions data from another incinerator (combustor and waste) type may be the best estimate of projected emissions for a new facility.

LITERATURE CITED

1. Trichon, M., and J. Feldman, "The Formation of Trace Toxic Emissions Resulting from Incineration," Poster paper presented at the 80th Annual APCA Meeting, New York, June 1987.
2. Siebert, P. C., D. R. Alston, J. F. Walsh, and K. H. Jones, "Statistical Properties of Available Worldwide MSW Combustion Dioxin/Furan Emissions," Paper No. 87-94-1 presented at the 80th Annual APCA Meeting, New York, June 1987.
3. Siebert, P. C., D. R. Alston, and K. H. Jones, "Effect of Control Equipment and Operating Parameters on Municipal Solid Waste (MSW) Incinerator Trace Emissions," Paper No. 88-98.3 presented at the 81st Annual APCA Meeting, Houston, Texas, June 1988.
4. Gilbert, R. O., *Statistical Methods for Environmental Pollution Monitoring,* Van Nostrand Reinhold Company, Inc. New York, pp. 148, 164 (1987).
5. Crawford, M., *Air Pollution Control Theory,* McGraw-Hill Book Company, New York, p. 133 (1976).
6. White, H. J., *Industrial Electrostatic Precipitation,* Addison-Wesley Publishing Company, Inc., Reading, MA, pp. 58–63 (1963).
7. Kolomogoroff, A. N., "Uber das Logarithmisch Normale Verteilungsgesetz der Dimensionen der Teilchen bei Zerstückelung," *C. R. Dokl. Acadi Sci. URSS (Akad, Nauk USSR)* Vol. 31, No. 2, pp. 99–101 (1941).
8. U. S. Environmental Protection Agency, Interim Procedures for Estimating Risks Associated with Exposures to Mixtures of Chlorinated Dibenzo-p-Dioxins and -Dibenzofurans (CDDs and CDFs) and 1989 Update, EPA/625/3-89/015, Risk Assessment Forum, U. S. Environmental Protection Agency, Washington, DC (1989).
9. Anderson, C. L., K. L. Wertz, and W. P. Gergen (Radian Corporation), Metals Analysis by NAA for the Marion County Emission Test Program Performed in September 1986. Revised October 20, 1987 personal memorandum.

Integrated Model for Predicting the Fate of Organics in Wastewater Treatment Plants

Rakesh Govind, Lei Lai

Department of Chemical Engineering, University of Cincinnati, Cincinnati, OH 45221

and

Richard Dobbs

Risk Reduction Engineering Laboratory, U.S. Environmental Protection Agency, Cincinnati, OH 45268

An integrated Fate Model has been developed for predicting the fate of organics in a wastewater treatment plant. The Fate Model has been validated using experimental data from a pilot-scale facility. The biodegradation kinetic constants for some compounds in the Fate Model were estimated using the group contribution approach. The Fate Model has been compared with other existing models in the literature. Potential applications of the Fate Model include assessment of volatile organic compound (VOC) emissions from a wastewater treatment plant, evaluate pretreatment requirements prior to discharge to the sewer system, predict concentrations of toxic compounds on sludges, and provide a general framework for estimating the removal of toxic compounds during activated sludge treatment.

INTRODUCTION

Removal of toxic compounds in a wastewater treatment plant occurs primarily by four different mechanisms: stripping, due to mechanical mixing and/or bubble aeration, volatilization at the air-liquid interface, sorption on solids, and biodegradation. Usually the removal is governed by a combination of these mechanisms. In this paper, a mathematical model has been developed to quantify the distribution of an influent organic compound in the air, liquid, and solid phases based on (a) the physical properties of the compound; and (b) the design and operating parameters of the wastewater treatment plant.

The development of an integrated fate model for predicting the concentrations of organics in a treatment plant is needed due to the large number of compounds that need to be regulated, the potentially large number of combinations of compounds that can exist in a wastewater matrix, and problems with the discharge of these compounds due to inherent toxicity. Recently, there has been concern regarding the emission of volatile organic compounds (VOCs) from wastewater treatment plants due to volatilization and stripping losses into the air phase.

The main objectives of this paper include: (1) development of an integrated fate model for predicting the fate of organic compounds in a wastewater treatment plant; (2) testing the fate model using experimental data from a pilot plant facility; (3) comparison of this model with other mathematical models; and (4) studying the impact of the physical properties, design and operating parameters on the intermedia distribution of the compound.

BACKGROUND

Several attempts have been made to develop a model for describing the fate of organics in a treatment plant. These

Table 1 Summary of the main features of the overall fate model studies in the literature

Author (year)	Mechanisms included[a]	Validation Testing	Computerized	Extent of Database[b]	Parameter Estimation
Hwang (1981)	Vol, ST, Sor, Bio in aeration tank	None	No		None
Kincannon (1983) and Stover and Kincannon (1983)	ST, Sor, Bio in aeration tank	None	No		None
Clark (1986)	Vol, ST, Sor, Bio in aeration tank & primary clarifier	None	Yes		None
Barton (1987)	Vol, ST, Sor, Bio in aeration tank	Full-scale plant	Yes	11	None
Namkung and Rittmann (1987)	Vol, ST, Sor, Bio in aeration tank	Full-scale plant	No		None
Blackburn et al. (1987)	ST, Sor, Bio in aeration tank	Full-scale plant	No		None
Govind et al. presented in this paper	Vol, ST, Sor, Bio in aeration tank & primary clarifier	Pilot scale and full-scale plant	Yes	196	Biodegradation kinetic rate constant

[a] Vol—Volatilization ST—Stripping
Sor—Sorption on solids Bio—Biodegradation
[b] Number of compounds in the database

studies in the literature can be classified into the following types: (1) treatment studies of single compounds; (2) studies on individual mechanisms; (3) empirical studies with little predictive capability; and (4) overall fate studies. While the first three types of studies were important, it is the last type of overall fate models that are relevant to this paper and hence have been discussed in detail.

Hwang [*18*] made the first attempt to develop an overall fate model for a continuous flow, single basin, activated sludge plant with sludge recycle and natural or mechanical surface aeration. The model used a non-linear Langmuir type isotherm for adsorption on sludge, and a first-order (Grau *et al.* [*13*]) equation for biodegradation kinetics. Laboratory-scale studies were used to determine various components of the model. No data were presented on the testing of the model for a broad range of compounds using pilot- or full-scale plant data.

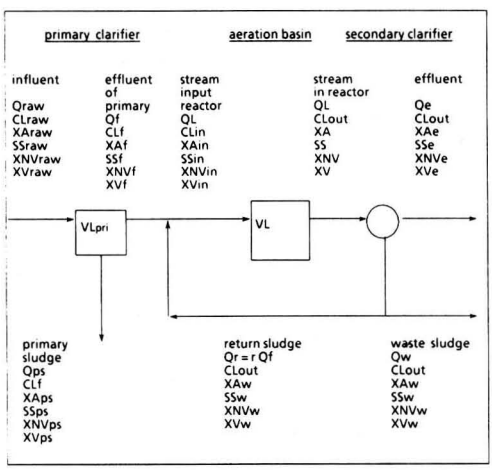

FIGURE 1. A schematic of an activated sludge treatment process.

Stover and Kincannon [*29*] and Kincannon *et al.* [*20*] models generated specific chemical biodegradation rate constants by measuring the influent and effluent compound concentrations. The removal equations were not explicitly stated in the papers. Blackburn [*4*] developed a model that gave overall removals for a continuous flow, single basin, diffused aeration, activated sludge plant. The model was validated against laboratory-scale and bench-scale tests and the model results were consistent with full-scale plant surveys, such as the EPA study of forty plants (Burns and Roe [*6*]). Although the model was not computerized, it requires as input compound properties, such as octanol-water partition coefficient, Henry's Law constant, first-order biotransformation rate constant, and various plant parameters (Blackburn [*4*]).

Clark *et al.* [*8*] presented a general fate model using a fugacity modeling technique. The model calculates removals in each tank (aeration tank, settling tank, etc.) by taking the ratio of the removal rates. The total removals are calculated by simply adding the removals for each tank. The biodegradation rate constants are computed from the user-input biodegradation half-life, assuming a MLSS concentration of 2,000 g/m3. The computerized version of the model has data for ten organic compounds. The model has been tested with 16% maximum error against laboratory-scale results for chlorobenzene, naphthalene, pentachlorophenol, and toluene.

Namkung and Rittmann [*26*] presented a model for a continuous flow, single basin, diffused aeration, activated sludge plant which was tested using data from two full-scale treatment plants. Assuming reasonable values for the biodegradation rate constant, the model predicted with good accuracy the removal of 11 volatile organic compounds. The model results were also reported to be consistent with other previous models.

Barton [*2*] presented a model for continuous flow, completely mixed single basin, bubble and surface aerated, activated sludge plant, which was tested with actual removals for two compounds from full-scale paper mill treatment plants.

The stripping equations used in this model were presented earlier by Roberts *et al.* [28]. The computerized version of the model required several input parameters for the compound and has input data for ten organic compounds. Table 1 provides a summary of the previous overall fate models and indicates the major similarities and differences among the various models.

DEVELOPMENT OF THE FATE MODEL

A schematic of a typical continuous flow, well-mixed single aeration basin, activated sludge plant is shown in Figure 1. Alternative systems that can be considered are secondary treatment only with or without recycle of sludge. Each stream in the plant is defined by the following variables (under the assumption of steady-state)

total flowrate (Q)
concentration of the organic compound in aqueous phase (CL)
suspended solids concentration (SS)
biomass concentration (XA)

The total suspended solids concentration (SS) consists of the concentration of volatile solids (XV) and non-volatile solids (XNV), i.e.,

$$SS = XV + XNV \tag{1}$$

The active biomass concentration is a fraction of the volatile solids concentration, XV. Furthermore, there exists a specific fraction of the active biomass responsible for the biodegradation of the compound. When evaluating experimental data from treatability studies, where the biomass consists of a mixed culture, the kinetic constants are generally related to the total biomass population. In the presented FATE model the biodegradation kinetic constants are based on the active biomass concentration (XA).

Primary Treatment System: Primary system is a gravity sedimentation process. The primary clarifier is used to remove solids from the waste stream entering the plant. For the primary effluent, the overall balance is

$$Q_f = Q_{raw} - Q_{ps} \tag{2}$$

and the suspended solids balance

$$SS_f = (Q_{raw}SS_{raw} - Q_{ps}SS_{ps})/Q_f \tag{3}$$

Assuming the ratio of volatile solids concentration and suspended solids concentration is maintained

$$XV_f = (SS_f/SS_{raw})XV_{raw} \tag{4}$$

$$XNV_f = (SS_f/SS_{raw})XNV_{raw} \tag{5}$$

The solids separation efficiency, $\eta 0$, is a known operating parameter, so for the sludge stream leaving the primary system the following equations can be written

$$Q_{ps} = \eta 0 Q_{raw}(SS_{raw}/SS_{ps}) \tag{6}$$

$$XV_{ps} = (SS_{ps}/SS_{raw})XV_{raw} \tag{7}$$

In the primary system, a certain part of compound, usually small compared with that in secondary system, is removed via sorption and volatilization. To simplify calculation, assume a uniform compound concentration. The exit compound concentration from primary system is calculated from the following mass balance equation

$$Q_{raw}CL_{raw} = Q_fCL_f + Q_{ps}CL_f + Q_{ps}K_p/1000XV_{ps}CL_f + V_{Lpri}K_L^{vol}aCL_f \tag{8}$$

The parameters in the above equations are calculated using equations presented later in this paper.

Secondary Treatment System: The system consists of a well-mixed single aeration basin and a secondary clarifier. Two streams enter the aeration basin. One stream is the primary effluent, and the other is recycled sludge from the secondary clarifier which contains the concentrated slurry of microorganisms. If the recycle ratio of return sludge is defined as follows

$$r = Q_r/Q_f \tag{9}$$

then the input variables of the aeration basin can be expressed as:

$$Q_L = (1+r)Q_f \tag{10}$$

$$CL_{in} = (CL_f + rCL_{out})/(1+r) \tag{11}$$

$$XA_{in} = (XA_f + rXA_w)/(1+r) \tag{12}$$

$$XV_{in} = (XV_f + rXV_w)/(1+r) \tag{13}$$

$$XNV_{in} = (XNV_f + rXNV_w)/(1+r) \tag{14}$$

Assuming steady-state and completely mixed condition (CSTR), the compound mass balance equation for the aeration basin is:

$$\begin{aligned} Q_L(CL_{in} - CL_{out}) &= V_L 24K_bXACL_{out} && (\textit{Biodegradation}) \\ &+ Q_wK_p/1000XV_wCL_{out} && (\textit{Sorption}) \\ &+ V_LK_L^{vol}a\,CL_{out} && (\textit{Volatilization}) \\ &+ V_LK_L^{mec}a\,CL_{out} && (\textit{Stripping via Surface Aeration}) \\ &+ Q_GH_C\left[1 - EXP\left(-\frac{K_L^{bub}aV_L}{H_CQ_G}\right)\right]CLout && (\textit{Stripping via Diffused Aeration}) \end{aligned} \tag{15}$$

Using a yield coefficient Y for the growth of biomass, the concentration of biomass in the aeration basin can be written as follows:

$$XA = XA_{in} + V_L/Q_L 24K_bYXA\,CL_{out} \tag{16}$$

The non-volatile solids and volatile solids balances in the aeration basin are

$$XNV = XNV_{in} \tag{17}$$

$$XV = XV_{in} + V_L/Q_L 24K_bYXA\,CL_{out} \tag{18}$$

Assuming no reaction in the secondary clarifier, the following ratios can be written

$$XNV/XNV_w = XA/XA_w \tag{19}$$

$$XV/XV_w = XA/XA_w \tag{20}$$

Combining equations (14), (17) and (19) gives

$$XNV_w = \frac{XNV_f/(1+r)}{XA/XA_w - r/(1+r)} \tag{21}$$

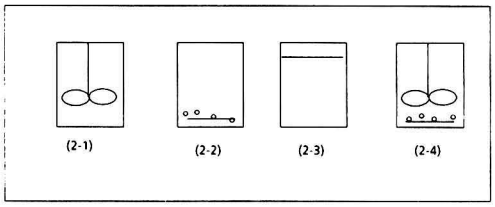

FIGURE 2. Typical aeration methods: (2-1) surface aeration (mechanical aeration) (2-2) diffused aeration (2-3) volatilization (quiescent surface) (2-4) submerged turbine aeration.

Similarly, for volatile solids

$$XV_w = \frac{XV_f/(1+r) + V_L/Q_L 24 K_b YXA\, CL_{out}}{XA/XA_w - r/(1+r)} \qquad (22)$$

Substituting XA and XVW into (15), and solving this equation by iteration gives both the compound concentration CL_{out} and active biomass concentration XA, and then the effluent and waste sludge streams become known.

In the above model equations, the rates of stripping, volatilization, sorption on solids and biodegradation need to be further quantified. The following sections detail the required equations for obtaining the rate terms in the above equations.

MODELS FOR STRIPPING AND VOLATILIZATION

Knowledge of volatilization and stripping rates is necessary to determine the amount of chemical that enters the atmosphere and the consequent change of pollutant concentration in water. The transfer process from the water to the atmosphere is dependent on the chemical and physical properties of the pollutant, the presence of other pollutants, and the physical (e.g., flow velocity, depth and turbulence) properties of the water body and the air above it.

The factors that control stripping and volatilization rates are pollutant properties such as Henry's Law constant, solubility, molar volume, chemical reactivity, and matrix contributions, such as presence of emulsifiers, dissolved salts, total suspended solids, temperature, pH, and concentration of oily phase.

Assumptions used in estimating rates of stripping and volatilization were as follows:

1. Equilibrium exists between the bulk gas and bulk liquid phases, which is quantified by the Henry's Law constant;
2. Equilibrium exists between the gas-liquid phases at the interface, with mass transfer coefficient based transport resistances between the bulk phase and the interface, and
3. Utilize measured constants, such as oxygen reaeration coefficient and the compound/oxygen mass transfer ratio estimated from diffusivities.

In our fate model, four types of stripping/volatilization systems (shown in Figure 2) have been included, which are as follows:

1. Surface mechanical aeration, where mechanical agitation is used to promote gas/liquid mass transfer (Figure 2-1);
2. Diffused aeration, where air is introduced below the surface through porous diffusers or nozzles (Figure 2-2);
3. Volatilization, which occurs at the air/water interface of an open aeration basin, and depends on wind velocity (Figure 2-3); and
4. Submerged turbine aeration, where air diffusers are accompanied by mechanical mixing causing high liquid shear rates around the air bubbles (Figure 2-4).

Surface Aeration: The rate of transport can be expressed as

$$\mathrm{Re}^{mec} = V_L K_L^{mec} a CL_{out} \qquad (23)$$

The overall liquid phase mass transfer coefficient can be written in terms of the liquid phase pure oxygen mass transfer coefficient, a function based on the ratio of compound/oxygen diffusivities, Ψ_i, and a correction factor, $ALPHA$, to account for differences between wastewater and clean water (Roberts 1984)

$$K_L^{mec} a = \Psi_i K_{L\,oxy}^{mec} a\,(ALPHA) \qquad (24)$$

$$\Psi_i = (D_i/D_{oxy})^{0.62} \qquad (25)$$

$$ALPHA = \frac{KLa \text{ in wastewater}}{KLa \text{ in clean water}} \qquad (26)$$

where the diffusivity and the molar volume of the compound can be estimated using the following equations

$$D_i = 7.410^{-8}[(18^{*}2.6)^{0.5} Tk/(\mu_{water} V_b^{0.6})] \qquad (27)$$

$$Vb = Mw_i/\rho_i \qquad (28)$$

The pure oxygen overall liquid phase mass transfer coefficient $K_{Loxy}^{mec}a$ can be calculated using the following equation, which contains the power expended for mechanical mixing

$$K_{L\,oxy}^{mec} a = 24\,(NcPower)/(CL_{oxy}^{*} V_L)\,(1.024)^{(T-20)} \qquad (29)$$

Diffused Aeration: The diffusers used in aeration systems can produce fine, medium, or coarse (relatively large) bubbles. The efficiency of oxygen transfer depends on the type of porosity of the diffuser, the size of the bubbles produced, the depth of submergence, and other factors. Table 2 gives a brief description of diffused-air aeration devices, a range of typical transfer efficiencies, and average values used in our model (Metcalf and Eddy [24]).

Using the oxygen transfer efficiency, β from Table 2, the oxygen concentration in the exit gas phase is

$$CG_{oxy}^{out} = (1-\beta)\, CG_{oxy}^{in} \qquad (30)$$

Table 2 Table of average oxygen transfer efficiencies for coarse, medium and fine bubbles in the aeration basin

Type of Aeration Device	Bubble Size	Typical[a] transfer efficiency	Average transfer efficiency
Orifice devices or slot-orifice injectors	Coarse	4–8%	6%
Plastic wrapped diffuser tubes, woven fabric sock or sleeve diffusers	Medium	6–15%	10%
Ceramically bonded grains of fused crystalline aluminum oxide or resin bonded grains of pure silica	Fine	10–30%	15%

[a] Depends on depth

The inlet oxygen concentration in the air is

$$CG_{oxy}^{in} = 32.0 P_{oxy}^{in}/(RTk) \quad (31)$$

Following the analysis of Roberts *et al.* [28], the following equation is used to quantify the oxygen absorption

$$CG_{oxy} = CL_{oxy} H_{Coxy} + (CG_{oxy}^{in} - CL_{oxy} H_{Coxy}) EXP[-\phi_{oxy}(Z_s - Z)] \quad (32)$$

where by definition

$$(\phi_{oxy} Z_s) = (k_{Loxy}^{bub} a V_L)/(Q_G H_{Coxy}) \quad (33)$$

Evaluating equation (32) at $Z = 0$ with $GC_{oxy} = CG_{oxy}^{out}$ and $CL_{oxy} = CL_{oxy}^{dis}$, the dissolved oxygen concentration in the wastewater, gives

$$(\phi_{oxy} Z_s) = -\ln[(CG_{oxy}^{out} - CL_{oxy}^{dis} H_{Coxy})/(CG_{oxy}^{in} - CL_{oxy}^{dis} H_{Coxy})] \quad (34)$$

Combining equations (34) and (33) gives

$$k_{Loxy}^{bub} a = -\ln[(CG_{oxy}^{out} - CL_{oxy}^{dis} H_{Coxy})/(CG_{oxy}^{in} - CL_{oxy}^{dis} H_{Coxy})](H_{Coxy} Q_G)/V_L \quad (35)$$

For the compound

$$k_L^{bub} a = \Psi_i k_{Loxy}^{bub} a \quad (36)$$

The overall liquid phase mass transfer coefficient can be written in terms of the liquid and air phase mass transfer coefficients

$$1/K_L^{bub} a = 1/k_L^{bub} a + 1/H_C k_G^{bub} a \quad (37)$$

For highly volatile compounds ($H > 3 \times 10^{-3}$ atm.m^3/mol), the liquid-phase resistance will control the rate of mass transfer, and the gas-phase resistance should have little influence (Roberts [28]).

$$K_L^{bub} a = k_L^{bub} a \quad (38)$$

The rate of transport due to bubble aeration is given by

$$\mathrm{Re}^{bub} = Q_G H_C [1 - EXP(-K_L^{bub} a V_L / H_C Q_G)] CL_{out} \quad (39)$$

Volatilization: The transport rate due to volatilization can be expressed as

$$\mathrm{Re}^{vol} = V_L K_L^{vol} a \, CL_{out} \quad (40)$$

The overall liquid phase mass transfer coefficient is

$$1/K_L^{vol} a = 1/k_L^{vol} a + 1/H_C k_G^{vol} a \quad (41)$$

For prediction of k_L, Cohen *et al.* [9] suggested that three wind velocity regions be considered: (1) below 3 m/sec where k_L is 2-3 cm/hr and strongly influenced by the water turbulence; (2) between 3-10 m/sec, which is the region of greatest interest, k_L is correlated with a roughness Reynolds number Re^*, given by equation (42); and (3) at high velocity region where wave breaking may occur.

$$k_L = (11.4 \mathrm{Re}^{*0.195} - 5.0)(D_i/D_{Toluene,water}) \quad (42)$$

In our case

$$k_L^{vol} a = (11.4 \mathrm{Re}^{*0.195} - 5.0) \frac{D_i}{D_{Toluene,water}} \left(\frac{24}{100d}\right) \quad (43)$$

The $k_G^{vol} a$ is rate of natural oxygen reaeration across the basin surface (Mills [25])

$$k_G^{vol} a = 700(18.0/Mw_i)^{0.25} V_{wind} \left(\frac{24}{100d}\right) \quad (44)$$

The extent of volatilization in aeration would depend not only on factors like wind speed, basin depth etc., but also on the degree of turbulence generated at the liquid-gas interface due to the turbulence. This turbulence increases the liquid phase mass transfer coefficient and also increases the liquid-gas interface area. In our current model, the effect of this increased turbulence due to aeration has not been quantified yet.

Submerged Turbine Aeration: This type of aeration is considered to be a combination of diffused aeration with fine bubbles and surface aeration. The transport rates for diffused aeration with fine bubbles and surface aeration are calculated using the equations presented for each type of aeration, and these transport rates are then added to obtain the transport rate for submerged turbine aeration. It is assumed that mechanical mixing results in the formation of fine bubbles.

MODELS FOR SORPTION ON SOLIDS

Sorption on solids is one of the processes controlling the removal of toxic organic compounds in wastewater treatment plants. There is ample evidence in the literature that organics accumulate in sludges at concentration levels several orders of magnitude greater than influent concentrations. Furthermore, high rates of sorption onto biological solids has been demonstrated by Blackburn [4]. Hence equilibrium between the solid and liquid phases can be assumed in a wastewater treatment plant.

Previous studies conducted in our laboratory (Dobbs *et al.* [11]) on sorption of toxic organic compounds on primary, mixed-liquor, and digested solids from municipal wastewater treatment plants resulted in the development of a correlation of the Freundlich adsorption parameter K_p' with the octanol/water partition coefficient K_{ow}. It was shown that the correlations are the same for all three types of wastewater solids if the partition coefficients are calculated on the basis of organic content of the solids. The following equation was obtained for the relationship between partitioning on wastewater solids and octanol/water partition coefficient:

$$\log(K_p') = 1.14 + 0.58 \log K_{ow} \quad (45)$$

The solid/liquid partition coefficient, K_p, is calculated as follows

$$K_p = (\%VSS/100) K_p' \quad (46)$$

and the amount of the compound sorbed per unit weight of the biomass is then given by

$$q = K_p/1000 \, CL_{out} \quad (47)$$

The removal rate of the compound by sorption on solids is:

$$Re^{sor} = Q_w X V_w q \quad (48)$$

MODELS FOR BIODEGRADATION

Biodegradation is an important mechanism for the removal of organic compounds in an activated sludge treatment plant. However, it is also the most difficult to quantify due to scarcity of experimentally determined biokinetic constants in the literature. Hence, any attempt to quantify extent of biodegradation in a wastewater treatment plant must include methods for estimating and predicting the biokinetic constants for a variety of compounds.

At low substrate concentrations, a first order equation is obtained with respect to the substrate concentration, and the removal rate of biodegradation can be expressed as

$$Re^{bio} = V_L K_b X A\, CL_{out} \quad (49)$$

The growth of biomass due to biodegradation is given by

$$Re^{biomass} = V_L K_b Y X A C L_{out} \quad (50)$$

There are three important aspects that are not taken into account in the present model:

1. Parameters other than substrate concentration, such as nutrients (Calcium, Nitrogen, Phosphorus etc.) or vitamins may limit the biodegradation rate. It is assumed in our model that in municipal wastewater, nutrients, vitamins etc. are present in sufficient concentrations and they are not limiting parameters; this may not be the case for industrial wastewaters;
2. Inhibition from the substrate or from metabolites formed during the degradation;
3. Biodegradation through co-metabolism has not been included.

To used the above equations in the Fate Model, it is necessary to know the first order biodegradation kinetic constant, K_b. There are basically three options, listed below, that are presented to the user in the Fate Model:

1. Enter the value of K_b for the compound;
2. Use the value of K_b given in the literature which is stored in a database; or
3. Estimate the value of K_b using the group contribution method.

The group contribution method is an estimation technique that we have developed for obtaining a reasonable value for the biodegradation kinetic constant. The basis for the group contribution method will be described in the following section.

GROUP CONTRIBUTION METHOD FOR ESTIMATING BIODEGRADATION KINETICS

The group contribution method has been widely used in chemical engineering thermodynamics for estimating a variety of pure component properties, such as liquid densities, heat capacities and critical constants for organic compounds. It has also been used for predicting adsorbability on activated carbon (Chitra and Govind [7]).

Several attempts have been made to correlate a compound's chemical structure with its tendency to be biodegraded (Ludzack and Ettinger [21]). Lyman *et al.* [22] has summarized rules of thumb for making qualitative predictions about biodegradability of organic chemicals. Geating [12] developed an algorithmic procedure for predicting biodegradability based on type and location of substituent groups. Recently a group contribution method for relating chemical structure to the first order biodegradation kinetic constant has been presented (Desai *et al.* [10]).

In the group contribution method, the chemical structure is decomposed into chemical groups (functional groups, fragments), and it is assumed that each chemical group has a unique contribution towards the biodegradation kinetics of the compound. This approach is attractive because a very large number of compounds can be constituted from perhaps a few hundred functional groups. Positional (ortho, meta, para), geometric (L-isomers, D-isomers) and other features can be incorporated in the group contribution method by treating these as distinct chemical groups.

The first order biodegradation kinetic constant, K_b, can be expressed as a function of its contribution, $\alpha_1,\ldots\alpha_L$, as follows:

$$\ln(K_b) = f(\alpha_1, \alpha_2, \ldots \alpha_L) \quad (51)$$

where L is the number of groups.

The above equation can be reduced to its linear form:

$$\ln(K_b) = \sum_{i=1}^{L} N_i \alpha_i \quad (52)$$

where N_i is the number of type i chemical groups present in the structure, and α_i is the contribution of type i group. The above equation can be written for each compound whose K_b is known and its chemical structure can be decomposed into these groups. The set of established linear equations was solved for the unknown group contributions α_i, using the method of least squares.

It should be noted that the above analysis has some shortcomings. First, a compound structure can be dissected in many ways, and this leads to some ambiguity in defining the chemical groups present in the structure. Secondly, since the above model is a first order approximation, interaction among the groups is neglected. This limitation has been recently overcome by using a neural network to calculate the biodegradation kinetic constant from the chemical groups present in the structure (Govind *et al.* [14]). Finally, the above analysis requires that each chemical group be present in at least five distinct compounds used to generate the linear equations for solving the unknown group contributions α_i. This is necessary to minimize the existence of chance correlations.

The above analysis was applied using experimental data obtained from electrolytic respirometry, which measures the cumulative oxygen demand. The experimental conditions were: temperature 20 C, pH of solution 7.0, sludge concentration 30 mg/L, and compound concentration 100 mg/L. The oxygen uptake data was analyzed using non-linear regression to obtain

Table 3 Values for the Group contributions (αi) for a variety of chemical groups

Number	Group Name		αi
1	Methyl	CH3	−3.460
2	Methylene	CH2	−0.1354
3	Ketone	CO	−0.9650
4	Amine	NH2	−4.061
5	Acid	COOH	−3.201
6	Hydroxy	OH	−2.983
7	Aromatic CH	ACH	−0.834
8	Aromatic C	AC	1.973
9	Chlorine	CL	−2.352
10	Aliphatic C	CH	3.223
11	Nitro	NO2	−2.448
12	Aldehyde	CHO	−3.909
13	Nitrile	CN	−5.272
14	Bromine	Br	−4.657

the first order biodegradation kinetic constant (Desai *et al.* [*10*]). The values of the group contributions, α_i, are tabulated in Table 3. Note that these values are used in equation (52) to calculate the first order biodegradation kinetic constant K_b. Also limited validation of the group contribution values has been achieved by predicting the degradation kinetic constant for compounds that were not used in the calculations of α_i, and it was found that the reported results agree within 20% with the predicted values (Govind *et al.* [*15*]). Extensive validation of the group contribution values will require further experimental investigations of biodegradation kinetics using electrolytic respirometry.

ORGANIZATION OF THE FATE PROGRAM

The above mathematical model, including the group contribution method for estimating the biodegradation kinetic constant, was automated, and this program, written in FORTRAN, has been referred to as the Fate Model in this paper. The Fate Model can run on any IBM or compatible microcomputer or can be compiled and run on a Digital Equipment VAX operating system.

Currently there are 196 compounds in the Fate Model database including their respective physical properties required for estimating their removals in the activated sludge system.

There are three default cases of plant sizes [1 million gallons per day (mgd), 10 mgd, and 100 mgd] in the Fate Model. The user is given the option of changing any or all of the default parameters. The default cases have been included in the program to facilitate the use of the Fate Model even if the user does not know all the input parameters.

The Fate Model can calculate the percent removals for three plant configurations: (1) primary with secondary treatment and sludge recycle; (2) secondary treatment with sludge recycle; and (3) secondary treatment without sludge recycle. For the type of diffused aeration, the user is given three choices: (1) coarse bubble aeration with low oxygen transfer efficiency (4–8%), usually obtained from orifice devices or slot-orifice injectors; (2) medium bubble aeration, with medium transfer efficiency (6–15%), usually obtained from plastic-wrapped diffuser tubes or woven-fabric sock or sleeve diffusers; and (3) fine bubble aeration, with high transfer efficiency (10–30 + %), usually obtained from ceramically bonded grains of fused crystalline aluminum oxide, or resin-bonded grains of pure silica.

The output of the Fate Model is presented in two ways: (1) a short summary which provides the user with influent and effluent concentrations for the primary and secondary treatment system and the amount of the compound removed by each mechanism (The percent removals by each mechanism and the total percent removal is also included in this summary report); and (2) a detailed report which lists the important plant parameters, such as sludge recycle ratio, gas/liquid ratio in the aeration basin, etc. and gives the flowrate, composition, suspended solids and biomass concentration for each stream in the plant. The user can review the summary or detailed results on the computer screen or generate a report, which is stored as a file on the disk for subsequent printing.

Table 4 Comparison of removal percentages calculated from the Fate Model and experimental data for RCRA compounds. Flowrate = 50400gpd, Influent concentration of compound = 0.25 mg/L, Aeration basin volume = 15780 gal, Basin area = 175.8 ft2, Gas flowrate = 5600 L/min, SRT = 4 days, Temperature = 20°C, Wind speed = 2 miles/hr.

	University of Cincinnati Fate Model				Experimental Data From T&E[c]			
Compound	Total	Sorp	Strip/Vol	Bio[a]	Total	Sorp	Strip/Vol	Bio
Acetone	69.3	0.6	2.1	66.6	$91.7_{5.9}$	$0.6_{0.4}$	$1.8_{0.6}$	$94.1_{5.9}$
Cyclohexanone	85.5	0.7	1.1	83.6	$82.1_{12.9}$	$0_{1.1}$	—	$81.1_{12.9}$
2-Butanone	69.0	7.0	3.5	58.6	$96.7_{1.6}$	$0.6_{0.2}$	$.8_{0.4}$	$94.3_{1.6}$
4-Methyl-2-pentanone		NA[b]			$97.5_{3.5}$	$1_{.2}$	2_{1}	95_{6}
Tetrahydrofuran	99.5	0.6	0.8	98.1	$89.1_{17.2}$	$1.2_{0.5}$	$10.2_{3.0}$	$77.9_{20.2}$
Carbon tetrachloride	97.1	3.6	91.8	1.7	$98.8_{0.5}$	$0.6_{0.4}$	$103_{22.5\ 4}$	$5_{22.9}$
Chlorobenzene	98.6	4.6	12.8	81.3	$99.1_{0.9}$	$2.8_{1.5}$	$12.6_{2.2}$	$83.6_{3.2}$
Chloroform	86.3	0.4	85.6	0.8	$84.3_{5.1}$	$2_{1.}$	104_{12}	-21_{17}
1,2-Dichloroethane	71.0	1.3	53.1	16.6	$53.0_{18.8}$	3_{2}	67_{11}	-17_{32}
1,2-Dichloropropane	83.7	2.0	72.3	9.4	$77.3_{10.2}$	2_{1}	97_{9}	-25_{12}
Methylene chloride	98.1	0.9	11.8	85.5	$73.0_{15.6}$	—	24_{40}	1
Tetrachloroethylene	97.1	4.8	92.2	0.0	$97.3_{1.1}$	$2.5_{1.1}$	110.8_{25}	$-16_{25.7}$
Trichloroethylene	94.6	2.9	88.6	3.1	$99.7_{0.3}$	$1.8_{0.7}$	$52.4_{7.2}$	$45.5_{6.7}$
1,1,1-Trichloroethane	97.4	3.1	94.2	0.1	$98.6_{0.6}$	$1.7_{0.5}$	$108.7_{15.9}$	$-11.9_{16.2}$
1,1,2-Trichloroethane	68.2	2.4	47.5	18.3	$70.8_{6.6}$	$2.1_{0.3}$	$37.0_{13.3}$	$31.7_{7.6}$
Ethylbenzene	96.9	6.7	38.2	52.1	$98.3_{1.7}$	$5.1_{3.4}$	$15.9_{3.3}$	$77.2_{6.3}$
Toluene	99.8	4.3	6.1	89.4	$99.0_{0.9}$	1_{1}	$25_{.6}$	72_{8}
Total Xylenes	95.2	4.3	46.0	42.7	$98.7_{0.6}$	1_{1}	32_{10}	66_{9}
Bis-(2-ethylhexyl)phthalate	99.9	99.9	0.0	0.0	$96.7_{0.6}$	11_{8}	—	85_{8}
Butylbenzyl phthalate	98.3	38.9	30.0	29.4	$91.0_{3.5}$	11_{6}	—	81_{9}
1,4-Dichlorobenzene	93.1	11.2	42.2	39.7	$94.3_{2.1}$	2_{1}	—	93_{3}
Naphthalene	99.8	7.9	2.8	89.1	$96.3_{1.5}$	2_{1}	—	94_{2}
Nitrobenzene	92.7	1.6	0.3	92.7	$95.7_{1.5}$	1_{1}	—	93_{6}
4-Nitrophenol	99.8	0.9	6.4	92.5		NA		
Phenol	97.2	1.0	5.2	90.9	$98.0_{1.0}$	1_{1}	—	97_{2}

[a] TOTAL—total removal percentages SORP—removal percentage by sorption
STRIP/VOL—removal percentage by stripping and volatilization
BIO—removal percentage by biodegradation
[b] NA—Data is not available in database of the model
[c] In this column the subscript numbers are the standard deviation

Table 5 Comparison of removal percentages calculated from the Fate Model and experimental data for CERCLA compounds. Flowrate = 50400gpd, influent concentration of compound = 0.5 mg/L, Aeration basin volume = 15780 gal, Basin area = 175.8 ft2, Gas flowrate = 5600 L/min, SRT = 8 days, Temperature = 20°C, Wind speed = 2 miles/hr.

	University of Cincinnati Fate Model			Experimental Data From T&E[c]		
Compound	Total	Sorp	Strip/Vol + Bio[a]	Total	Sor	STR/Vol + Bio[d]
Dichlorobenzene, 1,2	99.5	10.7	88.8	93_4	0_9	73_{10}
Dichlorobenzene, 1,3	90.0	11.4	78.6	89_5	16_{10}	72_{11}
Dichlorobenzene, 1,4	94.9	11.1	83.8	95_5	17_9	79_{10}
1,2,4-Trichlorobenzene	99.7	23.6	76.1	85_9	37_{12}	48_{14}
Nitrobenzene	96.9	1.6	95.3	93_3	1_1	91_3
2,6-Dinitrotoluene		NA[b]		68_{15}	12_{15}	57_{38}
p-Cresol	96.8	1.8	95.0	74_{22}	2_1	69_{21}
4-Chloroaniline		NA		88_{23}	2_1	78_{28}
Hexachloroethane	90.6	35.6	55.0	97_3	2.	100
Hexachloro-1,3-butadiene	98.0	38.2	59.8	96_5	50_{16}	47_{17}
Dimethyl phthalate	91.7	2.1	89.6	98_2	1_0	97_1
Diethyl phthalate	99.9	2.0	97.9	98_2	1_1	96_2
Di-n-butyl phthalate	97.1	66.0	31.1	96_4	42_{10}	54_{10}
Butylbenzyl phthalate	98.8	38.7	60.1	97_4	49_{12}	47_{12}
Naphthalene	99.9	7.9	92.0	98_1	14_9	84_8
Lindane	66.3	0.8	65.5	56_{40}	27_{10}	28_{38}
Dieldrin	84.5	20.3	64.2	81_9	48_{19}	36_{24}

[a] TOTAL—total removal percentages SORP—removal percentage by sorption
STRIP/VOL + BIO—removal percentage by stripping and volatilization and biodegradation
[b] NA—Data is not available in database of the model.
[c] In this columnn the subscript numbers are the standard deviation
[d] Only lumped removal of stripping + biodegradation provided

VALIDATION OF THE OVERALL FATE MODEL

Experiments were conducted on two parallel pilot-scale conventional activated sludge systems at the U.S. EPA Testing and Evaluation facility in Cincinnati, Ohio (Battacharya, *et al.* [3]). Screened municipal raw wastewater from the Metropolitan Sewer District's Mill Creek Plant in Cincinnati, Ohio was used as a common feed to both systems. The two activated sludge systems were operated at a flow rate of 35 gallons per minute (gpm) and a hydraulic retention time (HRT) of 7.5

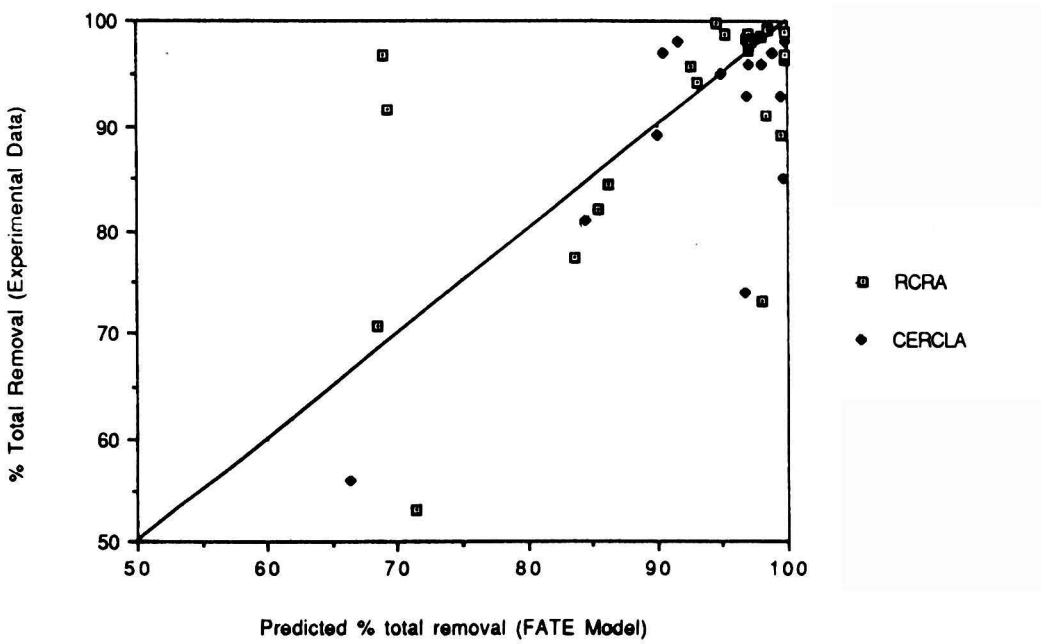

FIGURE 3. Comparison of total % removal predicted by the Fate Model and experimental data for RCRA and CERCLA compounds. The total removal numbers have been given in Tables 4 (RCRA) and 5 (CERCLA).

hours. Twenty-eight RCRA semi-volatile and volatile compounds and 19 CERCLA (semi-volatile) only were spiked into the system. An operational sludge retention time (SRT) of 4 days was used in the RCRA study period. In the CERCLA study period, the SRT was 8 days. Each compound was spiked at 0.25 mg/L for the RCRA study and 0.5 mg/L for the CERCLA study.

The air space above the primary clarifiers was swept with air to simulate a 2 mile per hour wind speed over the water surface. The aeration basins were closed from the top and the average air flow to the basins was 5,600 liters/min.

The toxic organic compounds were analyzed by GC/MS procedures, while the conventional pollutants were monitored using analyses for COD, BOD, NH4-N, NO3-N, and TKN. RCRA samples were analyzed by PEI Associates, Inc., Cincinnati, Ohio. Air samples were collected in stainless steel containers and analyzed by GC/MS. Details of the analytical procedures have been reported elsewhere (Bhattacharya *et al.* [3]). A total of three sampling events were performed during the RCRA study and eleven sampling events on the CERCLA study.

The Fate Model, described in the previous sections, was used to calculate the removal of each compound by volatilization/stripping, sorption on solids, and biodegradation. Results of these calculations and the actual experimental data from the pilot plant are shown in Table 4 for the RCRA study and in Table 5 for the CERCLA study.

In Table 4 for the RCRA study, 4-methyl-2-pentanone was not in our Fate Model database, and hence the experimental results could not be compared. For the chlorinated compounds, such as methylene chloride, tetrachloroethylene, the experimental percent removals for stripping/volatilization are greater than 100%. This was mainly due to analytical difficulties, resulting in high standard deviations, and formation of some of these compounds due to biodegradation of other chlorinated species, such as carbon tetrachloride, etc. The Fate Model predicted very high removals due to volatilization/stripping due to the high volatility of these chemicals. Methylene chloride was mainly removed by biodegradation, due to a high value for its biodegradation kinetic constant. In general, the Fate Model gave good predictions for most of the RCRA compounds. In cases where the calculated results are significantly different from the experimental data, it was found that a major part of the error was in estimating the value of the biodegradation kinetic constants K_b.

In the CERCLA study, the results shown in Table 5 provide further validation for the Fate Model. Comparing the calculated values with the experimental results, which provided only lumped removal of stripping/volatilization + biodegradation, we can see that there is good agreement for most of the compounds. Again here we find K_b accounts for the errors.

The RCRA and CERCLA validation results have been summarized graphically in Figure 3, where the experimental % total removal has been plotted versus the % values calculated by the FATE model.

In the RCRA case study the compounds that show large deviations between the experimental % total removal values and the calculated values are 2-Butanone, Acetone, 1,2-Dichloroethane and Methylene chloride. In the case of 2-Butanone and Acetone, the error is mainly due to biodegradation. As noted earlier, this is mainly due to errors in K_b values. In the case of 1,2-Dichloroethane and Methylene chloride, due to highly volatility and analytical problems, there were significant errors in the experimental data.

In the CERCLA study the largest error between the experimental % total removal and calculated value is for p-Cresol. This is mainly due to biodegradation which means problems in K_b values.

SUMMARY AND CONCLUSIONS

A Fate Model has been developed and the percent removal predicted by the model agreed well with the experimental pilot plant data. The model gave results which were consistent with full-scale treatment plant data for VOC emissions. The model offers significant advantages over existing models, as previously summarized in Table 1. Some of these advantages include: (1) all treatment mechanisms have been quantified for primary and secondary treatment; (2) the model database has properties for 196 compounds; (3) capability to estimate first-order biodegradation kinetic rate constants for a variety of compounds using the group contribution method; (4) default values for small, medium, and large scale wastewater treatment plants; (5) can handle user input values for the plant operating parameters; and (6) easy to use on any IBM compatible personal computer.

Potential applications of the Fate Model include: (1) assessment of VOC emissions from wastewater treatment plants; (2) determine acceptability of various aqueous wastes for treatment at central facilities; (3) evaluate pretreatment requirements prior to discharge to the sewer system; (4) establish local limits; (5) predict concentrations of toxics in sludge which impact disposal options; (6) predict fate of new chemicals in biological treatment plants; and (7) provide a general basis for estimating the effect of operating parameters on removal of toxic organics during treatment.

Further developments of this Fate Model will involve extension of the group contribution approach (estimating biodegradation kinetic constants) to include additional chemical groups, capability to handle complex flow patterns, such as combinations of plug and mixed flow, possible interactions between compounds which may affect adsorption and biodegradation kinetics, development of estimation methods for compound properties, and improved user interface.

NOTATION

$ALPHA$ = KLa in wastewater/KLa in clean water
CG_{oxy} = Oxygen gas phase concentration, depending on vertical position (g/M^3)
CG_{oxy}^{in} = Inlet gas phase oxygen concentration (g/M^3)
CG_{oxy}^{out} = Outlet gas phase oxygen concentration (g/M^3)
CL_f = Compound concentration in primary effluent (mg/L)
CL_{in} = Compound concentration input the aeration basin (mg/L)
CL_{out} = Compound concentration in the aeration basin (mg/L)
CL_{oxy} = Oxygen concentration in wastewater (g/M^3)
CL_{oxy}^{dis} = Dissolved oxygen concentration (g/M^3)
CL_{oxy}^{*} = Oxygen saturation concentration (kg o_2/M^3)
CL_{raw} = Compound concentration in influent (mg/L)
d = Depth of the aeration basin (m)
D_i = Diffusivity of compound in water (cm^2/sec)
$D_{toluene,water}$ = Diffusivity of toluene in water (cm^2/sec)
D_{oxy} = Diffusivity of oxygen (cm^2/sec)
H = Henry's Law constant of compound, $atm.m^3/mol$
H_{coxy} = Henry's Law constant of oxygen, dimensionless
H_c = Henry's Law constant of compound, dimensionless
K_b = First order rate constant of biodegradation (L/mg.hr)

$k_G^{bub}a$ = Gas phase mass transfer coefficient, diffused aeration (1/day)
$k_G^{vol}a$ = Gas phase mass transfer coefficient, volatilization (1/day)
k_L = Liquid phase mass transfer coefficient in Cohen's equation, cm/hr
$k_L^{bub}a$ = Liquid phase mass transfer coefficient (1/day)
$k_{L\,oxy}^{bub}a$ = Liquid phase transfer coefficient of oxygen (1/day)
$k_L^{vol}a$ = Liquid phase mass transfer coefficient (1/day)
$K_L^{bub}a$ = Mass transfer coefficient of compound by diffused aeration (1/day)
$K_L^{mec}a$ = Mass transfer coefficient of compound by surface aeration (1/day)
$K_{L\,oxy}^{mec}a$ = Mass transfer coefficient of oxygen by surface aeration (1/day)
$K_L^{vol}a$ = Mass transfer coefficient by volatilization (1/day)
K_{ow} = Octanol/water partition coefficient
K_p = Solid/liquid partition coefficient
K_p' = Corrected partition coefficient
L = Total number of groups in the compound
Mw_i = Molar weight of compound (g/mol)
N_c = Oxygen transfer rate (kg o_2/kw hr)
N_i = Number of groups of type i in the compound
P_{oxy}^{in} = Partial pressure of oxygen in air (atm)
P_{ower} = Brake power of aerator (kw)
q = Amount of the compound sorbed per unit weight of biomass (g/g)
Q_f = Flowrate of primary effluent (M^3/day)
Q_G = Gas flow rate (M^3/day)
Q_L = Flowrate in the aeration basin (M^3/day)
Q_{ps} = Flowrate of primary waste sludge (M^3/day)
Q_r = Recycle flowrate (M^3/day)
Q_{raw} = Influent flowrate (M^3/day)
Q_w = Flowrate of secondary waste sludge (M^3/day)
R = General gas constant (atm.M^3/mol.°K)
r = Recycle ratio of return sludge
Re* = Roughness Reynolds Number in Cohen's equation
Re^{bio} = Removal rate in secondary by biodegradation (g/day)
$Re^{biomass}$ = Biomass generate rate in the reactor (g/day)
Re^{bub} = Removal rate in secondary by diffused aeration (g/day)
Re^{mec} = Removal rate in secondary by surface aeration (g/day)
Re^{sor} = Removal rate in secondary by sorption (g/day)
Re^{vol} = Removal rate in secondary by volatilization (g/day)
SS = Suspended solids concentration in the aeration basin (mg/L)
SS_f = Suspended solids in primary effluent (mg/L)
SS_{ps} = Suspended solids in primary sludge (mg/L)
SS_{raw} = Suspended solids in primary influent (mg/L)
T = Temperature (°C)
T_k = Temperature (°K)
V_b = Molar volume of compound at normal boiling point (cm^3/mol)
V_L = Volume of aeration basin (M^3)
V_{Lpri} = Volume of primary clarifier (M^3)
V_{wind} = Wind speed (m/sec)
XA = Biomass concentration in the aeration basin (mg/L)
XA_f = Biomass concentration in primary effluent(mg/L)
XA_{in} = Biomass concentration input the aeration basin (mg/L)
XA_{ps} = Biomass concentration in primary sludge (mg/L)
XA_{raw} = Biomass concentration in primary influent (mg/L)
XA_w = Biomass concentration in secondary waste sludge (mg/L)
XNV = Nonvolatile solids in the aeration basin (mg/L)
XNV_f = Nonvolatile solids in primary effluent (mg/L)
XNV_{in} = Nonvolatile solids input the aeration basin (mg/L)
XNV_{raw} = Nonvolatile solids in primary influent (mg/L)
XNV_w = Nonvolatile solids in secondary waste sludge (mg/L)
XV = Volatile solids in the aeration basin (mg/L)
XV_f = Volatile solids in primary effluent (mg/L)
XV_{in} = Volatile solids input the aeration basin (with return sludge) (mg/L)
XV_{ps} = Volatile solids in primary sludge (mg/L)
XV_{raw} = Volatile solids in primary influent (mg/L)
XV_w = Volatile solids in secondary waste sludge (mg/L)
Y = Activated cell yield coefficient (mg/mg)
Z = Submergence vertical position (m)
= 0 at the bottom of the basin
= Z_s at the surface of the basin

Greek Letters

α_i = Contribution of group of type i
β = Oxygen transfer efficiency for diffused aeration
$\eta 0$ = Efficiency of primary clarifier
μ_{water} = Viscosity of water (centipoise)
ρ_i = Density of compound (g/cm^3)
ϕ_{oxy} = parameter for oxygen
Ψ_i = ratio of diffusivities of compound to oxygen

LITERATURE CITED

1. Ambrose, R. B., et al., "Waste Allocation Simulation Models," *J. WPCF,* 60(9) (1988).
2. Barton, D., "Intermedia transport of organic compounds in biological wastewater treatment process," *Environ. Prog.,* 6:246–256 (1987).
3. Bhattacharya, S. K., R. V. R. Angara, S. A. Hannah, Jr., D. F. Bishop, R. A. Dobbs, and B. M. Austern, "Fate and effects of selected RCRA and CERCLA compounds in activated sludge system," *USEPA Report,* Cincinnati, Ohio (1989).
4. Blackburn, J. W., "Prediction of organic chemical fates in biological treatment systems," *Environ. Prog.,* 6:217–223 (1987).
5. Bishop, D. F., "Estimation of removability and Impact of RCRA toxics," *USEPA report* (1985).
6. Burns and Roe Industrial Services Corporation, "Fate of priority toxic pollutants in publicly-owned treatment plants," *Final report, Washington, DC: USEPA Report No.* EPA 1440/1-82/303 (1982)
7. Chitra, S. P., R. Govind, "Application of a group contribution method for predicting absorbability on activated carbon," *AIChE J.,* 32:167–169 (1986).
8. Clark, B., G. Henry, D. Mackay, and S. Salenieks, "The fate of toxic organic chemicals in sewage treatment plants," Technology Transfer Conference, Toronto, Ontario (1986).

9. Cohen, Y., W. Cocchio, and D. Mackay, "Laboratory Study of Liquid-Phase Controlled Volatilization Rates in Presence of Wind Waves," *Environ. Prog.*, **12**:553–558 (1978).
10. Desai, S. M., R. Govind, and H. Tabak, "Development of Quantitative Structure-Activity Relationships for Predicting Biodegradation Kinetics," *Environ. Toxicology and Chemistry*, **9**:473–477 (1990).
11. Dobbs, A. R., W. Leping, and R. Govind, "Sorption of Toxic Organic Compounds on WasteWater Solids: Correlation with Fundamental Properties," *Environ. Sci. Technol.*, **23**:1092–1097 (1989).
12. Geating, J., "Literature study of the biodegradability of chemicals in water," *Report No.* EPA-600/2-81-175, USEPA, Cincinnati, Ohio (1981).
13. Grau, P., M. Dohanyos, and J. Chudoba, "Kinetics of multicomponent substrate removal by activated sludge," *Water Research*, **9**:637 (1975).
14. Govind, R., S. Desai, and H. Tabak, "Prediction and Modeling of Biodegradation Kinetics of Hazardous Waste Constituents," Paper presented at the EPA Biosymposium, Cincinnati, Ohio (1989[a]).
15. Govind, R., S. Desai, and H. Tabak, "Estimating biodegradation kinetic constant using Group Contribution Approach," Paper presented at the 1989 Pacichem meeting, Honolulu, Hawaii (1989[b]).
16. Grady, C. P. L., and H. C. Lim, "Biological Wastewater Treatment," Marcel Dekker, Inc. (1980).
17. Grady, C. P. L., "A Model for Single-Sludge Wastewater Treatment Systems," *Water Sci. Technol.*, **18** (1980).
18. Hwang, S. T., "Treatability and pathways of priority pollutants in the biological wastewater treatment," *AIChE Symposium Series*, **77**:316–326 (1981).
19. Jacobsen, B. N., "Behavior of Organic Micropollutants in Biological Waste Water Treatment," (1987).
20. Kincannon, D. F., E. L. Stover, V. Nichol, and D. Medley, "Removal mechanisms for toxic priority pollutant," *J. WPCF*, **55**:157–163 (1983).
21. Ludzack, F. J., M. B. Ettinger, "Chemical structures resistant to aerobic biochemical stabilization," *J. WPCF*, **32**:167–1200 (1960).
22. Lyman, W. J., W. F. Rechl, and D. H. Rosenblatt, "Handbook of Chemical Property Estimation Methods," McGraw-Hill, Inc., New York (1982).
23. MacKay, D., and S. Paterson, "Calculating fugacity," *Environ. Sci. and Technol.*, **15**:1006–1014 (1981).
24. Metcalf & Eddy Inc., "Wastewater Engineering Treatment/Disposal/Reuse," McGraw-Hill, New York, NY (1979).
25. Mills, W. B., et al., "A Screening Procedure for Toxic and Conventional Pollutants Part 1," USEPA EPA report 600/6-82-004a (1982).
26. Namkung, E., and B. E. Rittmann, "Estimating volatile organic compound emissions from publicly-owned treatment works," *J. WPCF*, **59**:670–678 (1987).
27. Perry, R. H., and C. H. Chilton, "Chemical Engineers' Handbook Fifth Edition," McGraw-Hill, New York (1973).
28. Roberts, P. V., "Modeling volatilization organic solute removal by surface and bubble aeration," *J. WPCF*, **56**:157–164 (1984).
29. Stover, E. L., et al., "Biological treatability of specific organic compounds found in chemical industry wastewaters," *J. WPCF*, **55**:97–109 (1983).
30. Sundstrom, D. W., and H. E. Klei, "Wastewater Treatment," Prentice-Hall (1979).
31. Technology Transfer, "Process design manual for upgrading existing wastewater treatment plants," USEPA, EPA report, 625/1-71/004a (1974).

FATE corrected 6/20/35

A commercial PC version of the Fate model is available from Morris Computer Systems Inc., 1020 Wayne Ave., Cincinnati, OH 45215.

Oxygen Membrane Electrode Used as a Toxicity Biosensor

David K. Goldblum, Steven E. Holodnick, Khalil H. Mancy
School of Public Health, The University of Michigan, Ann Arbor, MI 48109

and

Dale E. Briggs
College of Engineering, The University of Michigan, Ann Arbor, MI 48109

Three biosensor configurations that included a dissolved oxygen electrode and yeast cells (Saccharomyces cerevisiae) were evaluated as a means to assess the environmental effects of toxic chemicals. The configurations were: closed suspension—assay medium closed to air and cells suspended in the medium; open suspension—assay medium open to air and cells suspended in medium; and biofilm electrode (BFE)—assay medium open to air but cells immobilized on the surface of the electrode. The BFE was the most advantageous configuration based on assay times and detection limits.

INTRODUCTION

Toxic chemicals in the environment have prompted increased public awareness of environmental concerns. Two main issues are environmental effects (damage), and control and management of the risks associated with toxic chemicals. When addressing environmental effects, the human health, ecology, and abiotic sectors need to be considered. For control aspects, risk of exposure and regulatory aspects need to be addressed.

There is a need to develop simpler and more rapid procedures for assessing environmental effects of toxic chemicals [1]. A biofilm electrode consisting of a dissolved oxygen (DO) membrane-covered electrode coupled with immobilized yeast (*Saccharomyces cerevisiae*) cells was developed in the present work. This biosensor constitutes a simple and rapid procedure for screening toxic chemicals in the environment based on changes in respiratory activity of the test cells.

The DO membrane-covered electrode under consideration is amperometric, i.e., it generates a current which is proportional to the oxygen concentration on the plastic (polyvinyl chloride) membrane surface. The base electrode uses a silver cathode and a lead anode. At the cathode, the oxygen is reduced to hydroxide ion, whereas at the anode, the lead is oxidized. The DO electrode is also said to be Galvanic, since it does not require an external voltage for its operation. This DO membrane-covered electrode was first described by Mancy, et al. [2]. In the present work, this DO electrode will be referred to as a DOE.

In the three configurations considered in Figure 1, the DOE is used as the oxygen sensor and indicates the oxygen level on the surface of the plastic membrane of the DOE. The first configuration is the closed suspension, where the assay medium is closed to the atmosphere, and the yeast cells are suspended in the assay medium. The second configuration is the open suspension, where the assay medium is open to the atmosphere, and the yeast cells are suspended in the assay medium. The third configuration is the biofilm electrode (BFE), where the assay medium is open to the atmosphere, and the yeast cells are immobilized on the surface of the DOE. A detailed schematic of the BFE is illustrated in Figure 2.

BACKGROUND

There has been a widespread use of membrane-covered electrode systems to monitor gases and metabolites in biological

David Goldblum is currrently a Captain, USAF, Occupational and Environmental Health Laboratory, Brooks AFB, TX 78235.

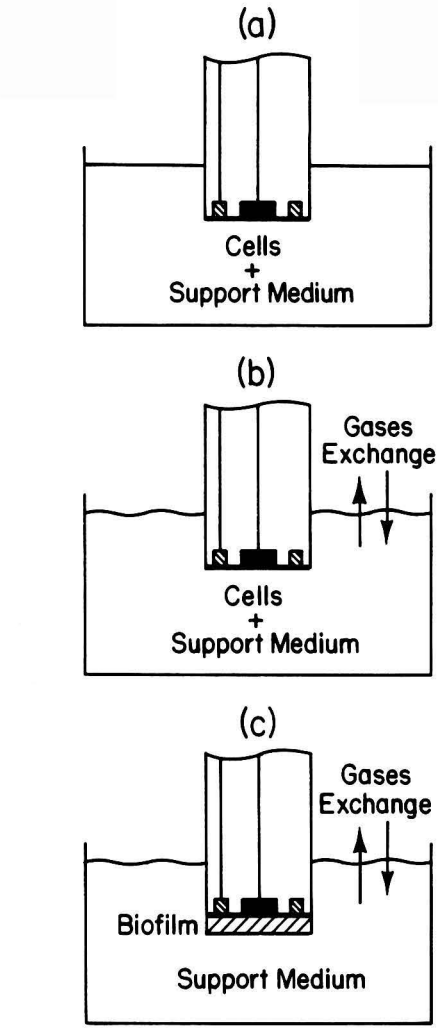

FIGURE 1. Biosensor Systems.

as well as environmental media, e.g., enzyme electrodes, and biofilm electrodes [3]. Membrane-covered electrodes are those with a selectively permeable membrane, e.g., polymeric membranes, which separates the electrode itself from the test solution. In the galvanic cell oxygen analyzer the membrane is permeable to gases such as oxygen. Surface active and electroactive substances, which may interfere with the electrode reactions, are screened out. Several authors [4,5] have specifically addressed the issue of selectively permeable membranes. Oxygen has been the gas most extensively measured with membrane covered electrodes [2,6–9]. Other gases so measured include carbon dioxide [6,7,10], ozone [11], and chlorine dioxide [12].

Enzyme electrodes are membrane-covered electrodes such that the membrane is an enzyme layer on the surface of the base electrode and monitor a metabolite (substrate) through that particular enzymatic reaction. These highly selective bioelectrode systems have been used to monitor glucose [13–18], urea [19], lactate [20–24], pyruvate [25], cholesterol [26], creatinine [27], salicylate [28], and 1-alanine [29].

The BFE is an extension of the membrane-covered enzyme electrode. In the BFE, a film of microorganisms is immobilized on the DOE and the rate of respiration of the biofilm is determined by monitoring changes in the oxygen concentration within the biofilm, or at the interface between the biofilm and the membrane of the DOE. Recent applications of the BFE are the cellular electrode for antitumor drug screening by Liang and Wang [30] as well as the present BFE's use in viral screening by Holodnick [31]. Another BFE example is the bacterial electrode for determination of monomethyl sulfate [32], which consists of the physical entrapment of the monomethyl sulfate degrading bacteria, *Hyphomicrobium*. A multispecies biofilm model was developed for computer simulation of symbiosis and/or competition for space and common substrates between several microbial species [33]. The concentrations of microbial cells in suspension were determined with a graphite electrode [34].

THEORY

The assumptions, mass balance, boundary and/or initial conditions, and final solution for the oxygen concentration are considered for three configurations illustrated in Figure 1. Oxygen excess ($C \gg K_s$) in the Monod Equation [35–37] (Equation 1) is assumed for all configurations.

$$RESPIRATION\ RATE = \frac{kNC}{K_s + C} = kN. \qquad (1)$$

Moreover, the yeast cells are in the exponential growth phase during the test runs and their growth rate follows 1st order kinetics (Equation 2).

$$N = N_o e^{k't} \qquad (2)$$

The mathematical analysis begins with an overall mass balance on oxygen (Equation 3).

$$ACCUMULATION\ (ACC) = IN - OUT + GENERATION\ (GEN) \qquad (3)$$

The GEN term is the negative of the Monod Respiration Rate

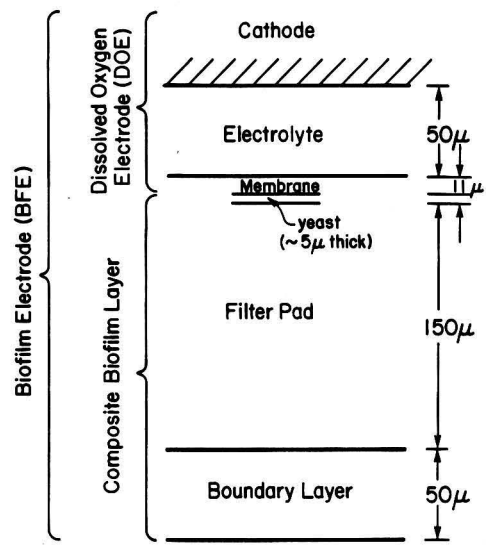

FIGURE 2. Composite Structure of DOE Biofilm.

corrected 27 Jul 93/AP In Equation (6) should read

$$C = C_s - \frac{kN_o}{k'}\left(e^{k't} - 1\right) \quad \text{---} \quad (6)$$

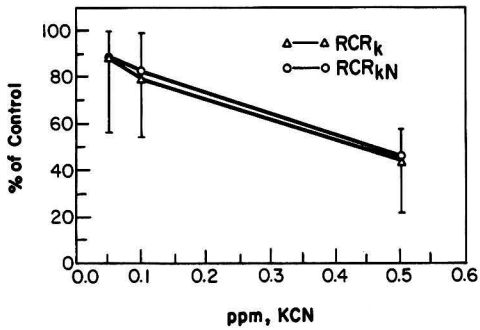

FIGURE 3. Open Suspension Response to Potassium Cyanide (KCN).

from equation 1 multiplied by the volume of the system, i.e., $GEN = -kNV$. The ACC term is VdC/dt.

In the closed suspension, IN = OUT = 0, so that Equation 3 reduces to:

$$\frac{dC}{dt} = -kN = -kN_o e^{k't} \tag{4}$$

The initial condition is that the assay medium is air-saturated at $t = 0$, i.e., $C = C_s$ @ $t = 0$. If the number of cells is taken as constant during the test run, i.e., the yeast cell growth is negligible, then the oxygen concentration as a function of time is:

$$C = C_s - kNt \tag{5}$$

If the growth of the yeast cells is considered, then the oxygen concentration is represented by:

corrected 1 Aug 93/AP

$$C = C_s - \frac{kN_o}{K_s}\left(e^{k't} - 1\right) \tag{6}$$

For the closed suspension, the oxygen in the assay medium is depleted rapidly, so that Equation 5 would apply.

In the open suspension $IN - OUT = k_L A_L (C_s - C)$, which is the oxygen mass transfer from the air atmosphere into the assay medium. Thus, the oxygen mass balance becomes:

$$\frac{dC}{dt} = \frac{k_L A_L}{V}(C_s - C) - kN = \frac{k_L A_L}{V}(C_s - C) - kN_o e^{k't} \tag{7}$$

The assay medium is air-saturated at $t = 0$, as is the case with the closed suspension, i.e., $C = C_s$ @ $t = 0$. If the number of cells is taken as constant during the test run, i.e., the yeast cell growth is taken as negligible, then the oxygen concentration as a function of time is:

$$C = C_s - \frac{kVN}{k_L A_L}\left(1 - e^{\frac{-k_L A_L t}{V}}\right) \tag{8}$$

If the growth of the yeast cells is considered, then the oxygen concentration becomes:

$$C = C_s - \frac{kN_o}{k' + \frac{k_L A_L}{V}}\left(e^{k't} - e^{\frac{-k_L A_L t}{V}}\right) \tag{9}$$

There is the potential of losing sensitivity in the open suspension analysis if the oxygen mass transfer from the air is much larger than the respiratory consumption by the yeast cells. The determination of k for the open suspension, is discussed in detail by Goldblum [38].

In the BFE configuration, steady state is attained quite rapidly, so that ACC in the mass balance vanishes (i.e., $dC/dt = 0$) and the number of cells can be taken as constant during the test run. Thus, the oxygen mass balance becomes:

$$0 = D\frac{d^2C}{dz^2} - kN \tag{10}$$

The boundary conditions are that $C = C_s$ @ $z = 0$, and $dC/dz|_{z=b} = -(P_m C_b)/(L_p D)$, where $C_b = C$ at $z = b$. Note that $z = 0$ at the biofilm-assay medium interface, and $z = b$ at the biofilm-plastic membrane interface, and the thickness of the biofilm is b. The assay medium is maintained at air-saturation during the test run by vigorously stirring, so the outer surface of the biofilm is assumed to be air-saturated. The second boundary condition results from the oxygen flux at the plastic membrane interface, which is proportional to the current produced by the DOE, or,

$$flux = \frac{i}{nFA} = -D\left.\frac{dC}{dz}\right|_{z=b} \tag{11}$$

using Fick's law of diffusion [39] along with the electrode sensitivity coefficient (ϕ) from Mancy's analysis [2].

$$\phi = \frac{nFAP_m}{L_p} \tag{12}$$

It is important to note that ϕ is the proportionality constant between the current produced by the DOE and $C_b (i = \phi * C_b)$. Equation 10 can be solved for C. Then, if $z = b$, the solution or C_b is:

$$C_b = \frac{C_s - \frac{kNb^2}{2D}}{1 + \frac{P_m b}{L_p D}} \tag{13}$$

In the biofilm, the steady state condition simplifies the analysis considerably. From Equation 13, k is computed from the observed C_b, which leads to:

$$k = \frac{2D}{Nb^2}\left[C_s - C_b\left(1 + \frac{P_m b}{L_p D}\right)\right] \tag{14}$$

For the open suspension and the biofilm electrode, results are expressed as a respiratory control ratio (RCR):

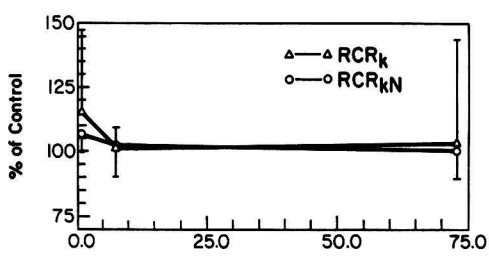

FIGURE 4. Open Suspension Response to 2,4-Dinitrophenol.

$$RCR = RCR_k = \frac{k_{test}}{k_{control}} \quad (15)$$

or

$$RCR = RCR_{kN} = \frac{kN_{test}}{kN_{control}} \quad (16)$$

It is noteworthy that RCR is based on the cellular respiration rate (Equation 15) or on the respiration rate of the entire biomass (Equation 16).

For open suspension analyses, the control and test data on respiration rates are obtained from separate runs. Although, the experimental design is to have the same number of cells for each run in a given series, there is variation in cell counting as well as in the cell-assay medium suspension so that the number of cells in the control run need not be exactly the same as the number of cells in the test run. Thus, RCR based on k will differ slightly from RCR based on kN (see Figures 3 and 4). For the biofilm electrode analyses, the control and test data on respiration rates are obtained from the same run, so that the number of cells in the test and control data is the same. Thus, RCR based on k will be equal to RCR based on kN.

METHODS

Two test chemicals used in the present work were: (a) potassium cyanide (KCN), which is a strong respiratory inhibitor; and (b) 2,4-dinitrophenol (2,4 DNP), which is strong respiratory uncoupler [*40*], i.e., it stimulates respiration. The yeast cells are incubated [*41*] at 30°C in acetate buffer growth medium with shaking. The acetate growth media consists of 0.0182 kg sodium acetate + 1.15 mL glacial acetic acid + 0.014 kg yeast nitrogen base (Difco Laboratories, Detroit) in 1 liter volume of aqueous solution (pH = 5.8). The acetate buffer assay medium is the growth medium less the 0.014 kg yeast nitrogen base. An inoculum of yeast is added to 75 mL of growth medium in an Erlenmeyer flask, which is put on a shaker for 36-48 hours for the suspensions and 24-36 hours for the biofilm electrode. After incubation, cell counts are taken using a hemocytometer (Spencer Brightline 0.1 mm, American Optical Co.) coupled with a Zeiss microscope (10 × oc/10 × obj). Standards for the two chemicals were prepared using distilled water. The DOE current was converted to voltage and recorded with a strip chart recorder.

The system was built in house for the most part. The stir plate assembly was constructed from a turntable (Bang and Olufson model 2400) with two preset stir rates (340 and 440 rpm). A Teflon coated stir bar was rigidly held in place at the bottom of the center of the assay chamber, about 1.8 cm from the magnet in the stir plate assembly. The assay chamber was set in an isothermal bath at 30°C, using a constant temperature circulator (Polyscience Corporation, Evanston, IL).

For the suspension test runs, it is necessary to incubate for a somewhat longer (36-48 hours) period to assure that the cell count has reached approximately 3×10^6 cells/mL. Without adequate biomass, the atmospheric aeration will drive the current to near saturation values, i.e., atmosphere reaeration would dominate cellular respiration. If the cells grow unusually fast, it becomes necessary to dilute the cell suspension with acetate buffer assay media (1:3 to 1:5) to get the final cell count near 3 million cells per mL, since this condition was observed to be experimentally optimal. In these open suspension respiration test runs, 55 mL of yeast cell suspension was monitored for three hours. For a given yeast cell suspension the first test run is the control, and subsequent test runs involve progressively higher levels of KCN or 2,4 DNP.

In the closed suspensions the oxygen in the assay medium is depleted within approximately 20 minutes, so that the closed suspension is of limited value, albeit its theoretical analysis is quite simple [*42*].

For the biofilm electrode, it is necessary to incubate for 24-36 hours to produce yeast cells in the exponential growth phase. For these test runs, 55 mL of acetate buffer assay medium is used and the yeast cells are center-filtered onto a microporous filter pad (Gelman Sciences, Ann Arbor, MI). The present configuration responds well when approximately 3 million cells are immobilized. This cell mass consumes dissolved oxygen at a rate which yields approximately 40% of the current of the base DOE, a condition which allows for the measurement of respiratory inhibition as well as respiratory uncoupling. During these test runs, the control datum is obtained after steady state is obtained then a dose of either KCN or 2,4 DNP is added to the assay medium. After steady state is again achieved, the test datum for the run is obtained. At this point, 100 ppm of KCN is added to totally inhibit biofilm respiration. In these runs, C_b is obtained for both the control and test data to give the cellular respiration rate k for both data. After 100 ppm KCN is added, C_k is then obtained, which is C_b when $k = 0$.

RESULTS

For the open suspension, the process for obtaining k was complex, due to the changing response for the initial (1-5 min) and later (130-180 min) time regimes [38]. These time regimes result from the analysis of the time derivative of C from Equation 9.

The assay chamber surface area available for oxygen mass transfer from the air was approximately 14.6 cm^2. This was based on the electrode having a 1-inch (2.54 cm) diameter and the assay chamber having a 2-inch (5.08 cm) diameter. From reaeration experiments, the oxygen mass transfer coefficient, k_L was about 0.19 cm/min. The growth rate constant, k', was found to be 0.002 min^{-1} in a separate incubation experiment.

From studies of control cell respiration, k was obtained for both the initial and later time regimes. It was concluded that k from the later time regime was more reliable, due to the uncertainty in the initial slope and the high variability in the k value obtained from the initial time regime. The best reproducibility was obtained using the k' and k values in the later time regime, and is the reason the respiration run lasts for three hours. Furthermore, when doing a series of increasing doses, the runs are done sequentially. Therefore, evaluating one concentration and a control takes about 5 hours.

Open suspension tests with the chemicals resulted in a detection limit of 0.2-0.4 ppm for KCN (correlation coefficient between RCR and [KCN] > 0.99 up to approximately 0.5 ppm KCN, see Figure 3). Respiratory uncoupling by 2,4, DNP was not detected at concentrations less than or equal to 73 ppm 2,4 DNP, see Figure 4. Thus, the open suspension detected the effect of the respiratory inhibition of KCN, but not the respiratory stimulatory uncoupling of 2,4 DNP.

For the biofilm electrode, k was obtained from Equation 14. The working surface area of the electrode was 1.33 cm^2, the number of cells was about 3-4 million, and the biofilm thickness was 205 μm. The biofilm consists of the yeast cell layer (5 μm), the micropore filter pad (150 μm), and the boundary layer (50 μm). The biofilm is taken as one composite diffusion layer, but can be taken as three diffusion layers in series. The one diffusion layer biofilm model and the three diffusion layer biofilm model are compared by Goldblum [*43*]. The overall effective O_2 diffusivity is about $3\text{-}4 \times 10^{-6} cm^2/sec$, the thickness of the plastic membrane is 0.428 mil (10.86 μm), and the permeability of the plastic membrane, P_m, is approximately $10^{-7} cm^2/sec$. Average values for the oxygen concentrations are: $C_s = 7.40 mg/L$, $C_k = 4.66 mg/L$, and $C_b = 2.79$ mg/L [*38*]. The assay time in this test is about 1.5 hours, which allows for the acquisition of both the control and test data.

Biofilm electrode tests with the chemicals resulted in a de-

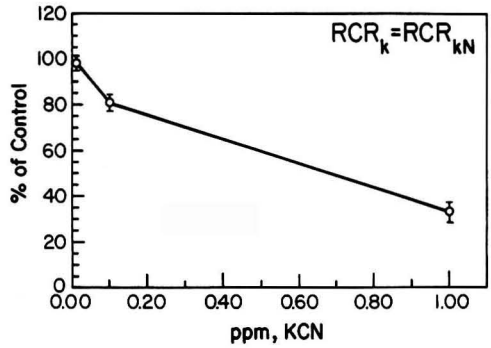

FIGURE 5. Biofilm Electrode (BFE) Response to Potassium Cyanide (KCN).

tection limit of 0.05-0.2 ppm for KCN (correlation coefficient between RCR and [KCN] > 0.99 up to 1 ppm KCN, see Figure 5), and a detection limit of 10-20 ppm for 2,4 DNP (correlation coefficient between RCR and [2,4 DNP] is approximately 0.97 up to 42 ppm 2,4 DNP, see Figure 6). Thus, the biofilm electrode detected the effect of both the respiratory inhibition of KCN and the respiratory stimulatory uncoupling of 2,4 DNP.

CONCLUSIONS

In comparing the open suspension with the biofilm electrode configuration, the open suspension test has advantages in its relative simplicity in experimental set up and mathematical analysis. The open suspension oxygen concentration is a function of time but independent of the spatial coordinate in the assay chamber. In open suspension respiration test runs, there is little vulnerability to variation in experimental technique. The open suspension would have much smaller assay times if the initial time regime could be made to show more reproducibility, otherwise its assay times are considerably longer using the later time regime. However, the biofilm electrode has advantages in its shorter assay times and lower detection limit capabilities, but the mathematical analysis would be rather difficult if the steady state condition were not justified. The oxygen concentration is a function of the distance from the assay medium-biofilm interface, and is independent of time in the steady state condition.

The biofilm electrode is the most advantageous configuration evaluated. The BFE allows for the rapid and reproducible measurement in inhibition and uncoupling of yeast respiratory activity. This configuration can be used most feasibly when in-situ measurements are required. It is possible to have this toxicity biosensor serve as an effective screening tool for toxic chemicals in environmental samples, based on changes in the respiration rate of the immobilized cells.

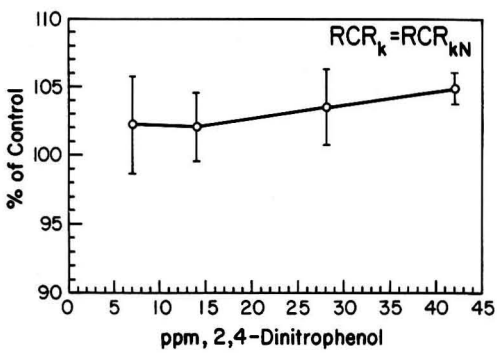

FIGURE 6. Biofilm Electrode (BFE) Response to 2, 4-Dinitrophenol.

NOTATION

Open Suspension

A_L = area available for O_2 mass transfer from the atmosphere into the aqueous solution
C = O_2 concentration in the aqueous solution
C_S = O_2 concentration in the aqueous solution under air-saturation conditions
k = maximum specific or cellular O_2 utilization (consumption) rate via respiration per unit volume
k_L = O_2 mass transfer coefficient in the liquid part of the boundary layer at the gas-liquid interface
k' = first order growth rate constant in Equation 2
N = total number of cells in the aqueous solution
N_0 = total number of cells in the aqueous solution initially (t = 0)
RCR = respiratory control ratio = ratio of a respiration parameter for the test run to the same respiration parameter for the control run expressed as a percentage

Biofilm Electrode (BFE)

A = cross-sectional area of the biofilm (actually area of the working electrode surface)
C = O_2 concentration in the biofilm
C_b = O_2 concentration in the biofilm at the plastic membrane/cell layer interface
C_k = O_2 concentration in the biofilm at the plastic membrane/cell layer interface after the biota are killed off by 100 ppm KCN
C_S = O_2 concentration in the biofilm under air-saturation conditions
D = diffusivity of O_2 in the biofilm
F = Faraday's Constant
i = current readout from the electrode
k = maximum specific or cellular O_2 utilization (consumption) rate via respiration per unit volume
N = number of cells filtered onto the filter pad
n = number of equivalents per mole of O_2 reduced to hydroxide ion (n = 4)
P_m = permeability of plastic membrane
RCR = respiratory control ratio = ratio of a respiration parameter for the test run to the same respiration parameter for the control run expressed as a percentage
z = axial distance into biofilm away from the aqueous bulk solution (diffusion path)

LITERATURE CITED

1. Mancy, K. H., "Development and Application of Biosensors in Pollution Control Programs," *International Symposium on Electrochemical Sensors,* June 12–14, 1984, Rome, Italy.
2. Mancy, K. H., D. A. Okun, and C. N. Reilley, "A Galvanic Cell Oxygen Analyzer," *J. Electroanal. Chem.,* **4**, 65 (1962).
3. Davis, G., "Advances in Biomedical Sensor Technology: a Review of the 1985 Patent Literature," *Biosensors,* **2**, 101 (1986).
4. Kunze, K., and D. W. Lubbers, "Absolute P_{O_2}-Measurements with Pt-Electrodes Applying Polarizing Voltage

Pulsing," *Oxygen Transport to Tissue,* Editors, H. I. Bicher and D. F. Bruley, Plenum, New York, 35 (1973).
5. Tang, T. E., V. G. Murphy, A. W. Hahn, and R. E. Barr, "The Operation of Platinum Oxygen Sensing Microelectrodes," *J. of Bioengineering,* **2**, 381 (1978).
6. Hahn, C. E. W., "Techniques for Measuring the Partial Pressures of Gases in Blood. Part I - In Vitro Measurements," *J. Phys. E.: Sci Instrum.,* **13**, 470 (1980).
7. Hahn, C. E. W., "Techniques for Measuring the Partial Pressures of Gases in Blood. Part II - In Vivo Measurements," *J. Phys. E.: Sci Instrum.,* **14**, 783 (1981).
8. Hitchman, M. L., "Measurement of Dissolved Oxygen," *Chemical Analysis,* Editors, P. J. Alving, J. D. Winefordner, and I. M. Kolthoff, **49**, John Wiley & Sons, New York, (1978).
9. Lilley, M. D., J. B. Story, and R. W. Raible, "The Chronoamperometric Determination of Dissolved Oxygen Using Membrane Electrodes," *J. Electroanal. Chem.,* **23**, 425 (1969).
10. Opdycke, W. N., and M. E., Meyerhoff, "Development and Analytical Performance of Tubular Polymer Membrane Electrode Based Carbon Dioxide Catheters," *Analytical Chemistry,* **58**, 950 (1986).
11. Smart, R. B., R. D. Herrera, and K. H. Mancy, "In Situ Voltammetric Membrane Ozone Electrode," *Analytical Chemistry,* **51**, 2315 (1979).
12. Herrera, R. D., and K. H. Mancy, "Voltammetric Membrane Chlorine Dioxide Electrode," *Analytical Letters,* **13(A7)**, 561 (1980).
13. Clark, L. C., and C. A. Duggan, "Implanted Electroenzymatic Glucose Sensors," *Diabetes Care,* **5**, No. 3, 174 (1982).
14. Cleland, N., and S. O. Enfors, "Monitoring Glucose Consumption in *Escherichia Coli* Cultivation with an Enzyme Electrode," *Analytica Chimica Acta,* **163**, 281 (1984).
15. Gough, D. A., J. Y. Lucisano, and P. H. S. Tse, "Two-Dimensional Enzyme Electrode Sensor for Glucose," *Analytical Chemistry,* **57**, 2351 (1985).
16. Olsson, B., H. Lundbock, and G. Johanson, "Theory and Application of Diffusion-Limited Amperometric Enzyme Electrode Detection in Flow Injection Analysis of Glucose," *Analytical Chemistry,* **58**, 1046 (1986).
17. Sonawat, H. M., S. P. Ratna, and G. Govil, "Covalent Immobilization of FAD and Glucose Oxidase on Carbon Electrodes," *Biotechnology and Bioengineering,* **26**, 1066 (1984).
18. Wiech, H. J., G. H. Heider, and A. M. Yacynych, "Chemically Modified Reticulated Vitreous Carbon Electrode with Immobilized Enzyme as a Detector in Flow-Injection Determination of Glucose," *Analytica Chimica Acta,* **158**, 137 (1984).
19. Szuminsky, N. J., A. K. Chen, and C. C. Liu, "A Miniature Palladium-Palladium Oxide Enzyme Electrode for Urea Determination," *Biotechnology and Bioengineering,* **26**, 642 1984).
20. Cenas, N., J. Rozgaite, and J. Kulys, "Lactate, Pyruvate, Ethanol, and Glucose-6-Phosphate Determination by Enzyme Electrode," *Biotechnology and Bioengineering,* **26**, 551 (1984).
21. Durliat, H., M. Comtat, and A. Baudras, "Spectrophotometric and Electromechanical Determination of L(+)-Lactate in Blood by Use of Lactate Dehydrogenase from Yeast," *Clinical Chemistry,* **22**, No. 11, 1802 (1976).
22. Durliat, H., M. Comtat, and J. Mahnec, "A Device for the Continuous Assay of Lactate," *Analytica Chimica Acta,* **106**, 131 (1979).
23. Mascini, M., D. Moscone, and G. Palleschi, "A Lactate Electrode with Lactate Oxidase Immobilized on Nylon Net for Blood Serum Samples in Flow Systems," *Analytica Chimica Acta,* **163**, 45 (1984).
24. Soutter, W. P., F. Sharp, and D. M. Clark, "Bedside Estimation of Whole Blood Lactate," *Br. J. Anaesth.,* **50**, 445 (1978).
25. Suand-Chagny, M. F., and F. G. Gonon, "Immobilization of Lactate Dyhydrogenase on a Pyrolytic Carbon Filter Microelectrode," *Analytical Chemistry,* **58**, 412 (1986).
26. Satoh, I., I. Karube, and S. Suzuki, "Enzyme Electrode for Free Cholesterol," *Biotechnology and Bioengineering,* **19**, 1095 (1977).
27. Meyerhoff, M. E., and G. A. Rechnitz, "An Activated Enzyme Electrode for Creatinine," *Analytica Chimica Acta,* **85**, 277 (1976).
28. Fonong, T., and G. A. Rechnitz, "Enzyme Electrode for the Determination of Salicylate," *Analytica Chimica Acta,* **158**, 357 (1984).
29. Pau, C. P., and G. A. Rechnitz, "Bound Cofactor/Dual Enzyme Electrode System for L-Alanine," *Analytica Chimica Acta,* **160**, 141 (1984).
30. Liang, B. S., X. M. Li, and H. Y. Wang, "Cellular Electrode for Antitumor Drug Screening," *Biotechnology Progress,* **2**, No. 4, 187 (1986).
31. Holodnick, S. E., "The Biofilm Electrode Sensor System for Acute Toxicity and Viral Screening," PhD Thesis in Environmental Health Science, University of Michigan, (1988).
32. Schar, H. P., and O. Ghisalba, "*Hyphomicrobium* Bacterial Electrode for Determination of Monomethyl Sulfate," *Biotechnology and Bioengineering,* **27**, 897 (1985).
33. Wanner, O., and W. Gujer, "A Multispecies Biofilm Model," *Biotechnology and Bioengineering,* **28**, 314 (1986).
34. Matsunaga, T., and Y. Namba, "Selective Determination of Microbial Cells by Graphite Electrode Modified with Adsorbed 4,4′- Bipyridine," *Analytica Chimica Acta,* **159**, 87 (1984).
35. Benefield, L., and F. Molz, "Mathematical Simulation of a Biofilm Process," *Biotechnology and Bioengineering,* **27**, 921 (1985).
36. Rittman, B. E., and P. L. McCarty, "Model of Steady-State-Biofilm Kinetics," *Biotechnology and Bioengineering,* **22**, 2343 (1980).
37. Rittman, B. E., and P. L. McCarty, "Evaluation of Steady-State-Biofilm Kinetics," *Biotechnology and Bioengineering,* **22**, 2359 (1980).
38. Goldblum, D. K., "Biofilm Electrode for Screening of Toxic Chemicals: Electrode System Characterization," PhD Thesis in Chemical Engineering and Environmental Health Science, University of Michigan, (1988).
39. Fahien, R. W., *Fundamentals of Transport Phenomena,* McGraw-Hill, New York, 60 (1983).
40. Lehninger, A. L., *Biochemistry,* 2nd Ed., Worth Publishers, New York, 519 and 611 (1975).
41. Parulekar, S. J., G. B. Semones, M. J. Rolf, J. C. Lievense, and H. C. Lim, "Induction and Elimination of Oscillations in Continuous Cultures of *Saccharomyces Cerevisiae,*" *Biotechnology and Bioengineering,* **28**, 700 (1986).
42. Haubenstricker, M. E., "Development of a Toxicity Biosensor Based on Changes in Mitochondrial Respiration Rates," PhD Thesis in Environmental Health Science, University of Michigan, (1984).
43. Goldblum, D. K., S. E. Holodnick, K. H. Mancy, and D. E. Briggs, "Oxygen Transport in Biofilm Electrodes for Screening of Toxic Chemicals," *AIChE Journal,* **36**, 19 (1990).

Development of an Immobilized Microbe Bioreactor for VOC Applications

David D. Friday and Ralph J. Portier

Institute for Environmental Studies, Louisiana State University, Baton Rouge, LA 70895.

In this paper, the technical challenges to building a bioreactor capable of removing significant amounts of chlorinated VOCs (ethylene dichloride specifically) from groundwater or wastewater effluents is discussed. Key considerations include appropriate construction materials, selection of a low cost microbial immobilization support, identification of microorganisms with high VOC metabolic uptake rates, reactor instrumentation and control system, optimum reactor mixing environment, and reactor aeration methods. Operating configuration and techniques to maximize performance in a 75-liter pilot reactor are presented with field performance data.

INTRODUCTION

This paper describes the development of a bioprocess system for removing significant concentrations of volatile organic compounds (VOCs) from contaminated water sources. The core of the system is an immobilized microbe bioreactor in which specific adapted microbial strains can be established within an inert porous packing. The process design minimizes stripping phenomenon to maintain volatiles as a substrate in the aqueous phase under aerobic conditions. The reactor can be thermally sterilized to allow propagation of desirable axenic or mixed cultures on the internal surface of the porous packing. Few applications have focused on hazardous waste effluent/groundwater biotreatment in which non-indigenous microbial assemblages have been immobilized to effect biotreatment. To show the selectivity that can be obtained with this approach, the halogenated aliphatic, ethylene dichloride (EDC), was targeted for bacterial mineralization using this process.

A step-wise approach was used in the design of the process. Both a literature search and laboratory effort were carried out concurrently to identify a pure or mixed microbial culture with demonstrated EDC metabolizing capabilities. Next, a cost-effective immobilization/adsorption media was identified, to provide a means of retaining the target bacterial species within the reactor. Then a reactor configuration with associated mixing and transport attributes was selected. Additionally, a set of design constraints was adopted with the intent of driving the final design toward maximum productivity (observed organic removal rate), maximum suitability for the assumed operating environment, high reliability, low maintenance, and low cost. Finally, material and construction specifications were developed to yield an operating prototype consistent with the above.

LITERATURE REVIEW/DESIGN CONSIDERATIONS

The main commodity uses of ethylene dichloride are in the synthesis of the gasoline anti-knock compound tetraethyl-lead (TEL) and as an intermediate to the synthesis of vinyl chloride. Since 1986, the EPA has limited the amount of lead in leaded gasoline to 0.25 grams/liter, eliminating this industrial application in the United States. However the solvent continues to be produced in large quantities for export to foreign TEL manufacturers. Vinyl chloride is the monomeric reactant used in PVC synthesis. Enormous quantities of EDC are produced for this application alone. In 1989, the estimated world production capacity for EDC was estimated to be 9.3 billion pounds per year [*12*]. EDC has been demonstrated to be both mutagenic and tumorogenic, and is a suspected carcinogen [*16,31*].

David D. Friday is presently at Environmental Remediation Inc., Baton Rouge, LA.
Correspondence concerning this paper should be addressed to Ralph J. Portier.

Table 1 Selected Physical Properties of EDC

Chemical Formula[a]:	CH_2ClCH_2Cl
Molecular Weight[a]:	98.96 gm/gmole
Boiling Point[a]:	83.5 deg. C
Liquid Density[a]:	1.2569 gm/cm^3 @ 4 deg. C
Flash Point[a]:	13 deg. C.
Henry's Law Constant (dimensionless mole fraction)[b]:	0.050
Water Solubility[b]:	8700 ppm @ 25 deg. C
Vapor Pressure[c]:	40 mm Hg @ 10 deg. C
	60 mm Hg @ 18.1 deg. C
	100 mm Hg @ 29.5 deg. C

[a] Source: The Merck Index, 10th Edition, Windholz M. editor, Merck & Co., Inc., Rahway, NJ, 1983, p. 3743.
[b] Source: Reference 13.
[c] Source: Reference 27.

EDC is also a remarkably persistent compound, with an estimated half-life due to abiotic hydrolysis of approximately 50 years [37]. Table 1 indicates some selected physical properties of EDC.

Even accepting biodegradation as a viable means of removing chlorinated hydrocarbons from the environment, the volatile nature of these compounds precludes carrying out such a process in a conventional open system. Dilling [13] made a comprehensive study of the evaporation kinetics of chlorinated hydrocarbons in well-mixed aqueous systems. His results show that none of the compounds tested had half-lives greater than one hour, and most were between 20 and 30 minutes. Even when sorptive materials (dolomite, bentonite clay and peat moss) were added, the disappearance rates were depressed by less than a factor of two, indicating the major pathway for loss from natural systems is evaporation [14].

Selection of Biocatalyst

Several groups have reported on the microbial metabolism of 1,2-dichloroethane. Stucki et al. [35] used batch enrichment techniques to develop aerobic populations capable of using dichloromethane, 2-chlorethanol and 1,2-dichloroethane as sole carbon and energy sources, but succeeded in obtaining pure cultures for only the first two compounds. Later by using terminal dilution techniques the same investigator isolated a pure culture capable of metabolizing up to 5mM EDC in batch culture with a specific growth rate of 0.08/h [36]. No degradation products other than chlorides were detected in cell culture supernatants.

A good deal of study has been devoted to employing methanogenic bacteria to degrade low concentrations of halogenated methanes and ethanes. McCarty and Bouwer [8] observed 1,2-dichloroethane transformation to carbon dioxide in an anerobic mixed culture under methanogenic conditions. However, the initial concentration was small (about 0.6 mM), and the half-life of the reactant was about 25 weeks. An attempt to exploit this activity in continuous culture was unsuccessful. Belay and Daniels [5] tested the degradative ability of three strains of methanogens on various brominated and chlorinated solvents, including EDC. They observed the production of ethylene as a metabolic end product concomitant with the disappearance of EDC. EDC also became inhibitory to microbial growth at concentrations between 0.2 and 1 mM.

Janssen and co-workers isolated a pure aerobic culture using enrichment techniques with chemostat cultivation [21]. The bacterial strain (GJ10) was capable of degrading EDC in concentrations up to 15 mM and grew exponentially on either 1,2-dichloroethane or chloroethanol with a specific growth rate 0.11/h and 0.13/h, respectively. Cell-free extracts of GJ10 contained 1,2-dichloroethane dehalogenase and chloroacetate dehalogenase, both of which formed constitutively. Growth rate was decreased by almost 50% if vitamins were withheld from the growth media. Subsequent studies [20] revealed that

Table 2 Biotransformation of Halogenated Ethanes By Microorganisms

Compound	Product(s)	System
Ethanes		
1,1-Dichloroethane	Chloroethane	A/M/m
1,2-Dichloroethane	Carbon Dioxide	O/P/p
	Chloroethanol	O/P/x
	Carbon Dioxide	A/M/m
1,1,1-Trichloroethane	1,1-Dichloroethane	A/S
		A/M/m
		A/M
	Not identified	A/M/m
1,1,2,2-Tetrachloroethane	1,1,2-Trichloroethane	A/M/m
		A/M
Hexachloroethane	Tetrachloroethane	O/M/s
Bromoethane		O/P/x
1,2-Dibromoethane	Ethene	O/S
	Ethene	A/M/m/r
	Carbon Dioxide	O/S

[a] Comma separates different experimental systems that result in similar products. Slashes separate information regarding each experiment. O = aerobic, A = anaerobic, which often is methanogenic (m), but often is not explicitly stated; M = mixed culture; P = pure culture; S = soil or aquifer used as biological seed; E = enzyme derived from microorganism; m = methanogenic culture; x = *Xanthobacter*; mo = monooxygenase; mb = *Mycobacterium*; p = *Pseudomonas*.
Source: Reference [37].

Table 3 Utilization of Halogenated Compounds by *Xanthobacter autotrophicus* GJ10

Growth Medium[a]	Generation time[b,c] (h)	Halide Production[b] (mM)	
		Inoculated	Sterile Control
1,2-Dichloroethane	6.3	9.8	<0.1
2-Chloroethane	5.3	5.0	0.1
Dichloroacetic acid	13	7.1	<0.1
Bromoethane	23	2.1	0.6
Dibromoacetic acid	6.5	8.8	<0.1
1-Chloropropane	5.6	4.2	<0.1
1,3-Dichloropropane	7.8	8.0	<0.1
2-Chloropropionic acid	9.0	3.5	0.2
1-Chlorobutane	6.9	5.0	<0.1

[a] Carbon sources were added at 5 mM; gases were added at 0.25 mmol/50 ml of medium.
[b] Growth and halide levels were scored after 10 days of cultivation in liquid medium at 30 deg. C.
[c] Generation times were determined after inoculation of fresh medium with cells from a preculture grown on the same carbon source.
Source: Reference [20].

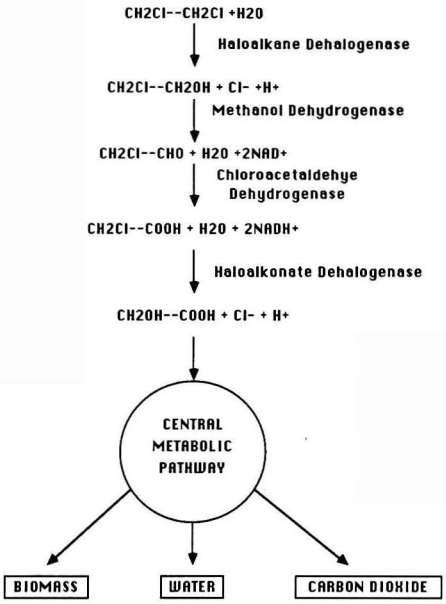

FIGURE 1. Metabolic pathway of EDC by *X. autotrophicus*

the organism could metabolize a number of other halogenated compounds as carbon and energy sources (Table 3). A taxonomic study indicated the bacterium should be classified as a strain of *Xanthobacter autotrophicus* [*39*]. The species is a member of a biologically unique group of bacteria which have the ability to grow chemolithoautotrophically in gas atmospheres containing hydrogen, oxygen, and carbon dioxide. That is, they are able to obtain energy from the oxidation of hydrogen and concomitantly synthesize cell material by the reductive assimilation of carbon dioxide via the ribulose bisphosphate cycle [*1*], which is the same cycle used by plants to produce biomass.

Janssen and others [*22*] studied the biochemistry of *Xanthobacter autotrophicus* GJ10 and reported the path from 2-chloroethanol to chloroacetate is mediated by two separate inducible dehydrogenase proteins. The first, an inducible methanol dehydrogenase, catalyzes the transformation of 2-chloroethanol to chloroacetaldehyde. The second is an NAD-dependent chloroacetaldehyde dehydrogenase, which permits chloroacetaldehyde to be converted to chloroacetate. The full dehalogenation pathway is shown in Figure 1 [*22*].

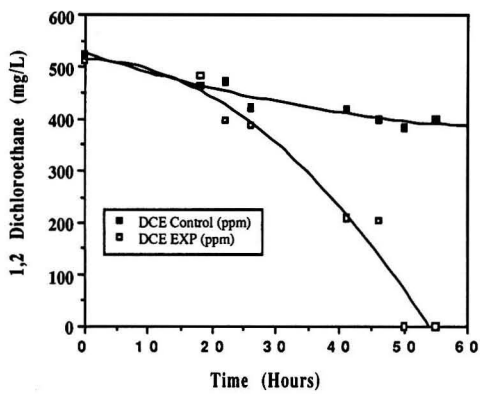

FIGURE 2. Removal of EDC from *X. autotrophicus* culture

To confirm the novel enzymatic capability of *Xanthobacter autotrophicus*, a controlled growth experiment was conducted. MMZ media spiked with ethylene dichloride and chloroethanol to yield aqueous concentrations of 6 mM and 3 mM, respectively, was added to each of four 500 ml sterile Kimax serum bottles fitted with vapor-tight closure assemblies. Two of the bottles were inoculated with 2 ml of a fresh *Xanthobacter autotrophicus* culture which had been propagated on nutrient broth media. The other two bottles were used as comparative sterile controls. Samples were asceptically removed periodically from the bottles and chromatographed for EDC. Concentration data obtained were averaged for both the control and inoculated replicates. The results are plotted in Figure 2. The existence of an EDC-metabolizing culture is evidenced by the rapid concentration decrease in the inoculated systems.

Biocatalyst Immobilization

Immobilization refers to either the process of confining a biocatalyst (either a cell or an enzyme) within a porous matrix, or to fixing the catalyst to a solid surface. There are a number of notable advantages to this approach as follows:

- Higher culture densities can be attained with cell immobilization versus suspended cell systems.
- Flowrates can be in excess of the washout dilution rate, since washout cannot occur when the biocatalyst is immobilized.
- The carrier may have sorptive capacities which increase the surface concentration of the substrate. Portier et al. [*29*] used the sorptive properties of the aminopolysaccharide chitin to concentrate soluble PCB fractions at the material surface, increasing the substrate availability to PCB-adapted microbial populations. The concentration effect resulted in a doubling of the rate at which PCB was removed from the system.
- Intrinsic catalytic activity may increase or decrease, possibly due to physiological changes in the biocatalyst. Bandyopadhyay and Ghose [*3*] presented electron microscope evidence to show physiological changes upon immobilization.
- Immobilization may have a stabilizing effect on enzyme activity. Chibata and his colleagues [*9*] found the half-life of aspartase deactivation was 120 days for immobilized cells, compared to 11 days in suspended cells of *E. coli*.
- The composition of the carrier support material may be used to affect both product yield and selectivity. Welsh and his coworkers [*38*] examined the distribution and total yield of solvent products from *Clostridium acetobutylicum* immobilized on eight types of supports. They found a marked increase in yield when the organism was immobilized on kaolinite versus a decisive decrease with Cab-o-sil fused silica.

A number of methods relating to the immobilization process have been developed. Rosevear [*33*] classifies them by three categories including (i) entrapment within a support, (ii) adsorption to a support, and (iii) covalent binding to a support. For this work, adsorption method and mechanisms were the primary focus, since category (i) and (iii) methods generally gave higher unit cost and/or yield immobilized moieties with low mechanical strength. Physical adsorption involves the attachment of cells to some adsorbing surface without covalent bonding taking place. The bonding mechanism may be due to van der Waals forces, hydrophobic or hydrophilic interactions, hydrogen bonding, or ionic bonding. Adsorption is widely observed in natural ecosystems in which microorganisms attach to surfaces in nutrient-poor environments, such as soil.

Both the properties of the solid support and the biological phase influence sorption tendencies. Mattiasson [*24*] reports that the chemical composition, surface charge, surface area, and pore size of the sorbent are key properties. In many cases,

Table 4 Properties of Immobilization Substrates

Mechanical Properties	Chemical Properties
Compressibility	Surface pH
Impact Resistance	Sorptive Capacity
Shear Sensitivity	Hydrophobicity
Packing Density	Hydrophilicity
Porosity	
Surface Area	
Pore Size Distribution	
Temperature Sensitivity	

Source: Reference [2].

the molecular binding characteristics of a surface can be made more favorable by a thermal or chemical modification. Portier [28] has patented a process for an aqueous delivery system to deposit chitosan on the surface of a porous support. This treatment is useful for scavenging dissolved metals in waste water systems and makes the support surface more favorable for biological colonization. Properties of the cells, such as wall composition, charge, and age are also important in the process. A potential problem with a microbial sorption process is its reversible nature. Most investigators now agree, though, that the attachment proceeds in two phases, with the first being a reversible sorption, and the second an irreversible fixation [11].

Key physical attributes of the carrier affect the performance of an immobilized system in practice. Pore dimensions and surface characteristics govern both the degree of biological colonization and transport of substrate and metabolic products. Mechanical properties may limit hydraulic loading and affect the choice of gas-liquid contacting schemes, and thus influence the process environment in which the carrier can be used. Table 4 lists some key properties which must be considered before choosing an immobilization substrate.

Optimizing Ideal Reactors

Several authors have considered various reactor schemes useful for fermentation systems. Herbert [18] presents a rather comprehensive summary of associated design calculations. Reusser [31] presented calculations presuming a series arrangement of plug flow and/or back mix reactors for the production of novobiocin and showed that a combination of the two types was most effective. Bischoff [6] emphasized the autocatalytic nature of many biological reactions, comparing the growth of microorganisms with the evolution of heat from a reversible chemical reaction occurring in an adiabatic reactor. Assuming a Monod rate function with parameters characteristic of the lactic acid fermentation, and 95% conversion of substrate, he showed the optimized holding time for a CSTR and PFR in series was 1/3 that of a single CSTR and 72% that of two equal sized, series CSTRs. Bischoff also showed the superiority of this arrangement increased as the conversion increased.

The similarity of these systems with wastewater detoxification systems is noteworthy. While industrial wastewater feed streams generally have lower substrate concentrations, a conversion magnitude of 90 to 99.9% is considered a typical target. This parallel lends a good deal of support to considering a "hydrid" process configuration which has both CSTR and PFR type attributes.

Packed Bed Reactors

In packed bed (or fixed bed) reactors, a solid phase inert support (usually inorganic) provides a surface on which whole cells or cell products can be attached. Typically these particles are loaded into tubular reactors and utilized in steady state processes. The simplest description of packed bed performance employs a plug flow model modified to account for the physical presence and chemical reaction activity due to the packing. If reaction occurs both in the fluid and solid phases, and diffusion effects are not negligible, the material balance becomes complex. This system is simplified if intraparticle and external mass transfer resistances are negligible (i.e., relatively fast superficial liquid velocity, small particle size, low catalyst density, and slow reaction rates). If this is not the case, effectiveness factors must be introduced [17].

Packed bed reactors offer advantages over their open tubular counterparts. Since the cell populations remain within the vessel, the problem of maintaining a stable culture with sterile inlet feed is solved. Process design is simplified since it is not necessary to provide a means of separating the fluid from the solid phase (as in fluidized beds), since the bed is fixed. Finally, the amount of axial backmixing is generally lower than that of a fluidized system, while the amount of catalyst per unit reactor volume is higher. Thus, for positive order reaction kinetics, higher conversions can be obtained for the same holding time in static packed systems than in fluidized systems.

The problems inherent in packed beds relate to gas and solid phase interactions. In aerobic systems, oxygen transfer is made difficult by the tortuous path a bubble must take through the column. The presence of the packing encourages coalescence of air bubbles, along with gas phase "channeling." Channeling occurs when air introduced continually seeks the path of least resistance through the bed, creating saturation conditions in some sections of the bed and driving other portions into an anoxic state. Eddies set up in the liquid phase by the fast-rising air bubbles may cause a substantial backmixing effect, with a concommitant loss in reactor performance. Finally, momentum transfer from the gas to the solid carrier may cause particle attrition over time.

A fluidized bed configuration was also considered for this project. Disadvantages of the fluidized bed include physical attrition of carrier particles, possibility for development of anoxic zones, and retention/recycling of carrier particles. Attrition of the carrier is caused by mechanical damage sustained from collisions with the vessel walls or other particles. Ngian and Martin [25] have shown that the time for a layer of identical tracer particles to disperse in a typical fluidized bed reactor is on the order of ten minutes, and thus aerobic to anaerobic metabolic transition is unlikely. However, axial substrate concentration gradients may induce particle density gradients within the reactor, which in turn can lead to oxygen depletion in the upper sections. Vogel and others [37] have shown that substrate uptake by an aerobic biomass in an oxygen depleted zone is zero. Thus, a fraction of the bed may be wasted if steps are not taken to maintain the dissolved oxygen concentration above some minimum concentration. Finally, the high liquid velocities required in fluidized systems require special operating considerations. If the high velocities are to be maintained by pumping, a means of rapidly separating and recycling particulates must be provided upstream of the pump to prevent impeller damage and carrier destruction.

Distributor Design

Mass transfer rates in gas/liquid systems are directly proportional to interfacial contact area between the two phases. Accordingly, a key consideration in such systems is selecting a method of introducing the discontinuous phase which results in maximum surface area for transport. Blenke [7] has quantitatively demonstrated the benefits of introducing both the air and liquid phase as a commingled jet at the base of the draft tube in his treatise on loop reactors. The high velocities and turbulence produced at the jet nozzles result in an effective dispersion of the air phase as very small gas bubbles entrained in the liquid feed along with any cell flocs. This type of distributor seems particularly well suited to the current case, in which well-defined mixing is desired to maximize oxygen mass

transfer, but air flow rate must be minimized. For example, at a total specific power input/reactor volume ratio of 1 W/L, the specific interfacial area for mass transfer is approximately 300 m^2/m^3 reactor volume for an air lift system alone. If fifty percent of this power is provided by a liquid jet, the resulting specific interfacial area more than triples to approximately 1100 m^2/m^3 reactor volume.

The mass transfer and specific power characteristics of various types of aeration equipment is reviewed in *Chemical Engineer's Handbook* [26]. Of the equipment evaluated, the two devices which used the energy in jets to produce intimate air/liquid mixing and high shear effects (to reduce average bubble diameter) provided the highest oxygen transfer efficiencies. One of the two jet mixing devices also exhibited the highest specific oxygen transfer rate, but at the expense of the highest specific energy consumption. Presumably for this device, a good portion of the increased specific energy input went into enhanced mixing of the air-water system.

Oxygen Absorption and EDC Stripping Considerations

The compelling kinetic rates available from *Xanthobacter autotrophicus* necessitated that an aerobic environment be maintained within the reactor. Thus, the problem of how to provide efficient oxygen transfer to the culture while minimizing stripping effects became critical. For oxygen transfer, the familiar transport equation can be written:

$$N_o = k_L a (C^* - C) V_T$$

By adopting the commonly held assumption that the exiting sparge gas comes to equilibrium with the dissolved volatile species, the equation for the molar rate of removal of the VOC from the groundwater due to evaporation is:

$$N_S = x_i H_i N_T / P$$

While the specific interfacial transfer area can be increased by increasing the gas sparge rate, this can be seen to have a negative effect on the volatile stripping rate since the total molar flux N_T increases proportionally. On the other hand, by increasing the total system operating pressure, the oxygen driving force C^* increases while the volatile flux rate decreases. While increasing the pressure works to minimize evaporation rate and improve oxygen mass transfer, the actual increase in gas to liquid transfer rate has been shown to be proportional to the 0.4 to 0.8 power of total pressure in the reactor [34]. A second alternative might be simply to sparge the reactor with pure oxygen. This would obviously increase the oxygen concentration driving force and reduce the volatile evaporation rate from the reactor, since the total molar gas sparge rate N_t would be significantly reduced. The application of a pure oxygen sparge was eventually rejected for several reasons, including the high operating costs associated with this strategy and the increased flammability hazard.

System Pressure Considerations

An obvious benefit to operating an air-sparged aerobic reactor at pressures above ambient is the increase in the driving force for oxygen mass transfer. The partial pressure of oxygen in the air increases in direct proportion to the total pressure. In a system which is oxygen transfer limited, the only means of increasing the oxygen mass transfer rate may be to increase oxygen concentration, either by increasing the air supply pressure or by admixing pure oxygen into the sparge gas.

Constraints on the maximum operating pressure of fermentation systems are mechanical, biochemical, and physiological. Mechanically, the only impediment to operation at higher pressures are securing dissolved oxygen and pH transducers which can function at the desired hydrostatic conditions. Naturally the pressure vessels would have to be constructed from steel with increased wall thickness or a higher yield strength.

At least two potential problem areas must be considered when contemplating effects of elevated operating pressure on the bacterial population. The first is end product concentration inhibition due to increased solubility of primary metabolites, such as CO_2. If the equilibrium concentration of this species were to become large, catabolic reactions in the cell might be slowed or even cease. Physiologically, the effect of pressure on cell wall integrity is also an impediment at high operating pressure. Kim [23] reported the leakage of cellular constituents increased as the culture incubation temperature was reduced from 40 to 25°C at 500 atm.

VOC BIOPROCESS DESCRIPTION

Literature Review Implications

From the literature review, several critical points emerge which influence the development of the bioprocess. These points are summarized below.

The only biological systems in the current literature capable of mineralizing EDC at kinetically useful rates without excretion of poisonous intermediate metabolites are Janssen's *Xanthobacter autotrophicus* and the organism isolated by Stucki. Both are aerobic organisms with roughly equivalent growth rates. A monoculture as the biocatalyst was appealing since it might make the system more amenable to future math modeling and scale-up. Janssen's organism was chosen due to its availability and the fact that it has been biochemically better characterized. Both use EDC as the sole source of carbon and energy.

Key attributes of the reactor and the system configuration were also identified. Assuming Monod-type kinetics for substrate utilization, the work of Bischoff indicates a reactor with CSTR-type characteristics followed by plug-flow behavior would minimize holding time. Highest productivity would be accomplished by operating in a continuous fashion. Maximum operating flexibility could be attained by recycling effluent from the PFR section into the influent to the CSTR section. The well-mixed requirement of the CSTR is consistent with the conditions for rapid gas-liquid mass transfer. This is beneficial from the standpoint of oxygen transfer from gas to liquid, but also enhances gas stripping of the chlorinated volatile from solution. Oxygen transfer could be improved by increasing the driving force (oxygen gas concentration), through increasing reactor operating pressure and/or increasing the fraction of oxygen in the sparge gas feed. A vessel with a moderate height to diameter ratio, as in a bubble column, increases the contact time between gas and liquid, and improves the transfer efficiency. A commingled jet of gas and liquid seemed to provide the best sparger configuration due to the excellent oxygen and momentum transfer qualities.

The plug flow portion of the process would accomplish the major portion of the bioconversion. An immobilized bacterial system would allow the reactor to be operated at high dilution rates, might improve kinetic rates, and would provide a continuous biological inoculum to the wastewater contacting it. By separating sparge gas from the VOC contaminated liquid prior to entering the PFR section, liquid dispersion effects would be minimized, creating fluid conditions more representative of plug flow. Also, attrition of the carrier would be minimized by eliminating mechanical shock from gas/liquid oscillations through the packed bed. By avoiding slow liquid velocities through the packed section, several advantages are realized. First, anoxic conditions are avoided since not enough contact time is allowed to completely deplete the dissolved oxygen content of the liquid. Second, film resistance to mass

Table 5 VOC Bioreactor Design Goals

Construction Goals	Process Goals
Economical Vessel Construction	Maximize Reactor Productivity
Industrial-Grade Materials	*Continuous Flow
Explosion-proof Field Instrumentation	*Rapid Microbial Uptake
Automated Control Loops	Minimize Stripping Losses
*Thermal	*Minimize Sparge Air Flow
*pH	*High Recycle Rate
*Dissolved Oxygen	*Elevated Pressure Operation
	Maximize Culture Performance
	*Thermally Sterilize Reactor
	*Immobilized Cell Support

transfer is reduced, so substrate concentration at the packing surface should be almost the same as that in the bulk fluid. Finally, the fluid shear effect near the particle surface should prevent adjacent biofilms from growing together and plugging the void spaces. Fluid channeling would thus be limited, preventing the development of anoxic sections in the bed.

High recycle rates decrease the effective concentration of the VOCs within the reactor, which in turn reduces the driving force for air stripping. However, lower substrate concentration also leads to lower metabolic rates in suspended systems, as long as the bacterial kinetics are positive order and substrate concentration has not reached an inhibitory level. By choosing an immobilization substrate which also exhibits sorptive tendencies for the target VOC, the local organic concentration could be effectively increased in the vicinity of the attached microorganisms. An obvious additional benefit which accrues from the partitioning effect is the lowering of the VOC concentration in the liquid phase. Thus sorption and recycle effects both serve to decrease volatilization losses.

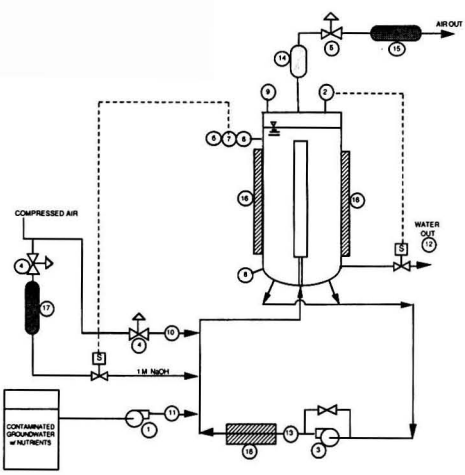

FIGURE 3. Process flow diagram for reactor.

Volatile Organic Immobilized Microbe Process System

Engineering process design goals established for the project are shown in Table 5. A process flow diagram (PFD) for the system is provided in Figure 3. The current system consists of two functionally distinct subsystems. The first is a raw influent conditioning system which removes suspended particulates down to 100 microns, dilutes recovered groundwater to the degree required to achieve biologically acceptable toxicant concentrations, and adjusts/maintains media pH and temperature. A high velocity jet of air is continuously injected into the water just prior to entering the reactor. Biological conversion occurs in the second subsystem (reactor vessel).

Several different control functions maintain process conditions optimal for continuous culture of the biocatalyst. A primary thermal control system maintains the reactor at some predetermined temperature set point. A secondary heating system provides additional thermal input to the recycle stream under high demand conditions (cold ambient temperature or sterilize mode of operation). Reactor operating pressure is controlled by regulating the pressure at which sparge gas is delivered to the reactor. Oxygen concentration is increased by raising the air delivery pressure, but can also be increased by admixing pure oxygen into the sparge air supply. The flowrate of contaminated feed water is controlled by a positive displacement pump. Recycle flow to the reactor is independently set by a centrifugal pump. Overpressure conditions can be controlled by relief valves on both the influent piping and the reactor vessel.

Since continuous liquid flow control based on level was considered too expensive, a semi-continuous scheme was developed. In this approach, flowrate out of the reactor is set slightly below the inlet feed rate by a manual flow control valve. Since the inlet flowrate is slightly more than the export flowrate, liquid accumulates in the reactor, and a two-position level switch is used to keep the reaction volume within acceptable limits. A high level condition causes a dump valve to open in parallel with the export flow control valve. This action causes a moderate rate of fluid loss from the reactor. System operating pressure is maintained fairly constant though, since the sparge air regulator increases the air supply rate to keep the delivery pressure steady as the headspace volume increases. Once the liquid level reaches the low level position on the level switch, the export dump valve closes and normal operation resumes.

The pH is controlled by adding concentrated acid or base reagents to the recycle stream as needed. If the pH sensed in the reactor drops below a low set point or exceeds a high set point, the appropriate valve on the acid or base reagent tank opens for some preset time interval. Reagent tank pressure is set slightly above the recycle line pressure to create a positive hydrostatic head.

Reactor off-gases are dehydrated, and VOC concentration slightly reduced, by the operation of a condensing unit in the head space. Cooling fluid is circulated through copper tubing,

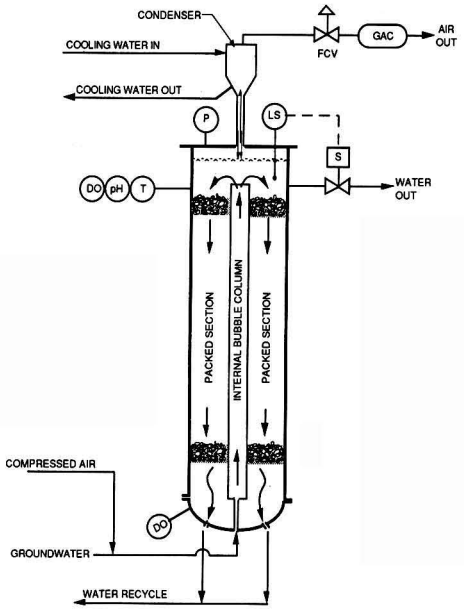

FIGURE 4. VOC bioreactor cross section

which causes condensation and reflux of water from the saturated air passing across the coils. Exit gas is droplet free, reducing the risk of the operator ingesting or inhaling airborne bacteria from the process.

The reactor (Figure 4) is fitted with a concentric internal tube which partitions the inner volume into two distinct sections. In the first, air sparged into the recirculation loop mixes and aerates the influent water. The tube volume is unpacked, and thus functions as a bubble column, promoting the efficient transfer of oxygen to the water. Admixed air separates by density from the water before it enters the second reaction stage. Fluid exiting the top of the column flows in a downward direction through the annular space between draft tube and vessel interior wall. The annular space is packed with the biological support and functions as a fixed biocatalytic bed. A recycle pump takes suction from the bottom of the reactor, drawing fluid through the bed as it does so. The recycle pump discharges fluid back into the reactor at the base of the draft tube, completing the fluid circuit. By adjusting the recycle flowrate, both the dispersion and oxygenation characteristics of the system can be varied.

In the sterilize mode, a steam source can be connected directly into the recirculation line. Admixing steam into the nutrient-amended groundwater greatly increases the rate of approach to sterilization temperature (120°C). This action has the obvious effect of diluting the initial concentration of nutrient and substrate constituents. During sterilize mode, the headspace pressure is maintained at 50 psig to avoid boiling. This condition is maintained for a minimum of twenty minutes to achieve a complete biological kill. The biocarrier selected is capable of withstanding the sterilization conditions, so the packing can be loaded into the vessel and sterilized along with the nutrient amended groundwater. Once the water cools to about 30°C, a biological inoculum is introduced through a port in the headplate. Sparge air filtered through a 0.45 micron filter provides a sterile air supply to the jet sparger. The broth is then circulated through the vessel over a 30–40 hour period to develop the culture and allow adequate time for it to partition onto the support.

Table 6 VOC Bioreactor Data

Reactor Vessel
- Type: Bubble column/packed bed series combination
- Wetted Materials: Stainless steel, baked phenolic coated carbon steel, Teflon, and glass.
- Packed Section Volume: 37,930 cm^3
- Bubble Column Volume: 8,553 cm^3
- Total Liquid Volume (excluding pore volume): 68,120 cm^3

Packing
- Manufacturer: Manville R-630 Celite Biocatalyst Carrier.
- B.E.T. Surface Area: 1.3 m^2/gm
- Bed Density: 0.3364 gm/cm^3
- Mass Used: 12.76 kg

Continuous Flow Test Operating Conditions
- Air Sparge Rate: 450 std. cm^3/min
- Pressure: 3 atm absolute
- Liquid Feed Rate: 2.85 L/hr
- Recycle Rate: 4.12 L/min
- Recycle Ratio: 86.7

Construction Specifications

The VOC-degrading pilot plant includes an instrumented bioconversion vessel, storage reservoirs for pH adjustment solutions, interconnecting piping and valve manifold, and a free-standing control panel which houses process monitoring devices and signal conditioning electronics.

The bioconversion vessel is constructed from welded carbon-steel components and has a nominal capacity of 75 liters. A summary of the reactor attributes and operating conditions is presented in Table 6. The vessel body is fabricated from a four foot section of 0.375″ wall thickness, Grade B steel line pipe with a nominal diameter of one foot. All flange fittings used are rated ANSI 150 and have raised faces to accommodate gasket seals. All gaskets were cut from 3/16″ Teflon sheets. A 6″ diameter sight window unit is installed at the liquid level to provide visual observation of reactor fluids. Vessel components were joined by welding with 0.9 mm, 65,000 psig yield strength wire using a TIG electrode. All internal corners were ground to a minimum radius of 1/4″ to accept a protective coating. The vessel was subsequently hydrostatically tested at 325 psig to verify mechanical integrity. The internal surface of the vessel is coated with a .006″ thick baked phenolic resin to prevent corrosion and biological interaction with the steel walls. Ports are provided for the continuous import/export of VOC-contaminated feedwater and for pH, dissolved oxygen, and temperature sensors. A condensing unit at the top of the vessel is fabricated from 6″ diameter pipe and steel weld fittings. Fifty feet of 1/4″ diameter coiled copper tubing provides the condensing heat exchange surface.

The internal design of the vessel features a stainless steel bubble column mounted to a coated, carbon steel cross-piece. The cross-piece is covered with a coated wire mesh which retains the bed packing. The packing used is a solid-phase inorganic cell support provided in 3/5 mesh size spheres. The selected support is manufactured by the Manville Corporation, and features an internal surface area of 1.3 m^2/g and a mean pore diameter of 6.6 microns. The carrier is composed of diatomaceous earth in a silica matrix. Approximately 3 kg of glass marbles were placed on the meshed cross-piece to form a base for the packing. Next, 1.12 kg of ceramic packing was placed as a layer above the marbles. Finally, 12.76 kg of the above referenced R-630 support material was placed in the annular space, to a height approximately 3″ below the top of the bubble column.

The feed pump is a positive displacement type with a 0-50 mL/min flowrate range and discharge pressure limit of 100

psig. A ceramic piston and stainless steel pump head give the unit a limited ability to pump liquids which have some suspended particulates.

Sparge air is supplied from compressed air cylinders through a high pressure regulator. The air supply is then sequentially routed through a 1 micron particulate filter, an oil vapor removal filter, and a 0.45 micron filter. The 0.45 micron filter is used only during asceptic culture development. Air is delivered through a section of 1/8″ diameter stainless steel tubing as a high velocity jet. The air line is tee'd into the 3/8″ diameter recirculation line approximately two feet upstream of the point where the recirculation line enters the bubble column section of the rector.

Instrument air is purified through high efficiency particulate and oil vapor filters, and a desiccant to remove moisture. Instrument air is used to operate acid and base addition valves and an effluent dump valve. In addition, instrument air is used to pressurize the acid and base reservoirs.

The selected recirculation pump is an open impeller centrifugal with all stainless steel construction and a 1/2 horsepower, explosion-proof motor. A portion of the discharge flow can be returned to the suction through a bypass line. Recirculation flowrate thus can be continuously varied between about 1 and 6 L/min. Rate measurements are made with a rotometer.

All interconnecting piping between the vessel and associated feed reservoirs is constructed of stainless steel tubing. All valves selected for the system have stainless steel bodies and plugs, with Teflon seating materials. All wetted material components were selected to withstand sterilization temperatures of 121°C, pressures in excess of 100 psig, and are inert to chemical attack by most organic compounds. Overpressure relief valves are installed on both the reactor and the piping manifold. Both were laboratory calibrated to relieve at 75 psig. The system was designed to "fail-safe" in the event of operator error or control equipment failure. The plant is skid-mounted to facilitate easy transport to industrial sites for demonstrating the system capabilities.

All instruments and transducers selected for the plant are industrial-grade, and of the best possible accuracy and reliability. Transducers and electrical devices located on and adjacent to the vessel are rated for Class I, Division II, Groups C and D environments (periodically explosive). Electrical equipment was selected and installed to conform to standards and recommended practice published by ISA and NFPA (10, 15, 19, 30). All instruments are protected from power surges and electrical transients by an isolation transformer. A temperature control system maintains the reactor within 1°C of a setpoint, regardless of the ambient temperature conditions. Sterilization of the reactor and feed piping is achieved by augmenting the thermal energy of the electric heaters with direct steam injection through the recirculation piping. Both dissolved oxygen and pH of the broth can be controlled automatically. A mass measurement system precisely measures air sparge rates to the fermentor. A digital chart recorder provides a continuous record of all critical operating parameters.

RESULTS/RECOMMENDATIONS

Eighteen hours after thermal sterilization, the reactor was inoculated with 3 L of an axenic *Xanthobacter autotrophicus* culture. 1.5 L of a sterile nutrient solution was added, along with 100 mL of sterile vitamin concentrate. Recirculation flow rate was set at approximately 4 L/min. Compressed air was introduced at the base of the well-mixed section of the reactor at approximately 500 standard cc/min. The reactor operating pressure was regulated to 30 psig and temperature was controlled at 30°C. The pH of the groundwater was automatically maintained between 6.5 and 7.5 by addition of 1 M sodium hydroxide solution. Twenty hours later, the turbidity within the reactor was high enough to obscure all internal reactor components located below the air/liquid interface.

Contaminated groundwater obtained from a monitoring well was treated in both batch and continuous operating modes over a period of 26 days. Data in Figures 5 and 6 were obtained during the last 72 hours of the continuous flow test period. Influent feed concentrations entering the system averaged 5.68 mM EDC. Effluents from the reactor averaged 0.009 mM EDC. Chloride concentrations increased by approximately 14 mM through the reactor. With an influent flowrate of 2.85 L/h, the average removal rate was 1599 mg EDC/h (Molecular Weight EDC-98.96 g/mole). During this period, a carbon trap in series with the reactor off-gas line adsorbed volatilized EDC at the rate of 4.84 mg/h, suggesting that in excess of 99% of the observed removal rate was due to biodegradation. GC/MS analysis of an off-gas sample collected downstream of the carbon trap just prior to removing it showed non-detectable levels of EDC, indicating that no organic breakthrough occurred.

Process conditions in the field demonstration reactor were purposely set to yield very high biological removal efficiencies. The high removal efficiency was realized at the expense of

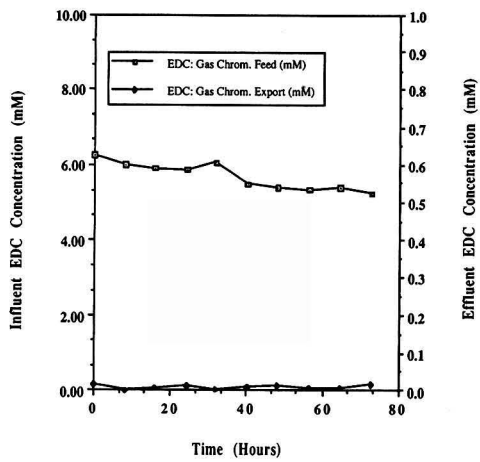

FIGURE 5. EDC concentrations in continuous flow operation

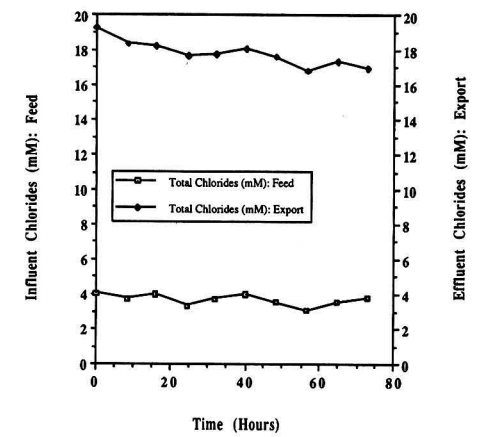

FIGURE 6. Chloride concentrations in continuous flow operations

process productivity, however. To evaluate the maximum productivity of the process, the EDC concentration in the bubble column should be increased to a level at or just below the inhibition concentration of the culture (about 500 ppm). This condition can best be imposed by adjusting the feed concentration and/or flowrate to the reactor, while keeping the recirculation rate approximately constant. The operating pressure of the system may also need to be raised in order to provide oxygen transfer rates sufficient to satisfy the increased respiration demand of the culture. Under these conditions, the removal rates should increase significantly. Obviously, the effluent EDC concentration will increase, along with stripping losses.

ACKNOWLEDGMENTS

Research presented in this paper was supported by funds from the State of Louisiana Board of Regents. Donation of the Cellite R-630 carrier material from Manville Service Corporation is gratefully acknowledged. The contribution of Kuniko Fujisaki, Mao Huazhong, Daniel Linarello, Charles Henry, and Steven Livesay are acknowledged and gratefully appreciated.

LITERATURE CITED

1. Arangno, M., and H. G. Schlegel, "The Hydrogen-Oxydizing Bacteria," *The Prokaryotes,* Vol. I, p. 865, M. P. Starr, H. Stolp, H. G. Truper, A. Balows, H. G. Schlegel, eds., Springer-Verlag, New York (1981).
2. Bailey, J. E., and D. F. Ollis, *Biochemical Engineering Fundamentals,* 2nd Edition, p. 599, McGraw-Hill Book Company, 1986.
3. Bandyopadhyay, K. K., and T. K. Ghose, Biotechnology and Bioengineering, Vol. 24:805, p. 48 (1982).
4. Basket, A. C., and C. Hinselwood, Proc. R. Society, Lond. B., Vol. 138, pp. 75-88 (1957).
5. Belay, N., and L. Daniels, "Production of Ethane, Ethylene, and Acetylene from Halogenated Hydrocarbons by Methanogenic Bacteria," Appl. Environ. Microbiol. (47) 1604-1610 (1987).
6. Bischoff, K. B., Optimal Continuous Fermentation Reactor Design, The Canadian Journal of Chemical Engineering, October 1966.
7. Blenke, H., Loop Reactors, *Advances in Biochemical Engineering: Mass Transfer and Process Control,* Vol. 13, T. K. Ghose, A. Fiechter, N. Blakebrough, eds., Springer-Verlag Publishers (1979).
8. Bouwer, E. J., and P. L. McCarty, Transformation of 1- and 2-Carbon Halogenated Aliphatic Organic Compounds Under Methanogenic Conditions, Applied and Environmental Microbiology, pp. 1286-1294 (April 1983).
9. Chibata, I. (ed.), Immobilized Enzymes, p. 140, Kodansha Ltd., Tokyo (1978).
10. Class I Hazardous Locations for Electrical Installations in Chemical Plants, Publication No. NFPA 497-1975, National Fire Protection Association, Stamford, CT, May 15, 1975.
11. Costerton, J. William, Thomas J. Marrie, and K. J. Cheng, Bacterial Adhesion: Mechanisms and Physiological Significance, Dwayne C. Savage and Madilyn Fletcher, eds., Plenum Press, New York and London (1985), p. 11.
12. Demand for PVC Outstrips Supply, Chemical and Engineering News, Vol. 50, 1987 (65), p. 9.
13. Dilling, Wendell L., Interphase Transfer Processes II. Evaporation Rates of Chloro Methanes, Ethanes, Ethylenes, Propanes, and Propylenes from Dilute Aqueous Solutions, Comparisons with Theoretical Predictions, Environmental Science and Technology, Vol. 11, No. 4, pp. 405-409 (1977).
14. Dilling, W. L., N. B. Tefertiller, and G. J. Kallos, Evaporation Rates and Reactivities of Methylene Chloride, Chloroform, III-Trichloroethane, Trichloroethylene, Tetrachloroethylene, and Other Chlorinated Compounds in Dilute Aqueous Solutions, Environmental Science and Technology, Vol. 9, No. 9, pp. 833-837 (1975).
15. Electrical Instruments in Hazardous Atmospheres, Publication No. ISA-RP12.1, Instrument Society of America, Research Triangle Park, N.C., April 1960, pp. 2-7.
16. Ethylene Dichloride, Current Intelligence Bulletin 25, April 19, 1978, pp. 1-5, U.S. Department of Health and Human Services, Public Health Service, Centers for Disease Control, National Institute for Occupational Safety and Health.
17. Froment, G. F., and K. B. Bischoff, Section 3.6 Transport Processes with Fluid-Solid Heterogeneous Reactions—Chemical Reactions with Pore Diffusion, Chemical Reactor Analysis and Design, John Wiley and Sons (1979).
18. Herbert, D., Continuous Culture of Microorganisms, Soc. Chem. Ind., Monograph No. 12, p. 21, London (1961).
19. Instrument Purging for Reduction of Hazardous Area Classification, Publication No. ISA-S12.4, Instrument Society of America, Research Triangle Park, N.C., pp. 4-11 (1970).
20. Janssen, D. B., A. Scheper, L. Dijkhvizen, and B. Witholt, Degradation of Halogenated Aliphatic Compounds by *Xanthobacter autotrophicus* GJ10, Applied and Environmental Microbiology, Vol. 49, No. 3, pp. 673-677 (1985).
21. Janssen, D. B., A. Scheper, and B. Witholt, Biodegradation of 2-Chloroethanol and 1,2-Dichloroethane by Pure Bacterial Cultures, Innovations in Biotechnology, E. H. Hoowink, R. R. Van der Meer, eds., Progress in Industrial Microbiology, Vol. 20, Elsevier Biomedical Press, Amsterdam (1984).
22. Janssen, D. B., S. Keuning, and B. Witholt, Involvement of a Quinoprotein Alcohol Dehydrogenase and an NAD-Dependent Aldehyde Dehydrogenase in 2-Chloroethanol Metabolism in *Xanthobacter autotrophicus* GJ10, Journal of General Microbiology, Vol. 133, pp. 85-92 (1987).
23. Kim, J., Disinfection by Increased Hydrostatic Pressure, Developments in Industrial Microbiology, Vol. 24, pp. 519-525 (1983).
24. Mattiasson, B., Immobilization Methods, Immobilized Cells and Oranelles, B. Mattiasson, ed., CRC Press, pp. 4-25 (1983), Boca Raton, FL.
25. Ngian, K. F., and W. R. B. Martin, Biologically Active Fluidized Beds: Mechanistic Considerations, Biotechnology and Bioengineering, Vol. XXII, pp. 1007-1014 (1980).
26. Perry, R. H., and C. H. Chilton, Section 18—Liquid-Gas Systems, *Chemical Engineer's Handbook,* 5th Edition, McGraw-Hill Book Company, pp. 18-78 (1973).
27. *Ibid,* p. 3-55.
28. Portier, R. J., U. S. Patent No. 4,775,650.
29. Portier, R. J. and K. Fujisaki, Enhanced Biotransformation and Biodegradation of Polychlorinated Biphenyls in the Presence of Aminopolysaccharides, Aquatic Toxicology and Hazard Assessment: 10th Volume, ASTM STP 971, W. J. Adams, G. A. Chapman, W. G Landis, eds., American Society for Testing and Materials, Philadelphia, pp. 517-527 (1988).
30. Purged and Pressurized Enclosures for Electrical Equipment in Hazardous (Classified) Locations, Publication No. NFPA 496-1982, National Fire Protection Association, 1982, pp. 4-14.
31. Registry of Toxic Effects of Chemical Substances, 1981-82, Vol. 2, p. 223, U.S. Department of Health and Human Services, Public Health Service, Centers for Disease Control, National Institute for Occupational Safety and Health.
32. Reusser, F., Appl. Microbiol., 1961(9), 361.
33. Rosevear, A., Immobilized Biocatalysts—A Critical Review, pp. 127-150 (1984).

34. Sato, S., S. Mukataka, H. Kataoka, and J. Takahashi, Oxygen absorption rate in an aerated stirred tank under increasing pressure, J. Ferment, Technol., 59, 221, 1981.
35. Stucki, G., W. Brunner, D. Staub, and T. Leisinger, Microbial Degradation of Chlorinated C1 and C2 Hydrocarbons in Microbial Degradation of Xenobiotics and Recalcitrant Compounds, T. Leisinger, A. M. Cook, R. Hutter, H. Nuesch, eds., Academic Press (1981).
36. Stucki, G., U. Krebser, and T. Leisinger, Bacterial Growth on 1,2-Dichloroethane, Experientia, Vol. 39, pp. 1271-1273 (1983).
37. Vogel, T. M., C. S. Criddle, and P. L. McCarty, Transformations of Halogenated Aliphatic Compounds, Environmental Science and Technology, Vol. 21, No. 8, pp. 722-736 (1987).
38. Welsh, F. W., R. E. Williams, and I. A. Veliky, Solid Carriers for a *Clostridium acetobutylicum* That Produces Acetone and Butenol, Enzyme Microb. Technol., Vol. 9, pp. 500-502 (August 1987).
39. Wiegel, J., D. Wilke, J. Baumgarten, R. Opitz, and H. G. Schlegel, Transfer of the Nitrogen-Fixing Hydrogen Baterium *Cornyebacterium autotrophicum* Baumgarten et al. to *Xanthobacter* Gen. Nov., Journal Syst. Bacterial, Vol. 28, pp. 573-581 (1978).

Thermal Treatment for The Removal of PCBs and Other Organics from Soil

Robert D. Fox and Edward S. Alperin
IT Corporation, Knoxville, TN

and

Hubert H. Huls
IT Corporation, St. Paul, MN

Thermal separation is an emerging technology for the treatment of contaminated soils and solids. The process removes organic contaminants by indirectly heating the soils and solids to temperatures sufficient to vaporize the hazardous components. The organic vapors in the desorber off-gas are treated either by oxidation in a RCRA-standard secondary combustion chamber or by condensation and conventional treatment of the small amount of the resultant condensate.

This process had its first successful pilot demonstrations in treating Herbicide Orange contaminated soils at the Naval Construction Battalion Center and at Johnston Island, where dioxin contamination was reduced to less than 1 ppb.

This paper summarizes the results of a series of pilot tests, conducted under a TSCA R&D permit, on 3 soils contaminated with PCBs at concentrations ranging from 250 ppm to 4%. To demonstrate the process on an engineering scale, IT made 13 runs in the pilot thermal separator at rates ranging from 18 to 32 kg/hr. Reported are results on the effect of temperature and residence time on the quality of treated soil. The report also summarizes pilot results on a mixed waste soil and soils contaminated with PAHs.

INTRODUCTION

Thermal separation is an emerging technology for the treatment of contaminated soils and solids. The process removes organic contaminants by indirectly heating the soils and solids to temperatures sufficient to vaporize the hazardous components. Key variables in volatilization performance are soil temperature, time at temperature, and particle size. The organic vapors in the off-gas are treated by either oxidation in a high temperature combustion chamber or by condensation and conventional treatment of the small amount of the resultant condensate.

Indirect heating of soils and solids in a rotating metal chamber as a means of separating contaminants by volatilization offers several process advantages. For example, multiple temperature control zones along the rotating chamber are possible; solids residence time can be readily varied; and the composition and rate of purge gas can be controlled. Indirect heating prevents contact between the contaminants, the direct flame and the combustion products. With indirect heating, the gases exiting the separator consist of containment and soil moisture vapors, entrained particulates, and purge gas. Because the volume of these gases is quite low compared to an incinerator, downstream equipment is small and solids entrainment is min-

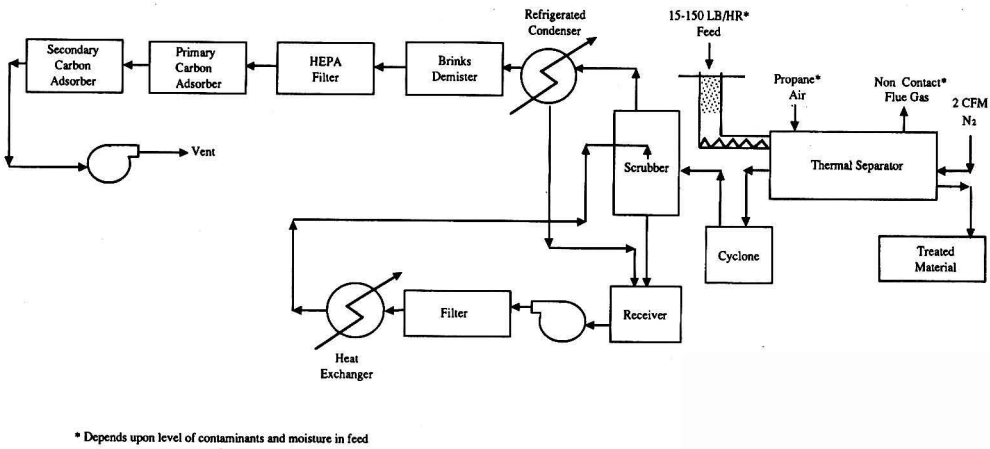

FIGURE 1. Schematic flow diagram of ITs thermal desorption system.

imized. This also enables condensation to be used as a method to collect the contaminants for either recovery or treatment.

Because it is an alloy metal instead of firebrick, the rotating chamber should require less maintenance. It can be transported easier and the unit can undergo faster heat-up/cool-down cycles.

Another advantage occurs when a lack of contact between the contaminated soil and a direct flame is coupled with the condensation option. In this configuration the system has received a RCRA RD&D permit as a physical/chemical treatment process rather than as an incinerator.

LITERATURE SURVEY

Initial testing of the time, temperature, and particle size relationships for decontamination of soils involved laboratory tests in support of the EPA's Mobile Incineration System [*1*].

Pilot-scale testing of the indirectly-heated separator was performed at two U.S. Air Force sites contaminated with dioxin from leaking drums of Herbicide Orange [*2,3*]. Additional pilot-scale tests, which are summarized in this paper, on PCBs are presented in detailed technical reports [*4,5*]. Treatment of soils contaminated with polynuclear aromatic hydrocarbons (PAHs) by indirectly-heated thermal separation have been reported [*6,7,8*]. Fundamental studies on the thermal desorption of organics from soil particles have been reported by researchers at the University of Utah [*9*]. Bench-scale test results have been reported on thermal separation treatment of contaminated soils from three Superfund sites [*10*].

Thermal separator systems for treatment of contaminated soils at temperatures of 340°–455°C have been described [*11*]. This technology will also be demonstrated in the EPA-SITE program [*12*]. Demonstration of the technology on soil contaminated with volatile organic compounds [*13*] was funded by the U.S. Army Toxic and Hazardous Materials Agency and the report is available from them.

Two new processes using direct heating of soil to volatilize contaminants at low temperatures have been described [*14,15*]. One will also be demonstrated in the EPA-SITE program, and the other is scheduled to treat Waukegan Harbor sediment.

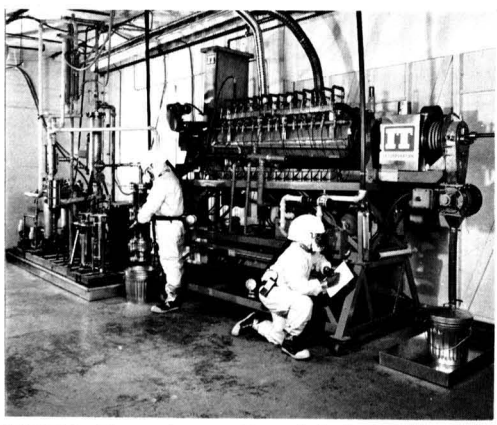

FIGURE 2. Thermal separation pilot plant.

EQUIPMENT DESCRIPTION

IT has a thermal separation pilot plant for engineering scale testing and demonstration of the technology on large quantities of contaminated site soils. The pilot plant has a quench and condensation system for handling the desorbed organic contaminants. The pilot plant can treat up to 68 kg/hr of soil at temperatures from 200 to 600°C and residence times of ten minutes to one hour. A block flow diagram of the pilot plant is shown in Figure 1 and a photograph of the thermal separation pilot plant is presented in Figure 2.

The thermal separator pilot plant consists of a continuously rotating 16.5 cm diameter tube (chamber) partially enclosed in a 4.3 meters long gas fired shell. The system is fired with propane at a rate of up to 337 MJ/hr (320,000 BTU/hr) and it transfers ≈1/3 of the heat to the test material.

Soil is fed continuously into the sealed system through a screw feeder and exits through a rotary valve. Purge gas is introduced at the soil discharge end, flows counter current to the soil flow, and exits into the gas quenching and condensing system.

UNIVERSITY OF MINNESOTA TESTS

Under a TSCA R&D permit for the University of Minnesota, pilot scale testing was performed on soil from the Rosemount Research Center (RCC) site. The site was contaminated with PCBs by small businesses, operating between 1968 and 1985,

Table 1 University of Minnesota, Pilot Plant Demonstration Test Conditions and PCB Analytical Results

Run	Total Soil Retention Time (min)	Soil Temp (°C)	Soil Feed Rate (lbs/hr)[3]	PCB Concentration (ppm)[1]		
				Soil Type[2]	Feed Soil	Treated Soil
01	39	375	40	F	216	<2.0
02	38	452	40	F	220	<2.0
03	39	545	40	F	183	<2.0
04	21	373	74	F	199	<2.0
05	20	449	72	F	247	<2.0
06	21	551	72	F	231	<2.0
07	22	372	70	O	489	<2.0
08	15	380	71	O	546	<2.0
09	22	371	70	O	642[4]	<2.0
10	15	300	70	O	642[4]	<2.0
11	39	379	45	S	44500[5]	10.9
11A	23	377	40	S	44500[5]	52.3
12	45	450	40	S	44600[6]	3.85
12A	22	449	39	S	44600[6]	<2.0
13	21	551	70	S	35500	<2.0

[1] DCMA Analytical Method
[2] Soil type: O = organic; F = Fill, S = Sand
[3] 2.2 lbs = 1 kg
[4] Same feed for runs 9 & 10
[5] Same feed for runs 11 & 11A
[6] Same feed for runs 12 & 12A

that leased portions of the site for electrical equipment salvage. IT tested three different types of site soils:

- a fill soil classified as silty sand and clayey silt contaminated with ≈200 ppm of Aroclor 1260;
- an organic soil classified as black to brown stiff clayey and organic silt contaminated with ≈500 ppm of Aroclor 1260; and
- a sandy soil consisting of medium dense fine to medium sand contaminated with ≈40,000 ppm of Aroclor 1242.

Table 1 provides a summary of the operating conditions and the starting and final concentration of PCBs in the test soils. Each type of soil was successfully treated to a residual PCB concentration of less than 2 ppm as calculated using the Dry Color Manufacturing Association (DCMA) analytical procedure. This method for the analysis of PCBs in soil was required by the USEPA as a condition of the TSCA R&D permit.

Starting and treated soil samples were also analyzed for 2,3,7,8-tetrachlorodibenzo-p-dioxin (TCDD), 2,3,7,8-tetrachlorodibenzo-furan (TCDF), and total tetrafurans using GC/MS. All starting and treated soils were below detectable levels (typically 0.66 ppb) for TCDD. Table 2 shows the results for 2,3,7,8-TCDF and total TCDF. All feed soils had low levels of TCDFs. The fill material and the sandy soil were treated to below detectable levels of both 2,3,7,8-TCDF and total TCDF in experiments at 550°C. The organic soil was not subjected to run conditions above 380°C and, therefore, contained residual levels of the compounds.

Table 2 University of Minnesota, Thermal Separation of PCB Contaminated Soils, Analytical Data Summary Total and 2,3,7,8-TCDF Results

Run	Soil Temp. °C	Feed Soils (ppb)		Treated Soils (ppb)	
		2,3,7,8-TCDF	Total TCDF	2,3,7,8-TCDF	Total TCDF
01	375	0.78[1]	3.4[1]	0.44	2.2
02	452	0.78	3.4	ND[2]	0.12
03	545	0.78	3.4	ND	ND
04	373	0.78	3.4	0.2	0.71
05	449	0.78	3.4	ND	ND
06	551	0.78	3.4	ND	ND
07	372	NA[3]	5.3[4]	1.8	7.0
08	380	NA	5.3	1.8	7.6
09	371	NA	5.3	2.5	10.5
10	300	NA	5.3	1.9	6.8
11	379	1.6[5]	5.2[5]	2.9	16.9
11A	377	1.6	5.2	2.9	16.9
12	450	1.6	5.2	0.2	1.4
12A	449	1.6	5.2	0.2	1.4
13	551	1.6	5.2	ND	ND

[1] Composite Feed Sample Runs 1-6
[2] ND = Not Detected
[3] NA = Not Analyzed
[4] Composite Feed Sample Runs 7-10
[5] Composite Feed Sample Runs 11-13

Table 3 Summary of Typical Pilot Plant Test Results

Soil Source/ Type	Soil Treatment Conditions: Temp. °C	Retention Time Minutes	PCBs ppm	Feed Soil: 2,3,7,8 TCDD ppb	2,3,7,8 TCDF ppb	Total TCDF ppb	Treated Soil, ppm: 2,3,7,8 PCBs ppm	2,3,7,8 TCDD ppb	Total TCDF ppb	TCDF ppb.
USAF-	560	40	NA	260	NA	NA	NA	ND[1]	NA	NA
Gulfport/sand	560	19	NA	236	NA	NA	NA	ND	NA	NA
	560	10.5	NA	266	NA	NA	NA	ND	NA	NA
	460	24	NA	233	NA	NA	NA	0.5	NA	NA
USAF-	550	5.6	NA	48	ND	ND	NA	<0.084	ND	ND
Johnston Island/ crushed coral	555	20	NA	56	ND	ND	NA	0.23	ND	ND
DOE Mixed Waste soil/silty sand	550	19	37.5	ND	1.0	ND[2]	<2	ND	ND (0.75)	ND[2]

[1] Detectability ranged from 0.018 to 0.051 ppb
[2] Detectability ranged from 0.22 to 1.0 ppb
ND = Not detected
NA = Not applicable

Table 4 Effect of Temperature and Residence Time on PAH Treatment Efficiency

Soil	Temperature (°C)	Time (Minutes)	PAH Removal (%)
A	300	5	96
A	300	9	93
A	400	5	99.5
A	400	9	99.95
B	300	5	96.5
B	300	9	98.9
B	400	5	99.6
B	400	9	99.92
C	300	9	88
C	350	9	96.7
C	400	9	99.1

Interpretation of the PCB and the TCDF data indicates that the PCBs can be removed from actual site soils to below 2 ppm—at temperatures between 300°C and 375°C for low levels of contamination (Runs 1, 4, 7, 9, 15), or 450°C for high levels of contamination (Run 12A). However, removal of the TCDF to below detectable levels required treatment at ≈550°C for 20 minutes (Run 13).

OTHER TESTING PROGRAMS

IT has also performed tests for the U.S. Air Force using the thermal separation system on soils contaminated with Herbicide Orange (including dioxin) [2,3]. These tests were conducted in Mississippi and on Johnston Island in the South Pacific. One of the first RCRA RD&D permits issued by the EPA was for The Johnston Island project. The thermal separation process reduced the dioxin content of the treated soils to less than 1 ppb. The organic contaminant vapors were condensed by quenching in an organic solvent and were destroyed by UV photolysis.

Table 5 Types of Contaminated Soils and Other Wastes Tested

Soil	Others
PCBs	Oily mill sludge
PAHs	Tetraethyl lead sludge
2,4,-D	Kerosene contaminated clay
2,4,5-T	K106 (Hg-sulfide contaminated sludge)
Dioxins	
Low level radioactivity and organics	Styrene tars
	API separator sludges
Pentachlorophenol	Creosote Sludge
	Mercury and thorium contaminated sludge

The IT thermal separation technology has also been demonstrated in pilot scale tests on two mixed waste soils contaminated with PCBs and low levels of uranium and technetium [5]. Thermal separation treatment separated the PCBs from the radioactive soil, thus, making the latter suitable for disposal as a low level radioactive waste. The PCBs were condensed and collected for off-site disposal; negligible radioactivity was found in the condensate. Table 3 summarizes typical results from these pilot runs.

Pilot scale tests have also demonstrated the ability of the thermal separation technology to treat soils from old manufactured gas plant sites. The contaminants of concern at these sites were polycyclic aromatic hydrocarbons (PAH). Table 4 shows the effect of temperature and residence time on treatment efficiency.

In addition to these pilot plant tests, IT has developed a data base in the application of the IT thermal separation technology for soils contaminated with a wide variety of organic and inorganic contaminants. Table 5 lists the types of contaminants previously tested in laboratory or pilot scale equipment. In addition, three types of laboratory test equipment have been used to understand the key treatment process requirements, such as temperature and residence time, to achieve specific removal efficiencies and clean-up criteria for widely different organic contaminants.

The laboratory testing apparatuses are:
- the tray furnace,
- the tube furnace, and
- the Rotary Thermal Apparatus.

The tray furnace test uses a static but very thin layer of soil to minimize the potential effects of temperature gradients and gas phase diffusion. The test sample is rapidly heated to the test temperature and maintained for a predetermined period. The residue from the test is analyzed for the constituent of interest.

The tube furnace test uses a static 2.5 cm diameter by 15 cm long aliquot of soil confined in an indirectly heated quartz tube. Upon heating, the off-gas from the soil can be collected and analyzed, condensed, or scrubbed to evaluate down-stream processing options.

The rotary thermal apparatus (RTA) shown in the Figure 3 photographs is a 12.5 cm diameter by 36 cm long rotating metal chamber which is indirectly heated with an electric furnace. One to two pound aliquots of soil are batch charged and

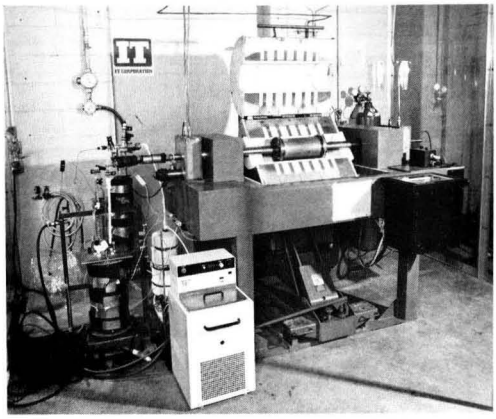

FIGURE 3. Rotary thermal apparatus.

heated to the desired temperature and maintained for the test period. Off-gas from the test apparatus is condensed or scrubbed depending on process applications. Residue can be analyzed for constituents of interest and a sufficient amount of treated material is generated for use in TCLP testing.

THERMAL SEPARATION COSTS

The cost considerations in remediating soils or solids contaminated with hazardous materials are:

1. planning and procurement,
2. permitting,
3. site preparation,
4. equipment mobilization,
5. equipment erection/startup,
6. operations,
7. equipment demobilization, and
8. site closure.

The non-operational cost components are highly specific depending on the contaminants involved and the site conditions. The estimated direct operating cost of the thermal separation technology is ≈$80/ton ($0.088/kg) based on a 10 ton/hr (9,000 kg/hr) system treating soil with 20% moisture. This cost includes $20/ton ($0.022/kg) for depreciation and $60/ton ($0.066/kg) for labor, utilities, fuel, materials and supplies, and administrative costs.

SUMMARY

Thermal separation offers a cost-effective alternative to incineration for decontaminating soils and solids. The use of a thermal desorption treatment system for a particular contaminated soil problem must be selected based on projected technical performance and cost, along with such factors as regulatory permitting, site characteristics/location, and the presence of other contamination problems at the site (e.g., drummed waste, impounded sludges, etc).

LITERATURE CITED

1. Freestone, F., et al, "Evaluation of On-Site Incineration for Cleanup of Dioxin Contaminated Materials," 1986 Hazardous Material Spills Conference Proceedings, May 5-8, 1986, Government Institutes Inc. publisher, Rockville, MD, p. 371 ff.
2. Helsel, R. W., et al, "Thermal Desorption/Ultraviolet Photolysis Process Technology Research, Test, and Evaluation Performed at the Naval Construction Batallion Center, Gulfport, MS, for the USAF Installation Restoration Program, Volume I, Report No. ESL-TR-87-28, AFESC, Tyndall, AFB, FL.
3. Helsel, R. W., et al, "Thermal Desorption/Ultraviolet Photolysis Process Research Test and Evaluation Performed at Johnston Island for the USAF Installation Restoration Program, Volume I, Report No. ESL-TR-87-37, AFESC Tyndall AFB, FL.
4. "Engineering Scale Demonstration of Thermal Separation Technology for PCB-Contaminated Soil," July 1988, Available for inspection at Minnesota Pollution Control Agency, St. Paul, MN.
5. "Removal of PCBs from Mixed Waste Soils by Thermal Separation," DOE Model report, Martin-Marietta Energy Systems, Oak Ridge, TN, November 1988.
6. McCabe, Mark M., "Evaluation of Thermal Technology for the Treatment of Contaminated Soils and Sludges," Proceedings of the 6th National Conference on Hazardous Wastes and Materials, April 12-14, 1989, p. 339 ff.
7. Beckstrom, B. D., "Destruction of Hazardous Waste and Cleanup of Contaminated Soils by Pyrolysis," 1989 AICHE National Summer Meeting.
8. Nielson, R. K., and M. G. Cosmos, "Low Temperature Thermal Treatment of Volatile Organic Compounds from Soil: A Technology Demonstrated," *Environmental Progress,* May 1989, p. 139.
9. Lighty, I. S., et al, "Fundamental Experiments on Thermal Desorption of Contaminants from Soils," *Environmental Progress,* Vol. 8, No. 1, February 1989, p. 57.
10. Lauch, R., et al, "Evaluation of Treatment Technologies for Contaminated Soil and Debris," Proceedings of Third International Conference on New Frontiers in Hazardous Waste Management, September 10-13, 1989, EPA/600/9-89/072, p. 1.
11. Swanstrom, C., "X*Trax^{R} Transportable Thermal Separator for Solids Contaminated with Organics," presented at International Symposium on Hazardous Waste Treatment: Treatment of Contaminated Soils, Cincinnati, OH, February 5-8, 1989.
12. The Superfund Innovative Technology Evaluation Program: Technology Profiles, EPA/540/5-89/013, November 1989, p. 29.
13. Installation Restoration General Environmental Technology Development: Task II—Pilot Investigation of Low Temperature Thermal Stripping of Volatile Organic Compounds (VOCs) from Soil, Report No. AMXTH-TE-CR-86074, June 1986.
14. The Superfund Innovative Technology Evaluation Program: Technology Profiles, EPA/540/5-89/013, November 1989, p. 17.
15. The Hazardous Waste Consultant, March/April 1990, p. 1-5.

The Incineration System "Thermal Siphon" Effect

Peter J. Kroll and Robert C. Chang
International Waste Energy Systems (WES)
2150 Kienlen Avenue, St. Louis, MO 63121

An anomalous phenomenon known as the "thermal siphon" effect has been observed in four operational incinerators with vertical secondary combustion chambers (SCCs). The kiln and air pollution control (APC) system pressures in all four cases have, under certain conditons, been observed to be negative while the pressure at the top of the SCC is positive. This paper will focus on an explanation of this unusual fluid flow phenomenon.

INTRODUCTION

The occurrence mentioned above can be explained in a qualitative manner as being primarily due to differences in elevation between the two combustion chambers. Since incinerators are usually kept under slightly negative (less than −25 mm water column [wc]) pressure, and chamber pressure transmitters use ambient air as a reference point, the normally insignificant change in ambient air pressure with elevation becomes quite important.

VERTICAL SCC DESIGN CONCEPTS

Incineration is a combustion process that utilizes excess air and relatively high temperatures to produce conditions which will degrade and consume the organic portion of a waste. The effectiveness of combustion in an excess-oxygen environment in the SCC is related to a combination of the "three Ts": time, temperature, and turbulence.

- Time refers to gas residence time. Residence time requirements are related to reaction rate ("incinerability"), which is an exponential function of absolute temperature.
- Temperature is normally maintained above the auto-ignition temperature of organic waste constituents to complete the combustion of organics in the flue gas.
- Turbulence relates to the intimate mixing of excess air with the residual organics present. The Reynolds number (Re) is a dimensionless quantity which is usually used to measure turbulence.

Fluid turbulence is dependent upon vessel geometry as well as the velocity and kinematic viscosity of the flue gas. Since kinematic viscosity is inversely proportional to the gas temperature, temperature is an important factor in achieving proper levels of turbulence.

One or more "pinch point," at which the cross-sectional flow area is greatly reduced, are generally provided to increase local gas velocity and thus areas of turbulence in the SCC. Many SCC designs provide for the gases entering the SCC to pass through a pinch point prior to flowing through the area where the burners are mounted. This highly turbulent regime will ensure that virtually all combustion gases pass through the flame zone, where destruction efficiency is greatest.

Another important combustion process variable is the oxygen content of the combustion gas. The SCC excess oxygen content is normally maintained at 4% to 10% on a dry-volume basis. At a given waste and fuel firing rate and temperature, increasing excess air will increase combustion gas flow and turbulence, therefore reducing gas residence time. In addition, since excess air is a heat sink, it can be used to control temperature.

While the kiln is always horizontal, vertical SCCs are becoming the industry standard. The gradual accumulation of slag in the SCC is one of the major reasons for utilizing a vertical configuration. A vertical SCC can be designed to provide a means of accommodating slag buildup and meltdown from the walls. A vertical SCC with a bottom which incorporates a wet ash/slag quench and submerged drag conveyor for removing slag, or an "ash can" for accumulating slag, is often used to address this problem.

The SCC diameter is normally chosen to maintain a high bulk gas velocity (3 to 6 m/sec), and thus turbulence, throughout the chamber, even at the expected maximum turndown ratio.

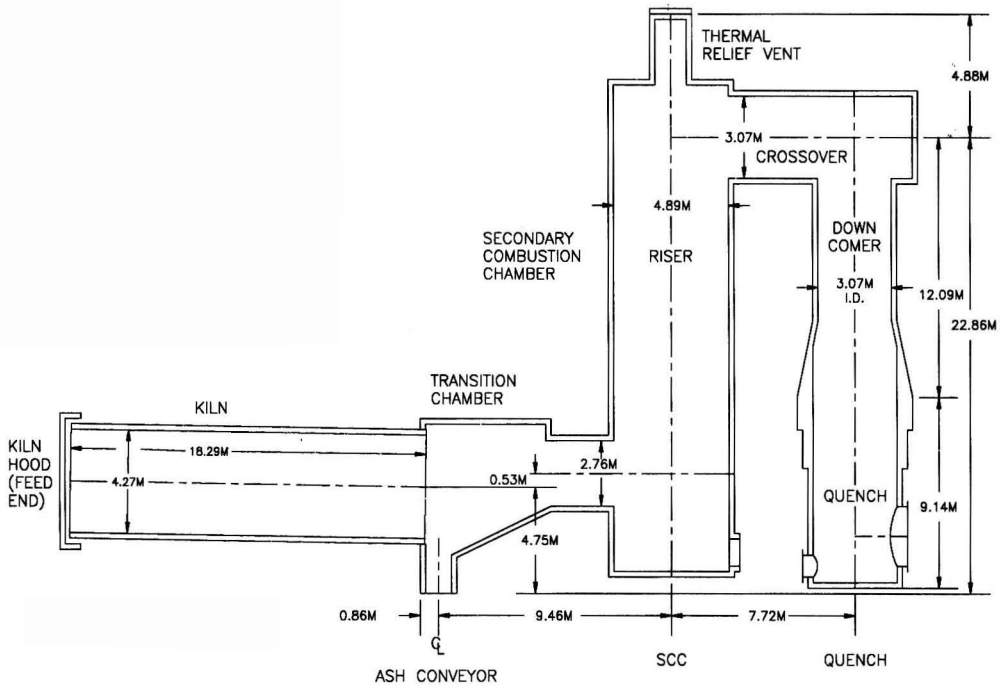

FIGURE 1. Incinerator cross-sectional view

The requirement for two or more seconds of gas residence time in the SCC usually determines the chamber length. A high residence time in the post-flame zone under oxidative conditions, high temperature, and high turbulence will ensure optimum destruction efficiency.

As requirements for gas residence time increase, a design compromise must be considered to avoid having a very long, tall SCC. The most economical approach seems to be increasing the SCC diameter as much as possible and "bending over" the vertical chamber where practical. Figure 1 illustrates a typical rotary kiln incinerator with a vertical SCC.

OVERALL FLUID FLOW CONCEPTS

For simplicity, let us consider the incinerator system to be a case with the following assumptions:

- The flow is steady and one-dimensional.
- Fluid friction is restricted to wall shear.
- The fluid is an ideal gas.
- Each incinerator chamber has a uniform temperature profile.

Although real combustion gas flow is much more complex, these restrictions will allow us to concentrate on the effects of basic flow processes.

The mechanical energy balance equation for the combustion gas can be written in a differential form as[1]

$$Vdp + vdv + dF + (g \cdot \sin\theta)dx = 0 \qquad (1)$$

Where V = fluid specific volume, p = pressure, v = bulk fluid velocity, ($\sin\theta$) $dx = dZ$ = vertical distance through which the fluid is raised when it moves distance (dx) along the incinerator, F = frictional loss and g is a constant.

The first term of this equation related to differential pressure, the second to velocity head (or kinetic energy), the third to frictional loss (or heat) and the last to elevation head (or potential energy). This equation for compressible fluid flow is analogous to the familiar Bernoulli equation for incompressible flow.[2]

The frictional loss for a compressible fluid can be expressed as

$$dF = \frac{f \cdot v^2}{2D} dx \qquad (2)$$

Where f = Darcy friction factor, which can be calculated from the Colebrook equation for turbulent flow[3] as

$$\frac{1}{\sqrt{f}} = -2 \log\left[\frac{\epsilon}{3.7D} + \frac{2.51}{Re\sqrt{f}}\right] \qquad (3)$$

where ϵ = duct roughness and D = duct diameter.

Substituting equation (2) into equation (1), one can solve for the pressure loss along the incinerator by the relationship

$$Vdp + vdv + \frac{f \cdot v^2}{2D} dx + g \cdot \sin\theta dx = 0 \qquad (4)$$

SAMPLE CALCULATIONS FOR TYPICAL INCINERATOR

A computer program was written to solve equation (4) with a boundary condition of -25 mm wc kiln feed-end pressure. Finite element analysis was used to divide each chamber into 20 small increments. After each iteration (dx increment), the pressure at a new location was obtained. Results were calculated for each pressure tap for one set of operating conditions. The operating conditions to be assumed (for the purpose of

Table 1 Incinerator Average Operating Conditions

	KILN	SCC
Heat release, KW	21,982	21,982
Temperature, °C	955	1,220
Combustion air rate, NM^3/min	633	392
Excess air, %	100	17
Bulk gas velocity, m/sec	3.81	5.58
Gas specific volume, m^3/kg	3.46	4.23

analysis) for the incinerator in Figure 1 are shown in Table 1. These conditions represent a case of maximum heat release and maximum combustion gas flow, and thus the velocity head and friction loss should be greatest.

In order to simplify the discussion, let us consider the separate terms of the velocity head, elevation head and friction loss. The individual terms in equation (4) can be integrated separately to analyze how each term contributes to the overall pressure drop.

VELOCITY HEAD

The velocity head, which is caused by the difference in gas velocities at the kiln feed end and at the SCC exit, can be calculated as

$$Velocity\ Head = \int_1^3 \frac{v}{V} = 2.18\ mm\ wc \qquad (5)$$

FRICTION LOSS

The friction loss for the compressible fluid is given by equation (2). This term can be calculated as

Friction Loss = Fitting Friction Loss + Line Friction Loss

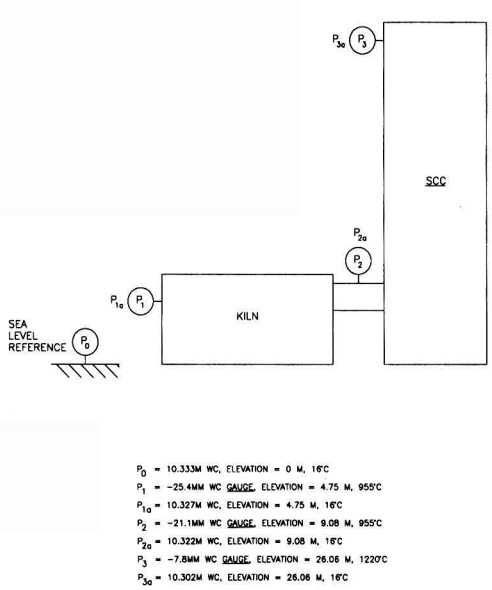

FIGURE 2. Location of pressure measurement ports

Table 2 Calculated Pressures for Base Conditions

Location	Pressure (wc)
p_0	10.333 m
P_{1a}	10.327 m
P_1	10.302 m
$P_1 - P_{1a}$	−25.4 mm
P_{2a}	10.322 m
P_2	10.301 m
$P_2 - P_{2a}$	−21.1 mm
P_{3a}	10.302 m
P_3	10.294 m
$P_3 - P_{3a}$	−7.8 mm

$$= \sum_i \left[K_f \cdot \frac{v^2}{2V} \right] + \int_1^3 \frac{f \cdot v^2}{2D \cdot V} \cdot dx = 2.05\ mm\ wc \qquad (6)$$

The "two-K" method[4] was chosen to predict the K-factors ($K = f \cdot L/D$) for the friction loss of the "fittings." The "fittings" in this case include the contraction and expansion of the transition chamber and the 90° turns in the SCC, which were all taken into account in the friction loss calculations.

ELEVATION HEAD

Figure 2 illustrates the location of the various pressure measurement points for this example. The elevation at the kiln feed-end pressure transmitter (p_1) is 4.75 m, at the transition chamber pressure transmitter (p_2) is 9.08 m, and at the SCC top pressure transmitter (p_3) is 26.06 m. Let us assume that the ambient pressure at p_0 (sea level) is 10.33 m *wc*. The ambient pressure at p_1 can be represented as p_{1a}. This pressure is therefore

$$p_{1a} - p_0 = -4.75m\ air\ column\ (ac) \qquad (7)$$

The density of ambient air at 16°C is 1,203 kg/m^3 and water density is 1000 kg/m^3; therefore, we can express this as

$$1000\ mm\ ac/m\ ac \cdot \frac{1.203}{1000} = 1.2\ mm\ wc/m\ ac \qquad (8)$$

$$p_{1a} - p_0 = -4.75\ m\ ac = -5.71\ mm\ wc \qquad (9)$$

$$p_{1a} = 10.333\ m - 5.71\ mm = 10.327\ m \qquad (10)$$

Similarly, we can calculate the ambient pressure at p_{2a} to be 10.322 m wc, and at p_{3a} to be 10.302 m wc.

The elevation head, or pressure drop caused by elevation difference, can be calculated as

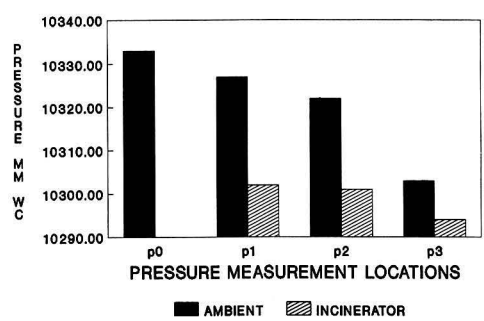

FIGURE 3. Pressure variation throughout incinerator

Table 3 Effect of temperature and elevation pressures

	Kiln at 927°C SCC at 1010°C	SCC Pressure Tap @10.67 m elevation
$P_1 - P_{1a}$	−25.4 mm wc	−25.4 mm wc
$P_3 - P_{3a}$	− 8.9 mm wc	−21.6 mm wc

$$Elevation\ Head = \int_1^3 \frac{g \cdot \sin\theta}{V} dx = 3.76\ mm\ wc \qquad (11)$$

TOTAL PRESSURE DROP

The total system pressure drop is a summation of the velocity head, friction loss and elevation head, from equations (5), (6) and (11).

$$\text{Total Pressure Drop} = \text{Velocity Head} + \text{Friction Loss} + \text{Elevation Head}$$
$$= 2.18\ mm + 2.05\ mm + 3.76\ mm = 7.99\ mm\ wc \qquad (12)$$

RESULTS

The resultant pressures for the operating conditions of Table 1 area summarized in Table 2 and Figure 3. The pressure transmitter readings are really *differential pressure*, since each transmitter uses ambient air pressure as reference.

The absolute pressure p_1 is equal to 10.302 m wc, and the pressure drop between p_1 and p_3 is 7.99 mm wc; therefore, $p_3 = 10{,}302 - 7.99 = 10.294$ m wc. Since p_{3a} is at 10.302 m wc, this is a differential pressure of 7.80 mm wc.

Thus the SCC pressure transmitter would read −7.8 mm wc while the kiln feed hood pressure transmitter would indicate −25.4 mm wc. Note that the great majority of this 17.6-mm wc difference is due to elevation differences in the pressure transmitters and the resultant ambient air pressure change. As the actual fluid pressure drop decreases at lower flow, the effect of the elevation difference is even more dominant.

Note that the ambient air pressure differential between P_{1a} and P_{3a} is 25 mm, which is about equal to the kiln feed end pressure transmitter ($P_1 - P_{1a}$) setpoint of −25.4 mm.

To compare the relative effects of gas temperature and elevation variations on the SCC pressure, two more cases were run and the results are given in Table 3. As can be seen, increasing the SCC temperature or height will enhance the thermal siphon effect. Elevation change, however, has a much more dramatic effect on pressure than does temperature change.

CONCLUSIONS AND RECOMMENDATIONS

The results clearly show what has been observed at several incinerators: the kiln gauge pressure can be as low as −25.4 mm wc while the top of the SCC can be −7.8 mm wc. It has thus been shown that the thermal siphon effect is a real factor which must be accounted for in incinerator design. Merely relocating the SCC pressure transmitter is not a feasible solution if the SCC must remain under negative pressure.

As we discussed earlier, the SCC diameter is normally chosen to maintain a high bulk gas velocity, and thus turbulence, throughout the chamber. The requirement for two or more seconds of gas residence time in the SCC usually determines the chamber length. As requirements for gas residence time increase, a design compromise must be considered to avoid having a very tall SCC.

The most practical solution seems to be increasing the SCC diameter as much as possible and "bending over" the vertical chamber in an inverted "J" or "U" configuration, depending upon downstream equipment orientation. In some cases, pinch points and/or high-velocity air jets can be added to increase combustion gas turbulence.

Performance of a new or existing incinerator with a vertical SCC can be improved by using the SCC instead of the kiln as the negative pressure (draft) control point. Most incinerators use the kiln pressure as the input to the combustion system draft controller, since it is the point furthest from the induced draft (ID) fan. As we have seen, however, the SCC can attain positive pressure while the kiln is still at negative pressure; thus, it is more appropriate to use the SCC as the draft control point.

NOTATION

D = Inside diameter of duct, m
F = Frictional loss, N-m/kg
f = Darcy friction factor, dimensionless (equal to four times the Fanning friction factor)
g = Gravitational acceleration, m/sec^2
K = Fitting friction loss factor, dimensionless
L = Length of duct or equivalent length of fittings, m
p = Pressure, m of water column
Re = Reynolds number, dimensionless
V = Fluid specific volume, m^3/kg
v = Bulk fluid velocity, m/sec
x = Distance traveled by fluid, m
Z = Height above datum plane, m

Greek Letters

ϵ = duct roughness factor, m
ρ = density of fluid, kg/m^3
μ = viscosity of fluid, kg/m-s

LITERATURE CITED

1. McCabe, W. L., and J. C. Smith, "Unit Operations of Chemical Engineering," McGraw-Hill, New York, N.Y. third edition, pp. 119-120.
2. Perry, R. H., and C. H. Chilton, "Chemical Engineering Handbook," McGraw-Hill, New York, N. Y. fifth edition, p. 526.
3. Serghides, T. K., "Estimate Friction Factor Accurately," *Chemical Engineering,* Vol. 91, No. 5, p. 63 (1984).
4. Hooper, W. B., "Calculation of Head Loss Caused by Change in Pipe Size," *Chemical Engineering,* Vol. 95, No. 16, p. 89 (1988).

Application of Selective Catalytic Reduction (SCR) Technology for NOx Reduction From Refinery Combustion Sources

David Cobb, Lisa Glatch, John Ruud, and Scott Snyder
Fluor Daniel Inc., Irvine, CA 92730

Selective Catalytic Reduction (SCR) has been applied as a NOx abatement technique for stationary sources of nitrogen oxides (NOx) in Japan since the early 1970s. To date, there are over 100 SCR installations operating in Japan. During the 1980s, a number of SCR systems have been installed in the United States, primarily in California. Among these applications are fired heater, boiler, and gas turbine/heat recovery steam generator (HRSG) installations. These installations provide a basis to assess the state-of-the-art for applying SCR to comply with refinery NOx emission limitations.

BACKGROUND

Need for Stringent NOx Controls

Exposure to nitrogen dioxide (NO_2) decreases lung function and may increase susceptibility to disease. Table 1 outlines some of the detrimental effects attributed to NOx emissions. The National Ambient Air Quality Standard for NO_2 is 100 $\mu g/m$, annual average (about 0.05 ppm). California has also adopted a one-hour ambient standard for NO_2 of 470 $\mu g/m$ (0.25 ppm). The South Coast Air Basin of Southern California is the only area of the country which currently exceeds the federal ambient NO_2 standard. No ambient standards exist for nitrogen oxides other than NO_2. NOx emitted from combustion sources typically consists of more than 90 percent NO and the usual assumption is that emissions of nitric oxide (NO) are eventually oxidized to NO_2 in the atmosphere.

In addition to the adverse effects of direct NO_2 exposure, NOx emissions contribute to the formation of fine nitrate particulates and acidified moisture in the atmosphere (acid rain and fog) and, in combination with reactive organics, play an important role in the atmosphere chemistry of photochemical oxidant (ozone) formation. Several urban areas in the United States exceed the federal ambient ozone standard. There is some disagreement among the scientific community as to whether the ozone formation mechanism is limited by the concentration of NOx or organics. At the present time, the federal EPA and most states consider reduction in organic emissions alone as the preferable strategy for ambient ozone reduction. In contrast, California regulators have adopted a strategy of simultaneous reduction of NOx and organic emissions to achieve ozone attainment.

Table 1 Effects of NO_x Emissions

- Direct NO_2 Exposure
- Forms Fine Particulates (Nitrates)
- Acid Rain and Fog
- Photochemical Oxidant (Ozone) Precursor

The federal New Source Performance Standards (Code of Federal Regulations, Title 40, Part 60) for combustion sources such as process heaters, industrial and utility boilers, and combustion turbines, establish NOx emission limits which can be readily achieved with technology other than SCR, such as low NOx burners or steam injection. Federal, and most states', Prevention of Significant Deterioration (PSD) regulations, applicable to attainment areas, presently require the consideration of SCR as a candidate for Best Available Control Technology (BACT) for larger new sources. Agency policy currently requires that PSD applicants perform a "top-down" BACT analysis. In this procedure, the most stringent candidate technology is evaluated for technical and, to a certain extent, economic feasibility. It a technology can be eliminated on either basis the next most stringent control technique is evaluated.

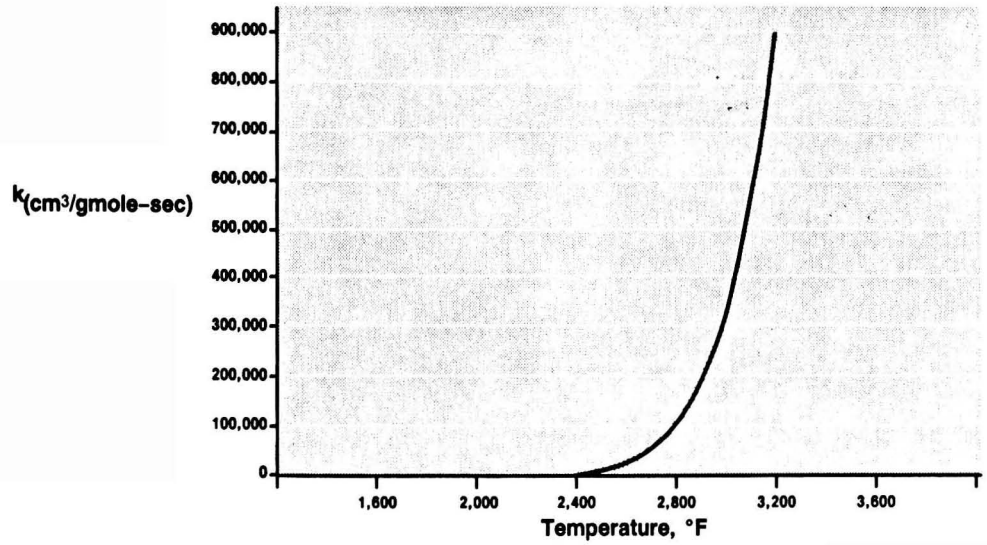

ADAPTED FROM: H.K. Newhall, "Kinetics of Engine Generated Nitrogen Oxides and Carbon Monoxide, "Twelfth Symposium (International) on Combustion (1969).

FIGURE 1. Effect of temperature on NOx formation rate

The process continues until a technology cannot be eliminated. This technology is then selected as BACT. Agencies have continually adjusted upward what they consider to be reasonable NOx control costs. This, in combination with increasing SCR commercial application experience, is making the elimination of SCR in a top-down BACT analysis increasingly more difficult.

The situation in most areas of California is more stringent than the nation as a whole. Frequent violations of the ozone ambient standards, the California ozone attainment strategy of NOx and organic reductions, and the continued NO_2 ambient standard violations have created a strong regulatory driving force for SCR installation. The South Coast Air Quality Management District, SCAQMD (Los Angeles area), has required SCR on all but the smallest new heaters, boilers, and combustion turbines for more than four years. The Bay Area AQMD (San Francisco area) and several other California air pollution control districts have followed suit and require SCR

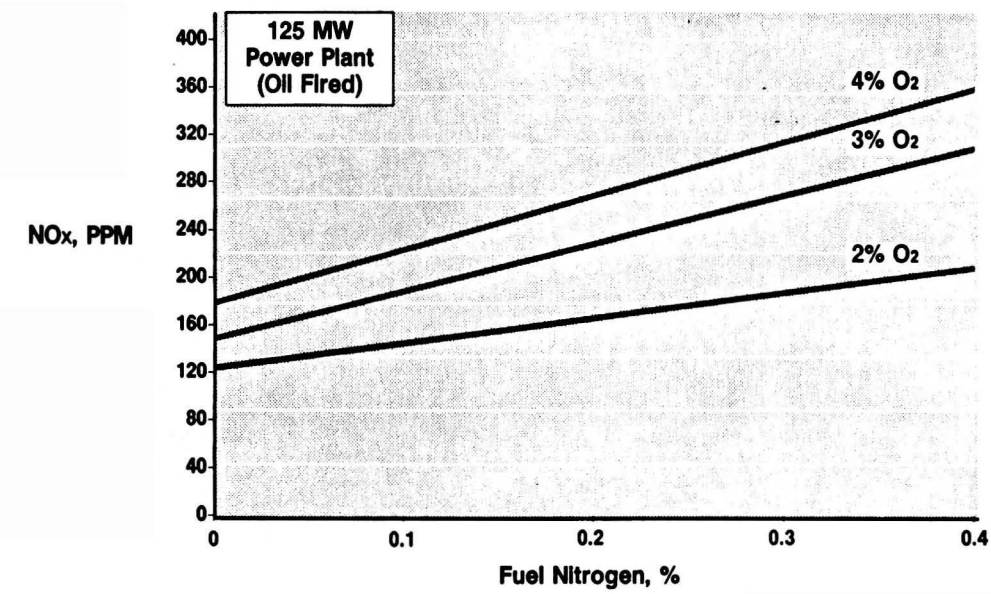

ADAPTED FROM: Ando, et al, NOx Abatement for Stationary Sources in Japan, EPA-600/2-76-0136, January 1976.

FIGURE 2. Effect of fuel nitrogen on NOx emissions

Table 2 NO_x Formation Control Techniques

Fired Heaters/Boilers
- Low NO_x Burners
- Gas Recirculation
- Staged Combustion
- Steam/Water Injection
- Reduced Heat Release Rate
- Reduced Air Preheat

Gas Turbines
- Steam/Water Injection
- Low NO_x Combustor

for major new sources. The SCAQMD is adopting rules for existing refinery heaters, boilers, and combustion turbines based on emission reductions achievable with SCR (recent developments in burner technology may displace the use of SCR in some heater applications).

Outside California, SCR is less frequently required. However, the application of SCR to flue gas from combustion turbines is gaining acceptance by non-California regulatory agencies because of the large NOx mass emission rate associated with these machines. The northeastern states in particular are increasingly pressing for SCR systems on combustion turbine installations.

NOx Formation

NOx is formed during combustion both from nitrogen contained in the combustion air and from nitrogen contained in the fuel. As illustrated in Figure 1, thermal NOx generated from nitrogen in the air is formed in the presence of oxygen when the flame temperature exceeds about 2600°F (1430°C). Compared to the triple-bonded nitrogen molecule, fuel-bound nitrogen more readily combines with oxygen or other intermediates to form NOx. Figure 2 shows the effect that fuel-bound nitrogen can have on total NOx emissions and also illustrates the increase in NOx formation which occurs with increasing oxygen concentration.

Combustion Modification

NOx can be controlled by modifying the combustion process or fuel to reduce its formation and/or removing it through treatment of the flue gas. It is generally more cost effective to prevent as much NOx formation as possible before considering additional steps to remove NOx which has already been formed.

Table 2 presents some of the NOx formation control techniques in general use. Although several different methods are used, the basic principle of each method is to lower the flame temperature and/or reduce oxygen concentration in the flame zone.

For fired heaters and package boiler systems used in refineries, the most widely applied control method is the use of low NOx burners. New advanced burner designs are being developed by some manufacturers, aimed at significantly reducing NOx formation compared with low NOx burners currently in widespread use [*1*].

Steam or water injection is typically used to reduce thermal NOx formation in gas turbines by acting as a diluent to reduce the flame temperature in the primary combustion zone. High temperatures in the primary combustion zone result in large yields of thermal NOx, and additional NOx emissions result from fuel nitrogen, if present. Several manufacturers are developing dry combustors designed to substantially reduce NOx formation without the use of steam or water injection.

Post Combustion Removal

Post combustion removal of NOx is required when NOx formation exceeds regulatory limits. In the United States, downstream removal of NOx formed in the combustion process has primarily been based on processes which convert NOx to nitrogen using injected ammonia or urea as a reducing agent. Selective non-catalytic reduction of NOx can be accomplished by mixing the reducing agent with the flue gas at a suitable temperature. Exxon's Thermal DeNOx Process, for example, is based on injecting ammonia into the flue gas within a temperature range of about 1500°F-2000°F (800°C-1100°C). [*2*] This process has been applied to many boilers and process fired heaters. Firebox temperatures on heaters often fall below the optimum temperature range for NOx conversion, making high conversion difficult to obtain.

For applications where very high percentage NOx removal is required or where it is difficult to inject ammonia within the temperature range required for effective use of Thermal DeNOx, SCR can be used to remove NOx from the flue gas. In the presence of the catalyst, the reduction reaction proceeds at much lower temperatures. Ammonia is added to the flue gas which then passes through layers of the catalyst. Table 3 summarizes some of the NOx conversion reactions which have been postulated to take place on the surface of the catalyst. The conversion products are nitrogen and water.

CATALYST TYPES AND SUPPLIERS

While the majority of SCR installations are in Japan, the Japanese are marketing their technology in both the United States and in Europe through license agreements with various manufacturers. U. S. catalyst manufacturers now also have several SCR installations in operation. For most applications, the Japanese and U.S. manufacturers utilize a rigid, honeycomb type catalyst with base metal oxides (primarily vanadium and titanium oxides). The catalysts differ among the manufacturers in the various compounds used to promote high activity, enhance durability, decrease oxidation characteristics, and provide resistance to contaminants. The methods by which the catalyst and substrate are manufactured and shaped also vary. The active materials (base metal oxides) are either impregnated on a metallic or ceramic substrate, or are integral with a homogeneous ceramic type substrate [*3*].

While base metal formulations are the predominant SCR catalyst types presently in use, two other types are emerging. The first is a zeolite molecular sieve catalyst wherein NOx and ammonia are adsorbed and react in the catalyst micro pore structure. The suppliers of this catalyst system claim higher operating temperatures are allowed than for the vanadium catalyst types and virtually no poisoning or fouling effects

Table 3 Reactions of NO_x Over SCR Catalyst

$4\ NO + 4\ NH_3 + O$	Catalyst	$4\ N_2 + 6\ H_2O$ (main reaction)
$6\ NO + 4\ NH_3$	Catalyst	$5\ N_2 + 6\ H_2O$
$2\ NO_2 + 4\ NH_3 + O_2$	Catalyst	$3\ N_2 + 6\ H_2O$
$6\ NO_2 + 8\ NH_3$	Catalyst	$7\ N_2 + 12\ H_2O$

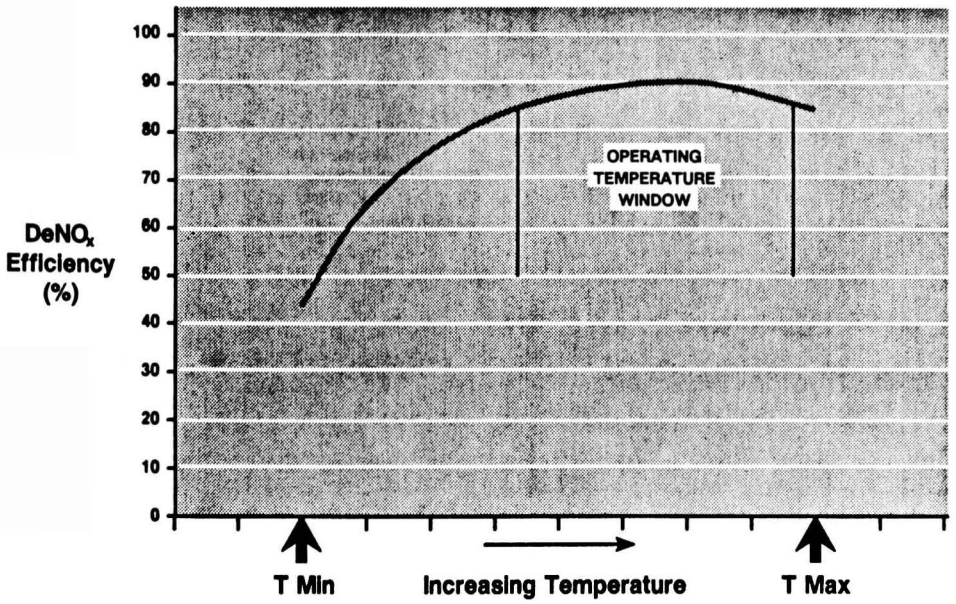

FIGURE 3. SCR efficiency vs. temperature

from fuel contaminants. The second is a noble metal-based formulation. According to the supplier, this catalyst converts excess ammonia to nitrous oxide (N_2O)—thus reducing potential concerns regarding the formation of ammonium salts which could cause fouling. (N_2O is specifically excluded from the federal definition of NOx.) This catalyst typically operates at lower temperatures than the vanadium-based systems and is more sensitive to sulfur contamination. Additional features of the noble metal catalysts are higher space velocities (less catalyst volume) and simultaneous carbon monoxide oxidation.

The following list identifies the principal SCR suppliers and the available catalyst types:

Japanese

Babcock Hitachi - Base metal/metallic plate substrate
Hitachi Zosen - Base metal/ceramic monolith or wire mesh
Ishikawajima - Harima Heavy Industries (IHI) - Base metal/ceramic monolith
Kawasaki Heavy Industries - Base metal/ceramic monolith
Mitsubishi Heavy Industries - Base metal/ceramic monolith
UBE - Base metal/ceramic monolith

Table 4 SCR Operating Temperatures – °F

	Maximum Range
Babcock Hitachi	480–780
Hitachi Zosen	625–790
IHI	400–750
KHI	570–750
MHI	400–750
Camet	437–527
Engelhard	575–750
JMI	650–800
Steuler	572–970
Norton	430–970
UBE	480–750

United States

Camet/W.R. Grace - Noble metal/metallic plate substrate
Engelhard - Base metal/ceramic monolith
Johnson Matthey - Base metal/metallic plate substrate
Norton - Zeolite

German

Steuler - Zeolite

EVALUATING AND IMPLEMENTING SCR TECHNOLOGY

Based on information obtained from various manufacturers and operating data from numerous installations both in Japan and the United States, a number of factors have been identified which should be considered when applying SCR technology to control NOx emissions. These considerations are listed below and discussed in the following sections:

- Operating temperature window
- Flue gas pressure drop
- Flue gas flow/temperature maldistribution
- Fouling potential and impact on emissions
- Operation in series with CO oxidation catalyst
- Flue gas contaminants
- Physical constraints
- Catalyst disposal
- Ammonia storage

Operating Temperature Window

One of the major operating constraints imposed on heat transfer equipment by the SCR system is that the catalyst must operate within a fairly narrow temperature window. Figure 3 is a typical curve of NOx reduction efficiency as a function of catalyst operating temperature at a fixed catalyst volume. Most

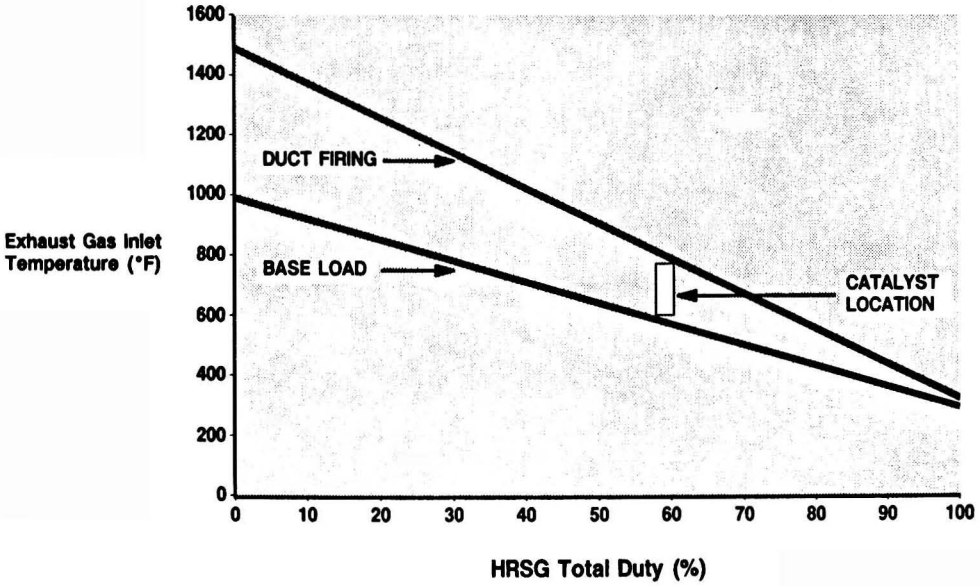

FIGURE 4. HRSG exhaust gas profile

suppliers offer several different catalyst compositions which have similar operating characteristics but with a different temperature range (which has the effect of shifting of the curve slightly to the left or right). Table 4 illustrates the span of operating temperature ranges for the catalyst formulations offered by each of the suppliers. The ranges shown may represent several different formulations offered by the same manufacturer. Depending on the catalyst system selected and the flue gas sulfur content, the minimum acceptable temperature may range from as low as 400°F (200°C) up to about 650°F (350°C), while the maximum acceptable operating temperature is typically between 750°F to 800°F (400°C to 425°C), with the notable exception of the zeolite catalyst.

As shown in Table 4, the operating temperature limitations dictate that, for a heater or boiler application, the SCR catalyst bed is located somewhere in the convection or economizer section. For a combustion turbine application, exhaust gas heat recovery is normally necessary to achieve the required catalyst bed temperature range, with the possible exception of the zeolite-type catalyst.

NOx conversion begins to decline gradually as the catalyst temperature decreases below or rises above the optimum conversion point. Catalyst systems are normally designed to operate within an acceptable range which means that the required catalyst volume must be adequate to achieve the required NOx conversion at temperatures away from the optimum. When the catalyst is operating below the minimum operating temperature, the catalyst activity declines rapidly and, in some cases, precipitates can deposit on the catalyst. Above the optimum operating temperature, NOx removal declines due to oxidation of ammonia. Operating above the maximum acceptable temperature can result in irreversible degradation of the catalyst. For most catalyst compositions, operating above about 800°F (425°C) may cause catalyst sintering, resulting in permanent deactivation [*4,5*].

A suitable catalyst must be selected and located where the temperature fluctuations stay within the specified catalyst operating range. For fired heater and boiler applications, the highest catalyst temperatures occur at full load operation. By contrast, duct firing is often required to increase the steam output of the heat recovery steam generator in a gas turbine combined cycle plant operating at reduced power output. In these installations, flue gas contacting the catalyst is colder during base load operation than during the duct firing condition. Figure 4 shows a typical heat curve for a heat recovery steam generator (HRSG) and the optimum location for the SCR catalyst. In this example, the unit is designed with a duct firing temperature of 1500°F (800°C), and the catalyst operates over a temperature range which approaches both the upper and lower operating limits of the catalysts. Firing above 1500°F (800°C) would subject the catalyst to an unacceptable temperature.

Flue Gas Pressure Drop

The pressure drop across the SCR catalyst bed will vary depending on the gas superficial velocity, catalyst configuration, and quantity of catalyst required to achieve specified NOx reduction efficiencies. Generally, the pressure drop for a high conversion SCR system is on the order of 1–4 inches of water column (250–1000 Pa) including the pressure drop across the ammonia injection grid located upstream of the catalyst bed. Typically, these added frictional losses more than double the pressure drop through a fired heater convection section, but amount to only about 15 to 30 percent of the drop through a HRSG. Frequently, catalyst manufacturers will allow additional space in the converter housing for future installation of catalyst as a safety margin in the event that the original catalyst charge does not perform to specification requirements during the warranty period. The pressure drop which would result by the addition of extra catalyst must be accounted for when sizing the heat transfer equipment and auxiliaries.

The additional system pressure drop in a boiler installation resulting from the addition of an SCR catalyst can be tolerated by increasing the size of the fan. Since most boiler installations include a fan anyway, this design modification can be handled easily and relatively inexpensively. However, most process fired heaters are natural draft units with stacks sized to provide adequate draft through the furnace and convection banks. Incorporating and SCR system into a fired heater convection section typically requires the addition of a fan. In a gas turbine combined cycle plant, the SCR catalyst adds to the heat re-

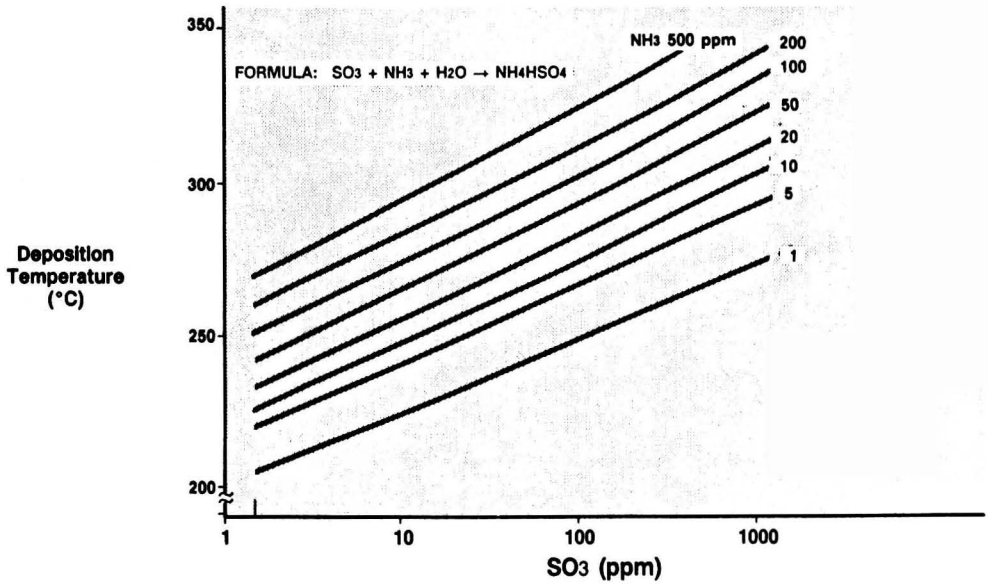

ADAPTED FROM: Pease, R.R., Status Report on Selective Catalytic Reduction for Gas Turbines, SCAQMD Engineering Division Report, July 1984.

FIGURE 5. Deposition temperature of ammonium bisulfate (NH4 HSO4)

covery steam generator (HRSG) back pressure at the gas turbine exhaust, which results in slightly lower power output of the gas turbine generator.

Flue Gas Flow/Temperature Maldistribution

All SCR manufacturers have imposed a limitation on the allowable maldistribution of flue gas flow and temperature across the front face of the catalyst. Generally, the limitation gas is ±10% and for temperature about ±20°F (±11°C). For most fired heater applications this restriction is not a major concern because the internal flue gas velocities are low (around 10 ft/sec [3m/sec]) and the catalyst is located downstream of convection section coils where the flue gas flow and temperature profiles are fairly uniform.

Unlike a heater application, the flue gas velocities from a gas turbine into a heat recovery steam generator are on the order of 80 ft/sec (24 m/sec). In addition, the flue gas velocity profiles are very nonuniform, especially for radial exhaust gas turbines. In some installations, the velocity profiles across the face of the ducting are so poor that flow straightening devices must be considered and the SCR catalyst may have to be positioned in a location where the operating temperature is not optimum.

Fouling Potential and Impact on Emissions

Efficient and cost-effective operation of an SCR system requires a slight excess inlet concentration of ammonia (NH_3) reducing agent above the required for stoichiometric conversion of the desired amount of NOx. While NOx conversion usually can be improved by increasing the ammonia injection rate, excessive unreacted NH_3 in the exhaust gas (termed "slip") can cause an objectionable odor nuisance. Most commercial SCR systems in the United States are designed for a maximum of 80 to 90 percent removal efficiency with an NH_3 slip of 10 to 20 ppmv. Regulatory agencies generally limit NH_3 slip to 20 to 30 ppmv.

When sulfur bearing fuels are combusted in an installation with a SCR system, unreacted ammonia may combine with sulfur trioxide to form precipitates at the lower temperatures which exist downstream of the catalyst. This can lead to increased particulate emissions and potential fouling of cold end heat transfer surfaces. Depending on the particular combustion process, about 3% to 5% of the sulfur in the fuel is oxidized to form sulfur trioxide (SO_3), with the balance forming sulfur dioxide (SO_2). The SCR catalyst can also promote the oxidation of SO_2 to SO_3. Depending on the formulation, the SCR catalyst may oxidize up to an additional five percent of the SO_2 to SO_3 [6].

Depending on the ammonia slip, the quantity of sulfur trioxide (SO_3) in the flue gas, and cold end operating temperatures, ammonium bisulfate (NH_4HSO_4) or ammonium sulfate ($(NH_4)_2SO_4$) may form. Ammonium bisulfate adheres to heat transfer surfaces which may result in corrosion and reduced performance. Figure 5 is a diagram indicating the approximate ammonium bisulfate deposition temperature given the quantities of sulfur trioxide and ammonia. Environmental agencies usually require that both ammonium bisulfate and sulfate emitted from the stack be counted as particulates.

Although not much can be done about SO_3 formation in the combustion process, there are SCR catalyst compositions which inhibit further oxidation. Figure 6 shows the sulfur oxidation characteristics and NOx removal efficiency as a function of catalyst temperature for three different catalyst formulations available from one manufacturer. The curves show that the lowest oxidation catalyst is also the least active which indicates that more catalyst would be required to achieve the same reduction efficiency as the formulation exhibiting higher oxidation characteristics. Another method of reducing the formation of sulfur trioxide is the treatment of fuels to remove sulfur. Pretreatment of the fuels can be quite costly depending on the type of fuel and quantity of sulfur to be removed. However, pretreatment may be less expensive than the alternative of reduced performance, replacement of heat transfer surfaces, costly equipment design, and down time for maintenance and cleaning.

Special considerations can be incorporated into the design

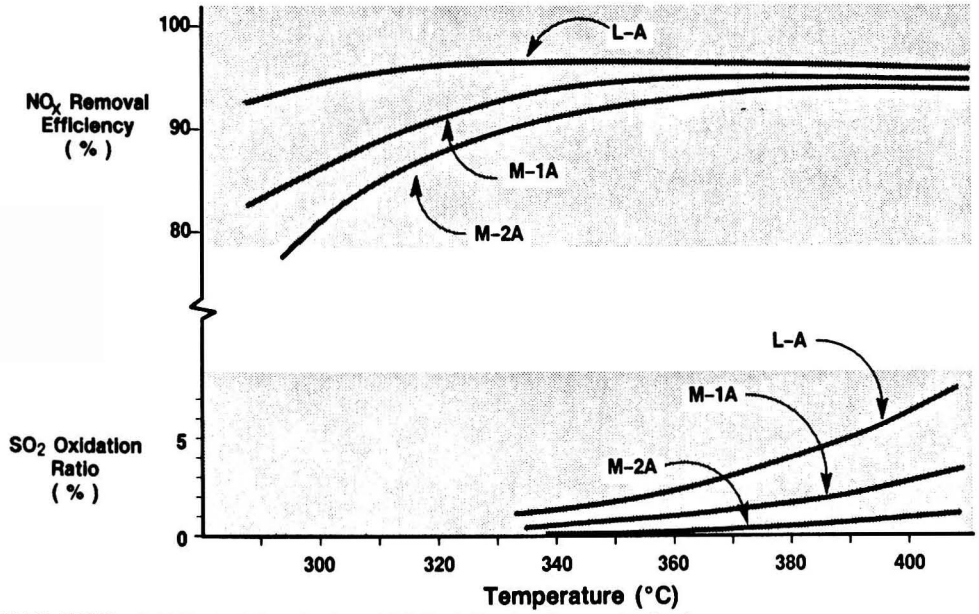

ADAPTED FROM: Aoki,H.,et al, Introduction of IHI Denitrification System for Coal Fired Steam Generator, EPRI CS-4360 Vol. 1, January 1986.

FIGURE 6. Typical NOx reduction and SO_2 oxidation performance of IHI type catalysts

of the heat transfer equipment when there is concern that ammonium bisulfate may form and deposit on cold end surfaces. Once desposited between extended surfaces or in air preheater baskets, ammonium bisulfate can be difficult to remove. Experience has shown that sootblowers are not very effective in removing this compound. However, when allowed to soak in water for a short period, ammonium bisulfate readily dissolves. Therefore, to accommodate bisulfate removal, heat transfer equipment can be designed to allow for water washing during maintenance periods. This includes adding access lanes between tube rows or in ducting, and making provisions in the floor. For fired heater and boiler designs where the flue gas flows vertically through the cold end of the unit, special care must be used when water washing since catalyst activity for some formulations can be reduced by contact with water.

Operation in Series with CO Oxidation Catalyst

In regions which are nonattainment for carbon monoxide (CO) ambient air quality standards, owners may be required to install a CO oxidation catalyst in addition to an SCR catalyst particularly for gas turbines. In this case, the CO catalyst should be installed upstream of the ammonia injection grid, since the CO catalyst will oxidize ammonia to NOx. Installing a CO catalyst in series with a SCR catalyst may present a problem if the fuel contains sulfur. Since the CO catalyst is highly oxidizing, it can convert a relatively large portion of the SO_2 to SO_3, and SO_3 will subsequently form ammonium sulfate compounds. In addition, if CO and SCR catalysts are supplied by different manufacturers, the compatability of the two systems should be evaluated.

Flue Gas Contaminants

There are a number of compounds which contaminate or poison vanadium/titanium based catalysts. The most prevalent is sulfur which can poison the catalyst by adsorption of SO_3 or by the fouling or masking of the catalyst by ammonium sulfate compounds. Although some irreversible damage may occur when operating on sulfur bearing fuels at low temperatures, this type of poisoning is generally reversible. By temporarily elevating the temperature it may be possible to thermally clean the catalyst and restore normal activity [5].

Other trace compounds found in flue gas streams, such as alkaline compounds, halogens, and heavy metals, can cause permanent catalyst poisoning [3]. In most applications, these compounds are not present in sufficient quantity to cause a problem. In oil-fired boiler applications, the soot can present a problem not only because it may contain catalyst poisons, but it also can cause plugging of some types of catalyst.

SO_2 inhibits the activity of the noble metal catalyst by competing for active catalysis sites. The manufacturer claims that the sulfur levels which occur in typical refinery fuel gas can be accommodated by providing additional catalyst to compensate for slight reductions in activity. Application for liquid or solid fuels with appreciable sulfur (>0.5 wt. percent) is not recommended by the manufacturer at this time.

One zeolite catalyst supplier claims that their formulation is virtually immune to all potential contaminants from gaseous, liquid, and solid fuels.

Physical Constraints

Most catalyst suppliers manufacture catalyst in standard dimensions. When the catalyst is configured for a specific application, the frontal cross sectional area of the catalyst will most likely have different dimensions than the boiler bank, economizer, or convection section. This requires that external or internal transition pieces be installed both upstream and downstream of the catalyst converter housing. These transition pieces must be sized to prevent flow disturbances in the flue gas path. This adds to the overall height or length of the heat transfer section and must be considered when designing structural supports, access ways, and crossover piping.

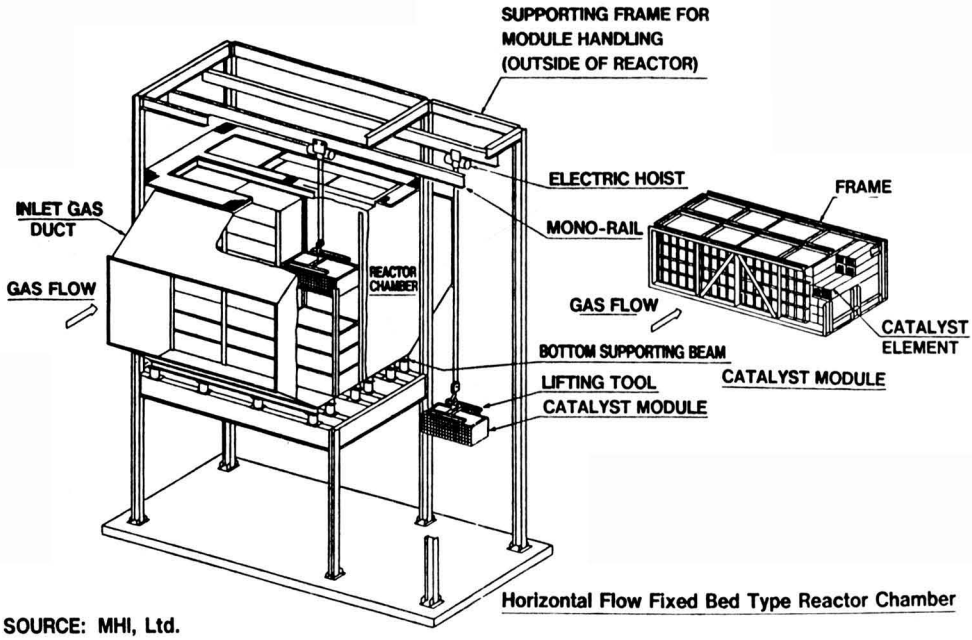

FIGURE 7. Horizontal flow fixed bed type reactor chamber. Reproduced by permission of Mitsubishi International Corporation.

In order for the SCR system to work properly, the ammonia injection grid must be installed such that there is good mixing with the flue gas prior to entering the catalyst. Some manufacturers have patented an injection grid which can be installed in the front of the SCR converter housing. Specially designed nozzles ensure adequate mixing upstream of the catalyst. Other manufacturers require that the injection grid be located several tube rows ahead of the catalyst, taking advantage of the flue gas turbulence around the tube banks to ensure good mixing. The injection grid installed upstream of the catalyst should be placed in a location where the flue gas temperature is less than about 1100°F (600°C) and the tube metal temperature is less than about 750°F (400°C), since significant decomposition of ammonia can occur above these temperatures [7]. One supplier recommends countercurrent ammonia injection to further enhance mixing.

The size of the converter housing which supports the catalyst can vary significantly depending on the selected catalyst. For example, for an 80 MW gas turbine installation, one manufacturer offers a catalyst with a very high catalyst surface area to volume ratio (designed for treating particulate free gas), requiring a converter housing depth of approximately 12 feet (4 m). Other manufacturers who offer lower area to volume ratio catalyst (designed for clean and dirty gas) might require a converter housing depth of more than 30 feet (9 m) for the same application. Although both designs will satisfy the NOx reduction requirements, one design may have a clear advantage over another depending on the fuel characteristics and other constraints.

Catalyst loading can present a problem when the heat transfer equipment is congested with support steel and crossover piping. Although most converter housings are loaded with catalyst from the top, as shown in Figure 7, many have been designed for side loading. In either case, space must be provided for loading and handling facilities and for pulling and lifting of the catalyst blocks and/or modules. Additional space is also required for installing the ammonia injection system including controls and monitoring equipment. This includes space required for insertion of the ammonia injection grid into the heat transfer equipment as well as additional plot area required for auxiliary equipment such as the ammonia tanks, vaporizer, dilution chamber, fans or air blower, and all interconnecting piping.

Catalyst Disposal

Spent vanadium-titanium catalyst is considered hazardous waste within the United States and must be specially processed and/or disposed of in specially designated dump sites. Most manufacturers will assume the responsibility of taking back spent catalyst and reprocessing and/or disposing of the hazardous material. This arrangement should be negotiated in the original purchase contract. Japanese suppliers will generally assume responsibility for disposal, but the shipping cost to return the catalyst to Japan is normally borne by the owner. There is no recovery value for stripping the base metals from the spent catalyst. Recently, the United States has adopted legislation which prohibits export of hazardous waste. This new requirement may prevent the return of spent catalyst to overseas suppliers in which case other arrangements would be necessary for proper disposal.

The zeolite catalyst systems do not contain hazardous materials and, thus, would not be considered hazardous waste unless contaminated with hazardous materials from the flue gas.

Spent noble metal catalysts have sufficient value to economically justify reclaiming, which partially offsets their higher first cost.

Ammonia Storage

Ammonia storage systems required for the SCR system have recently been subjected to increased review by regulators. Anhydrous ammonia required for the process is stored as a liquid in a pressurized vessel which is typically sized to allow filling at biweekly or monthly intervals. The possibility of vessel or piping failure resulting in the release of a large ammonia gas

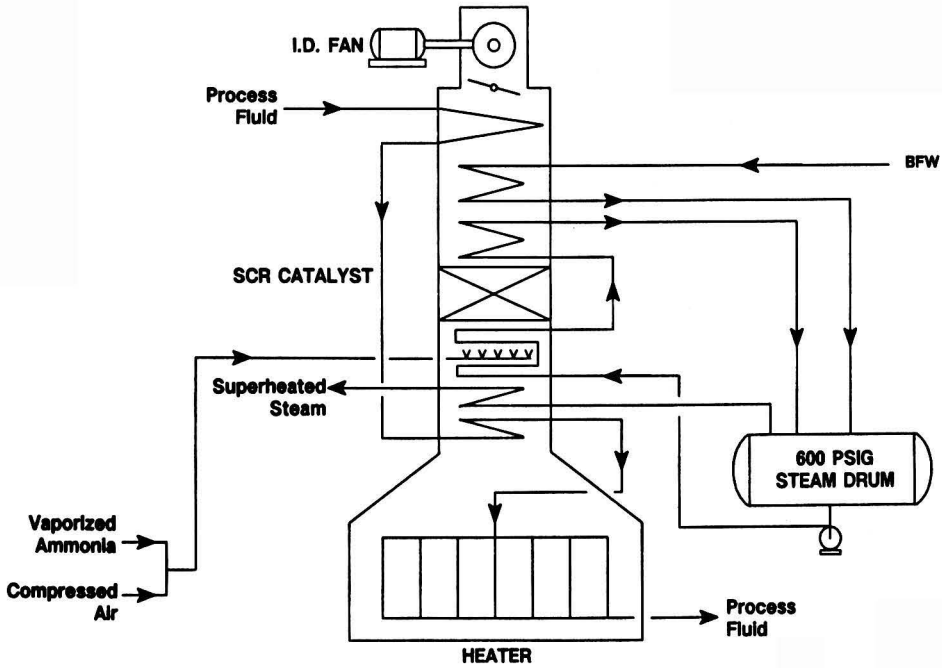

FIGURE 8. Reformer furnace system with SCR

cloud has attracted considerable attention where storage vessels are near populated or sensitive areas. Although the likelihood of a vessel rupture is extremely remote, the resulting ammonia gas cloud would present a major risk to a nearby populace. As a result, much less volatile aqueous ammonia (ammonia/water solution) in atmospheric tanks is being utilized for some projects. The disadvantages of aqueous ammonia storage include additional plot space required for the larger storage tank and the need a for more elaborate ammonia vaporization system.

SCR OPERATING EXPERIENCE

Fired Heater Installation

The additional pressure drop introduced by adding a catalyst bed to a fired heater virtually ensures that a fan will be required. This can be readily incorporated into the design of a new heater, but can be a major obstacle in the retrofit of an existing heater.

Also of concern in system design for fired heaters is the capability of maintaining flue gas temperature within the operating range required for the catalyst. For heaters generating high pressure steam in the convection section, placing the catalyst in the steam generation section typically is sufficient. However, since NOx conversion can drop off significantly at the lower end of the allowable catalyst temperature range, NOx removal requirements should be evaluated over the range of expected plant operation (turndown, clean vs. fouled tubes, etc.) to assure that removal will be adequate in all cases. Where low pressure steam is generated or process fluids are heated in the convection section, direct control of the catalyst inlet temperature is generally required. Methods which have been used to control gas temperature include providing a flue gas bypass around convection coils upstream of the SCR and using a circulating heat transfer fluid to control heat removal from the upstream convection coils [8]. The first method, while providing a simpler control scheme, must provide adequate mixing with the bypass stream to prevent temperature and flow gradients across the catalyst face.

Figure 8 shows a sketch of an SCR system installed in a new fired heater with an induced draft fan. Low-NOx burners were installed in combination with a 90% removal SCRE design to minimize NOx emissions from a heater. Temperature control is maintained by locating the catalyst between 600 psig steam generation coils.

Some of the difficulties in achieving high percentage removal of NOx are illustrated in Figure 9, which shows one set of data from a performance test on this heater. NOx concentration at the catalyst inlet varied significantly across the convection section, attributable to differences between burner operations. With the flexibility introduced by the SCR system design and with the capability of adjusting ammonia flow to individual injectors, these deviations were tolerable. During an earlier test, with hydrogen-rich fuel gas, NOx formation from the Low-NOx burners was 50% higher than predicted by the manufacturer. However, the high conversion catalyst design allowed permit requirements to be satisfied.

Controls for fired heater applications have typically been simpler than for gas turbine systems, where operating fluctuations occur more rapidly. Some systems are operated simply by adjusting ammonia flow based on laboratory analysis of gas samples, while others use analyzers either for automatic control or to provide a basis for operator adjustment of ammonia flow rate. Some regulatory agencies have recently required continuous monitoring of ammonia slip for larger combustion units.

SCR systems in fired heater applications have a good record of performance in meeting NOx removal specifications over an extended catalyst life, with at least one system being on line for over 5 years now. One drawback has occurred in heaters firing refinery gas with significant mercaptan sulfur content. Significant bisulfate fouling of downstream heat exchange surface has occurred in these cases. However, water washing during turnaround periods has been effective in removing the bulk of the deposits.

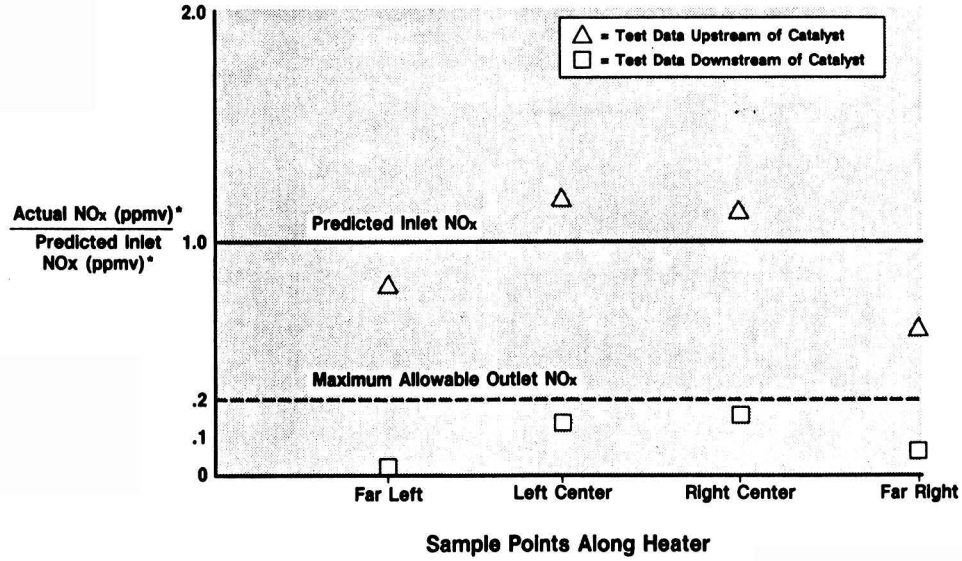

* Corrected to 3% O_2

FIGURE 9. Fired heater performance test results

Boiler Installation

Installation of an SCR system as part of a package boiler design is similar in nature to the other applications. Typically, the system is designed as three, interconnected elements, consisting of the boiler, SCR system and economizer or air preheater. Boiler forced draft fans must be sized to accommodate the additional pressure drop. If low pressure steam is generated in the boiler, a bypass around a portion of the boiler may be required to maintain temperature to the SCR catalyst.

Gas Turbine Combined Cycle Installation

Figure 10 shows the HRSG arrangement for one of four gas turbine/combined cycle trains located in a Southern California 385 MW cogeneration facility. The gas turbine generators utilize steam injection for NOx control to 42–69 ppmv (dry basis), depending on fuel type, corrected to 15% O_2-Steam generation reliability was built into the design by incorporating duct firing capability.

Since the installation is in an area which is nonattainment

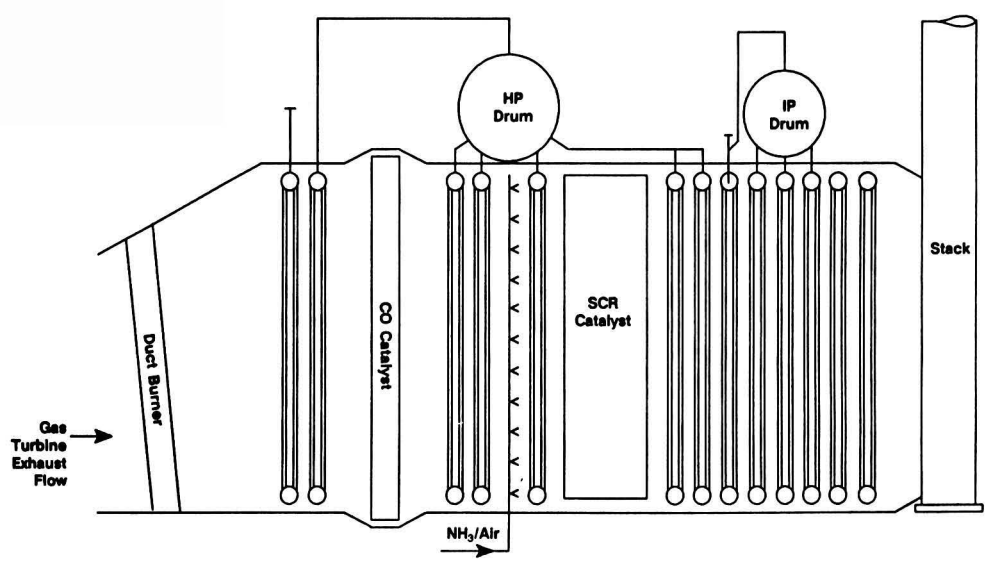

FIGURE 10. Heat recovery steam generator

for NO_2, CO, and ozone, a CO oxidation catalyst and a SCR catalyst were installed to achieve required emission limitations. The CO catalyst is located upstream of the SCR catalyst in a high temperature zone to achieve the most efficient oxidation of non-methane hydrocarbons (ozone precursors) as well as high CO oxidation efficiency. As shown on the diagram, the CO catalyst was installed after the first four rows of tubes (high pressure superheater) to ensure a more uniform velocity and temperature profile at the catalyst inlet. The SCR catalyst was installed in the middle of the high pressure boiler bank to ensure satisfactory operating temperature during both fired and unfired operating modes.

The gas turbines are designed to operate on three separate fuels; natural gas, butane, and refinery fuel gas. The duct burners are designed to fire on natural gas and refinery gas. While the natural gas and butane fuels are relatively sulfur-free, the refinery gas contains up to 800 ppmv of H_2S and mercaptans. Burning this sulfur-containing fuel in combination with the installation of a CO oxidation catalyst poses a high risk that significant ammonium-sulfate precipitates will form, increasing particulate emissions and the potential for fouling of cold end heat transfer surfaces. As a result of these possible problems, two alternatives were evaluated. The first option was to design the heat recovery steam generator to minimize fouling and enhance cleaning capability by decreasing fin density and providing access lanes between tube rows and providing drainage for water washing. The second option was to pretreat the fuel to remove sulfur. After careful consideration of all the economic, technical, and environmental issues, the owner opted to pretreat the fuel.

Since the optimum operating temperature required that the SCR catalyst be installed in the middle of the boiler bank, the crossover piping from the back end boiler modules to the steam drum became quite long (converter housing is about 30 feet [9m] in depth) and required special design consideration to maintain desired circulation ratios. The problem was further complicated by the fact that the catalyst is top loaded into the converter housing. An unusual crossover arrangement was required to allow top loading of the catalyst.

To assure steam system reliability, one spare catalyst charge for the four units was purchased and is stored on site (indoors). The contract with the supplier requires that the supplier dispose of the spent catalyst with shipping to be paid by the owner.

Experience to date with SCR applications for combined cycle systems has been mixed. While several systems are performing as expected, some installations have suffered major loss of catalyst activity prior to expiration of the catalyst guarantee [*9,10*]. These cases are still under investigation at this time.

SUMMARY

A number of SCR systems are currently in operation in the United States, with many more planned to come onstream in the next few years. Most of these systems are successful in meeting NOx removal specifications and are demonstrating catalyst life in excess of guarantees. In a few cases, however, problems have occurred involving loss of catalyst activity, demonstrating that uncertainty still remains in the application of this technology. Systems firing low sulfur fuels enjoy the advantage of avoiding fouling of low temperature heat transfer surfaces. At least with the moderate levels of fuel sulfur typical in refineries, operators are managing to cope with the drawbacks introduced with system fouling.

Selection of SCR for NOx control should evolve from an evaluation of alternative control strategies, including the latest developments in combustion modification (such as low NOx burner technology) to determine the most cost effective approach to meeting regulatory requirements. Once SCR is selected for an application, control requirements, design parameters, and system constraints for that application should be carefully reviewed to ensure selection of the best-suited system and adequate system performance.

LITERATURE CITED

1. Minden, C. A., and Gilmore, P. T., *NOx Control in Gas Fired Refinery Process Heaters Using Pyrocore Radiant Burners,* 1988 Fall Meeting, Western States Section of the Combustion Institute, (October 17-18, 1988).
2. Arand, J. K., et al., *Noncatalytic NOx Removal with Ammonia,* EPRI F-735, (April, 1978).
3. Makanski, J., Ed., *Reducing NOx Emissions,* Power, pgs. S.1-26 [528 Key], (September, 1988).
4. Pease, R. R., *Status Report on Selective Catalytic Reduction for Gas Turbines,* SCAQMD Engineering Division Report, (July, 1984).
5. Damon, J., Ireland, P., and Giovanni, D., *Updated Technical and Economic Review of Selective Catalytic NOx Reduction Systems,* Proceedings of the 1987 Symposium on Stationary Combustion Nitrogen Oxide Control, Volume 2, (August, 1987).
6. Aoki, H., Suzaki, T., and Ishimoto, R., *Introduction of IHI-Denitrification System for Coal Dired Steam Generator,* Proceedings: 1985 Symposium on Stationary Combustion Control, Volume 1, (May, 1985).
7. Kirk-Othmer Encyclopedia of Chemical Technology, 3rd Edition, pp. 471-2, (1978).
8. Blair, J. B., Massey, G., and Hill, H., *Refinery Catalytically Cuts NOx Emissions, Oil & Gas Journal,* (January 12, 1981).
9. Cogeneration Report, McGraw Hill, pp.1-2, (December 5, 1986).
10. Cogeneration Report, McGraw Hill, p. 7, (January 2, 1987).

RBC Nitrification of High Ammonia Leachates

Edward J. Opatken and James J. Bond

Environmental Protection Agency, 26 M. L. King Drive, Cincinnati, OH 45268

A study was conducted on treating a simulated leachate that contained high concentrations of ammonia-nitrogen ranging between 20 and 1000 mg/L. A pilot sized rotating biological contractor (RBC) was used to treat a surrogate leachate composed of primary effluent that was adjusted with glucose and ammonium chloride to achieve various concentrations of dissolved organic carbon (DOC) and ammonia-nitrogen. Experiments were conducted to determine:

- *The rate of ammonia conversion*
- *The drop in pH at high ammonia concentrations*
- *The effect of low pH on ammonia conversion*
- *The effect of high ammonia levels (1000 mg/L) on ammonia conversion*
- *The effect of temperature on the reaction rate constant*

The results from these experiments and the applicability of a RBC to treat leachates containing high concentrations of ammonia-nitrogen are reported.

BACKGROUND

Land disposal of solid waste is no longer regarded as an ultimate solution because of the potential for leachate formation and/or groundwater contamination. Leachate characterization at some Superfund sites has uncovered concentrations of ammonia-nitrogen at levels up to 500 mg/L [*1*]. This level is at least 10 times greater than ammonia nitrogen levels typically experienced in municipal wastewater treatment. This study was undertaken to determine if biological treatment of leachate could effectively convert these high ammonia nitrogen concentrations into nitrate nitrogen and whether the required reaction time is compatible with reaction times necessary for organic carbon conversions. The rotating biological contractor (RBC) was selected as the biological treatment process for this project. Its applicability for converting the high ammonia-nitrogen concentrations in leachates into nitrates was evaluated. A pilot RBC unit was available at the U.S. Environmental Protection Agency's Test and Evaluation (T&E) Facility in Cincinnati, Ohio, to conduct such an investigation.

ROTATING BIOLOGICAL CONTRACTORS—GENERAL

The first RBC [*2*] introduced into the United States occurred in the early 1970's. Since that time the RBC has undergone significant design changes that have improved its competitiveness in the wastewater treatment field. The RBC consists of a multitude of plastic sheets mounted on a main shaft. The sheets are designed to permit ample space between adjacent sheets and to provide turbulence when moving through the wastewater to achieve the desired levels of liquid mixing and shear.

The sheets are partially immersed in wastewater so that 40% of the media area is always submerged. The RBC is rotated at a normal operating speed of 1 1/2 rpm and the media is alternately exposed to the air and wastewater. A biological slime growth develops on the plastic media using the soluble organics in wastewater, as their food source. As a section of the media leaves the wastewater it starts draining into the tank, providing a thin liquid film that allows a high oxygen transfer rate to occur between the air and the liquid film. The biomass continues to grow until the shearing action caused by the rotation of the RBC causes the biomass to slough from the media.

The RBC can be designed to produce effluents with less than 5 mg/L of soluble BOD. The only energy required is for rotating the RBC and the operation requires minimal attention.

PROJECT DESCRIPTION

The pilot RBC, as shown in Figure 1 contains 930 m^2 (10,000 sq ft) of media surface area, 10% of that of a full-scale unit

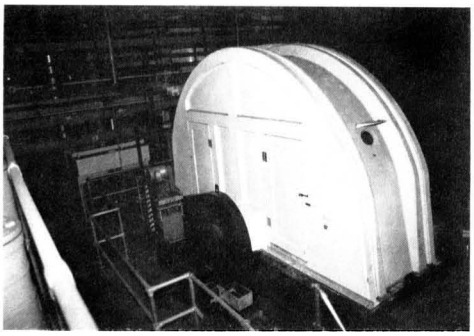

FIGURE 1. Rotating biological contractor (RBC).

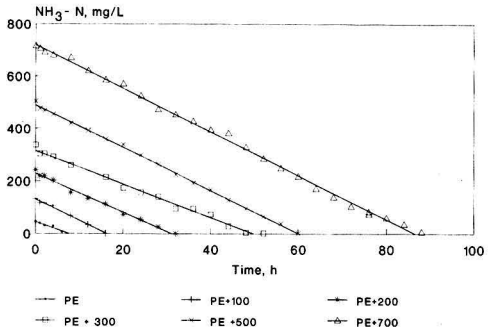

FIGURE 2. Conversion of ammonia

(100,000 sq ft) [3]. The media diameter is 3.6 m (12 ft), identical to that of a full-scale unit; however, the media length is less than 1 m (3.3 ft), whereas a full-scale unit is 7.6 m (25 ft) long.

The RBC was operated in a batch mode to obtain kinetic data on the conversion of ammonia nitrogen with time. The primary effluent (PE) from Cincinnati's Mill Creek Treatment Facility was used as the prime carrier and was adjusted by adding ammonium chloride, sodium phosphate, and glucose to simulate a leachate containing higher concentrations of ammonia nitrogen, phosphorus and dissolved organic carbon. The feed operation consisted of adding a standard volume of PE to a calibrated hold tank, adding the nutrients, and pumping the modified PE into the RBC. The RBC was operated at a constant speed of 1.5 rpm, which is equivalent to a peripheral speed of 17m/min (56 ft/min). Samples were removed from the RBC at specific time intervals and analyzed for:

- soluble biochemical oxygen demand (SBOD)
- soluble chemical oxygen demand (SCOD)
- dissolved organic carbon (DOC)
- ammonia-nitrogen (NH_3-N)
- total Kjeldahl nitrogen (TKN)
- nitrate nitrogen (NO_3-N)
- alkalinity

The influent and effluent were analyzed for the above parameters and:

- suspended solids (SS)
- volatile suspended solids (VSS)
- phosphorus (P)

During the experiment, pH, dissolved oxygen (DO), and temperature were measured hourly. The conversion of NH_3-N caused a drop in the pH [4], and sodium carbonate (SC) was added as a 10% slurry to maintain the pH above 7.2. After each experiment the RBC would undergo a daily change of unaltered PE to maintain an active biomass during periods when no experiments were being conducted.

RESULTS AND DISCUSSION

Biochemical Kinetics on the Disappearance of Ammonia Nitrogen

Biochemical kinetic rates of the disappearance of NH_3-N with time were determined for PE whose initial NH_3-N concentration ranged between 25 and 50 mg/L [5]. Higher concentrations were then studied by adding ammonium chloride to the PE at levels varying from 100 to 1000 mg/L NH_3-N.

Samples were withdrawn from the RBC after 1, 2, 4, 8, 12, ... hours, to obtain kinetic data on the disappearance of NH_3-N with time. When the concentration of NH_3-N was plotted against time, a straight line was obtained for experiments where the initial concentration ranged between 25 and 700 mg/L. The slope of the line varied between 6 and 9 mg/L × h. The pH was maintained above 7.2 during these experiments. These results are shown in Figure 2. A linear regression was performed with the data, and the intercept Co (initial concentration), slope k (reaction rate constant), and correlation coefficient r are given for each of these curves in Table 1.

Table 1 Linear Regression on Ammonia Nitrogen Conversion

Ammonia Addition mg/L	r	k mg/L × h	Co mg/L
—	.999	−6.4	45
+100	.996	−8.1	133
+200	.996	−7.3	228
+300	.996	−6.3	314
+500	1.000	−8.2	489
+700	.999	−8.3	720

The straight line relationship in Figure 2 indicates that the conversion of ammonia with time was zero order at initial NH_3-N concentrations up to 800 mg/L [6]. This relationship infers that:

- NH_3-N concentration will decrease at a constant rate with time
- at a constant temperature, any change in reactor configuration such as a plug flow reactor, a series of stirred reactors, a completely mixed reactor, or batch operation will not affect the reaction time.

Effect of pH on Conversion of Ammonia Nitrogen

There are references in the literature including the "Process Design Manual for Nitrogen Control" [4] and "Wastewater Engineering" [7] recommending that pH be maintained above 7.2 to obtain satisfactory biological conversion of NH_3-N. An experiment was designed to demonstrate the effect of pH on this conversion. Ammonium chloride was added to the PE to provide an additional 100 mg/L NH_3-N. Influent organic carbon was not altered, but influent phosphorus was adjusted to yield an additional 20 mg/L of phosphorus. pH was maintained during the experiment above 7.2 by adding a 10% slurry of SC whenever the pH approached 7.2. The data from this experiment indicated a zero-order rate equation with a reaction rate constant of 6.9 mg/L × h at a temperature of 15.2°C as illustrated in Figure 3. The adjustments with SC were made hourly, and the pH never dropped below 7.2 as shown in Figure 3. This experiment with SC addition to control pH followed a zero order relationship.

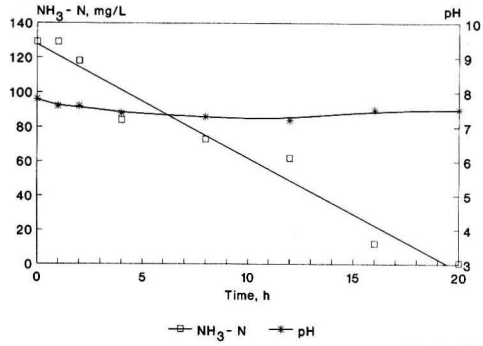

FIGURE 3. Ammonia conversion with controlled pH

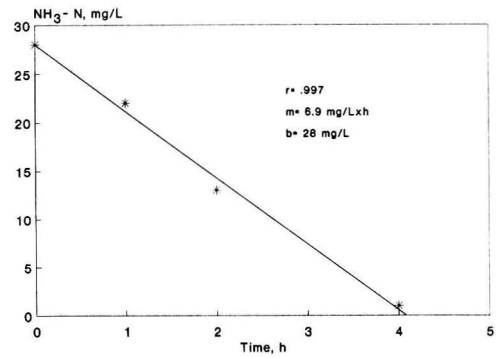

FIGURE 5. Effect of low pH on biomass

Influent NH_3-N was again raised by 100 mg/L in the next experiment. The organic carbon concentration was not altered, but influent phosphorus was adjusted by adding 20 mg/L of phosphorus using sodium phosphate. pH was not controlled during this experiment. The experiment exhibited a constant reduction in NH_3-N over the first 8 hours, from 138 mg/L to 81 mg/L. During this 8 hour period, the pH dropped from 7.9 to 5.9 as shown in Figure 4. After the pH dropped to 5.9, only a small reduction in NH_3-N occurred. The experiment was continued for 80 hours. NH_3-N in the RBC tank liquor fluctuated between 78 and 69 mg/L during this time period. The pH dropped slowly from 5.9 to 4.9 during these final 70+ hours. The kinetic curves given in Figure 3 with pH control and Figure 4 without pH control dramatically illustrate the inhibitory effect that pH values below 7.0 have on the biochemical conversion of ammonia. These data strongly support the past references that pH control above 7.2 is essential for the biochemical conversion of ammonia nitrogen.

After completing the experiment without pH control, the RBC underwent three changes of PE. Each change lasted one day. This was followed with a kinetic run on PE without supplemental addition of NH_3-N. The result was similar to other experiments in which the initial ammonia nitrogen concentration was approximately 28 mg/L. The reaction was essentially complete after 4 hours, and the residual NH_3-N level was below 1 mg/L. The reaction followed a zero-order relationship with a reaction rate constant of 6.9 mg/L × h as displayed in Figure 5. This experiment showed that the effect of the low pH on the biomass was inhibitory and not toxic, since the biomass performed normally on PE following three batch changes. The reaction rate constant for the follow-up experiment was similar to those found in previous experiments, indicating no permanent harmful effects to the biomass from the low pH experiment.

Upper Limit on Ammonia Nitrogen Concentration

The ammonia nitrogen concentration was incrementally increased to determine the upper concentration at which the biochemical reaction becomes inhibitory or toxic to the biomass. The concentration of NH_3-N was increased from 25 to 100, 200, 300, 500 and 700 mg/L without any adverse effects. At 1000 mg/L, however, a detrimental effect on the reduction of the NH_3-N was noted. The NH_3-N dropped from 1000 to 800 mg/L during the first 40h. It then took 60h for the NH_3-N to drop from 800 to 700 mg/L. These data are plotted in Figure 6. The pH was generally maintained in the range 7.2–8.0 in the experiment.

The system was purged three times with PE. Each purge lasted one day and then a standard kinetic run with PE was made to determine if the biomass had been irreparably harmed by the high ammonia concentration. The standard kinetic experiment started with an initial NH_3-N concentration of 45 mg/L. The NH_3-N concentration decreased to less than 1 mg/L after 8h of treatment. The reaction rate constant, k, was 6.4 mg/L × h, again indicating that the high ammonia concentration imposed on the biomass during the first portion of the experiment was inhibitory rather than toxic. The standard kinetic run data are displayed in Figure 7.

Effect of Temperature

The plots of the ammonia nitrogen concentration with time result in straight lines whose slopes are equal to the reaction rate constant, k, i.e.:

$$dc/dt = k \qquad (1)$$

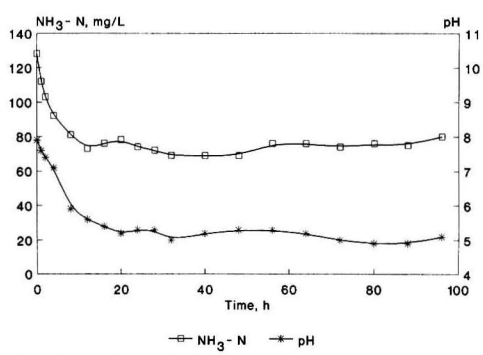

FIGURE 4. Effect of pH on ammonia conversion

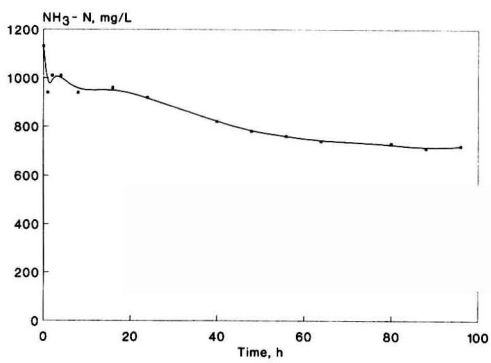

FIGURE 6. Effect of high ammonia concentration

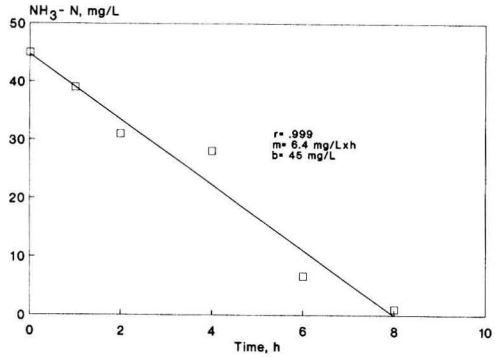

FIGURE 7. Effect of high ammonia on biomass

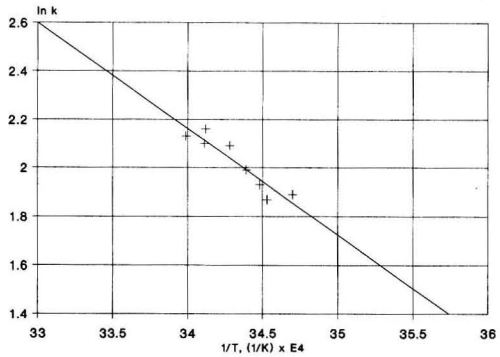

FIGURE 8. Temperature effect on rate constant

Table 2 Reaction Rate Constant Summary

Experiment No.	T °C	T °K	1/T $°K^{-1} \times E4$	k mg/L×h	ln k
01269	18.5	291.7	34.28	8.1	2.09
01049	16.4	289.6	34.53	6.5	1.87
11158	19.9	293.1	34.12	8.7	2.16
10278	21.0	294.2	33.99	8.4	2.13
10178	20.0	293.2	34.11	8.2	2.10
02139	15.0	288.2	34.70	6.6	1.89
03139	16.8	290.0	34.48	6.9	1.93
03209	17.6	290.8	34.39	7.3	1.99

The units of k are mg/L × hr. The k values obtained from the experiments ranged from 6.5 to 8.7 mg/L × hr, while the temperature varied between 15.0 to 21°C. These data are summarized in Table 2.

The effect of temperature on the reaction rate constant is related by the Arrhenius equation

$$k = Ae^{-E/RT} \tag{2}$$

where, k = reaction rate constant
A = frequency factor
E = activation energy, cal/g-mol
R = gas constant, 1.97 cal/g-mol
T = temperature, °K

The Arrhenius equation can be rearranged to obtain the following expression:

$$\ln k = -E/RT + \ln A \tag{3}$$

A plot of ln k against $1/T$ yields a straight line with the slope equal to E/R. The Arrhenius plot for ammonia conversion is shown in Figure 8. The curve shows that at 12.5°C, where $1/T$ is approximately 35×10^{-4}, the ln k is 1.72, which converts to a k value of 5.58 mg/L × hr. Doubling the reaction rate constant from 5.58 to 11.16 mg/L × hr results in a ln k value of 2.41. From the curve in Figure 8 the reciprocal of the temperature at this point is approximately 33.4, which converts to 26.2°C. Therefore, a temperature increase of 13.7°C from 12.5 to 26.2°C will double the reaction rate. The activation energy for the conversion of NH_3-N was calculated from the slope of the Arrhenius curve in Figure 8.

$m = E/R = 4400$
$R = 2.0$ cal/g-mol × °K
$E = 4400 \times 2.0$ cal/g-mol × °K = 8.8 kcal/g-mol

This value is lower than those obtained by Knox [8] who reported 13.8 kcal/g × mol in his study with leachate and Steiner et al. [9] who obtained 12.3 kcal/g mol.

SUMMARY

The results from this study on ammonia nitrogen conversion can be summarized as follows:

- The disappearance of NH_3-N with time follows a zero order biochemical kinetic relationship.
- The pH must be maintained above 7.2 to obtain a constant and satisfactory reaction rate for the conversion of NH_3-N.
- The maximum concentration of NH_3-N that can be satisfactorily converted at a constant reaction rate lies between 700 and 1000 mg/L.
- The Arrhenius equation can be used to predict the effect of temperature on the reaction rate constant.

LITERATURE CITED

1. Memo "Operating Industries at Monterey Park—Leachate Characterization," from E. J. Opatken to Brian Ullensvang, April 29, 1988.
2. *Envirodisc Rotating Biological Contactor System,* Clow Corporation, WTD 880-0510.
3. Brenner, R. C., J. A. Heidman, E. J. Opatken, and A. C. Petrasek, *Design Information on Rotating Biological Contractors,* EPA-600/2-84-106 (June 1984).
4. *Process Design Manual for Nitrogen Control,* U. S. Environmental Protection Agency (October 1975).
5. Antonie, R. L., *Fixed Biological Surfaces-Wastewater Treatment.* CRC Press (1976).
6. *Perry's Chemical Engineers Handbook,* McGraw Hill Book Company, Sixth Edition.
7. *Wastewater Engineering: Treatment, Disposal, Reuse,* Metcalf & Eddy, Inc. (1979).
8. Knox, K., "Leachate Treatment with Nitrification of Ammonia," *Water Resources,* Volume 19, No. 7 (1985).
9. Steiner, L., et al., "Demonstrating Leachate Treatment," U. S. Environmental Protection Agency, Solid Waste Management Series, Report SW-758 (1979).

Feasibility, Modeling and Economics of Sequestering Power Plant CO_2 Emissions In the Deep Ocean

H. Herzog, D. Golomb and S. Zemba

Energy Laboratory, Massachusetts Institute of Technology, Cambridge, Massachusetts 02139

The capture and disposal of carbon dioxide from the flue gas of fossil-fueled power plants is technically feasible, albeit it requires a significant fraction of the energy content of the fossil fuel and additional equipment with large capital expenditures. The five processes investigated for capturing CO_2 from the flue gas of coal-fired power plants are (a) combustion of coal in an atmosphere of oxygen and recycled flue gas; (b) scrubbing the flue gas with a recyclable solvent (monoethanolamine); (c) cryogenic CO_2 fractionation of the flue gas; (d) separation of CO_2 by selective membrane diffusion; and (e) scrubbing of the flue gas with seawater. The captured CO_2 is envisioned to be liquefied at 150 atm, piped to the deep ocean, and released through a diffuser. Model calculations show that with appropriate release conditions the formed CO_2 drops can be completely dissolved in seawater. The process that requires least incremental energy is air separation/flue gas recycling. In this process about 30% of the total energy content of the coal is consumed, and the thermal efficiency of a power plant is reduced from 35% to about 25%. Excluding pipeline and deep water disposal costs, we estimate that electricity production costs will increase by about 80%.

The ever-increasing fossil fuel usage worldwide causes the atmospheric build-up of carbon dioxide (CO_2) concentrations. At present rates of emission, the CO_2 concentrations are expected to double in the middle of the next century. This may cause significant perturbations of the Earth's radiative budget and consequently cause significant climatological and geohydrological changes. The options for preventing CO_2 build-up are few: greater reliance on nuclear energy; greater utilization of solar, wind, geothermal and renewable energy; greater energy efficiency and conservation; and CO_2 capture from the flue gas products resulting from fossil fuel combustion. This study is limited to the last option, the capture and removal of CO_2 from the flue gas of fossil fuel combustion with sequestering of the captured CO_2 in the deep ocean. The capturing and sequestering of CO_2 from power plant flue gas has been considered previously by several authors. The process steps, end goals, and consequently the assessment of the technological feasibility, energetics and economics of the CO_2 sequestering varies greatly from author to author. Furthermore, the mode of release of CO_2 in the deep ocean has not been considered previously in detail, causing considerable uncertainty about the ultimate fate of the released CO_2. A brief review of the previous studies concerning the capture and sequestering of power plant CO_2 follows.

Marchetti [*1,2*] proposed first the idea of disposing CO_2 in the deep ocean. A 1000 km pipeline would carry CO_2 from

about 10 large power stations to a disposal site, e.g. at the outflow of the Mediterranean Sea into the Atlantic Ocean at the straits of Gibraltar. There, the outflow carries over one million tons of water per second, gently sinking into the deep layers of the Atlantic. Similar, but smaller thermohaline currents exist in the Red, Weddell, and Norwegian Seas. Marchetti considered for CO_2 separation from the flue gas both a scrubbing process, and burning the coal in pure oxygen.

Mustacchi et al. [3] analyzed the disposal of flue gas CO_2 in the ocean. They considered first the direct (unseparated) flue gas bubbling at a depth of about 240 m. While they estimated that absorption of the CO_2 in seawater will be complete before the bubbles ascend to the surface, the compression energy of the total flue gas resulted in unacceptable costs. A second option was the release into the ocean of separated, liquefied CO_2 at a depth of about 160 m. This process requires the construction and operation of a chemical processing plant that separates the CO_2 from the rest of the flue gas. Mustacchi et al. considered the use of solutions of alkalis (KOH, NaOH), salts (K_2CO_3, Na_2CO_3, K_3PO_4) or amines (mono-, di- or trimethylethylamine) to strip the CO_2 from the flue gas and disposal into the deep ocean. Preliminary estimates of this process also resulted in unacceptable costs. The third process involved the release at a depth of only 10 m a seawater solution of CO_2. This latter process was estimated to yield the lowest cost.

Albanese and Steinberg [4] assessed two separation processes: the absorption of CO_2 in seawater, and the absorption of CO_2 in monoethanolamine (MEA). Captured CO_2 is injected into the ocean via a pipeline, as a gas or liquid, or dropped from a barge as solid blocks. Of the processes considered, absorption by MEA was considered the least energy intensive. Steinberg et al. [5] also analyzed the process of CO_2 absorption/stripping by monoethanolamine, liquefying the CO_2, and injection into the ocean at 300 m depth. They concluded that if this CO_2 control process were integrated into the power plant operation, a 90% removal of CO_2 would reduce the power plant thermal efficiency by only 3%! As will be shown later, this estimate is erroneous.

Baes et al. [6] analyzed CO_2 separation from the flue gas by amine stripping, and production of a relatively pure CO_2 flue gas by burning coal in oxygen. They concluded that the latter process is more energy efficient than the former. Baes et al. also investigated the behavior of a jet of carbon dioxide enriched seawater discharged into stagnant seawater of lower density below the thermocline; the behavior of a liquid CO_2 release in the deep ocean; and the dropping of dry ice blocks from barges. Total energy and capital expenditures were given for a *new* power plant to be built on a floating platform over the ocean disposal site. Baes et al. considered the most attractive means for CO_2 disposal from a floating plant the dissolving of the compressed gas in seawater at depth.

Hendriks et al. [7] considered two processes of CO_2 capture: a conventional coal-fired power plant with chemical absorption by MEA and an integrated coal gasification/combined cycle (IGCC) power plant with physical absorption by selexol. The latter proved to be more efficient. They estimated that with CO_2 capture, an IGCC plant thermal efficiency falls from 43.6% to 38.1% and electricity production costs increase by 24%. Hendriks et al. proposed to sequester the CO_2 from Dutch power plants in exhausted North Sea natural gas fields. Snyder and Depew [8], in a study sponsored by the Electric Power Research Institute, estimated that with CO_2 capture, the thermal efficiency of an IGCC plant decreases from 34.4% to 27.8%.

SCOPE OF STUDY

Because the feasibility and economic assessments of the previous studies vary greatly, we undertook this study to evaluate in detail the most promising processes of capturing CO_2 from the flue gas of *existing* power plants and sequestering the CO_2 in the deep ocean. The deep layers of the ocean are highly unsaturated in regard to CO_2, hence they could serve as practically unlimited sinks for the captured CO_2. Once a reliable and quantitative estimate emerges from such an assessment, we can more confidently evaluate the role of this strategy in future efforts to ameliorate the CO_2-caused greenhouse effect.

This study is constrained by the following guidelines:

a. Consider electric power plants only. Fossil-fueled power plants contribute about one-third of the world's CO_2 emissions from fossil fuel sources. Generally, power plants have the highest density of CO_2 emissions in terms of mass per area per time.
b. Consider retrofit options only. Replacement of an existing coal or oil fired boiler with a natural gas fired turbine combined cycle, while reducing significantly the emission rate of CO_2 per kWh electricity produced, is not considered a retrofit option because of the large capital investment and the limited reserves of natural gas. Obviously, replacing a fossil fueled power plant with a nuclear one is also not a considered retrofit option.
c. Consider only techniques which separate CO_2 directly from the flue gas. Global capturing of CO_2 from the atmosphere by forestation and/or biomass farming is not within the scope of this research.
d. Consider only closed systems, that is, the requisite energy for CO_2 capture and disposal must come from the fossil fueled power plant, not from external nonfossil fueled power sources.
e. Consider only commercially proven, or at least demonstrated, technology. Because of activities in the chemical process industry and interest in enhanced oil recovery, there has been considerable experience in separating CO_2 from flue gases and other gases (e.g. methane).

Using the above criteria, we narrowed the scope of the investigation to the following processes:

1. **Air Separation/Flue Gas Recycle.** Oxygen is separated from the air in a preprocessor plant. Pulverized coal is combusted in an atmosphere of oxygen and recycled flue gas. Part of the flue gas is recycled into the furnace to maintain original heat transfer rates to the various boiler elements. Water vapor is separated from CO_2 by condensation and absorption in a recyclable dehydrant (triethylene glycol).
2. **Recyclable Solvent.** The CO_2 from the flue gas is scrubbed with a solvent, monoethanolamine (MEA). The solvent is stripped of CO_2 in a regeneration step and recycled.
3. **Cryogenic Fractionation.** The CO_2 from the flue gas is separated from the other gases by multiple stage cryogenic absorption and distillation.
4. **Membrane Separation.** The CO_2 from the flue gas is separated from the other gases by polymer membranes.
5. **Seawater Scrubbing.** The CO_2 from the flue gas is directly absorbed at atmospheric or elevated pressures in seawater.

In the first four processes, the CO_2 from the flue gas is captured, compressed and released as a supercritical fluid in the deep ocean. The fifth process, seawater scrubbing, results in a saturated solution of CO_2 in seawater. While this solution may not be required to be discharged at great depth, it requires huge flow rates of seawater.

CO_2 CAPTURE TECHNOLOGIES

The first four selected processes are modeled in detail on the ASPEN PLUS™* process simulator to generate overall

ASPEN PLUS™ is a trademark or Aspen Technology, Inc. of Cambridge, MA. The original development of ASPEN PLUS was carried out at the MIT Energy Lab.

material and energy balances. The fifth process, seawater scrubbing, is only evaluated quantitatively in regard to the required flow rates of seawater and the necessary pipeline diameters.

Key steps in assembling the ASPEN PLUS model include:

- Specifying the chemical components.
- Choosing the physical property methods and models for calculating thermophysical properties.
- Defining the feed streams of the process.
- Breaking the process into unit operation blocks and selecting a unit operation model for each block.
- Specifying the operating conditions of each unit operation block.
- Imposing design specifications.

ASPEN PLUS uses its built-in library of component data, physical property and unit operation models, and mathematical algorithms to generate material and energy balances based on the above input. Detailed ASPEN PLUS energy and material balances have been reproduced in a technical report [*9*] and will not be repeated here.

For each process, we calculate the energy required to capture the CO_2 generated by burning coal and to compress the captured CO_2 to 150 atm. The energy requirement is expressed as a percentage of the heat content of the coal. The energy required for pipeline transport and deep ocean disposal is highly dependent on the distance between the power plant and the disposal site, so the transport/disposal energy component is not included in our analysis. However, for power plants near to the ocean, the energy required for transport and disposal will be small compared to the energy required for capture and compression.

The flue gas that feeds each process is taken from a 500 MW coal-fired power plant with an assumed overall thermal cycle efficiency of 35%. The power plant is assumed to burn a bituminous coal with a low sulfur content and a mid-range ash and moisture content. The assumed coal composition is as follows [*10*]:

Component	wt. %
C	68.3
H	4.16
S	0.874
N	0.666
O	10.8
H_2O	7.7
Ash	7.5
Heating Value	0.029 GJ/kg coal

Based on the above coal, the following parameters are calculated:

Molecular Formula	$CH_{0.731}O_{0.119}N_{0.008}S_{0.005}$
CO_2 Generated	2.50kg CO_2/kg coal 86kg CO_2/GJ 0.88kg CO_2/kWh$_e$

The combustion air flow is determined by requiring the concentration of oxygen in the furnace effluent to be 3.5 mole percent. This corresponds to about 17% excess air.

Air Separation/Flue Gas Recycling

Most of the methods proposed for the capture of CO_2 are based on the separation of CO_2 from the other components of the flue gas. Since CO_2 typically constitutes only 15% by volume of the flue gas, energy requirements are high for the separation. The following scheme is based on prior enrichment of CO_2 in the flue gas by combusting coal in an atmosphere

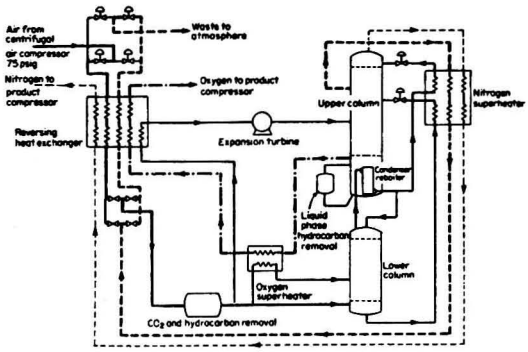

FIGURE 1. Typical air separation plant [*48*].

of oxygen and recycled flue gas instead of air. For retrofit applications, the main challenges are maintaining the flame and heat transfer characteristics of the boiler and preventing air ingress. The U.S. Department of Energy is funding research on the air separation/flue gas recycling process at the Argonne National Laboratory. The three basic process steps are air compression and separation; combustion and power generation; and flue gas compression and dehydration. The key energy requirements are compression of the inlet air prior to separation (17% of the combustion energy of the coal) and compression of the flue gas for pipeline transport (9-14% of the combustion energy of the coal).

Air compression and separation is a very common process found in industry today. A 500 MW power plant requires on the order of 9,000 metric tons/day of oxygen. The largest standard commercial units available today are roughly 2,000 metric tons/day. However, development of larger units (about 9,000 metric tons/day) is currently underway to help satisfy projected needs of the steel industry [*11*]. Processes available for air separation include membranes, pressure swing adsorption (PSA), and cryogenic distillation. However, for large scale air separation, cryogenic distillation is the only practical choice [*11,12*]. The cryogenic process consists mainly of heat exchangers and distillation columns (Figure 1). The oxygen produced from the air separation plant is mixed with recycle flue gas to approximate the combustion characteristics of air. In air, the N_2/O_2 ratio is about 3.65. A CO_2/O_2 ratio of 2.42 gives similar flame temperatures as well as similar ratios of radiant heat transfer to convective heat transfer [*13*]. Fly ash is removed from the power plant effluent. Water vapor may also be removed from the flue gas by condensation prior to recycling. The trade-offs of wet versus dry flue gas recycling are not evaluated in this study, which models a dry recycle. About 70-75% of the dried flue gas is recycled and the rest is sent to compression and dehydration prior to pipeline transport.

The major operational problem associated with the tests to data is air ingress. This problem has shown up in several of the experimental programs [*14,16*]. Many existing boilers were not designed for leak tight settings and may be difficult to retrofit [*15*]. By using oxygen instead of air, it may be possible to redesign the boiler to take advantage of a higher flame temperature and thereby improve the overall thermal cycle efficiency. This possibility would be worthwhile exploring in follow-up work.

Amine Scrubbing

The use of amines for gas sweetening (i.e., removal of CO_2 and H_2S) was first patented by R. R. Bottoms in 1930. Triethanolamine (TEA) was the first commercially available amine. Today, several amines are widely available, with monoethanolamine (MEA) and diethanolamine (DEA) being of prime commercial interest. MEA is used primarily for

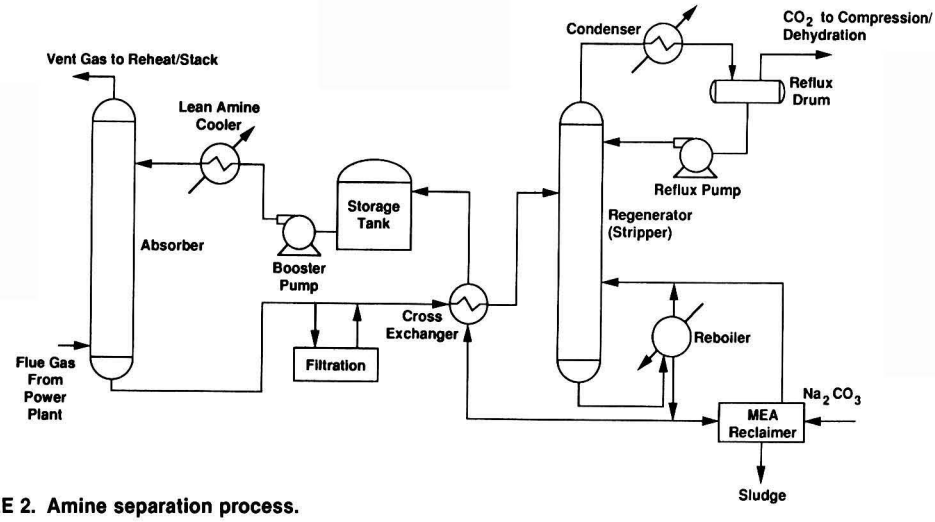

FIGURE 2. Amine separation process.

sweetening natural gas streams, while DEA is used primarily for refinery or manufactured gas sweetening [*17*]. The greatest advantage of MEA is its relatively high carrying capacity or load (amount of CO_2 absorbed per unit volume of solvent). This means that less solvent circulation is required for a given system performance specification, which leads to lower capital and operating costs. The Dow Chemical Company has developed a new amine technology, called FT technology, specifically targeted to remove large amounts of CO_2 from flue gas. Dow's technology is based on a 30% MEA solution with additives to control corrosion and inhibit the oxidative degradation of amines [*18*]. Dow's technology provides the best available amine for our purpose and forms the basis for the evaluation of the regenerable solvent process.

The simplified chemistry of this process is:

$$C_2H_4OHNH_2 + H_2O + CO_2 \rightleftharpoons C_2H_4OHNH_3^+ + HCO_3^- \quad (1)$$

Lower temperatures favor the forward reaction, while elevated temperatures favor the reverse reaction. A flowsheet of the basic amine process is shown in Figure 2. The key process units are the absorption tower, the regeneration (stripper) tower, and the lean/rich exchanger. An MEA recovery unit (reclaimer) is required to regenerate amine that reacts with SO_2 and NO_x. Also, solution filtration is required to control foaming. In the absorption tower, CO_2-lean amine solution absorbs CO_2 from the flue gas. The absorption tower consists of a packed section for absorption and a water wash at the top to reabsorb vaporized MEA. The tower operates at close to atmospheric pressure to avoid high compression costs. Some flue gas compression is required to overcome the pressure drops in the system. Operating temperatures are normally 40-65°C. This means that the flue gas must be quenched before entering the absorber and that the vent gas may need to be reheated (to have the required buoyancy) before being exhausted to the atmosphere. The regeneration column operates at elevated temperatures (100-120°C) to strip the CO_2 from the amine solution. The key energy requirement for the process is the regenerator reboiler duty (32-53% of the energy in the coal). The reboiler provides the heat of reaction, heats the feed to the temperature of the reboiler, and vaporizers H_2O (which is later condensed in the condenser). The column overhead product contains the CO_2 which is ready for compression, dehydration, and pipeline transport.

Key operational concerns are corrosion, foaming, and solvent degradation. Corrosion is a standard problem with amine systems. The presence of oxygen increases this problem because the oxygen slowly reacts with amine to form corrosion causing products. Traditionally, amine concentrations were kept low (less than 20%) to minimize corrosion problems. The Dow

Table 1 Commercial CO_2 Recovery Plants

Operator	Location	Capacity (tons/day CO_2)	CO_2 Fuel Source	CO_2 Use	Technology	Status	Ref.
Carbon Dioxide Technology	Lubbock, TX	1200	gas	EOR	Dow MEA	Shut	[*20*]
Kerr-McGee	Oklahoma City, OK	600	coal	Carbonation of brine to produce soda ash	Conventional MEA	Operational	[*21*]
Mitchell Energy	Bridgeport, TX	493	gas	EOR	Conventional MEA	Shut	[*43*]
N-ReN Southwest	Carlsbad, NM	104	gas	EOR	Retrofit to Dow MEA	Shut	[*44*]

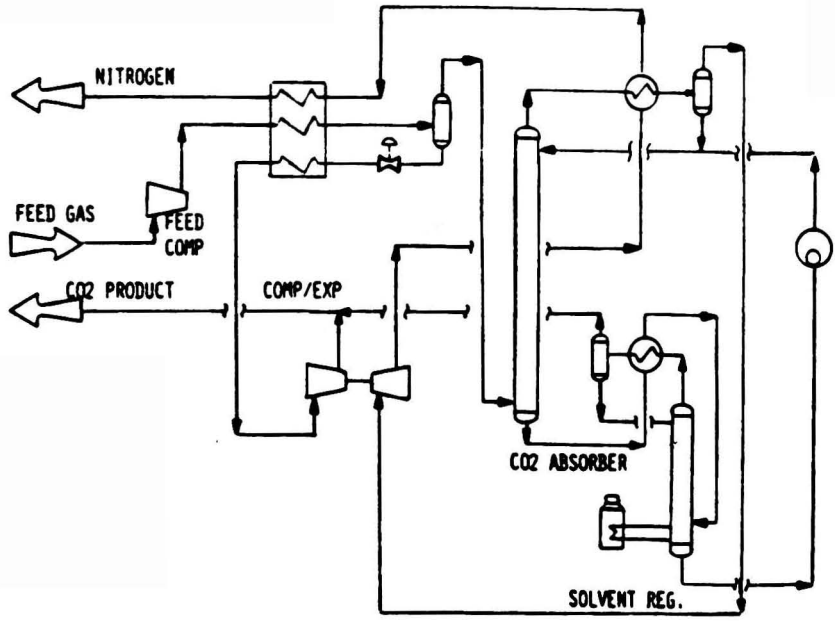

FIGURE 3. Cryogenic fractionation process [*49*].

amine contains inhibitors to reduce corrosion problems. It has been reported that flue gas concentrations up to 8% oxygen are acceptable [*19*]. Foaming is caused by a wide range of foreign materials and leads to reduced process efficiency. For a coal fired plant, particulates in the flue gas are a chief cause of foaming. Foaming can be controlled by pre-treating the flue gas to remove particulates and proper filtering of the amine solution during CO_2 capture. Two standard methods of particulate removal are electrostatic precipitation and fabric filtration. Solvent degradation is caused by the reaction of the amine with SO_2 and NO_x to form heat stable salts which cannot be regenerated in the stripping column. Since most SO_2 removal schemes only remove 50-90% of the SO_2, an MEA reclaimer is required for flue gases containing significant SO_2. In the reclaimer, sodium carbonate (Na_2CO_3) is added to the amine to precipitate out salts containing SO_2 and NO_x (e.g. Na_2SO_3, Na_2SO_4, $NaNO_3$). The regenerated amine is steam stripped and combined with the regenerator's reboiler vapor. In addition to solvent degradation, other sources of solvent losses include entrainment, vaporization, spills and leaks. Dow quotes that the solvent loss rate for its FT technology is 2-4 pounds solvent per ton of CO_2 recovered [*19,20*]. Data have been presented in the literature on 4 plants that have successfully produced CO_2 from flue gas (Table 1). Only Kerr-McGee has extensive flue gas pre-treatment because only they use coal (as opposed to gas) as a fuel source. In the Kerr-McGee plant, fly ash is removed with an electrostatic precipitator (99.8% efficient) and SO_2 is removed by Na_2CO_3 wet scrubbing (90% efficient) [*21*].

In summary, for amine scrubbing of a flue gas from a coal fired power plant, the flue gas must be pre-treated by removing particulates and SO_2. Also, solution filtration and an MEA reclaimer need to be included in the amine system. The total energy requirement for this process is 47–79% of the combustion energy of the coal.

Cryogenic Fractionation

A considerable amount of work exists on the cryogenic fractionation of methane and CO_2 for Enhanced Oil Recovery (EOR). However, very little work has been done on the cryogenic fractionation of nitrogen and CO_2. It is known that the N_2/CO_2 system has similar behavior and distillation limitations as the CH_4/CO_2 system, but the N_2/CO_2 system requires different operating pressures and temperatures [*22*]. A review of the literature reveals several approaches to CH_4/CO_2 or N_2/CO_2 fractionation, including straight distillation, double column systems, use of an additive, and controlled freezing.

The problem with straight distillation is the possible formation of solid CO_2 in the distillation column [*22*]. In CH_4/CO_2 systems, solid formation can be avoided by operating at pressures above 48 atm. However, this requires large compression costs. As an alternative, a number of schemes have been suggested using double column systems operating at different pressures to avoid CO_2 freezing [*23*]. These schemes required operation close to the critical point or close to the CO_2 freezing zone and are uneconomical due to high energy use and high capital costs [*24*]. The controlled freezing zone (CFZ) process was patented by Exxon Production Research (EPR) Co. Rather than avoiding the CO_2 freezing zone, this process takes advantage of it. The fractionation column is designed to allow for CO_2 freezing, followed by a melting tray [*25*]. The technique was proven in a demonstration pilot plant, but a commercial unit has not yet been built. Operating pressure is 38 atm for a CH_4/CO_2 system. The Ryan-Holmes process for CO_2 fractionation, patented by Koch Process Systems of Westborough, MA, avoids freezing by using an additive (such as butanes and aromatics) to alter the phase diagram. The distillation of CO_2 becomes easier and higher recoveries and purities are achieved compared to straight distillation. Typical operating pressures are 25-35 atm [*22,24*]. The Ryan-Holmes approach was chosen as the best process upon which to base our analysis of the cryogenic fractionation of N_2 and CO_2. The Davy McKee Co. has designed an N_2/CO_2 cryogenic fractionation process. This design forms the basis of our scoping study (Figure 3).

The cleaned flue gas is dehydrated and compressed to about 30 atm. The compressed gas is then cooled in an exchanger against the vent gas and vaporizing CO_2. This liquefies approximately half the CO_2, which is separated out in a knockout drum. The gas is next fed to an absorber, where CO_2 is

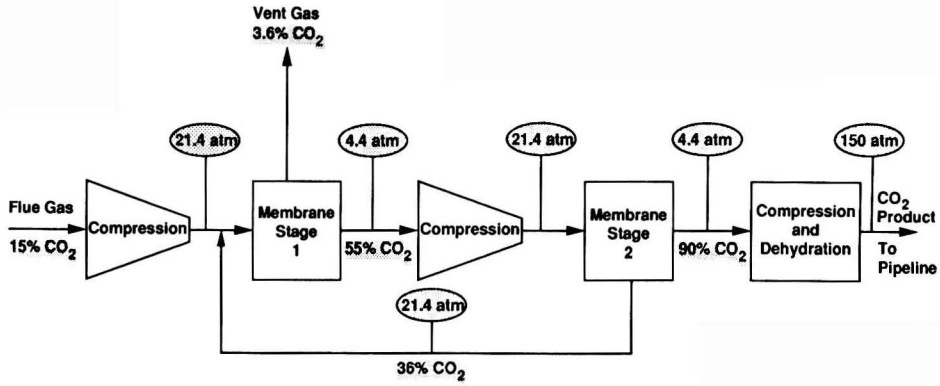

FIGURE 4. Membrane separation process.

selectively absorbed by a solvent. The Davy McKee Co. studied a variety of solvents and determined the best solvent is a mixture of aromatics. The absorber overhead containing nitrogen with some oxygen and CO_2 is vented, while the absorber bottoms are sent to the solvent regeneration column. The solvent regeneration column drives off the CO_2 overhead by raising the solvent temperature. The regenerated solvent is cooled with external propane refrigerant and recycled to the absorber. Over 90% of the CO_2 is recovered at a purity of about 97% [*26*]. Prior to fractionation, the flue gas must be cleaned and dehydrated. Both fly ash and SO_2 must be removed, but the acceptable levels of these contaminants is currently undefined. Dehydration of the flue gas is essential because CO_2 hydrates will form at column operating conditions. The key energy requirements are flue gas compression prior to fractionation and production of the external refrigeration required for the fractionation process. In general, a higher system pressure means higher energy consumption for flue gas compression, but lower energy consumption for refrigeration. Overall energy consumption for this process is 55-95% of the energy of the coal.

Membrane Separation

Polymeric membranes separate gases by selective permeation of gas species in contact with the membrane. The gases dissolve in the polymer and are transported across the membrane barrier under an imposed partial pressure gradient. The pressure gradient is accomplished by feeding high pressure gas to the outside of the hollow fiber membrane while the permeate side is operated at substantially lower pressure. Typically the feed to permeate pressure ratio is greater than three. The relative rate at which gas species will permeate across the membrane in also dependent upon the polymer selected for the membrane. In the PRISM separators currently marketed by Monsanto, water vapor, carbon dioxide, and hydrogen sulfide are fast species in comparison to methane, nitrogen, and other hydrocarbon gases [*27*]. For a flue gas, only partial separation and concentration of CO_2 can be achieved in a single membrane stage. Based on Pope [*28*], a two stage process was selected, as shown in Figure 4.

The flue gas from the power plant (after fly ash removal) is compressed to about 21 atm, mixed with a recycle stream of non-permeate from stage 2, and fed to stage 1 of the membrane separator. The non-permeate is vented to the atmosphere, while the permeate, containing about 55% CO_2 at 4.4 atm, is recompressed to 21 atm and fed to stage 2 of the membrane separator. The permeate from stage 2, containing 90% CO_2 at 4.4 atm, is compressed to 150 atm for pipeline transport. The overall CO_2 recovery of this process is about 80%. In order to recover 90% of the CO_2, the cost of the membranes may double [*28*]. Overall energy consumption for this process is in the range of 50-75% of the energy of the coal.

Seawater Scrubbing

In this process, the flue gas at atmospheric or elevated pressure is brought into contact with seawater. The seawater absorbs CO_2 from the flue gas. For operating at atmospheric pressure the key energy requirement is to overcome frictional losses of a fluid flowing in a pipe. The frictional loss is:

$$F = \frac{32 f Q^2 L}{\pi^2 g_c D^5} \tag{2}$$

where F is the friction loss in energy per mass of fluid flowing; f is the fanning friction factor (0.0015 used); Q is the volumetric flow rate; g_c is a dimensional constant; D is the pipe diameter; and L is the pipe length. The power needed to pump the seawater is the friction loss F times the flow rate. This results in a relationship of power to pipe length, pipe diameter, and volumetric flow rate:

$$P \alpha \frac{Q^3 L}{D^5} \tag{3}$$

At atmospheric pressure, assuming the inlet water contains no CO_2 and the outlet water is saturated, 413,000 kg/sec of seawater is needed to absorb 90% of the CO_2 from a 500 MW power plant. To pipe this water 16 km in a 4.6 m diameter pipe requires 3600 MW, while a 7.6 m diameter pipe requires 300 MW. It can be seen that to reduce the power requirement to an acceptable level requires a very large diameter pipe. However, this drives up capital costs dramatically. The capital cost of the absorbers is another problem with this scheme. The seawater flow of 413,000 kg/sec is about 250 times the solvent flow rate in the amine scrubbing process. With realistic CO_2 concentrations in the inlet and outlet seawater streams (as opposed to zero and saturated, respectively), this factor will rise to 500-1000. Since the absorber capital cost is a function of the solvent flow rate, the capital cost of the absorbers for seawater scrubbing will be one to two orders of magnitude greater than the capital cost of the absorbers for amine scrubbing.

By operating the absorbers at elevated pressures, the solubility of CO_2 in the seawater is increased, thereby reducing the seawater flow rate. However, some of the savings in capital

Table 2 Energy Requirement Comparison

Process	Energy Requirement		Coal Requirement		Net CO_2 Emissions		Recovered CO_2	
	% Combustion Energy of Coal	Thermal Eff (%)	kg Coal per kWh	Relative to Base Case	kg CO_2 per kWh	% of Base Case	% CO_2 Recovery	% CO_2 Purity
Base Case—No CO_2 Removal	0	35	0.35	1	0.88	100	0	---
Air Separation/FG Recycling	26-31	24-26	0.48-0.51	1.35-1.45	0	0	100	90
Amine Scrubbing	47-79	7-19	0.66-1.68	1.89-4.76	0.17-0.42	19-48	90	99+
Cryogenic Fractionation	55-95	2-16	0.78-7.04	2.22-20	0.20-1.76	22-200	90	97
Membrane Separation	50-75	9-18	0.72-1.41	2-4	0.35-0.70	40-80	80	90

costs due to reduced seawater flow rate will be offset by the higher capital costs associated with the higher design pressure. In addition, significant energy is now required to compress the flue gas and pressurize the seawater feeds to the absorbers. In other words, by increasing operating pressure, much of the benefit of the reduced seawater flow rate is offset by thicker wall requirements and higher compression requirements. This point is illustrated by looking at an absorber operating pressure of 10 atm. The seawater flow rate is 41,000 kg/sec (assuming CO_2-free inlet and saturated outlet) and the energy requirement is 42-56% of the combustion energy of the coal (including pipeline transport of 100 km). This energy requirement is approaching that of the amine scrubbing process, but a pipeline diameter of at least 5 m is still needed and the seawater flow is still two orders of magnitude greater than the amine flow. We conclude that seawater scrubbing of the total flue gas, either at atmospheric or elevated pressure, is not a viable option and, therefore, is not included in the following comparisons.

ENERGY REQUIREMENT AND COST

For each of the four selected processes, the energy requirement is calculated as the percent of the total energy (calorific value) of the coal required to capture a certain percentage of the CO_2 and compress it to 150 atm for transport as a one-phase supercritical fluid. Another comparative measure is to estimate the power plant's overall thermal efficiency (i.e., the coal's calorific value that is converted to electrical energy). The energy requirement for each process is presented in Table 2 along with the coal requirement per unit of net electricity produced and the net CO_2 emissions per unit of net electricity produced. For comparison, the first line of Table 2 is the base case without any CO_2 capture. The last two columns give the fraction of the flue gas CO_2 that is captured and its purity. Note that these quantities vary for the different processes. The energy requirements in Table 2 are reported as ranges. Generally, the lower end of the energy range results from increased efficiency of the process. However, increased efficiency usually involves larger capital investment in equipment. For example, the efficiency of gas compression can be increased by adding compression stages and interstage cooling. Thus, there is a trade-off between energy efficiency and capital cost. A detailed economic evaluation to optimize the energy versus capital cost-trade-off for each process is beyond the scope of this study.

The results for the air separation/flue gas recycle process are compared to other studies in Table 3. Argonne National Laboratory (ANL) and Oak Ridge National Laboratory (ORNL) used an air plant energy requirement of 395 and 441 kWh per ton of oxygen, respectively. Brookhaven National Laboratory (BNL) and this study used approximately 200 kWh per ton of oxygen [*29*]. This lower energy requirement is achieved through economies of scale associated with a 9,000 metric tons per day oxygen plant. The compression energy requirements from this study fall in the middle of energy requirements predicted by the other studies. The variations are primarily due to assumptions made in the compressor calculations, particularly in regard to efficiencies. The ORNL energy requirements appears to be too small. It is based on the assumption that steam turbines drive the compressors. No details are presented on the energy requirement calculations, but we assume unrealistically high turbine efficiencies were used.

The results for the amine scrubbing process are compared to other studies in Table 4. The BNL and this study's results are based on the Dow amine process, while the ORNL and ANL results are based on a conventional 20% MEA solution [30]. Dow claims its process uses 11% less energy (5.6 versus

Table 3 Energy Requirements for Air Separation Flue Gas Recycle Process

Source	Energy Requirement as % of Combustion Energy of Coal		Reference
	Air Plant	Compression	
MIT	17	9-14	This report
BNL	16	9	[*45*]
ANL	45[a]	---	[*46*]
	---	16[b]	[*47*]
ORNL	32	5	[*6*]

[a] Includes oxygen compression to 30 atm.
[b] Based on a detailed equipment design and quotation prepared by Ingersoll-Rand.

Table 4 Energy Requirements for Amine Scrubbing Process

Source	Energy Requirement as % of Combustion Energy of Coal		Reference
	Amine Plant	Compression	
MIT	32-53[a]	7-10	This report
BNL	58[b]	8	[*5*]
ANL	48	---	[*46*]
ORNL	43[c]	3	[*6*]

[a] Thermal efficiency 35%, boiler efficiency 85%.
[b] Thermal efficiency 38%, boiler efficiency 90%, reboiler efficiency 85%.
[c] Thermal efficiency 38%, boiler efficiency 90%.

Table 5 Capital Cost for CO_2 Capture Retrofit of 500 MW Power Plant

Component	Cost ($10^6$$)
O_2 Plant (9,000 metric tons/day)[a]	135
CO_2 Compressor[b]	38
Other[c]	53
Contingency[d]	45
Total	271

[a] O_2 plant cost [29].
[b] CO_2 compressor costs calculated by ASPEN PLUS. Literature values (adjusted for inflation by cost indices and for capacity by .7 rule) range from $19-43 million [45,47].
[c] Other includes cost of piping for CO_2 recycle, dehydration system, etc. Based on estimate for a 600 MW power plant and adjusted by .7 rule [14].
[d] A 20% contingency factor is used.

6.3 MJ/kg CO_2 recovered) than the conventional 20% MEA process [20]. Other differences reflect different assumptions for power plant, boiler, and reboiler efficiencies. In general, these results show good agreement with each other. The compression energy requirement for amine scrubbing is slightly lower than the corresponding requirement for air separation/flue gas recycling because less gas needs to be compressed. Steinberg et al. [5] and Steinberg and Cheng [31] claim it is possible to reduce the energy requirement of the amine plant from 58% to 7% by cogenerating the steam required for the amine stripper boiler. However, they erroneously assume that the power plant's overall thermal conversion efficiency will remain at 38%, despite cogenerating large quantities of steam (over half the turbine steam needs to be extracted to satisfy the reboiler duty). We did not evaluate the amine scrubbing process with cogenerated steam in detail because it would be difficult--if not impossible--to retrofit existing boilers to cogeneration. Also, preliminary calculations indicate that this process is more energy intensive than the air separation/flue gas recycling process. However, it would be worthwhile exploring this process is the framework of a new plant where the amine scrubbing is fully integrated into the overall power plant design.

We conclude that the air separation/flue gas recycling process is the most energy efficient process analyzed, requiring 26-31% of the coal heating value. All the other processes studied require over 50% of the coal heating value. The air separation/flue gas recycling process reduces the thermal efficiency of the power plant from the 35% base case to 24-26%. In addition to being the most energy efficient process, the air separation/flue gas recycle process also has the highest CO_2 recovery rate (100% versus 90% or less for the other processes studied). Table 2 shows that even with recovering 90% of all the CO_2 generated, CO_2 emissions can still be significant because the capture processes require burning more coal per unit of net electricity produced. By capturing 100% of all the CO_2 generated, the air separation/flue gas recycling process eliminates this concern.

The capital cost estimate of the components of an air separation/flue gas recycling process for a 500 MW coal-fired power plant is presented in Table 5. The total cost is estimated at $271 million (1989 $), with a probable range of ±30%. The major costs are for the air separation plant and the flue gas compression and dehydration system. Costs for the CO_2 pipeline and ocean disposal system are not included in this estimate. Installed costs for a one meter diameter, high pressure pipeline is $2 million (1984 $) per mile [32]. An offshore pipeline may cost significantly more. For a typical 500 MW coal-fired power plant, the average U.S. cost of electricity is 46 mills/kWh (1986 $) [33]. For the air separation/flue gas recycling process, the amortization of the capital costs plus operating and maintenance costs excluding energy adds 13 mills/kWh. Taking into account the reduced overall thermal efficiency of the power plant from 35% to 24-26%, the cost of electricity with CO_2 capture by an air separation/flue gas recycling process is 80-86 mills/kWh. This represents an 80% increase in the cost of electricity.

Many power plants are currently being mandated to control their emissions of SO_2 and NO_x. Since both SO_2 and NO_x are disposed together with the CO_2 in the air separation/flue gas recycling process, it may be appropriate to consider the savings in not having to control SO_2 and NO_x emissions by other means. It is estimated that the mandated emission controls of SO_2 and NO_x will add about 15% to the electricity generating costs [33]. With joint disposal of CO_2, SO_2 and NO_x by air separation and flue gas recycling, the 15% SO_2 and NO_x emission control costs could be counted as a credit toward the CO_2 control costs.

CO_2 DISPERSAL IN THE DEEP OCEAN

The nature of the CO_2-seawater interaction depends on the release depth and the characteristics of the CO_2 stream. In equilibrium with seawater, CO_2 is in the gaseous phase down to a depth of about 500 m. At greater depths, liquid CO_2 is the stable phase. If CO_2 is released at ambient sea temperatures, the density of the liquid is less than that of seawater to a depth of 3000 m, and greater below this depth [34]. Thus, the released liquid CO_2 will have a tendency to rise (positive buoyancy) at all practical release depths.

A complicating factor is the possibility that in the release of liquid CO_2 in the deep ocean, a solid hydrate is formed by composition $CO_2 \cdot 6H_2O$ or $CO_2 \cdot 8H_2O$ [35,36]. Such hydrates are also called clathrates. Apparently, the clathrate is denser than either liquid CO_2 or seawater [34] and thus may sink to the ocean bottom. The amount of clathrate to be formed in the release cannot be estimated from available data. Probably, the amount of clathrate formation will be dependent on the microdynamic conditions at the interface of one liquid, that of seawater, penetrating the other, CO_2. In the absence of any relevant data on this non-equilibrium process, we refrain here from estimating the amount of solid hydrate that may form in the release, and its subsequent sedimentation rate and the accumulation on the ocean bottom. However, this is an interesting and important research problem that ought to be investigated before deep ocean release of CO_2 is contemplated. In the following exercise we shall assume that all the released CO_2 remains in the liquid form until fully dissolved in seawater.

For a given set of release conditions (fluid properties and orifice diameter), the dynamics of the liquid-liquid system depends on the rate at which CO_2 is injected. Clift et al. [37] define three regimes. At low flowrates, bubbles form slowly and break off when buoyancy forces become greater than the restraining surface tension. At moderate flowrates, fluid momentum becomes important and a jet forms at the release orifice. The jet lengthens with increasing flow to a point where instabilities become more important and disintegrate the jet into drops. At very high flowrates, no jet is formed; rather, the stream atomizes into tiny droplets at the orifice exit. The latter principle is the basis of spray drying techniques. Given the large volume of CO_2 produced by large generating plants, it is likely that the flow will be in either the jetting or atomization regime. Disintegrating jets produce the largest drops, roughly twice the diameter of the orifice [37]. Atomization produces droplets considerably smaller than the release orifice. Drop size is thus controllable in jetting and atomizing flows.

Stability considerations limit drop size. Competition between surface tension, viscous, and buoyant (inertial) forces tends to break up large drops. The largest drop radius is [37]

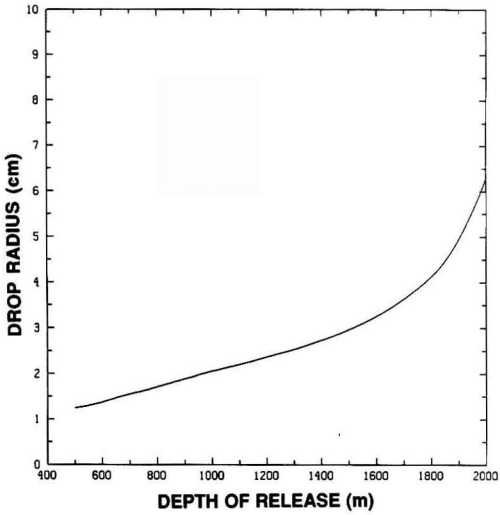

FIGURE 5. Largest stable drop radius as a function of depth.

$$r_{stable} = \sqrt{\frac{\sigma}{g(\rho_w - \rho)}} \tag{4}$$

where σ is the surface tension of liquid CO_2, ρ_w is the density of water, ρ the density of liquid CO_2, and g is the gravitational constant. The relationship is plotted as a function of depth in Figure 5 using literature values of the ocean water temperature profile, surface tension and CO_2 density. At intermediate depths, stable drops are at most 1-2 cm in radius. At these depths, the formed droplets are positively buoyant and will rise. Drag forces slow the drops. Simultaneous mass transfer will tend to dissolve the drops into the surrounding unsaturated seawater. The purpose of the disposal system is to dissolve the drops completely. In this study, we estimate the release depth such that by the time liquid CO_2 drops ascend to 500 m, they completely dissolve in seawater. This is a conservative approach, for even if the core of the drops were not dissolved at 500 m, they may flash into gaseous bubbles and still be dissolved before they ascend to the surface. Since ocean depths greater than 500 m are not accessible to many coastal power plants, future work should consider optimal release depths, including regimes where some flash vaporization may occur.

Consider a spherical drop of radius r at a depth z. The equation of motion for a hard sphere is given by

$$\ddot{z} = \frac{g(\rho_w - \rho)}{\rho} - \frac{3C_D u^2}{8r} \tag{5}$$

where u is the drop velocity and C_D is the drag coefficient which depends on the Reynolds number Re, defined as

$$\mathrm{Re} = \frac{2ur}{\nu} \tag{6}$$

where ν is the kinematic viscosity. Note that ν is related to the molecular viscosity μ by $\nu = \mu/\rho$. Initial integrations demonstrated that the acceleration term is important only for a very short time; for all practice purposes, it can be neglected, and Equation (5) solved for a steady state velocity.

$$u_f = \left[\frac{8gr(\rho_w - \rho)}{3C_D\rho}\right]^{1/2} \tag{7}$$

Because C_D depends on Re (and hence velocity), Equation (7) must be solved implicitly using the commonly available drag relationship for flow past a solid sphere [*38*]. The subscript f refers to force-balance velocity.

Treybal [*39*] noted that actual liquid drops are not well approximated by hard spheres. Rather, they tend to wobble and form internal circulation because of viscous interactions with the surrounding flow. Denoting the drop rise velocity u_t, Treybal suggests the following empirical relation:

$$u_t = \begin{cases} \dfrac{62.2(\rho_w - \rho)^{.58} r^{.7}}{\rho^{.45}\mu^{.11}} & r < r_t \\ \dfrac{17.6(\rho_w - \rho)^{.28}\mu^{.10}\sigma^{.18}}{\rho^{.55}} & r > r_t \end{cases} \tag{8}$$

The transition radius r_t is found by equating the two expressions for a given set of properties. Equations (7) and (8) are thus two different estimates of drop velocity. Equation (8) generally gives faster rise velocities. In the calculations that follow both equations are used to test model sensitivity.

A mass transfer equation which governs the rate of dissolution of a spherical drop is given by

$$\frac{d}{dt}\left[\frac{4}{3}\pi r^3 \rho\right] = -4\pi r^2 K[C_s - C_\infty] \tag{9}$$

where K is a mass transfer coefficient and C the CO_2 concentration in water. Subscripts s and ∞ designate surface and far stream concentrations. The surface concentration is the saturated solubility limit, which is large compared to the free stream value. Neglecting the latter and changing the subscript to *sat*, the mass transfer equation can be simplified to predict drop radius:

$$-\dot{r} = \frac{KC_{sat}}{\rho} + \frac{ru\dfrac{d\rho}{dz}}{3\rho} \tag{10}$$

The saturation concentration C_{sat} is relatively constant below depths of 500 m. A fixed value of 1 mole CO_2/kg seawater is adopted for this analysis. This value is somewhat conservative when compared with CO_2 solubility data in water [*40*]. The right-hand side of Equation (10) is composed of two terms; the first is the mass transfer term, and the second, which is usually small in comparison, is a compressibility term. The mass transfer coefficient is a function of fluid properties, drop size, buoyancy and velocity. Estimates of mass transfer coefficients are generally expressed as empirical correlations in a non-dimensional form, the Sherwood number (Sh)

$$\mathrm{Sh} = \frac{2Kr}{D} \tag{11}$$

where D is the molecular diffusion coefficient. Two mass transfer correlations are considered to provide a range of model estimates. The first, subscripted c, is suggested by Cussler [*41*] for liquid spheres in a liquid solvent:

$$\mathrm{Sh}_c = 0.42\left[\frac{8r^3 g(\rho_w - \rho)}{\rho\nu^2}\right]^{1/3}\left[\frac{\nu}{D}\right]^{1/2} \tag{12}$$

A more complex correlation, derived from numerical simulations, is subscripted with an x [*37*]:

$$Sh_x = \frac{2}{\sqrt{\pi}} Pe^{1/2} f(l,Re)$$

$$f(l,Re) = \begin{cases} \left[1 - \dfrac{2.89 + 2.15 l^{.64}}{Re^{1/2}}\right]^{1/2} & Re > 70 \\ \left[1 - \dfrac{\dfrac{2+3l}{3(1+l)}}{\left(1 + \left[\dfrac{(2+3l)Re^{1/2}}{(1+l)(8.67+6.45l^{.64})}\right]^{n}\right)^{1/n}}\right]^{1/2} & Re < 70 \end{cases} \quad (13)$$

where $l = \mu/\mu_w$
$n = 4/3 + 3l$
$Pe = 2ur/D$

The two options for mass transfer coefficient Equations (12) and (13) when combined with the two velocity estimations Equations (7) and (8), provide four distinct combinations to calculate drop absorption. Integrations are performed given an initial drop size and depth of release. Both drop radius and position are tracked as a function of time. Using depth dependent properties, velocity at the current depth is calculated using either Equation (7) or (8). The drop radius is then estimated using a 4th order Runge-Kutta method [*42*] to numerically integrate Equation (10) in conjunction with one of the two mass transfer correlations, Equation (12) or (13). The time-step and velocity are then used to update position. Release depths from 500-2000 m are considered. Figure 6 plots the maximum drop size which will be completely dissolved at the 500 m level as a function of release depth. The four velocity/mass transfer combinations are distinguished by symbols. Using the most conservative method, drops of 1 cm radius can be completely dissolved if released at or below a depth of 700 m. Two complications are not considered in the single drop analysis which may decrease the effectiveness of mass transfer. First, interactions may be caused by the proximity of multiple drops. Second, the formation of solid hydrate may appear at the liquid-liquid interface. These effects are probably small and are compensated by the conservative choice of saturated CO_2 concentration (C_{sat}). A diffuser type system design should provide further assurance that drops will spread over a large volume.

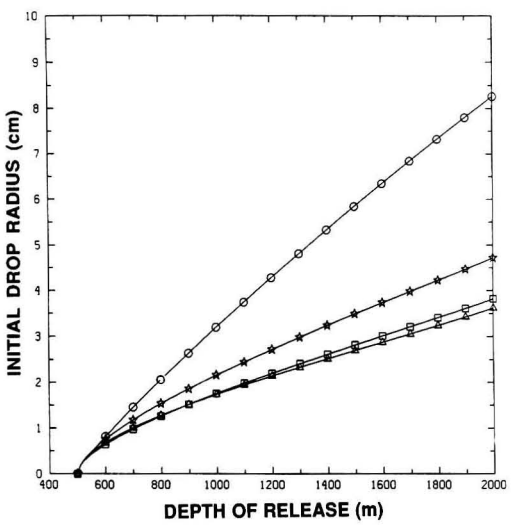

FIGURE 6. Initial drop radius versus release depth to assure drop will be completely dissolved by the time it rises to a depth of 500 m. Symbols refer to different velocity/mass transfer correlations:
□ - u_t / Sh_c; △ - u_t / Sh_x; ○ - u_t / Sh_c; ★ - u_t / Sh_x.

CONCLUSIONS

The air separation/flue gas recycling process is the least energy intensive retrofit process studied for capturing CO_2 from the flue gas of coal-fired power plants.

The capital cost of the air separation/flue gas recycling process is estimated at $271 million for a 500 MW power plant. The thermal efficiency of the power plant is reduced from 35% to 25% and the resulting cost of electricity production increases by 80%. These numbers include compression of the CO_2 to 150 atm for pipeline transport, but exclude pipeline and diffuser system capital and operating costs.

For new power plants using the air separation/flue gas recycling process, one may utilize the higher thermal efficiency of combusting coal in pure oxygen by reducing flue gas recycling. This would improve the overall energy efficiency and economics of such a plant compared to the retrofit case presented in this paper.

To ensure that liquid CO_2 is completely dissolved in seawater at a depth of 500 m, it should be released through a diffuser at depths greater than 700 m and drop radii less than 1 cm.

ACKNOWLEDGMENT

This research was funded by the Mitsubishi Research Institute, Society and Technology Department, Tokyo, Japan. That support is gratefully acknowledged. We are also grateful for stimulating discussions and suggestions by Drs. J. Tester and D. White of the MIT Energy Laboratory.

LITERATURE CITED

1. Marchetti, C., "On Geoengineering and the CO_2 Problem," in Climatic Change **1**, D. Reidel Publishing Company, Dordrecht, Holland (1977).
2. Marchetti, C., "Constructive Solutions to the CO_2 Problem," in Man's Impact on Climate, W. Bach, J. Pankrath and W. Kellogg (eds.), Elsevier Scientific Publ. (1979).
3. Mustacchi, C., P. Armenante and V. Cena, "Carbon Dioxide Removal From Power Plant Exhausts," *Environment International*, **2**, 453-456 (1979).
4. Albanese, A. S. and M. Steinberg, "Environmental Control Technology for Atmospheric Carbon Dioxide," Brookhaven National Laboratory, DOE/EV-0079 (1980).
5. Steinberg, M., "An Analysis of Concepts for Controlling Atmospheric Carbon Dioxide," Brookhaven National Laboratory, DOE/CH/00016-1 (1984).

6. Baes, E. F., Jr., S. E. Beall, D. W. Lee and G. Marland, "The Collection, Disposal, and Storage of Carbon Dioxide," in Interactions of Energy and Climate, W. Bach, J. Pankrath and J. Williams (eds.), D. Reidel Publishing Company, Boston, MA (1980).
7. Hendricks, C. A., K. Blok and W. C. Turkenbury, "The Recovery of Carbon Dioxide from Power Plants," in Proceedings Climate and Energy Symposium, Utrecht, The Netherlands (1989).
8. Snyder, W. G. and C. A. Depew, "Coproduction of Carbon Dioxide (CO_2) and Electricity," Electric Power Research Institute, AP-4827 (1986).
9. Golumb, D., H. Herzog, J. Tester, D. White and S. Zemba, "Feasibility, Modeling, and Economics of Sequestering Power Plant CO_2 Emissions in the Deep Ocean," Massachusetts Institute of Technology Energy Laboratory, MIT-EL 89-003 (1989).
10. Alexander, J. F., Jr., D. P. Swaney, R. J. Rognstad and R. K. Hutchinson, "An Energetics Analysis of Coal Quality," in Coal Burning Issues, A.E.S. Green (ed.), University Presses of Florida, Gainesville, FL (1980).
11. Moreira, P., Air Products and Chemicals, Allentown, PA, personal communication (1989).
12. Lagree, D. A., "Oxygen Enriched Air Production System," Union Carbide Corp., DOE/ID/12652-1 (1988).
13. Weller, A. E., B. W. Rising, A. A. Boiarski, R. J. Nordstrom, R. E. Barrett and R. G. Luce, "Experimental Evaluation of Firing Pulverized Coal in a CO_2/O_2 Atmosphere," Argonne National Laboratory, ANL/CNSV-TM-168 (1985).
14. Park, R. S., "Description of a North Sea CO_2 Enhanced Oil Recovery Project," in Recovery and Use of Waste CO_2 in Enhanced Oil Recovery, Argonne National Laboratory, ANL/CNSV-TM-186 (1988).
15. Tupper, R. J. and T. Fuller, "Description of a Planned CO_2 Recovery Project in Wyoming," in Recovery and Use of Waste CO_2 in Enhanced Oil Recovery, Argonne National Laboratory, ANL/CNSV-TM-186 (1988).
16. Payne, R., W. Richter and A. Abele, "Coal Combustion in Oxygen and Recycled Flue Gas Mixtures: Experimental Evaluation and Boiler Performance Prediction," in Recovery and Use of Waste CO_2 in Enhanced Oil Recovery, Argonne National Laboratory, ANL/CNSV-TM-186 (1988).
17. Maddox, R. N., Gas and Liquid Sweetening, Second Edition, Campbell Petroleum Series, Norman, OK (1977).
18. Thornton, B., Dow Chemical Company, Houston, TX, personal communication (1989).
19. Pauley, C. R., "CO_2 Recovery from Flue Gas," *Chem. Eng. Progress*, **80**, 59-62 (1984).
20. Kaplan, L. J., "Cost-Saving Process Recovers CO_2 from Power-Plant Fluegas," *Chem. Eng.*, **89**, 30-31 (1982).
21. Arnold, D. S., D. A. Barrett and R. H. Isom, "CO_2 Can be Produced from Flue Gas," *Oil & Gas Journal*, **80**, 130-136 (1982).
22. Holmes, A. S., "Recovery of CO_2 from Man-Made Sources Using Cryogenic Distillation Techniques," in Recovering Carbon Dioxide from Man-Made Sources, Argonne National Laboratory, ANL/CNSV-TM-166 (1985).
23. Schianni, G. C., "Cryogenic Removal of Carbon Dioxide from Natural Gas," *Institute of Chem. Eng. Symposium Series*, **44**, 50-55 (1976).
24. Holmes, A. S., J. M. Ryan, B. C. Price and R. E. Styring, "Process Improves Acid Gas Separation," *Hydrocarbon Processing*, **61**, 131-136 (1982).
25. Victory, D. J. and J. A. Valencia, "Methane-CO_2 Fractionation," *Hydrocarbon Processing*, **66**, 44-46 (1987).
26. Elliot, D. G. and R. Chen, formerly of Davy McKee Co., Houston, TX, personal communication (1989).
27. Stookey, D. J. and W. M. Pope, "Application of Membranes in Separation of Carbon Dioxide from Gases," in Recovery Carbon Dioxide from Man-Made Sources, Argonne National Laboratory, ANL/CNSV-TM-166 (1985).
28. Pope, W. M., Monsanto Company, St. Louis, MO, personal communication (1989).
29. Smith, A., Air Products and Chemicals Co., Allentown, PA, personal communication (1989).
30. Rump, W. M., M. Hare and R. E. Porter, "Supply of Carbon Dioxide for Enhanced Oil Recovery," Pullman Kellogg Div., FE-2515-10 (1977).
31. Steinberg, M. and H. C. Cheng, "Advanced Technologies for Reduced CO_2 Emissions," Brookhaven National Laboratory, BNL-40730 (1987).
32. "Technical and Cost Evaluation of Use of Idle Pipelines for Reverse Carbon Dioxide Service," Ford, Bacon and Davis, Inc., ANL/CNSV-TM-159 (1985).
33. National Acid Precipitation Assessment Program (NAPAP), Interim Assessment, Council on Environmental Quality, Washington, D. C. (1987).
34. Song, K. Y. and R. Kobayashi, "Water Content of CO_2 in Equilibrium with Liquid Water and/or Hydrates," in Society of Petroleum Engineers Formation Evaluation (1987).
35. Wroblewski, M. S., "Sur les Lois de Solubilite de l'Acide Carbonique dans l'Eau sous de Haute Pressions," *Compes Rendus*, **XCIV**, 1355-1357 (1882).
36. Villard, P., "Etude Experimental des Hydrates de Gaz," *Ann. Chim. Phys.*, **11**, 353-361 (1887).
37. Clift, R., J. R. Grace and M. E. Weber, Bubbles Drops and Particles, Academic Press, New York (1978).
38. White, F. M., Fluid Mechanics, McGraw-Hill Book Co., New York (1979).
39. Treybal, R. E., Liquid Extraction, McGraw-Hill Book Co., New York (1963).
40. Wiebe, R. and V. L. Gaddy, "The Solubility of Carbon Dioxide in Water at Temperatures from 12 to 40°C and at Pressures to 500 Atmospheres. Critical Phenomena," *J. Amer. Chem.*, **62**, 815-817 (1940).
41. Cussler, E. L., Diffusion: Mass Transfer in Fluid Systems, Cambridge University Press, Cambridge, UK (1984).
42. Hornbeck, R. W., Numerical Methods, Prentice-Hall, Inc., Englewood Cliffs, NJ (1975).
43. Hopson, S., "Amine Inhibitor Copes with Corrosion," *Oil & Gas Journal*, **83**, 44-47 (1985).
44. Pauley, C. R., P. L. Simiskey and S. Haigh, "N-ReN Recovers CO_2 from Flue Gas Economically," *Oil & Gas Journal*, **82**, 87-92, (1984).
45. Horn, F. L. and M. Steinberg, "A Carbon Dioxide Power Plant for Total Emission Control and Enhanced Oil Recovery," Brookhaven National Laboratory, BNL-30046 (1981).
46. Abraham, B. M., J. G. Asbury, E. P. Lynch and A. P. S. Teotia, "Coal-Oxygen Process Provides CO_2 for Enhanced Recovery," *Oil & Gas Journal* **80**, 68-75 (1982).
47. Lynch, E. P., "Compression and Dehydration of Carbon Dioxide for Oil Field Injection," Argonne National Laboratory, ANL/CNSV-TM-158 (1985).
48. Shen, S. Y., and A. M. Wolsky, "Energy and Materials Flows in the Production of Liquid and Gaseous Oxygen," Argonne National Laboratory, ANL/CNSV-15 (1980).
49. Aldana, G., R. Arai and D. G. Elliot, "An Evaluation of Sources of CO_2 for EOR in Venezuela," in Acid and Sour Gas Treating Processes, S. A. Newman (ed.), Gulf Publishing Company, Houston, TX (1985).

Design and Testing of a Moving Bed VOC Adsorption System

Eric S. Larsen and Michael J. Pilat

Department of Civil Engineering, University of Washington, Seattle, WA 98195

A 0.28–2.8 m^3/min (10–100 cfm) moving bed carbon adsorption pilot plant has been developed for testing of low (10–200 ppm) concentration VOC emissions. The pilot plant uses a cross-flow arrangement with the air flowing horizontally through the adsorption bed while the carbon adsorbent particles flow vertically downward. At the bottom of the system, the "used" activated carbon is regenerated using a direct contact heat exchanger. The regenerated carbon is then transported to the top of the moving bed via a screw feeder and pneumatic transport tube. A small gas flow containing the VOCs removed from the used adsorbent is emitted continuously from the adsorbent regenerator. When a carbon flow rate of 2.3 kg/hr (5 lbs/hr), a face velocity of 0.32 m/sec (63 ft/min), and an emissions stream containing 30 ppm ethanol were used, the observed collection efficiency was approximately 90%. The ability to regenerate the carbon was tested by first operating the system in a static mode, that is air being drawn into the system while the adsorption bed was not moving. This was continued until approximately 70% of the inlet gas VOCs passed through the system without being adsorbed. The carbon flow was then started and the VOC concentration in the off gases of the absorbent regenerator was measured as the partially saturated carbon passed through the system. The VOC concentration in the gases emitted from the adsorbent regenerator was about a factor of ten higher than the VOC concentration in the air entering the adsorption bed.

INTRODUCTION

Research Objectives

The purpose of this project was to investigate methods to reduce the size of VOC control equipment and in doing so determine if adsorption systems could be applied to applications where currently available systems are not appropriate. To address this, two areas were to be investigated. The first being whether continuously recycling of the adsorbent could minimize the amount of adsorbent necessary. Presumably, continuous recycling of the adsorbent should minimize the quantity of adsorbent required since adsorbent is either being used to adsorb VOCs or is being regenerated. In conventional fixed bed VOC adsorption systems, a portion of the adsorbent is not in use as the adsorption bed needs to have a depth such that as the initial portion of the bed is spent, additional bed depth is still available to collect VOCs until such time as the adsorption bed is shut down to be regenerated. In a moving adsorption bed arrangement, a minimum of adsorbent need be used as fresh adsorbent is continuously added and removed from the adsorbent bed.

The second objective was to investigate whether higher gas velocities through the adsorption system could be realized by using a thin moving bed. Higher gas velocities through an adsorption bed that is continuously recycling could lead to the design of more compact emissions control systems. Such higher gas velocities through the adsorption bed and continuously recycling the carbon may also allow carbon adsorption systems to be applied to lower concentration emission streams.

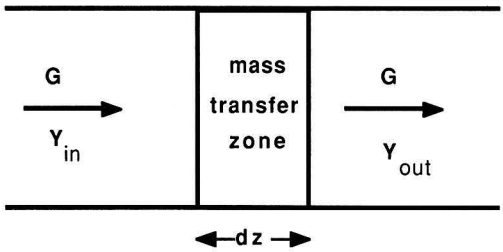

FIGURE 1. Differential element of adsorption bed.

Research Approach

To test the use of a moving bed adsorption system for the collection of VOCs, a 2.8 m^3/min (100 cfm) scale pilot plant was constructed. The pilot plant incorporated a moving bed adsorption section, a section where the adsorbed VOCs are thermally desorbed, and a mechanism to continuously recycle the adsorbent. In the adsorbent section the activated carbon adsorbent flows downward while the emissions stream to be treated flows across the bed. From the adsorbent section the carbon flows downward through a desorption section where the activated carbon is heated to remove adsorbed VOCs. The carbon is then continuously returned to the top of the adsorbent bed. As VOCs contact the activated carbon they are adsorbed according to the equilibrium established between the adsorbent particles and the VOC. The exchange between the air stream and the solid occurs in what is termed the 'mass transfer zone.' The mass transfer, dy/dz, in a differential element of adsorbent bed, depicted in Figure 1, is given by

$$\frac{dy}{dz} = \frac{K_G a}{G}(y - y^*)$$

where $K_G a$ is the overall gas phase mass transfer coefficient, G the gas superficial velocity, y the gas phase concentration, and y^* the concentration in equilibrium with the VOCs adsorbed on the carbon within the differential element. As more VOCs are adsorbed the equilibrium concentration, y^*, approaches the concentration in the bulk gas and the location of the mass transfer zone is moved toward the downstream side of the adsorption bed.

In this system, regenerated adsorbent is continuously added to the top of the system. The effect of the adsorbent moving down through the bed is to shift the location of the mass transfer zone downward in addition to towards the downstream side of the bed. This situation is depicted in Figure 2. By considering the VOC concentrations to be adsorbed, the equilibrium capacity of the adsorbent, and the mass transfer relationship between the gas and the solid, one should be able to determine optimum gas and solid flow rates that would result in minimum adsorbent use for a given gas velocity through the system.

The use of a pilot plant allows the identification, through testing, of not only potential problems due to the adsorption/desorption process itself, but also difficulties that can be expected to be encountered in applying such a process to actual installations. By using a pilot plant which incorporates both a moving adsorption bed and continuous recycling of the adsorbent the potential advantages, as well as difficulties with, these approaches when applied to actual emissions streams could be examined. A cross flow moving bed was selected primarily because one could be constructed relatively easily and yet still allow testing of a continuously recycling system. Contact heating in the desorption section was chosen, instead of steam or inert gas regeneration, because such a device could be made that would not require additional systems for steam or hot gas generation and thus would ease construction and operation of the system. Testing of the system was conducted to show that VOCs would be collected by the system and that the collected VOCs could be desorbed while the adsorption section continued collecting VOCs.

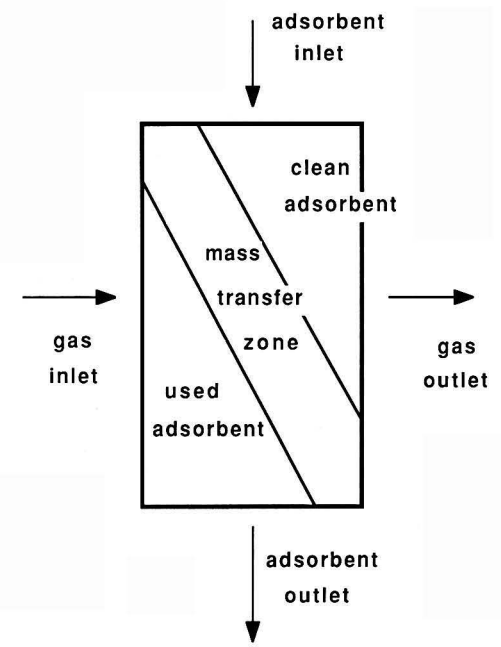

FIGURE 2. Mass transfer zone in moving adsorbent bed.

Difficulties in Controlling VOC Emissions

Solvent and coatings usage patterns in the aerospace industry are such that currently available VOC control systems may not be applicable or may not be economically feasible in many applications. Currently available options for controlling VOC emissions from low concentration, high volume emissions sources are limited to carbon adsorption using fixed bed systems, thermal incineration, catalytic incineration, and systems utilizing a combination of these control methods. The overall size of activated carbon VOC control equipment is directly related to the gas velocity through the system in that fans, ducting, and the size of the adsorbent bed are all dependent on the velocity of the gas through the system. As the size of the required equipment increases, the cost associated with building the equipment increases. At some point it becomes economically infeasible to apply the control equipment to an emission source. The point at which economic infeasibility (ie. cost per ton of VOC) is reached varies with geographic locality and specific application but in general, as the concentration of VOCs in the emissions source decreases the likelihood of a control device being economically feasible decreases. Costs associated with controlling emissions from surface coating operations are generally compared on the basis of the annual cost per ton of VOC controlled. As the concentration of the emissions stream decreases, the associated control cost increases.

In a review of six fixed-bed carbon adsorption VOC control systems, Nelson et al. [8] found that the annual cost of the systems on a per ton of VOC controlled basis varied from $260 to $600 per ton of VOC controlled. The capital cost for the systems on a per volume treated basis ranged from $850 to $2900 per SCM/min ($24 to $82 per cfm). The systems ex-

Table 1 VOC Adsorption System Costs

	Superficial Velocity (m/sec)	Inlet VOC Concentration (ppm)	Flow Rate (SCM/min)	Control Efficiency (%)	Capital Cost ($/SCM/min)	Annual Control Cost ($/ton VOC)
Plant 1 rubberized fabric manufacturer	0.45	2,190	317	84.9	2000	480
Plant 2 magnetic tape manufacturer	0.24	905–1330	275	93–99	1800	560
Plant 3 magnetic tape manufacturer	0.46	3000	561	92–97	2900	600
Plant 4 coated aluminum foil manufacturer	0.36	1200	501	99	2200	460
Plant 5 rubberized fabric manufacturer	0.33–0.30	2000	221–258	97	850	180
Plant 6 flexible packaging manufacturer	0.26	1000	946	98	1200	260
Superfund Site groundwater stripping tower effluent	—	1	142	>99	2500	600,000

Data for plants 1 through 6 from Nelson et al. (1985). Data for Superfund site from Byers (1988).

amined were designed to control emissions from continuous coatings processes in the rubberized fabric, magnetic tape, and flexible packaging industries. In these processes the VOC concentration was of the order of 1000 ppm. In comparison, Byers [*1*] presented data from a fixed-bed carbon adsorption system installed to control emissions from a groundwater stripping tower. In this case capital costs on a per volume treated basis were comparable to the continuous coating processes (approximately $2500 per SCM/min). The control cost, based on the amount of VOCs recovered, however was approximately $600,000 per ton of VOC controlled. The high control cost in the case of the groundwater stripping tower emissions control is due to the very low concentration being controlled (of the order of 1 ppm). Costs associated with the continuous coating operations and the groundwater stripping effluent are shown in Table 1.

The control cost associated with groundwater stripping emissions control perhaps represents an extreme in that the control system was installed as a remedial action at a Superfund site. The case does serve to illustrate how control costs increase dramatically when the VOC concentration is low. For low concentration (10–100 ppm) intermittent emissions sources the control costs can be expected to be significantly greater than costs for systems controlling higher concentration continuous emissions sources. According to an analysis of coating operations prepared for the aerospace industry [*9*], manufacturing processes in that industry involve intermittent coating of very large subassemblies and finished aircraft. The construction methods lead to very large exhaust volumes (greater than 2800 SCM/min) containing low concentrations of VOCs (on the order of 10–100 ppm). Control of these emissions with conventional technology, ie. fixed-bed adsorption systems, would involve quite high control costs.

Review of the Literature

Fixed bed adsorption devices are widely used for the control of VOC emissions. Numerous reviews and example applications of fixed bed adsorption devices are available in the literature [*3,7,8,13*]. The use of fixed bed adsorption systems to control emissions from groundwater air strippers is a typical application of fixed bed adsorption systems to very low concentration emissions streams. Reviews of such applications are available [*2,12*]. However, few investigations have been made of moving bed gas adsorption systems. Hori et al. [*5*] examined the breakthrough time of benzene in a fluidized bed of activated carbon. In the 1970's, Sakaguchi [*1*] described the development of a continuously flowing counter-current design using a special beaded activated carbon. Other research addressing the use of moving bed activated carbon systems for VOC emissions control has not been identified.

Moving bed control systems have, however, been investigated with regards to particulate control applications. Considerable research has been done towards the development of moving granular bed filters for controlling emissions from fluidized bed combustion devices. Rubow and coworkers [*10*] provide a review of several moving bed granular filter particulate collection systems. The effects of gas flow and solid flow on particulate collection efficiency in a granular cross flow moving bed have been investigated experimentally by Tsubaki and Tien [*14*]. Their research focused on collection of fine particulate by a moving bed filter. Ginestra and Jackson [*4*] investigated the ability of cross gas flow to prevent the downward flow of particles. The research in this case was directed towards understanding phenomena occurring in equipment such as continuously regenerated catalytic reactors in use in the petrochemicals industry. These investigators and others have demonstrated cross flow moving bed systems can be used to investigate particulate emissions control. Descriptions of other types of chemical process equipment with continuously flowing solids are available in standard reference texts (eg. Perry's Chemical Engineer's Handbook).

MOVING BED PILOT PLANT

Description of Apparatus

The pilot plant that was constructed incorporates a cross-

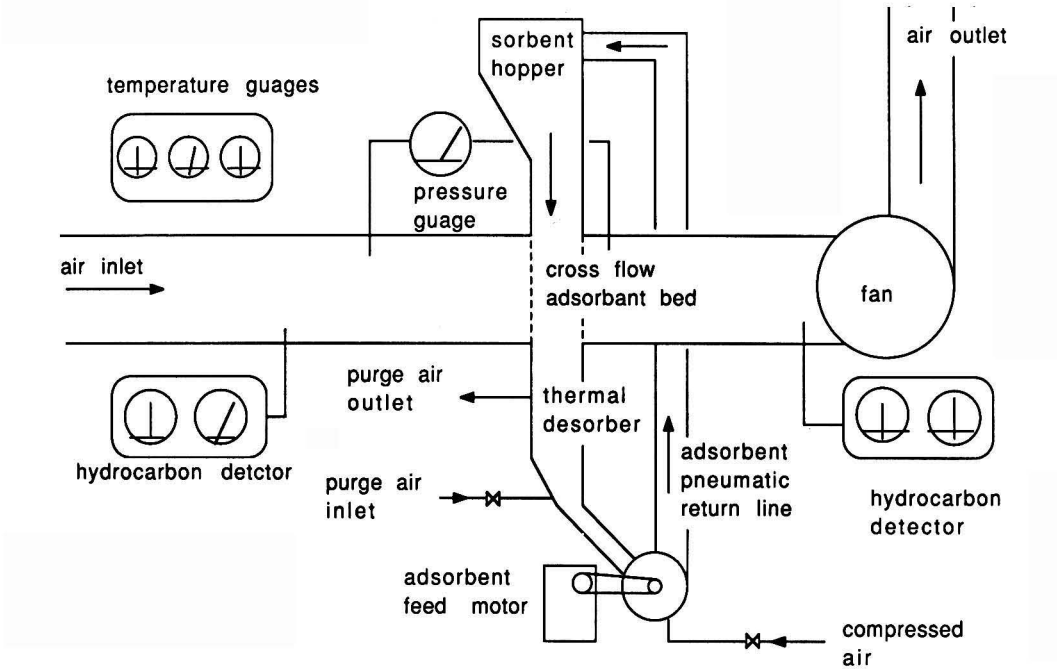

FIGURE 3. Cross-flow moving bed system schematic

flow adsorbent bed, a heated section to remove adsorbed VOCs, and a solids feeding and return mechanism which allowed for continuous recycling of the activated carbon adsorbent to the top of the adsorbent bed. The system is shown schematically in Figure 3. In the adsorption section, the activated carbon is supported between screens allowing VOC containing air to flow through the carbon while the carbon flows downward between the screens. The screen used was aluminum window screening having 1.2 mm openings. The depth of adsorbent bed used by 10.16 cm. The VOC containing air enters and exits the adsorbent bed through 15.24 cm diameter sheet metal ducting. All of the components above the desorption section were constructed from 6.35 mm thick plexiglass. The activated carbon flows downward through the adsorbent bed by gravity due to the action of the solids feeding mechanism located at the bottom of the apparatus.

Below the adsorber section, a desorption section is located where the activated carbon is heated to remove adsorbed VOCs. The desorption section is constructed of sheet metal which is heated using 500W heating tape. The temperature of the desorption section is controlled by adjusting the setting on a percentage time controller supplying power to the heating tape. The desorption section has a depth of 2.54 cm. The narrow depth was chosen to allow for more efficient heat transfer from the heated sheet metal to the activated carbon. Between the heated desorption section and the adsorption section of the device is a spacer that was manufactured from refractory brick. The spacer is necessary to prevent heating of the components above the desorption section when heat is applied to the desorber. Fittings located 2.54 cm from the top of the desorption section allow air to be withdrawn while the desorption section is heated. The desorbed VOCs are removed along with the air removed from the desorber outlet fittings. The flow rate of the desorber purge is very much less than the flow of the VOC containing emissions stream through the adsorption section. During testing of the desorber, a purge flow rate of 4 liters/min (0.14 cfm) was used while the air flow through the adsorbent bed was 354 liters/min (12.5 cfm). If all the VOCs collected in the adsorption section are desorbed and removed via the desorber purge, then the effect would be to increase the concentration and decrease the volume of VOC containing air to be dealt with. In the pilot plant, the air flow from the desorber purge is collected in a small fixed carbon bed although if the system were applied to a larger scale, the output stream from the desorber could be treated by thermal or catalytic incineration.

To enable continuous recycling of the activated carbon to the top of the adsorbent bed a solids feed mechanism was constructed by fitting a 2.54 cm diameter ship auger drill bit to the outlet of the heated desorber section. The sleeve for the auger bit was made from the length of slotted mild steel pipe and sealed to the desorption section using steel reinforced epoxy. The auger bit shaft was coupled to a 1/6 HP AC motor (1140 rpm) via a series of pulley wheels and v-belts such that the auger bit rotates at a speed of 26 rpm. The rotation speed of the auger bit, and thus the solids flow rate, can be changed by increasing or decreasing the diameter of the pulley wheels used. The outlet from the auger bit is fed into the pneumatic return line via a tee. The solids return line is 2.54 cm ID plastic tubing. Air supplied from a Lear Siegler compressor (0.48 HP) provides the driving force to return the activated carbon back to the top of the system. The solids return line empties into the system at a point well above the adsorbent bed such that the flow of the VOC containing air through the bed is not significantly affected by the returning carbon. The activated carbon returned to the top of the device then flows by gravity to the bottom of the system.

VOC containing air is drawn through the system by a fan located downstream of the adsorbent bed. Between the adsorbent bed and the fan is a fiberglass mat filter to collect dust created by the flow of air through the adsorbent bed. At the fan is located a bypass damper that can be used to adjust the volume of air that is drawn through the bed.

Experimental Test Procedure

To determine the ability of the system to collect VOCs a

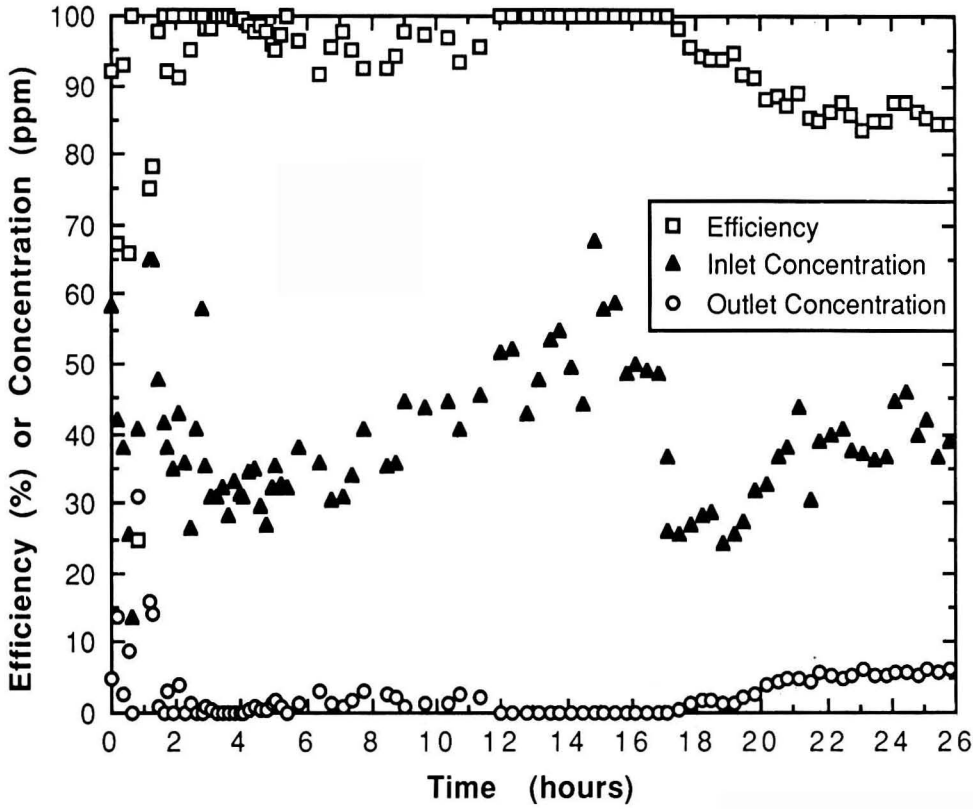

FIGURE 4. VOC concentrations and collection efficiencies during Test 1.

test gas was generated by bubbling air through a flask containing ethanol and introducing this air into the inlet of the system. The air flow rate through the bubbler was 1.8 liters/min. This ethanol saturated flow was mixed with the air flow entering the adsorption bed at the ducting inlet approximately 12 duct diameters upstream of the adsorption bed. The inlet and outlet concentration of ethanol was measured with a Photovac model TIP 1 portable hydrocarbon detector. This instrument employs a photoionization detector to detect hydrocarbons. The detector does not provide for identification of individual components, but rather provides an indication of total hydrocarbon concentration within the sample stream. The concentration measured at the desorber inlet was used to normalize all of the measurements taken. Inlet and outlet sampling probes (tubing extending into the duct) were located at the approximate center of the air duct. Air from the sampling ports was drawn to the PID through tygon tubing via a sampling pump. To measure the temperature of the inlet and outlet air, temperature probes were also placed in the air ducts close to the sampling probes. To measure the temperature of the desorption section and of the carbon being returned to the top of the system, temperature probes were inserted into the desorption section near the desorber outlet fittings, and in the top of the system were the carbon is returned. Temperatures measured by the probes were indicated on a multiple input thermocouple indicator. During each run, temperature and concentration measurements were recorded every 20 minutes. The activated carbon was used Westvaco Carbon BX-7450 pellets. The pellets are cylindrical in shape having a diameter of 4.4 mm. The air flow rate through the system was determining by making velocity traverses upsteam of the adsorbent bed with the fan damper in a fixed position. An Alnor model 8565 thermoanemometer was used to make the velocity traverses. The flow rate of activated carbon through the system was determined by disconnecting the compressed air supply to the solids return line and weighing the amount of carbon discharged from the auger bit outlet over a fixed time period. For the pulley wheel diameters used in these tests the activated carbon flow rate was 3.63 kg/hr (8 lbs/hr). This corresponds to a cycle time (the time for the activated carbon to complete one loop through the system) of 2.25 hours. The activated carbon moves through the bed at approximately 15 cm per hour. For test run #6, the pulley wheels were changed such that the carbon flow rate was reduced to 2.27 kg/kr (5 lbs/hr).

Results and Discussion

VOC Collection Efficiency

The initial system test was intended to determine if the system would operate stably for a prolonged time period. The velocity of the ethanol containing air stream entering the system was 0.32 m/sec. The flow rate of carbon through the system was 3.63 kg/hr. The VOC collection efficiency observed during this test is shown in Figure 4. Also shown in Figure 4 are the inlet and outlet ethanol concentrations as measured with the photoionization detector. The collection efficiency is shown in percent and the concentrations are shown in ppm. The variation shown in the first few hours of the test was due to measurement inaccuracies caused by electronic interference from a sampling pump affecting the background concentration indicated by the Photovac detector. After the first two hours

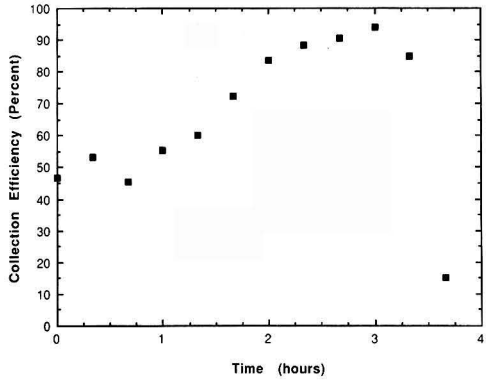

FIGURE 5. VOC collection efficiencies during Test 2.

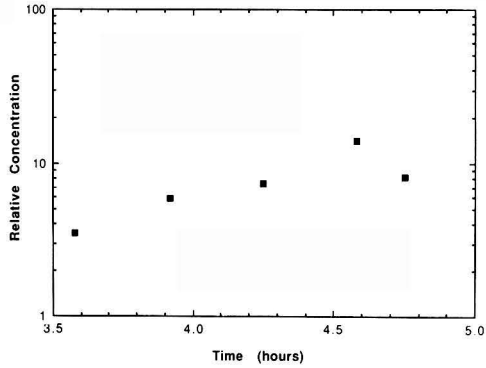

FIGURE 7. Ratio of outlet/inlet VOC concentrations of desorber versus time.

of testing this difficulty was eliminated. Figure 4 illustrates the moving bed system can be effective in collecting VOCs. The downward trend in collection efficiency towards the conclusion of the test is to be expected as the carbon begins to become more saturated.

In the second test, an initial gas velocity of 0.83 m/sec was used. The flow rate of carbon through the system was again 3.63 kg/hr. The VOC collection efficiency observed during the test is shown in Figure 5. This test was discontinued after 4 hours and 40 min due to apparent blockage of air flow through the system. The increased velocity through the system, and corresponding increased pressure drop, resulted in plugging of the support screen on the outlet side of the adsorber bed. Due to the arrangement of the system fan and bypass damper used to set the air flow rate through the system, the pressure drop measured across the adsorbent bed remained about constant even though the air flow rate through the system decreased. The apparent increase in collection efficiency shown in Figure 5 is also an effect due to screen plugging. Since the ethanol saturated air was being delivered to the air inlet at a constant rate, the concentration of ethanol in the inlet stream to the adsorber increased as the air flow rate decreased. The increase in collection efficiency indicated in Figure 5 is due to the inlet concentration increasing while the outlet concentration remains about constant. In later tests, the adverse effects of plugging of the adsorbent support screens were overcome by brushing the screens between test runs (about every 4 hours of operation).

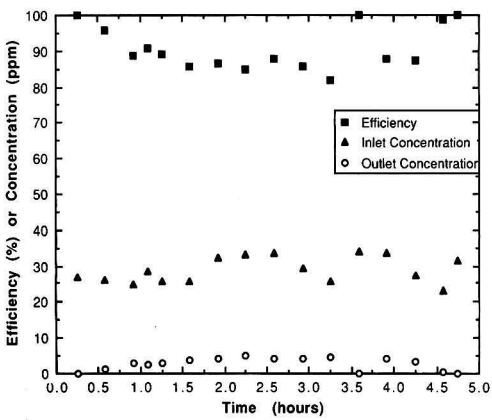

FIGURE 6. VOC concentrations and collection efficiencies during Test 6.

Third, fourth and fifth tests of the system were conducted using the same solids flow rate. VOC collection efficiencies observed during these tests were similar to those for the first test. The collection efficiency at a lower carbon flow rate was measured in the sixth test. The carbon flow rate during this test was 2.27 kg/hr. The air velocity into the adsorption bed was 0.32 m/sec. The collection efficiency observed during this test is shown in Figure 6. The inlet and outlet ethanol concentrations are also shown. Comparison with Figure 4 indicates the observed collection efficiency was not substantially different than at the higher carbon flow rate.

Desorption

To assess the effectiveness of the desorber section to remove collected VOCs, ethanol containing air was drawn through the system while the adsorbent bed was not moving. This was continued until approximately 70% of the VOC in the inlet gas passed through the bed without being adsorbed, as determined by inlet and outlet VOC concentration measurements. The solids feeding mechanism was then activated and the VOC concentration in the off gases of the adsorbent regenerator were measured as the partially saturated adsorbent passed through the regeneration section. The ratio of the desorber outlet concentration to the adsorption bed inlet concentration during this part of the test is shown in Figure 7. During this portion of the test, the desorber outlet concentration averaged 7.8 times the inlet concentration to the adsorption bed. To determine the amount of the adsorbed VOCs that were removed while the emissions from the desorption section were being measured, the weight of ethanol adsorbed while the adsorption bed was not moving and that which was emitted while the desorber emissions were being measured were determined. The gas flow rate through the adsorption bed and the difference between the inlet and outlet concentrations were used to determine the amount of ethanol adsorbed. The desorber outlet concentration measurements and the flow rate from the desorber were used to determine the amount of ethanol desorbed. The amount of ethanol adsorbed was 4.3×10^{-3} kg. The amount of ethanol desorbed was 1.0×10^{-4} kg, or about 2.4% of the total ethanol adsorbed. The temperature of the desorption section during this test ranged from 74 to 141°C and averaged 104°C. Since this test of the desorption section was concluded after approximately 1.5 hours, it is uncertain if the high concentration, relative to that of the inlet gas, emitted from the desorption section would be evident when this partially saturated carbon made another pass through the desorber. This carbon would be expected to re-enter the desorption section after completing another loop through the system, or in about another 2.25 hours.

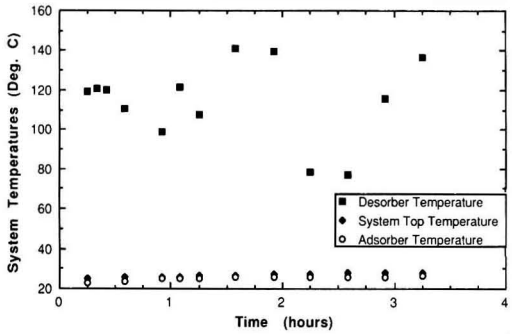

FIGURE 8. System temperatures during desorber testing (Test 6).

The temperature of the desorption section during this test is shown in Figure 8. Also shown in Figure 8 are the temperatures measured at the top of the system where carbon is returned to the adsorption bed and of the air in the outlet duct from the adsorption bed. These measurements indicate that a reasonably high temperature can be attained in the desorber and yet not adversely effect the temperature in the adsorption bed.

Carbon Attrition

To assess the attrition of the activated carbon pellets as they are circulated through the system, the compressed air supply to the return line was disconnected and the carbon collected from the auger bit outlet. Attrition of the carbon was assessed by determining the fraction of carbon that would pass a 30 mesh sieve. This screen size was chosen because it was felt that particles below this size should be considered 'dust' requiring some sort of collection device in the system to prevent the particles from being emitted out the exhaust of the fan. For a single pass through the auger bit feeding mechanism, the fraction less than 30 mesh was 2%. After the system had run for 6 hours and 40 minutes, the fraction less than 30 mesh was 6.8%. After the system had run for 26 hours, the fraction less than 30 mesh was 7.7%.

Pressure Drop

Figure 9 shows the pressure drop across the adsorption bed as a function of gas velocity through the bed. The pressure drop across the moving bed adsorber during tests 1 and 6 was 0.95 cm H_2O. The gas velocity through the bed was 0.32 m/sec. During test 2 the pressure drop across the bed was 6.67 cm H_2O. The gas velocity through the bed during test 2 was 0.83 m/sec.

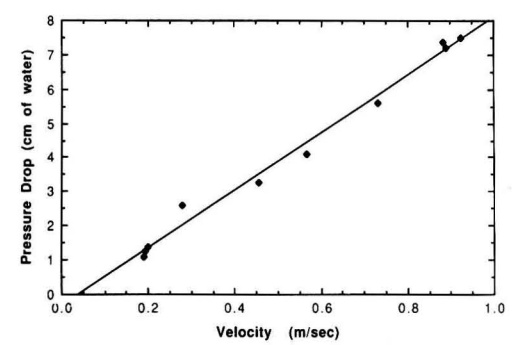

FIGURE 9. Gas pressure drop across the adsorption bed versus gas velocity through the bed.

CONCLUSIONS

A moving bed carbon adsorption system could be used to collect VOC emissions from low concentration emissions streams. The difficulties to be addressed in the use of the moving bed approach include attrition of the carbon as it is continuously recycled through the system and blockage of flow due to small particles being caught in the screening used to retain the carbon in the adsorbent bed. The tests conducted thus far with a small pilot scale system have indicated that VOCs can be collected in the slowly moving carbon bed. The two carbon flow rates used, approximately 2.27 kg/hr and 3.63 kg/hr, both resulted in collection efficiencies of the order of 90% without a discernible difference between the two rates. This may be due to the dimensions of the system, ie. the bed depth. It is anticipated that a thinner adsorbent bed of an inch or less thick would allow differences due to carbon flow rate to be measured.

Testing of the direct heated desorption section indicated that the carbon can be heated adequately as it flows through the section to produce an emission stream of considerably higher concentration than that which flowed through the adsorber. The results obtained indicate that removal of adsorbed VOCs could be accomplished in a flow through desorber. Further testing of such a continuous desorption system would need to be conducted to determine if such an approach is economically sound.

ACKNOWLEDGMENTS

The authors are grateful for the financial assistance provided by the Boeing Hazardous Waste Research Program. The loan of the Photovac portable hydrocarbon detector and the Alnor thermoanemometer by the University of Washington Department of Environmental Health is greatly appreciated. Also, the donation of the activated carbon by Westvaco Carbon is greatly appreciated. The use of the shop and lab facilities at the University of Washington Harris Hydraulic Laboratory to construct and test the pilot plant are acknowledged. The assistance of Tony McKay at the Harris Laboratory is appreciated.

NOTATION

G = gas flow rate, kg/hr-m^2 or lb/hr-ft^2
$K_G a$ = overall mass transfer coefficient, kg/hr-m^3 or lb/hr-ft^3
y = mole fraction of VOC in gas phase, dimensionless
y^* = mole fraction of VOC in gas phase in equilibrium with adsorbed phase, dimensionless
Z = depth of adsorbent bed in direction of gas flow, m or ft

LITERATURE CITED

1. Byers, W., "Control of Emissions From an Air Stripper Treating Contaminated Groundwater," *Environmental Progress*, **7**, No. 1, pp. 17-21 (1988).
2. Crittenden, J., Cortright, R., Rick, B., Tang, S., and

Perram, D., "Using GAC to Remove VOCs From Air Stripper Off-Gas," *American Water Works Association Journal,* **80**, May 1988, pp. 73–84 (1988).
3. Foster, M., "Evaluation of Parameters Affecting Activated Carbon Adsorption of a Solvent-Laden Air Stream," U.S. EPA, Report No. EPA/600/D-85/144 (1985).
4. Ginestra, J., and Jackson, R., "Pinning of a Bed of Particles in a Vertical Channel by a Cross Flow of Gas," *Industrial Engineering and Chemistry Fundamentals,* **24**, pp. 121–128 (1985).
5. Hori, H., Tanaka, I., and Akiyama, T., "Breakthrough Time on Activated Carbon Fluidized Bed Adsorbers," *Journal of the Air Pollution Control Association,* **38**, pp. 269–271 (1988).
6. Kunii, D., "Chemical Reaction Engineering and Research and Development of Gas Solid Systems," *Chemical Engineering Science,* **35**, pp. 1887–1911 (1980).
7. MSA Research Corporation, "Package Sorption Device System Study," U. S. EPA, Report No. EPA/R2/73/202 (1973).
8. Nelson, T., Blacksmith, J., and Randall, J., "Full-Scale Carbon Adsorption Applications Study," U.S. EPA, Report No. EPA/600/2-85/012 (1985).
9. Radian Corporation, "State of the Industry Report, Aerospace Surface Coatings/Solvents—Development of Low VOC Materials," Report prepared for the aerospace industry by Radian Corporation, Los Angeles (March 1987).
10. Rubow, L., Borden, M., Buchanan, T., Cramp, J., and Fischer, W., "Technical and Economic Evaluation of Ten High Temperature, High Pressure Particulate Cleanup Systems for Pressurized Fluidized Bed Combustion," U.S. DOE, Report No. DOE/MC/19196-1654 (1984).
11. Sakaguchi, Y., "Development of Solvent Recovery Technology Using Activated Carbon," *Chemical Economy and Engineering Review,* **8**, No. 12, pp. 36–43 (1976).
12. Singh, S., DePaoli, D., and Bergovich, J., "Review of Methods for Removing VOCs (Volatile Organic Compounds) from the Environment," Oak Ridge National Laboratory, Report No. CONF-871113-4 (1987).
13. Spivery, J., "Recovery of Volatile Organic from Small Industrial Sources," *Environmental Progress,* **7**, No. 1, pp. 31–40 (1988).
14. Tsubaki, J., and Tien, C., "Gas Filtration in Granular Moving Beds—An Experimental Study," *Canadian Journal of Chemical Engineering,* **66**, pp. 271–275 (1988).

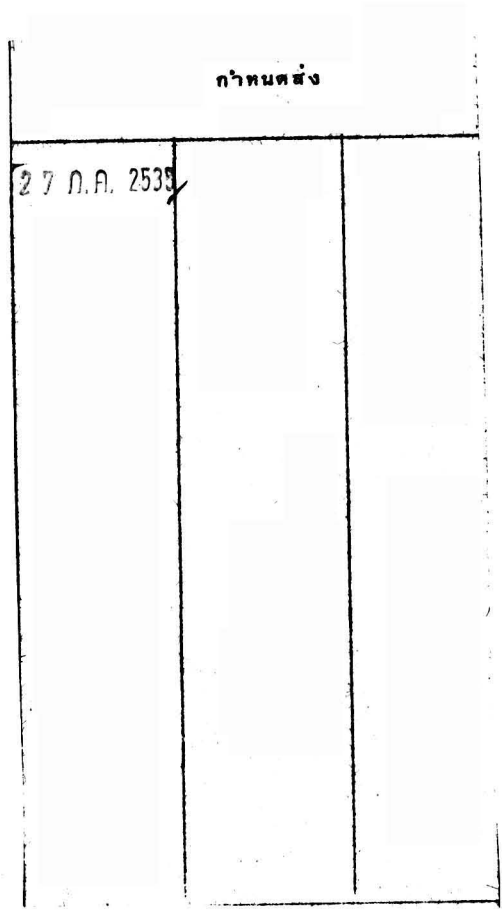

EMERGENCY RELIEF SYSTEM DESIGN

developed by AIChE's Design Institute for Emergency Relief Systems (DIERS)

SAFIRE COMPUTER PROGRAM & DOCUMENTATION

The *Systems Analysis for Integrated Relief Evaluation* (SAFIRE) computer program and accompanying manuals are useful for designing emergency relief systems for runaway reactions or fire exposure. Engineers can utilize this tool to estimate the pressure/temperature/time history for selected relief devices in a variety of applications and situations.

Your have a choice of one of two formats: Computer Tape for use with an IBM, VAX or UNIVAC Mainframe Computer.....or.....diskette for IBM Compatible Personal Computers.

Purchase of a single copy entitles a company to world-wide use of both versions of this computer program.

Pub# B-1 Computer Tape and/or PC Floppy Disk *plus* One set of 7 Manuals (782 pp) $7500

EMERGENCY RELIEF SYSTEMS FOR RUNAWAY CHEMICAL REACTIONS & STORAGE VESSELS: A SUMMARY OF MULTIPHASE FLOW METHODS

This technology summary presents the multiphase flow methods to calculate phenomena relevant to design of emergency relief systems for runaway reactions. The document will help users acquire, assimilate and implement the vast amount of DIERS information by serving as both a reference and a training tool.

Pub# B-2 Spiralbound (200 pp) $210

BENCH-SCALE APPARATUS DESIGN & TEST RESULTS

Methods to measure runaway reaction data under adiabatic conditions in a vessel with a very low thermal inertia are presented. Measurement of vessel liquid disengagement regimes and viscous vs. turbulent pipe flow behavior are discussed. Methods are also provided for sizing emergency relief devices without a comprehensive computer program.

Pub# B-4 Spiralbound (5 reports, 286 pp) $90

SMALL/LARGE SCALE EXPERIMENTAL DATA & ANALYSIS

Ten reports present test data useful for the better understanding of vessel and vent line multiphase flow behavior applicable to emergency relief of chemical systems. Time/temperature/pressure/void fraction history and analysis of each test are given. Complete apparatus design details to facilitate independent analysis are also provided.

Pub# B-3 Spiralbound (10 reports, 1218 pp) $250

SAFETY VALVE STABILITY & CAPACITY TEST RESULTS

This study addresses problems arising when a safety valve adjusted for vapor flow is used to vent low-quality steam. The report also covers the effect of valve exit to orifice areas on the flow capacity and stability of the valve and the prediction of saturated liquid mass flow rates through valves.

Pub# B-5 Spiralbound (77 pp) $100

Send Orders to: AIChE Publication Sales, 345 East 47 Street, New York, NY 10017. Prepayment in U.S. funds required (check, international money order or bank draft drawn on a New York bank). VISA or MasterCard orders: call (212) 705-7657 for details. U.S. bookrate shipments prepaid. Foreign Extra: $6 per book. *(Europe, Middle East & Africa: Contact Clark Associates-Europe Ltd, Unit 2, Pool Road Trading Estate, W. Molesey, Surrey KT8 OHE England.)*

AMERICAN INSTITUTE OF CHEMICAL ENGINEERS

find information fast

document delivery

fast precise searches

ESL information services

save time and money

online information retrieval

comprehensive bibliographies

ESL Information Services addresses the special needs of the Engineering and Technological community. Through the DIALOG information retrieval system, we can survey 'online' 15 years of the worldwide engineering and scientific literature in a few minutes at costs that are a fraction of manual searches.

WHAT ESL INFORMATION SERVICES HAS TO OFFER YOU

- Fast precise searches of the Engineering Literature
- Immediate access to engineering journals, numerous conference proceedings, reports, and books
- Over 65 databases covering engineering, physics, computers, energy, materials, patents, and chemistry
- Flexible and extensive search terms - authors, title words, subject categories, chemical abstracts register numbers
- More for your money and time... save hours of library research over manual techniques
- Document delivery... tap the vast resources of the Engineering Societies Library's engineering and technological literature... over 5000 serials from some 50 countries in 25 languages

For more information on this indispensable research tool, please call or write:

ESL Information Services

Engineering Societies Library

345 East 47th Street New York, New York 10017 (212) 705-7610

1984.094